

SYNTHESIS AND CHARACTERIZATION OF  
HYDROXYL AMMONIUM IONIC LIQUIDS AS  
CORROSION INHIBITOR FOR CARBON STEEL  
UNDER ACIDIC MEDIA

KIKI ADI KURNIA

DOCTOR OF PHILOSOPHY  
CHEMICAL ENGINEERING DEPARTMENT

UNIVERSITI TEKNOLOGI PETRONAS

AUGUST 2011



STATUS OF THESIS

Title of thesis

SYNTHESIS AND CHARACTERIZATION OF HYDROXYL  
AMMONIUM IONIC LIQUIDS AS CORROSION INHIBITOR  
FOR CARBON STEEL UNDER ACIDIC MEDIA

I, KIKI ADI KURNIA

hereby allow my thesis to be placed at the Information Resource Center (IRC) of  
Universiti Teknologi PETRONAS (UTP) with the following conditions:

- i) The thesis becomes the property of UTP
- ii) The IRC of UTP may make copies of the thesis for academic purposes only.
- iii) This thesis is classified as

<input type="checkbox"/>	Confidential
<input checked="" type="checkbox"/>	Non-confidential

If this thesis is confidential, please state the reason:

\_\_\_\_\_  
\_\_\_\_\_

The contents of the thesis will remain confidential for \_\_\_\_\_ years.

Remarks on disclosure:

\_\_\_\_\_  
\_\_\_\_\_

Endorsed by

\_\_\_\_\_  
Signature of Author

Permanent address:

Jln. Jend. Gatot Subroto No.173/118

Bandung, 40274, Indonesia

Date : \_\_\_\_\_

\_\_\_\_\_  
Signature of Supervisor

Name of Supervisor

Assoc. Prof. Dr. M. Ibrahim A. Mutalib

Date : \_\_\_\_\_

UNIVERSITI TEKNOLOGI PETRONAS

SYNTHESIS AND CHARACTERIZATION OF HYDROXYL AMMONIUM  
IONIC LIQUIDS AS CORROSION INHIBITOR FOR CARBON STEEL UNDER  
ACIDIC MEDIA

by

KIKI ADI KURNIA

The undersigned certify that they have read, and recommend to the Postgraduate Studies Programme for acceptance this thesis for the fulfillment of the requirements for the degree stated.

Signature : \_\_\_\_\_

Main Supervisor : ASSOC. PROF. DR. M. IBRAHIM A. MUTALIB

Signature : \_\_\_\_\_

Head of Department : ASSOC. PROF. DR. SHUHAIMI MAHADZIR

Date : \_\_\_\_\_

SYNTHESIS AND CHARACTERIZATION OF HYDROXYL AMMONIUM  
IONIC LIQUIDS AS CORROSION INHIBITOR FOR CARBON STEEL UNDER  
ACIDIC MEDIA

by

KIKI ADI KURNIA

A Thesis

Submitted to the Postgraduate Studies Programme

as a Requirement for the Degree of

DOCTOR OF PHILOSOPHY

DEPARTMENT OF CHEMICAL ENGINEERING

UNIVERSITI TEKNOLOGI PETRONAS

BANDAR SERI ISKANDAR,

PERAK

AUGUST 2011

DECLARATION OF THESIS

Title of thesis

SYNTHESIS AND CHARACTERIZATION OF HYDROXYL  
AMMONIUM IONIC LIQUIDS AS LOW COST CORROSION  
INHIBITOR FOR CARBON STEEL UNDER ACIDIC MEDIA

I, \_\_\_\_\_ KIKI ADI KURNIA \_\_\_\_\_

hereby declare that the thesis is based on my original work except for quotations and citations which have been duly acknowledged. I also declare that it has not been previously or concurrently submitted for any other degree at UTP or other institutions.

Witnessed by

\_\_\_\_\_  
Signature of Author

\_\_\_\_\_  
Signature of Supervisor

Permanent address:

Jln. Jend. Gatot Subroto No.173/118

Bandung, 40274, Indonesia

Date : \_\_\_\_\_

Name of Supervisor

Assoc. Prof. Dr. M. Ibrahim A. Mutalib

Date : \_\_\_\_\_

*To my parents and grandparents, for their love and support. Who worked tirelessly,  
so that their children could have better lives than they.*

## ACKNOWLEDGMENTS

First and foremost I would like to express my sincere gratitude and appreciation to my supervisor, Assoc. Prof. Dr. Mohamed Ibrahim Abdul Mutalib for his invaluable advice, support, encouragement, and his patience throughout this course of thesis study. I am forever grateful to him for believing in me and giving me the opportunity to work with him, and being such an inspiring mentor with his immense enthusiasm.

I am also greatly thankful to Assoc. Prof. Dr. Bambang Ariwahjoedi from Fundamental and Applied Science Department for his generous help, his expert advice, and his approach to me like as if I am one of his own students. I would also like to thank Assoc Prof. Dr. Mohamad Azmi Bustam, who gave generously imparted some of his vast knowledge on me through my symposiums.

Financial support provided by Postgraduate Office, Universiti Teknologi PETRONAS (UTP) in the form of graduate assistantship is gratefully acknowledged. I would also like to thank Postgraduate Study Programme staff members and Chemical Engineering Department staff members and technicians.

I would like to express my gratitude to the entire PETRONAS Ionic Liquids center and my lab mates in block 5 for their help and support, and friendship that you have given me over the years. Particularly, I would like to express my appreciation to Anisa Ur Rahmah, Ariyanti Sarwono, Sabtanti Harimukti, and Hasiah Kamarudin for not only making my days at UTP more fun and effective, but also for being great friends to me when I am thousand miles away from my home ways. I wish you all the best luck in your future endeavors!



I wish to thank all my friends, especially to Dini Amalia, Sri Krisna Wisnu Wardhana, Firman Syah, Abdul Munir, Tri Chandra, Fikri Irawan, Prantyo Rizkyantoro, Aryo Handoko, Luluan Lubis, Belinda, Ela Nurlaela, Yunita Sari, and Rere Rahardjati for carrying me with their presence, conversation, and their own nature, which inspire me and change my life during my study in UTP.

Most importantly, I would like to express my true appreciation to my family for their love, emotional support, understanding, and their patience. I would like to send my deepest appreciation to my parents and my grandmother that have made biggest sacrifices to enable me to achieve this goal, for their endless love and support, for that I will forever be indebted to them, and without their encouragement this study would not have been possible.

## ABSTRACT

The inhibition of carbon steel corrosion becomes of such interest because it is widely used as constructional materials in many industries, such as erecting boilers, drums, heat exchangers, pipe line, and many more. The acidization of oil and gas wells is probably the most widely used work over and stimulation practice in oil industry. HCl is widely used for stimulating carbonate-based reservoirs. Since HCl is strong aggressive medium for oil and gas well equipment, the effective way to protect these materials is to inject a suitable corrosion inhibitor. Accordingly, corrosion inhibitors must be injected with the HCl solution to avoid the destructive effect of acid on the surface of the pipe lines. Hence it is very important to measure the physical properties of the new corrosion inhibitor.

A variety of organic additives as corrosion inhibitors have been tested in these processes. However, there are some disadvantageous with the current inhibitor such as toxic, difficult preparation method and the high material cost. Also it has been reported that the lack of their physical properties data, has limited the design and application of these corrosion inhibitors. Even though ionic liquids have been proven as a potential inhibitor on carbon steel corrosion in acidic media, their price is relatively higher compared to the commercially available corrosion inhibitor. An alternative way is to find cheaper ionic liquids that can be applied as corrosion inhibitor on carbon steel corrosion in acidic media. Hydroxyl ammonium ionic liquids are relatively cheap and easy to produce in purity greater than 99%. In order to develop low cost inhibitors, the recent investigations on application of the hydroxyl ammonium ionic liquids as inhibitor on corrosion of carbon steel in 1 M HCl, seem really worthwhile.

The objectives of this research are to synthesis and characterize the range of ionic liquids, and to study their potential application as inhibitor on carbon steel corrosion in acidic media. For this study, sixteen hydroxyl ammonium ionic liquids were synthesized and characterized. The structures of synthesized ionic liquids were confirmed by infrared,  $^1\text{H-NMR}$ , and  $^{13}\text{C-NMR}$  spectra. Composition of synthesized ionic liquids was also confirmed from elemental analysis. Water content of these ionic liquids was found to be lower than 200 ppm. Physical properties of the ionic liquids such density, viscosity, and refractive index were measured at atmospheric pressure and temperature from 293.15 to 353.15 K, while refractive index was measured at temperature from (293.15 to 323.15) K. The coefficients of thermal expansions were calculated from experimental density data. In practical condition, corrosion inhibitors are mixture of active components, solvents, and surfactant. In this work, the effects of alcohol such as methanol, ethanol, and 1-propanol, as co-solvent on physical properties namely density, viscosity, and refractive index of the ionic liquids were also studied. The ionic liquids Bis(2-hydroxyethyl)ammonium formate, [BHEAF] was chosen as model due to the highest inhibition performance.

The inhibition performance of the synthesized ionic liquids on carbon steel corrosion in 1 M HCl was measured within concentration range of ionic liquids from 0.02 to 0.08 M while temperature range from 298.15 – 343.15 K using two methods, weight loss and electrochemical. The obtained results showed that the inhibition performance increased with increasing concentration of ionic liquids and decreasing temperature of system. Tafel Plot analysis showed that these ionic liquids were mixed type inhibitor, which reduced the corrosion rate by blocking both cathodic and anodic site. Electrochemical Impedance Spectroscopy analysis showed that the addition of ionic liquids did not change the mechanism of corrosion of carbon steel. The synthesized ionic liquids reduced the corrosion rate of carbon steel by adsorbing themselves on the carbon steel surface. The adsorptions of the ionic liquids on the surface of carbon steel obey the Langmuir's isotherm adsorption. The high values of equilibrium constant and standard free energy of adsorption indicated that the adsorption of ionic liquids on the surface of carbon steel was spontaneous and occurred only by physisorption. The apparent activation energy of corrosion of carbon

steel in the presence of ionic liquids was higher compared to without ionic liquids. This result indicated that the addition of ionic liquids give energy barrier for corrosion. These results were also supported by their enthalpy and entropy of adsorption. Addition of alcohol on ionic liquids did not alter the inhibition efficiency. Thus, it can be concluded that these alcohols can be used as co-solvent with ionic liquids, without reducing the ionic liquids performance. The organic solvent is particularly helpful for reducing the viscosity of ionic liquids which is known to be highly viscous

From these experimental results, it shows that hydroxyl ammonium ionic liquids have potential as inhibitor on corrosion of carbon steel in 1 M HCl. It suggests that all the synthesized hydroxyl ammonium ionic liquid in this work has the potential to be used as inhibitor on carbon steel corrosion in 1 M HCl.

## ABSTRAK

Penghambatan korosi baja karbon menjadi kepentingan kerana banyak digunakan sebagai bahan pembinaan di banyak industri, seperti boiler, drum, penukar panas, paip, dan banyak lagi. The acidization telaga minyak dan gas bumi mungkin adalah pekerjaan yang paling banyak digunakan di atas dan amalan stimulasi dalam industri minyak. HCl secara meluas digunakan untuk merangsang reservoir karbonat yang berpusat. Kerana HCl adalah sarana agresif yang kuat untuk minyak dan gas tetap, cara efektif untuk melindungi material ini adalah dengan menyuntikkan inhibitor korosi yang sesuai. Oleh kerana itu, inhibitor korosi harus disuntik dengan larutan HCl untuk mengelakkan kesan merosakkan asid pada permukaan garis paip. Oleh kerana itu sangat penting untuk mengukur sifat fizikal inhibitor korosi baru.

Berbagai aditif organik sebagai inhibitor korosi telah diuji dalam proses ini. Namun, ada beberapa merugikan dengan inhibitor saat ini seperti beracun, kaedah persiapan sulit dan kos bahan tinggi. Juga telah dilaporkan bahawa kurangnya data sifat fizikal mereka, telah menyekat desain dan aplikasi dari inhibitor korosi. Walaupun cecair ionik telah terbukti sebagai inhibitor berpotensi pada korosi baja karbon dalam media asam, harga mereka relatif lebih tinggi berbanding dengan inhibitor korosi tersedia secara komersil. Cara alternatif adalah untuk mencari cecair ionik murah yang boleh digunakan sebagai inhibitor korosi pada korosi baja karbon dalam media asam. Cecair ammonium ion hidrosil relatif murah dan mudah untuk dibuat dalam kemurnian lebih dari 99%. Dalam rangka untuk mengembangkan kos rendah dan persekitaran "ramah" inhibitor, penyelidikan baru pada penerapan cecair ammonium ion hidrosil sebagai inhibitor terhadap korosi baja karbon dalam 1 M HCl, tampak benar-benar berharga.

Tujuan kajian ini adalah untuk sintesis dan mengkarakterisasi pelbagai cecair ion, dan mempelajari aplikasi potensi mereka sebagai inhibitor korosi pada baja karbon dalam media asam. Untuk kajian ini, sebanyak enam belas hidroksil amonium cecair ionik yang disintesis dan disifatkan. Struktur cecair ionik disintesis disahkan dengan spektra IR,  $^1\text{H-NMR}$ , dan  $^{13}\text{C-NMR}$ . Komposisi ionik cecair disintesis juga disahkan daripada analisis unsur. Kadar air dari cairan ion dijumpai lebih rendah daripada 200 ppm.

Sifat fizikal dari cairan ionik tersebut, seperti kepadatan, viskositas, dan indeks bias diukur dan dilaporkan. Kepadatan dan viskositas cecair ionik diukur pada tekanan atmosfera dan suhu 293.15-353.15 K, sedangkan indeks bias diukur pada suhu dari (293.15-323.15) K. Pekali pengembangan terma dikira dari data kepadatan eksperimental. Sifat fizikal cecair ionik yang menurun dengan peningkatan suhu. Ketergantungan suhu sifat fizikal cecair ionik boleh dikorelasikan menggunakan persamaan empirik.

Dalam keadaan praktikal, inhibitor korosi adalah campuran komponen aktif, pelarut, dan surfaktan. Dalam karya ini, pengaruh alkohol seperti metanol, etanol, dan 1-propanol, sebagai cosolvent pada sifat fizikal dari cairan ionik juga dipelajari. Cecair ionik [BHEAF] dipilih sebagai model kerana prestasi inhibisi tertinggi. Sifat fizikal campuran binari ionik cecair [BHEAF] dengan alkohol dijumpai tertinggi pada cecair ionik murni dan menurun dengan peningkatan konsentrasi alkohol. Selain itu, kerapatan dan viskositas campuran cecair ion dengan alkohol menunjukkan penyimpangan negatif dari ideal, sedangkan indeks bias menunjukkan penyimpangan positif. Dari data percubaan, termodinamik sifat kelebihan seperti kelantangan molar kelebihan, deviasi viskositas, dan deviasi indeks bias dihitung dan juga dilengkapi dengan Redlich Kister persamaan polinomial. Kelantangan molar semu pada pencairan tak terbatas cecair ion di cosolvent juga dipelajari. Keputusan yang diperolehi menunjukkan bahawa cecair ionik mempunyai kelantangan molar lebih rendah berbanding dengan sistem murni.

Prestasi penghambatan cecair ionik disintesis pada korosi baja karbon dalam 1 M HCl diukur dalam liputan konsentrasi cairan ion 0.02 – 0.08 M sementara kisaran suhu 298.15-343.15 K menggunakan dua kaedah, berat badan dan elektrokimia. Keputusan yang diperolehi menunjukkan bahawa prestasi inhibisi meningkat dengan peningkatan kepekatan ion cecair dan penurunan suhu sistem. Analisis Tafel Plot menunjukkan bahawa cecair ionik adalah inhibitor jenis campuran, yang mengurangkan laju korosi dengan menghalang kedua-dua laman katodik dan anodik. Elektrokimia Spektroskopi Impedansi analisis menunjukkan bahawa penambahan cecair ionik tidak merubah mekanisme kakisan baja karbon. Cecair ionik disintesis mengurangkan laju korosi pada baja karbon dengan menyerap diri pada permukaan baja karbon. Para jerapan dari cairan ion pada permukaan baja karbon mematuhi jerapan isotherm yang Langmuir. Nilai tenaga yang tinggi keseimbangan tidak konstan dan standard jerapan menunjukkan bahawa jerapan ion cecair pada permukaan baja karbon spontan dan berlaku hanya oleh physisorption. Tenaga pengaktifan nyata dari korosi baja karbon di hadapan cecair ion lebih tinggi berbanding dengan tanpa cecair ionik. Keputusan ini menunjukkan bahawa penambahan cecair ionik memberikan penghalang tenaga untuk korosi. Keputusan ini juga disokong oleh entalpi dan entropi jerapan. Penambahan alkohol pada cecair ionik tidak mengubah kecekapan inhibisi. Dengan demikian, dapat disimpulkan bahawa alkohol boleh digunakan sebagai cosolvent dengan cecair ionik, tanpa mengurangkan prestasi cecair ionik. Pelarut organik sangat bermanfaat untuk mengurangkan viskositas cecair ion yang dikenal sangat kental

Dari hasil percubaan, hal itu menunjukkan bahawa cecair ion hidroksil amonium mempunyai potensi sebagai inhibitor terhadap korosi baja karbon dalam 1 M HCl. Ini menunjukkan bahawa semua cecair ammonium ion hidroksil disintesis dalam karya ini mempunyai potensi untuk digunakan sebagai inhibitor korosi pada baja karbon dalam 1 M HCl.

## COPYRIGHT

In compliance with the terms of the Copyright Act 1987 and the IP Policy of the university, the copyright of this thesis has been reassigned by the author to the legal entity of the university,

Institute of Technology PETRONAS Sdn Bhd.

Due acknowledgement shall always be made of the use of any material contained in, or derived from, this thesis.

© Kiki Adi Kurnia, 2011  
Institute of Technology PETRONAS Sdn Bhd  
All rights reserved.



## TABLE OF CONTENTS

STATUS OF THESIS.....	i
DEDICATION .....	v
ACKNOWLEDGMENTS .....	vi
ABSTRACT .....	viii
ABSTRAK .....	xi
COPYRIGHT .....	xiv
TABLE OF CONTENTS.....	xv
LIST OF TABLES .....	xviii
LIST OF FIGURES .....	xx
LIST OF SYMBOLS AND ABBREVIATIONS.....	xxvii
CHAPTER 1: INTRODUCTION.....	1
1.1 Background .....	1
1.1.1 Ionic Liquids Corrosion Inhibitor .....	5
1.2 Problem Statement.....	6
1.3 Research Objectives and Scope of Study.....	9
1.4 Thesis Layout .....	10
CHAPTER 2: LITERATURE REVIEW .....	13
2.1 Ionic Liquids.....	13
2.1.1 Synthesis of Ionic Liquids .....	16
2.1.2 Purification of Ionic Liquids.....	20
2.2 Physical Properties of Ionic Liquids.....	21
2.2.1 Density.....	22
2.2.2 Viscosity .....	25
2.2.3 Refractive Index .....	28
2.2.4 Effect of Co-solvent on Physical Properties of Ionic Liquids .....	30
2.3 Carbon Steel Corrosion in Acidic Media.....	40

2.3.1	Recent Development on Corrosion Inhibitor in Acidic Media .....	42
2.3.2	Method to Measure Corrosion Inhibition.....	47
2.3.3	Adsorption of Inhibitor on Carbon Steel Surface.....	54
2.3.4	Thermodynamic of Adsorption .....	57
2.3.5	The Apparent Activation Energy.....	61
CHAPTER 3: RESEARCH METHODOLOGY.....		65
3.1	Preparation of Ionic Liquids .....	65
3.1.1	Chemicals .....	67
3.1.2	Synthesis of Ionic Liquids.....	67
3.1.3	Characterization of Ionic Liquids .....	72
3.2	Measurement of Physical Properties .....	73
3.2.1	Density .....	74
3.2.2	Viscosity.....	75
3.2.3	Refractive Index.....	76
3.2.4	Preparation of Binary Mixture.....	77
3.3	Corrosion Study .....	78
3.3.1	Preparation of Solution .....	78
3.3.2	Preparation of Specimen .....	78
3.3.3	Weight Loss Method.....	80
3.3.4	Electrochemical Method .....	82
CHAPTER 4: SYNTHESIS AND PHYSICAL PROPERTIES OF IONIC LIQUIDS .....		87
4.1	Hydroxyl Ammonium Ionic Liquids.....	87
4.1.1	Infrared Spectrum .....	88
4.1.2	NMR Spectrum.....	91
4.1.3	Elemental Analysis .....	95
4.1.4	Water Content.....	96
4.2	Physical Properties of Ionic Liquids .....	97
4.2.1	Density .....	98
4.2.2	Coefficient of Thermal Expansion.....	107
4.2.3	Viscosity.....	108
4.2.4	Refractive Index.....	113
4.3	Effect of Alcohol on Physical Properties of Ionic Liquids.....	115
4.3.1	Density of Binary Mixture and Volumetric Properties.....	116



## LIST OF TABLES

Table 1.1	Price comparison of some precursor of imidazolium-based and hydroxyl ammonium ionic liquids .....	7
Table 2.1	Density for some alcohols and ionic liquids at $T = 298.15$ K.....	23
Table 2.2	Viscosity of some organic solvents and ionic liquids at $T = 298.15$ K...	26
Table 2.3	Refractive index of some organic solvents and ionic liquids at temperature 298.15 K.....	29
Table 2.4	Adsorption isotherm.....	55
Table 2.5	The enthalpy and entropy of activation for mild steel in 1M HCl solution in the absence and presence of [BMIM]Cl.....	61
Table 2.6	The apparent activation energy for mild steel in 1M HCl solution in the absence and presence of [BMIM]Cl.....	62
Table 3.1	The amount of ionic liquids needed to make 0.02, 0.04, 0.06, and 0.08 M of solution.....	79
Table 3.2	Chemical composition of carbon steel BS 970.....	79
Table 4.1	List of peak appear in the infrared spectrum of the synthesized ionic liquids in this work.....	91
Table 4.2	Elemental analysis of synthesized ionic liquids.....	96
Table 4.3	Water content of synthesized ionic liquids.....	97
Table 4.4	Comparison of density, $\rho$ , values for pure ionic liquids and alcohol at $T = 298.15$ K.....	98
Table 4.5	The predicted density for hydroxyl ammonium ionic liquids using COSMO-RS method.....	100

Table 4.6	Fit parameter for temperature dependence of density calculated using equation (2.1) and its standard deviation calculated using equation (4.1).....	104
Table 4.7	Comparison of viscosity values for pure ionic liquids at $T = 298.15$ K .....	109
Table 4.8	Fit parameter for temperature dependence of viscosity calculated using equation (2.4) and its standard deviation calculated using equation (4.1).....	112
Table 4.9	Fit parameter for temperature dependence of refractive index calculated using equation (2.5) and its standard deviation calculated using equation (4.1). .....	114
Table 4.10	Fit parameter for temperature dependence of density of 1 M HCl with the various concentrations of [BHEAF] calculated using equation (2.1) and its standard deviation calculated using equation (4.1).....	135
Table 5.1	Electrochemical impedance parameters and the corresponding inhibition efficiency for carbon steel in 1 M HCl in the presence of various concentrations of ionic liquids [BHEAF] at 298.15 K. ....	158

## LIST OF FIGURES

Figure 1.1 Structures of some recent discovered novel corrosion inhibitors in acidic medium.....	3
Figure 1.2 Ionic liquids inhibitors on steel corrosion in acidic medium.....	6
Figure 2.1 Structure of common cations and anions used for ionic liquids.....	14
Figure 2.2 General method to synthesis ionic liquids.....	17
Figure 2.3 Schematic formation of the protic ionic liquids ethylammonium nitrate through proton transfer. ....	18
Figure 2.4 Structure of common cations used in protic ionic liquids. ....	19
Figure 2.5 Structure of common anions used in protic ionic liquids.. ....	19
Figure 2.6 Effect of temperature on density of the ionic liquids.. ....	24
Figure 2.7 Effect of temperature on viscosity of the ionic liquids .....	27
Figure 2.8 Experimental and predicted viscosity for ionic liquids. ....	28
Figure 2.9 Effect of temperature on refractive index of ionic liquids [empy][EtSO <sub>4</sub> ] .....	30
Figure 2.10 Density and excess molar volume ([BMIM]SCN + 1-propanol) binary mixture at $T = 298.15$ K (a) Effect of composition on density of binary mixture, (b) Excess volume molar of binary mixture, (--) correlated using equation 2.11 .....	35
Figure 2.11 Viscosity of ([BMIM]SCN + 1-propanol) binary mixture at $T = 298.15$ K (a) Effect of composition on viscosity of binary mixture, (b) Deviation of viscosity of binary mixture, (-) correlated using equation 2.11.....	37

Figure 2.12 Refractive index of ([empty][EtSO <sub>4</sub> ] + 1-Propanol) binary mixture at $T = 298.15$ K (a) Effect of composition on refractive index of binary mixture, (b) Deviation of refractive index of binary mixture, (-) correlated using equation 2.11.....	39
Figure 2.13 The E-pH diagram of iron with the cathodic criterion at $25$ °C.....	42
Figure 2.14 Mechanism of carbon steel corrosion in HCl solution in the absence and presence of inhibitor.....	45
Figure 2.15 Corrosion rate and inhibition efficiency in the absence and presence of [BMIM]Cl for mild steel in 1 M HCl. ....	48
Figure 2.16 Experimentally measured Tafel plot.....	49
Figure 2.17 Effect of inhibitor concentration on the potentiodynamic polarization response for mild steel in 1M HCl solution at 303 in various concentration of [BMIM]Cl.....	50
Figure 2.18 Experimentally measured linear polarization resistance.....	51
Figure 2.19 Nyquist plot for mild steel in 1M HCl solution at 303.15 K in various concentration of 1-butyl-3-methylimidazolium chloride.....	52
Figure 2.20 Bode plot for mild steel in 1M HCl solution at 303.15 K in various concentration of 1-butyl-3-methylimidazolium chloride.....	53
Figure 2.21 Electrical circuit analog corresponded to the Figure 2.19 and 2.20 .....	53
Figure 2.22 Langmuir's isotherm adsorption for ionic liquids 1-Butyl-3-methylimidazolium chloride on the surface of mild steel at temperature 303 K.....	56
Figure 2.23 Equilibrium constant for mild steel in 1M HCl solution in the presence of 0.005 M [BMIM]Cl at different temperatures.....	57
Figure 2.24 Standard free energy for mild steel in 1M HCl solution in the presence of 0.005 M [BMIM]Cl at different temperatures.....	59

Figure 2.25 Plot the $\ln(CR/T)$ against. $1000/T$ for mild steel in 1M HCl solution in the presence of 0.005 M 1-butyl-3-methylimidazolium chloride at different temperatures.....	60
Figure 2.26 Arrhenius plot for mild steel in 1M HCl solution in the presence of 0.005 M 1-butyl-3-methylimidazolium chloride at different temperatures.....	62
Figure 3.1 Flow diagram of experimental in the present work.....	66
Figure 3.2 Schematic preparation of ionic liquids through protonation of alkanolamine using organic acid.....	67
Figure 3.3 Illustration of the working electrode used for measurement of corrosion experiment. ....	80
Figure 3.4 General setup for the measurement of corrosion rate using three electrodes configurations .....	83
Figure 4.1 Infrared spectra of ionic liquids [HEF], [HEA], [HEP], and [HEL].....	88
Figure 4.2 Infrared spectra of [BHEAF], [BHEAA], [BHEAP], and [BHEAL].....	89
Figure 4.3 Infrared spectra of [BHEMF], [BHEMA], [BHEMP], and [BHEML]... ..	89
Figure 4.4 Infrared spectra of [THEAF], [THEAA], [THEAP], and [THEAL] .....	90
Figure 4.5 $^1\text{H-NMR}$ spectrum of [BHEAF]. .....	92
Figure 4.6 $^{13}\text{C-NMR}$ Spectrum of [BHEAF].....	92
Figure 4.7 Density of ionic liquids Bis(2-hydroxyethyl)ammonium with different anion at temperature 298.15 K.....	101
Figure 4.8 Density of ionic liquids with acetate and different cation at temperature 298.15 K. ....	102
Figure 4.9 Density of ionic liquids with formate anion and different cation as function of temperature.. ..	105
Figure 4.10 Density of ionic liquids with acetate anion and different cation as function of temperature.. ..	105



Figure 4.11 Density of ionic liquids with propionate anion and different cation as function of temperature.....	106
Figure 4.12 Density of ionic liquids with lactate anion and different cation as function of temperature.....	106
Figure 4.13 Coefficient of thermal expansion of ionic liquids and methanol at several temperatures.....	107
Figure 4.14 Viscosity of ionic liquids as function of temperature.....	111
Figure 4.15 Viscosities of ionic liquids from temperature (293.15 to 353.15) K and its polynomial correlation using equation (4.2) (·····).....	112
Figure 4.16 Refractive index of ionic liquids as function of temperature and its polynomial correlation using equation (2.1) (·····).....	115
Figure 4.17 Densities of {[HEF](1) + methanol(2)} binary mixture at temperature 298.15 K.....	116
Figure 4.18 Densities of binary mixture of ionic liquids with alcohol at temperature 298.15 K.....	117
Figure 4.19 Density-temperature dependence of {[BHEAF](1) + methanol(2)} binary mixtures with different moles fraction of [BHEAF].....	118
Figure 4.20 Excess molar volume, $V_m^E$ , for {[BHEAF](1) + Alcohol(2)} binary mixture at temperature 298.15 K.....	120
Figure 4.21 Excess molar volume, $V_m^E$ , for {[BHEAF](1) + methanol(2)} binary mixture at several temperature.....	121
Figure 4.22 Partial molar volume, $V_\phi$ , for {[BHEAF](1) + methanol(2)} binary mixture at temperature 298.15 K.....	122
Figure 4.23 Coefficient of thermal expansion for binary mixture of ionic liquids with alcohol at temperature 298.15 K.....	124
Figure 4.24 Coefficient of thermal expansion for {[BHEAF](1) + methanol(2)} binary mixture at several temperatures.....	125

Figure 4.25 Viscosity of binary mixture of ionic liquids with alcohol at temperature 298.15 K. ....	126
Figure 4.26 Viscosity of {[BHEAF](1) + methanol(2)} binary mixture at several temperatures.....	127
Figure 4.27 Viscosity deviation, $\Delta\eta$ , for for {[BHEAF](1) + alcohol(2)} binary mixture at temperature 298.15 K. ....	128
Figure 4.28 Viscosity deviation, $\Delta\eta$ , for {[BHEAF](1) + methanol(2)} binary mixture at several temperature.....	129
Figure 4.29 Refractive index of binary mixture of ionic liquids with alcohol at temperature 298.15 K. ....	130
Figure 4.30 Refractive index of {[BHEAF](1) + methanol(2)} binary mixture at several temperatures. ....	131
Figure 4.31 Refractive index deviation, $\Delta n_D$ , for for {[BHEAF](1) + alcohol(2)} binary mixture at temperature 298.15 K. Symbols: $\square$ , {[BHEAF](1) + methanol(2)}; $\diamond$ , {[BHEAF](1) + ethanol(2)}; $\Delta$ , {[BHEAF](1) + 1-propanol(2)}.....	133
Figure 4.32 Refractive index deviation, $\Delta n_D$ , for {[BHEAF](1) + methanol(2)} binary mixture at several temperature.....	133
Figure 4.33 Density of 1 M HCl solution in the presence of various concentration of ionic liquids [BHEAF] at several temperatures. ....	134
Figure 4.34 Temperature dependence of density of 1 M HCl solution in the presence of various concentration of ionic liquids [BHEAF] at several temperatures.....	135
Figure 5.1 Effect of ionic liquids concentration on corrosion rate of carbon steel in 1 M HCl in 1 M HCl at 298.15 K determined using weight loss method. (a) Ionic liquids with formate anion. (b) Ionic liquids with 2-hydroxyethylammonium cation. ....	140
Figure 5.2 Corrosion rate of carbon steel in 1 M HCl in the presence of various concentrations of ionic liquids [BHEAF] at 298.15 K measured using	

	weight loss method. (a) Ionic liquids with formate anion. (b) Ionic liquids with 2-hydroxyethylammonium cation. ....	143
Figure 5.3	Effect of anion on concentration dependence of inhibition efficiency of ionic liquids on corrosion of carbon steel in 1 M HCl at temperature 298.15 K using weight loss method. ....	144
Figure 5.4	Effect of cation on concentration dependence of inhibition efficiency of ionic liquids on corrosion of carbon steel in 1 M HCl at temperature 298.15 K using weight loss method ....	145
Figure 5.5	Effect of the cation and anion on the inhibition efficiency of 0.02 M ionic liquids on carbon steel corrosion at 298.15 K. ....	148
Figure 5.6	SEM micrographs of carbon steel specimens (magnificent scale 3000x). (a) Before immersion, (b) After immersion in 1 M HCl solution without inhibitor, and (c) after immersion in 1 M HCl solution in the presence of 0.08 M of ionic liquids [BHEAF]. ....	149
Figure 5.7	Tafel Plots of carbon steel dissolution in 1 M HCl at 298.15 K in the presence of various concentrations of ionic liquids [BHEAF]. ....	151
Figure 5.8	The effect of concentration of the ionic liquids on corrosion current density of carbon steel in 1 M HCl at 298.15 K measured using Tafel Plots. ....	151
Figure 5.9	The inhibition efficiency of ionic liquids determined using Tafel Plot at 298.15 K. ....	152
Figure 5.10	The effect of concentration of the ionic liquids on polarization resistance of carbon steel in 1 M HCl at 298.15 K measured using Linear Polarization Resistance. ....	153
Figure 5.11	The inhibition efficiency of ionic liquids determined using Tafel Plot at 298.15 K. ....	154
Figure 5.12	Nyquist plot of carbon steel in 1 M HCl with various concentrations of ionic liquids at 298.15 K. ....	156

Figure 5.13 Electrochemical impedance spectrum of carbon steel in 1 M HCl with various concentrations of ionic liquids [BHEAF] at 298.15 K.....	157
Figure 5.14 Electrical Circuit Analog .....	158
Figure 5.15 Corrosion rate of carbon steel in 1 M HCl with the presence of various concentrations of ionic liquids [BHEAF] at several temperatures using weight loss method.....	161
Figure 5.16 Temperature dependence of inhibition efficiency of [BHEAF] on corrosion of carbon steel in 1 M HCl at several temperatures using weight loss method.....	162
Figure 5.17 Effect of alcohol on inhibition performance of 0.08 M of [BHEAF] on carbon steel corrosion in acidic medium. ....	163
Figure 5.18 Plots of Langmuir's isotherm adsorption of [BHEAF] at several temperatures using weight loss method.....	166
Figure 5.19 Plots of equilibrium constant of adsorption process of ionic liquids on carbon steel surface at several temperatures.....	167
Figure 5.20 Plots of standard free energy of adsorption process of ionic liquids on carbon steel surface at several temperatures.....	170
Figure 5.21 Plot of $\ln(CR/T)$ against $1/T$ for ionic liquids.....	172
Figure 5.22 Plots of enthalpy of activation for carbon steel corrosion in the presence of various concentrations of ionic liquids. ....	173
Figure 5.23 Plots of entropy of activation for carbon steel corrosion in the presence of various concentrations of ionic liquids. ....	175
Figure 5.24 Plot of $\ln(C/R)$ against $1/T$ for ionic liquids.....	177
Figure 5.25 Plots of entropy of activation for carbon steel corrosion in the presence of various concentrations of ionic liquids. ....	178

## LIST OF SYMBOLS AND ABBREVIATIONS

Symbol	Meaning	Unit
<b>Latin Symbols</b>		
$C$	Concentration	Molar
$C_{inh}$	Concentration of inhibitor	M
$C_{dl}$	Capacitance double layer	$\mu\text{F}\cdot\text{cm}^{-2}$
$CR_{corr}$	Corrosion rate	$\text{mg}\cdot\text{cm}^{-2}\cdot\text{h}^{-1}$
$CR_{corr}^{inh}$	Corrosion rate in the presence of inhibitors	$\text{mg}\cdot\text{cm}^{-2}\cdot\text{h}^{-1}$
$\Delta G_{ads}$	Standard free energy of adsorption	$\text{kJ}\cdot\text{mol}^{-1}$
$\Delta H_{act}$	Enthalpy of activation	$\text{kJ}\cdot\text{mol}^{-1}$
$\Delta n_D$	Refractive index deviation	
$\Delta S_{act}$	Entropy of activation	$\text{J}\cdot\text{K}^{-1}\cdot\text{mol}^{-1}$
$\Delta W$	Mass loss	g
$IE$	Inhibition efficiency	%
$E$	Potential of the metal	V or mV
$E_{corr}$	Corrosion potential	V or mV
$F$	Faraday Constant	$96.500\text{ C}\cdot\text{mol}^{-1}$
$f$	Frequency	Hz
$h$	Planck's constant	

$i$	Current	A or mA
$i_{corr}$	Corrosion current density	$A \cdot cm^{-2}$
$i_{ox}$	Oxidation current	A or mA
$i_{red}$	Reduction current	A or mA
$K_{ads}$	Equilibrium constant of adsorption	
$M$	Molecular weight	$g \cdot mol^{-1}$
	Molar mass	$g \cdot mol^{-1}$
$M_1$	Molecular weight of component 1	$g \cdot mol^{-1}$
$M_2$	Molecular weight of component 2	$g \cdot mol^{-1}$
$m$	Mass	g
$N_A$	Avogadro's constant	
$n$	Number of electron	
$n$	Mole	
$n_1$	Mole of component 1	
$n_2$	Mole of component 2	
$n_D$	Refractive index	
$T$	Temperature	$^{\circ}C$
	Absolute temperature	K
	Transmittance	
$t$	Time	h
$V$	Volume	$cm^3$

$V^0$	Volume ideal	$\text{cm}^3 \cdot \text{mol}^{-1}$
$V_1^0$	Volume molar of component 1	$\text{cm}^3 \cdot \text{mol}^{-1}$
$V_2^0$	Volume molar of component 2	$\text{cm}^3 \cdot \text{mol}^{-1}$
$V_m^E$	Excess molar volume	$\text{cm}^3 \cdot \text{mol}^{-1}$
$V_{m,1}$	Volume molar partial of component 1	$\text{cm}^3 \cdot \text{mol}^{-1}$
$V_{m,2}$	Volume molar partial of component 2	$\text{cm}^3 \cdot \text{mol}^{-1}$
$V_{m,1}^\infty$	Volume molar partial of component 1 at infinite dilution	$\text{cm}^3 \cdot \text{mol}^{-1}$
$V_{m,2}^\infty$	Volume molar partial of component 2 at infinite dilution	$\text{cm}^3 \cdot \text{mol}^{-1}$
$V_{\phi,1}$	Apparent molar volume of component 1	$\text{cm}^3 \cdot \text{mol}^{-1}$
$V_{\phi,2}$	Apparent molar volume of component 2	$\text{cm}^3 \cdot \text{mol}^{-1}$
$x$	Mole fraction	
$x_i$	Mole fraction of component $i$	
$x_j$	Mole fraction of component $j$	
$x_1$	Mole fraction of component 1	
$x_2$	Mole fraction of component 2	
$Z$	Atomic Weight	
$Z$	Impedance	
$Z'$	Real impedance	
$Z''$	Imaginary impedance	

## Greek Symbols

$\alpha$	Coefficient of thermal expansion	$K^{-1}$
$\beta_a$	Tafel constant for anodic	V·decade
$\beta_c$	Tafel constant for cathodic	V·decade
$\Delta\eta$	Viscosity Deviation	mPa·s
$\eta$	Viscosity	mPa·s
$\theta$	Degree of surface coverage	
$\rho$	Density	$g\cdot cm^{-3}$
$\rho_1$	Density of component 1	$g\cdot cm^{-3}$
$\rho_2$	Density of component 2	$g\cdot cm^{-3}$
$\rho_{mix}$	Density of mixture	$g\cdot cm^{-3}$

## Abbreviation      Meaning

AC	Alternating Current
[BHEAA]	Bis(2-hydroxyethyl)ammonium Acetate
[BHEAF]	Bis(2-hydroxyethyl)ammonium Formate
[BHEAL]	Bis(2-hydroxyethyl)ammonium Lactate
[BHEAP]	Bis(2-hydroxyethyl)ammonium Propionate
[BHEMA]	Bis(2-hydroxyethyl)methylammonium Acetate
[BHEMF]	Bis(2-hydroxyethyl)methylammonium Formate
[BHEML]	Bis(2-hydroxyethyl)methylammonium Lactate
[BHEMP]	Bis(2-hydroxyethyl)methylammonium Propionate



[BMIM]BF <sub>4</sub>	1-butyl-3-methylimidazolium tetrafluoroborate
[BMIM]Br	1-butyl-3-methylimidazolium bromide
[BMIM]Cl	1-butyl-3-methylimidazolium chlorides
[BMIM]HSO <sub>4</sub>	1-butyl-3-methylimidazolium hydrogen sulfate
[BMIM]PF <sub>6</sub>	1-Butyl-3-methylimidazolium
[BMIM]SCN	1-Butyl-3-methylimidazolium thiocyanate
[BMIM]Tf <sub>2</sub> N	1-Butyl-3-methylimidazolium bis[(trifluoromethyl)sulfonyl]imide
[empy][EtSO <sub>4</sub> ]	1-ethyl-3-methylpyridinium ethylsulfate
[MMIM]MeSO <sub>4</sub>	1,3-Dimethylimidazolium methylsulfate
DEA	Diethanolamine
DMSO	Dimethyl sulfoxide
EIS	Electrochemical Impedance Spectroscopy
EDL	Electrochemical Double Layer
[HEA]	2-Hydroxyethylammonium Acetate
[HEF]	2-Hydroxyethylammonium Formate
[HEL]	2-Hydroxyethylammonium Lactate
[HEP]	2-Hydroxyethylammonium Propionate
[HMIM]Tf <sub>2</sub> N	1-Hexyl-3-methylimidazolium bis[(trifluoromethyl)sulfonyl]imide
IR	Infrared
LPR	Linear Polarization Resistance
MDEA	Methyldiethanolamine
MEA	Monoethanolamine
NMR	Nuclear Magnetic Resonance

OCP	Open Circuit Potential
[OMIM]Tf <sub>2</sub> N	1-Octyl-3-methylimidazolium bis[(trifluoromethyl)sulfonyl]imide
TEA	Triethanolamine
TMS	Tetramethyl silane
[THEAA]	Tris(2-hydroxyethyl)ammonium Acetate
[THEAF]	Tris (2-hydroxyethyl)ammonium Formate
[THEAL]	Tris (2-hydroxyethyl)ammonium Lactate
[RHEAP]	Tris (2-hydroxyethyl)ammonium Propionate

# CHAPTER 1

## INTRODUCTION

### **1.1 Background**

The corrosion of metals is a common phenomenon in industry, and it has received considerable amount of attention. Corrosion is defined in different ways, but the usual interpretation of the term is “an attack on a metallic material by reaction with its environment” [1]. One of the most studied environments is acidic medium. Acidic medium is widely used in various industrial processes like pickling of metals to remove scale in metallurgical industries, deactivation of equipments in atomic power establishments, various chemical and petrochemical processes in an oil refinery, removal of scales from heat exchangers in electricity producing plants, and rocket fuel components in rocket technology [1].

There are several different approaches to reduce the effect of corrosion. These approaches can be divided into four major groups; upgrading of materials, blending of production fluids, process control, and use of corrosion inhibitor [1]. The right material selection and upgrading for the use as corrosion resistant could solve most problems encountered in any corrosive environment. Usually, the cost associated with these higher-end alloys is prohibitively expensive. The development of nonmetallic composites with corrosion resistant properties could become a potential option, but it is hard to compete against the versatility, good structural properties, and low cost of carbon steel. Blending is a process in which a production fluid with a high concentration of corrosive species is mixed with another production fluid with lower

concentration, thus reducing the overall concentration of the corrosive species to an acceptable level. Physical properties such as viscosity can also be reduced through the blending of two streams of production fluid, which leads to a lower shear stress of the production fluid and an increase in inhibitor efficiency. Process control reduces corrosion through the control of temperature and flow rates of production media. Reducing the temperature decreases the corrosion rate, but it will also increase viscosity, so the method is dependent on where in the production process it is applied. Controlling and lowering the flow rate of production media in particularly exposed areas will reduce corrosion and increase inhibition efficiency.

Among the several methods for corrosion prevention and control mentioned above, the use of corrosion inhibitors is highly popular. A corrosion inhibitor is a chemical substance that, upon small quantity addition to a corrosive environment, results in the reduction of corrosion rate to an acceptable level. Corrosion inhibitors are generally used in small concentrations. A corrosion inhibitor should not only mitigate the corrosion, but also be compatible with the environment in the sense that it should not lead to any repercussions [1].

One of the major consumers of the corrosion inhibitors is the oil industry which includes acid stimulation of oil and gas wells. The stimulation of oil and gas wells using concentrated solutions of 1 to 5 M of HCl is a common practice, performed to increase production and remove formation damage. The acid, which must be pumped through steel pumping equipment, casing, and production tubing prior to entering the formation, not only can create significant damage to those equipments, but also can damage the formation by forming corrosion by-products such as FeS and Fe(OH)<sub>3</sub>. Therefore, corrosion inhibitors are an indispensable part of the fluid mix pumped downhole when well is acidized [2, 3].

Figure 1.1 shows some chemical structure of recent discovered novel corrosion inhibitors. Organic inhibitors contain active functional groups that bond to the metal surface and protect it. Most of the efficient inhibitors are organic compounds which mainly contain oxygen, sulfur, nitrogen atoms and multiple bonds in the molecule through which they are adsorbed on metal surface [4-9].

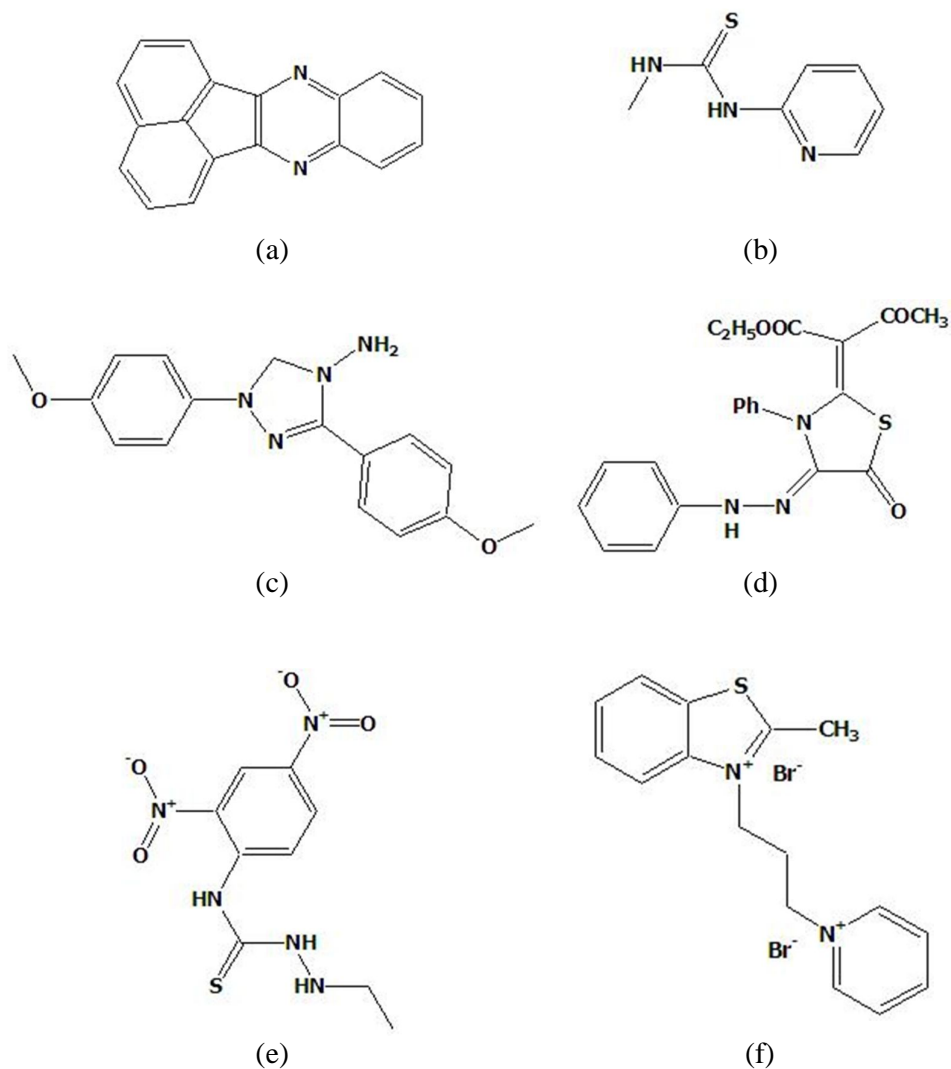


Figure 1.1 Structures of some recent discovered novel corrosion inhibitors in acidic medium. (a) Acenaphtho[1,2-b] Quinoxaline [4], (b) 1-methyl-3-pyridin-2-yl-thiourea [5], (c) 2,5-bis(4-methoxyphenyl)-4-amino-1,2,4-triazole [6], (d) 2-(acetyl-ethoxycarbonyl-methylene)-3-phenyl-4-(phenylhydrazono)-1,3-thiazolidin-5-one [7], (e) 1-ethyl-4-(2,4-dinitrophenyl)thiosemicarbazide [8], (f) 3-(3-Propylpyridinio)-2-methylbenzoathiazolium bromide [9].

Nitrogen compounds constitute the largest class of inhibitors for corrosion of steel in acidic medium. The most effective type of corrosion inhibitors for oil and gas wells stimulation is film-forming amines and its salts [3]. Long chain aliphatic amines like hexylamines, octylamines, decylamines, and dodecylamines are effective corrosion inhibitors in acidic media containing sulfuric acid or hydrochloric acid [10]. The behavior of quaternary ammonium compounds like tetraethyl ammonium chloride, tetrabutyl ammonium chloride, benzyltrimethyl ammonium chloride, benzyltriethyl ammonium chloride, benzyltributyl ammonium chloride, phenyltrimethyl ammonium chloride, alkylbenzyltrimethyl ammonium chloride, tetradecyltrimethyl ammonium bromide and cetyltrimethyl ammonium bromide was studied in 0.1 M HCl solutions [3]. It was found that inhibition efficiencies were closely related with the chain length of the alkyl group as well as the presence of benzene ring in quaternary ammonium compounds. Maximum inhibition efficiencies of cationic surfactants were observed around and above critical micelle concentration, while the inhibition efficiencies of the quaternary ammonium salts were found to increase with the increase in their concentrations [10]. Cetyltrimethyl ammonium bromide has been identified to be an effective corrosion inhibitor in both hydrochloric and sulfuric acid environments [11]. The inhibitors generally consist of a mixture of active component along with surfactant and solvent. Nitrogen compounds and acetylenic alcohols are often used together to give high levels of protection at elevated temperature and high acid concentrations [12].

As discussed above, a wide range of corrosion inhibitors formulations have been developed for carbon steel under acidic medium. However, there are some disadvantages with the current inhibitor such as difficulty in the preparation method and the high material cost. Also it has been reported that the lack of their physical properties data, has limited the design and application of these corrosion inhibitors [4-9].

### 1.1.1 Ionic Liquids Corrosion Inhibitor

Ionic liquids are generally defined as salts with a melting temperature below the boiling point of water [13]. Most of the ionic liquids are liquid at room temperature and are commonly known as room temperature ionic liquids. Ionic liquids are considered as a good substitute to those volatile organic solvents, because of its low vapor pressure and thus being environmental friendly. Furthermore, ionic liquids have many other attractive features, including chemical stability [14], high thermal stability [15-17], high ionic conductivity [18], and a wide electrochemical potential window [19]. Ionic liquids have a variety of properties that could potentially make them as ideal inhibitor for corrosion. For a start, preferred species of ionic liquids have larger liquid range from ambient temperature up to 300 °C [20]. Additionally, the preparation of ionic liquids is well known and the favorable viscosity and density characteristic of ionic liquids is likewise well-documented [21].

Recently, inhibition performance on corrosion of steel in 1 M HCl by ionic liquids, namely 1-butyl-3-methylimidazolium chlorides, [BMIM]Cl ; 1-butyl-3-methylimidazolium hydrogen sulfate, [BMIM]HSO<sub>4</sub> [22]; 1-butyl-3-methylimidazolium bromide, [BMIM]Br [23]; 1,3-Dioctadecylimidazolium bromide and *N*-Octadecylpyridinium bromide [24] has been investigated using electrochemical impedance, potentiodynamic polarization and weight loss measurements. These ionic liquids have showed good inhibition property for the corrosion of steel in 1M HCl solution and the inhibition efficiency was improved significantly with ionic liquids concentration. Figure 1.2 shows the structure of these ionic liquids corrosion inhibitors [22-24].

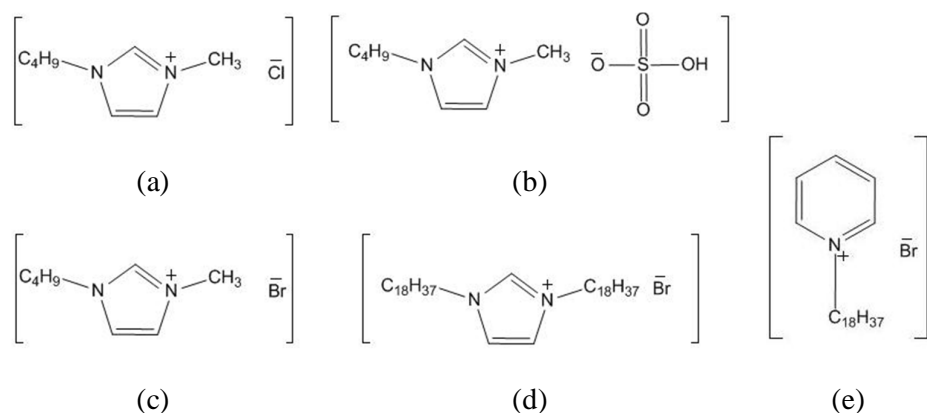


Figure 1.2 Ionic liquids inhibitors on steel corrosion in acidic medium (a) 1-butyl-3-methylimidazolium chlorides,  $[BMIM]Cl$ ; (b) 1-butyl-3-methylimidazolium hydrogen sulfate,  $[BMIM]HSO_4$  [22]; (c) 1-butyl-3-methylimidazolium bromide,  $[BMIM]Br$  [23]; (d) 1,3-Dioctadecylimidazolium bromide,  $[C_{18}C_{18}IM]Br$ ; (e) *N*-Octadecylpyridinium bromide,  $[C_{18}Py]Br$  [24].

## 1.2 Problem Statement

For industrial implementation, the physical properties of corrosion inhibitor must be known [25]. A screening of some properties such as density and viscosity of corrosion inhibitor must be examined and reported together with their efficiency of inhibition. However, most of the published reports on corrosion inhibitor lack these physical properties data [4-9].

Even though ionic liquids have been proven as a potential inhibitor on corrosion of mild steel in acidic medium, there are several considerations when choosing an inhibitor, namely: (i) cost of the inhibitors which can sometime be very high when the material involved is expensive or when the amount needed is huge and (ii) availability of the inhibitor which will determine the selection of it and if the availability is low, the inhibitor becomes often expensive. As can be seen from Table 1.1, it is obvious that 1-methylimidazole, a precursor for the manufacturing of imidazolium based ionic liquids, is considerably more expensive than the precursor for hydroxyl ammonium ionic liquids.



Table 1.1 Price comparison of some precursor of imidazolium-based and hydroxyl ammonium ionic liquids

Chemical	Package	Price (RM)*
<b>Precursor of Hydroxyl Ammonium Ionic Liquids</b>		
Monoethanolamine (reagentPlus <sup>®</sup> , ≥99%)	1 L	290.01
Diethanolamine (99%)	1 L	108.00
<i>N</i> -methyldiethanolamine (>99%)	1 L	134.91
Triethanolamine (>99%)	1 L	292.50
Formic acid (reagent grade, ≥99%)	1 L	498.51
Acetic acid (reagentPlus <sup>®</sup> , ≥99%)	1 L	258.51
Propionic acid (reagent grade, ≥99%)	1 L	164.00
Lactic acid (reagent grade, ≥99%)	1 L	125.03
<b>Precursor of Imidazolium-based Ionic Liquids</b>		
1-methylimidazole (99.9 %, Aldrich)	1 L	1596.52
<i>n</i> -butyl chloride (Anhydrous, 99.5 %, Aldrich)	1 L	560.01
<i>n</i> -butyl bromide (Anhydrous, 99.5 %, Aldrich)	1 kg	425.50
<b>Ionic Liquids</b>		
[BMIM]Cl (dry, ≥ 99.0 %, Fluka)	5 g	498.51
	25 g	1720.02
[BMIM]Br (≥ 98.5 %, Fluka)	5 g	512.51
	25 g	2142.53
Hydroxyl ammonium ionic liquids	NA	NA

\* Source: [www.sigmaaldrich.com](http://www.sigmaaldrich.com) (Date of access: 15 July 2011)

By the time this compound is processed to the final ionic liquid product, its cost will have increased to many times than of the commercial acid inhibitor. This is not helped by the fact that at present there is a very limited market for these compounds, keeping retail prices high. It is envisaged that if ionic liquid does become widely accepted, then the cost of production will decrease rapidly. An alternative way is to find cheaper ionic liquids corrosion inhibitor. Hydroxyl ammonium ionic liquids could potentially be the alternatives.

Hydroxyl ammonium ionic liquids are a new class of ionic liquids [26-33]. The first report on synthesis of hydroxyl ammonium ionic liquids was in 2008 [29]. It was prepared through direct protonation of alkanolamine using organic acid. Hydroxyl ammonium ionic liquids have been studied as potential solvent for CO<sub>2</sub> absorption [30, 31], removal of SO<sub>2</sub> from natural gas [32], and their application in electrochemical field [33]. However, no substantial information was available on using hydroxyl ammonium ionic liquids as inhibitors on carbon steel corrosion in acidic medium. Thus, the project is executed to study the inhibition effect of hydroxyl ammonium ionic liquids on carbon steel corrosion in hydrochloric acid.

In practical condition, corrosion inhibitors are mixture of active components, solvents, and surfactant [1, 25]. The corrosion inhibitor is used as its mixture with co-solvent and surfactant. In acid stimulation of oil and gas wells, before the acid is injected, it is mixed with the inhibitors solution [1]. Therefore, the corrosion inhibitor shall compatible with the co-solvent and surfactant used. Among some co-solvent used in the inhibitor solution, alcohol is widely used due to its stability and non-reactive against most of corrosion inhibitor [1, 25]. The physical properties of inhibitor solution, as well as its pure active components, shall be measured for the new corrosion inhibitor. In this work, the physical properties of hydroxyl ammonium ionic liquids as new corrosion inhibitor are measured. In addition, the effect of methanol, ethanol, and 1-propanol on physical properties of ionic liquids is also reported.

Another important parameter to design ionic liquids as corrosion inhibitor is their inhibition mechanism. Organic corrosion inhibitors, as well as imidazolium ionic liquids corrosion inhibitor, inhibit the corrosion of through adsorption of themselves onto surface of carbon steel [22-24]. Their adsorption is affected by concentration used and temperature. Therefore, the inhibition mechanism of the hydroxyl ammonium ionic liquids in acidic media is proposed.

### **1.3 Research Objectives and Scope of Study**

The objectives of this research are to synthesis and characterize hydroxyl ammonium ionic liquids, and to study the potential application of these ionic liquids as inhibitor on carbon steel corrosion in acidic medium. The objectives and scope of research approaches will be discussed in the following:

#### **1. Synthesis and Characterization of Hydroxyl Ammonium Ionic Liquids**

For this study, sixteen hydroxyl ammonium ionic liquids are synthesized and characterized. Alkanolamines such as monoethanolamine (MEA), diethanolamine (DEA), methyldiethanolamine (MDEA), and triethanolamine (TEA) are used as cation sources while organic acids such as acetic, formic, lactic, and propionic acid are used as anion sources. The synthesis is carried out by direct protonation of alkanolamines with acid. The characterizations of synthesized ionic liquids are carried out using spectroscopies  $^1\text{H-NMR}$ ,  $^{13}\text{C-NMR}$ , Infrared, Elemental Analysis, and water content. Spectroscopies NMR and infrared are used to study structure of all ionic liquids synthesized in the present work. Elemental analysis is used to determine the Carbon, Hydrogen, and Oxygen composition of ionic liquids, while measurement of water content is used to determine the water content and purity of synthesized ionic liquids.

## 2. Measurement of Physical Properties of Synthesized Ionic Liquids

In the present work, density, viscosity, and refractive index of the ionic liquids bis(2-hydroxyethyl)ammonium formate, [BHEAF], and its binary mixture with alcohol C<sub>1</sub>-C<sub>3</sub> are measured under atmospheric pressure within a whole composition range and at different temperature. Ionic liquids [BHEAF] is chosen as model for ionic liquids in binary mixture with solvent because it demonstrates the highest efficiency of inhibition compare to other studied ionic liquids in this research.

## 3. Measurement of Inhibition Efficiency of The Synthesized Ionic Liquids on Carbon Steel Corrosion in Acidic Medium

In this research, the inhibition efficiency is measured using two methods, namely, weight loss and electrochemical, within different concentrations of ionic liquids and at different temperatures. The concentration of ionic liquids is ranged from 0.02 to 0.08 M while temperature is ranged from (298.15 – 343.15) K. The inhibition efficiencies are discussed by looking at the effect of cation and anion of ionic liquids, concentration of ionic liquids, and temperature of solution. The present study is also devoted to understanding the process of corrosion inhibition by proposing inhibition mechanism of hydroxyl ammonium ionic liquids for carbon steel corrosion under acidic media.

### 1.4 Thesis Layout

Chapter 1 provides the reader with background knowledge of corrosion inhibitor and describes the motivation behind using ionic liquids as inhibitor on corrosion of carbon steel in acidic medium. The objective and scope of research is also provided.

Chapter 2 presents a detailed review of literature to support the present work. This chapter is divided into three sub chapters. The first sub chapter summarizes review of literature related to synthesis and characterization of ionic liquids. In the second sub chapter, a description on various techniques typically used in literature to measure physical properties of pure ionic liquids and binary mixture containing ionic liquids is

discussed. A current research on using ionic liquids as inhibitors on steel corrosion in acidic medium is presented in third subchapter.

Chapter 3 presents research methodology used in the present work. The list of chemicals and apparatus used in this study to synthesis and characterize ionic liquids are also given along with the detail experimental procedures. It also highlights the experimental procedures, methodology, and basis for calculating inhibition efficiency of ionic liquids on carbon steel corrosion in acidic medium.

Chapter 4 presents experimental results on synthesis and physical properties of ionic liquids. This chapter is divided into three subchapters. In the first subchapter, the analysis for synthesis and characterization of ionic liquids studied, include the spectrum  $^1\text{H-NMR}$  and  $^{13}\text{C-NMR}$ , Infrared, elemental analysis, and water content of the synthesized ionic liquids is presented. The spectroscopies methods, namely NMR and FTIR are used to analyze structure of synthesized Ionic liquids, while elemental analysis and measurement of water content are used to analyze the composition and purity of the synthesized ionic liquids, respectively. The second subchapter presents the results on measurement of physical property such as density, viscosity, and refractive index of ionic liquids. The temperature dependence of physical properties of ionic liquids is correlated using semi empirical equation. The third subchapter presents the effect of alcohol on properties of ionic liquids [BHEAF]. The excess thermodynamic properties are calculated to understand the interaction of ionic liquids and alcohol.

Chapter 5 focuses on the application of the ionic liquids as inhibitor on corrosion of carbon steel in acidic medium. The results are discussed using analysis of weight lost, potentiodynamic, and electrochemical impedance spectroscopy. The performance of corrosion inhibition of the ionic liquids are discussed in reference to the effect of cation and anion of ionic liquids, concentration of ionic liquids, effect of cosolvent and temperature. The mechanism of inhibition and its thermodynamic aspect are analyzed based on the adsorption phenomena.

Chapter 6 presents the conclusions of the present research work and few recommendations for future work.



## CHAPTER 2

### LITERATURE REVIEW

#### 2.1 Ionic Liquids

Ionic liquids are generally defined as salts with a melting temperature below the boiling point of water [13]. Most of the ionic liquids are liquid at room temperature and are commonly known as room temperature Ionic liquids (RTIL). Ionic liquids are considered as a good substitute to the volatile organic solvents, because of its low vapor pressure [14] and thus being environmental friendly. Furthermore, ionic liquids have many other attractive features, including chemical stability [14], high thermal stability [15-17], high ionic conductivity [18] and a wide electrochemical potential window [19].

Ionic liquids usually consist of nitrogen-containing organic cation combined with inorganic or organic anions. Figure 2.1 shows the common cation and anion for ionic liquids. Common cation for ionic liquids includes dialkylimidazolium, alkylpyridinium, tetraalkylammonium, and tetraalkylphosphonium. The R group usually represents alkyl chain, but the other functional groups such as aralkyl, amine and hydroxyl can also present. Common anion includes chloride ( $\text{Cl}^-$ ), bromide ( $\text{Br}^-$ ), hexafluorophosphate ( $\text{PF}_6^-$ ), tetrafluoroborate ( $\text{BF}_4^-$ ), nitrate ( $\text{NO}_3^-$ ), acetate ( $\text{CH}_3\text{COO}^-$ ), and bis(trifluoromethylsulfonyl)imide ( $(\text{CF}_3\text{SO}_2)_2\text{N}^-$ ).

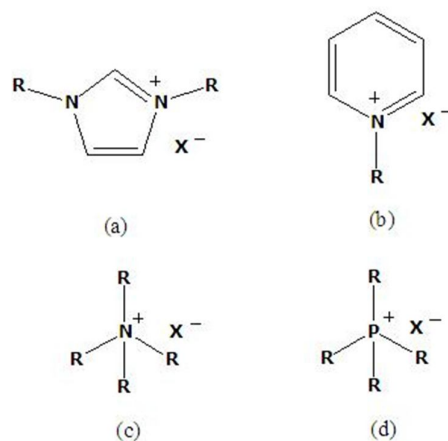


Figure 2.1 Structure of common cations and anions used for ionic liquids (a) dialkylimidazolium (b) alkylpyridinium (c) tetraalkyl ammonium (d) tetraalkylphosphonium. R is representing alkyl etc. and  $X^-$  could be Cl, Br,  $PF_6^-$ ,  $BF_4^-$ ,  $NO_3^-$ ,  $CH_3COO^-$ ,  $SO_4^{2-}$ , and  $(CF_3SO_2)_2N^-$ .

Ionic liquids have attracted rising interest in the last decades with a diversified range of applications. The types of ionic liquid available have also been extended to include new families and generations of ionic liquids with more specific and targeted properties. This expanding interest has led to a number of reviews on their physico-chemical properties, the design of new families of ionic liquids, the chemical engineering, and the wide range of arrangements in which ionic liquids have been utilized and piloted for industrial developments [34, 35].

### 1. Ionic liquids as alternatives to organic solvents

Ionic liquids are beginning to be used as alternatives to organic solvents. Wide ranges of ionic liquids have been used as solvent and catalyst for a number of different organic reactions. The use of Ionic liquids in organic synthesis typically involved many ionic liquids to achieve the desired activity such as alkylation of benzene [36-39], alkylation of naphthalene [40, 41], Friedel-Crafts acylation of aromatics [42-45], hydroformylation with carbon dioxide [46, 47], organocatalysis [48], hydrogenation [49], and esterification [50-55].



## 2. Ionic liquid in catalysis

Soluble ionic liquids have recently been used as supports for catalyst/reagent immobilization and synthesis in homogeneous solution phase. The wide range of ionic liquid supports available makes their use as supports compatible with most common chemistries [56-64]. The solubility properties of these ionic-liquids can be tuned by the variation made in the cations and anions used to make their phase separation possible from less polar organic solvents and aqueous media. The ionic-liquid-supported species can therefore be purified from the reaction mixture by simple washings. Ionic-liquid-supported catalysts and reagents have been prepared and used, and they are easily recovered and reused [65].

## 3. Ionic liquids in separation

The unique properties of modern imidazolium-based ionic liquids such as high viscosity, broad liquid range, high thermostability, low volatility, good wetting ability for fused silica capillary, and the possibility of multiple interactions with a variety of solutes make them suitable to be used as gas chromatography stationary phases coated on fused silica capillary columns [66-68]. Ionic liquids also have potential application as selective additives in extractive distillation. Adding ionic liquids to an azeotropic mixture has been shown to break the azeotrope and increase relative volatility of the mixture allowing for an easier separation [69-71]. Ionic liquids 1,3-Dimethylimidazolium methylsulfate [MMIM]MeSO<sub>4</sub> is suitable for use as solvent in the petrochemical extraction process for the removal of ethanol from its mixture with hexane [72].

## 4. Ionic liquids in electrochemical devices and processing

Many ionic liquids offer a range of properties that make them attractive to the field of electrochemistry [73]. A variety of electrochemical devices including solar cells [74, 75], high energy density batteries [76-78], fuel cells [79, 80], and super capacitors [81, 82] have become of immense interest as part of the various solutions proposed to continue sustaining the energy supply for current and future generation.

## 5. Gas solubility in ionic liquids

Study on gas solubility in ionic liquids have been conducted extensively [20, 30, 31, 83-90]. As ionic liquids are non-volatile, they could be easily separated and would not pose any contamination to a gas stream. This feature gives ionic liquids an advantage over traditional solvents used for absorbing gases [20].

## 6. Ionic liquids as corrosion inhibitor

Despite the rapid increasing number of papers describing the applications of ionic liquids, there are relatively few papers reported on using ionic liquids as inhibitor on corrosion of carbon steel in acidic medium [22-24]. Application of ionic liquids as corrosion inhibitor is given in section 2.3.1.1. To expand our knowledge in ionic liquids as corrosion inhibitor, it is thought worthwhile to study the corrosion inhibition behavior of hydroxyl ammonium ionic liquids on carbon steel corrosion in hydrochloric acid.

### 2.1.1 Synthesis of Ionic Liquids

The increasing interest in ionic liquids, especially in the light of their recent widespread commercial availability, has resulted in further developments in their synthesis and purification [13]. A subset of ionic liquids are protic ionic liquids, which are easily produced through the combination of a Brønsted acid and Brønsted base. In fact, the story of ionic liquids is generally regarded as beginning with the first report on the preparation of protic ionic liquids ethylammonium nitrate in 1914 [91]. The same method has been applied to prepare other protic ionic liquids [29, 92-95].

The synthesis of ionic liquids can be divided into two steps: (i) formation of the desired cation, and (ii) anion exchange to form the desired product. In some cases only the first step is required, as with the formation of ethylammonium nitrate. In other case, where the desired anion could not be formed directly from the first step, the second step is needed which involves anion exchange. Figure 2.2 illustrates the general formation of ionic liquids. Example of these is 1-butyl-3-methylimidazolium

chloride, [BMIM]Cl. The ionic liquid is formed through the first step only which the product can be used to form 1-butyl-3-methylimidazolium tetrafluoroborate [BMIM]BF<sub>4</sub>, using the second step involving anion exchange.

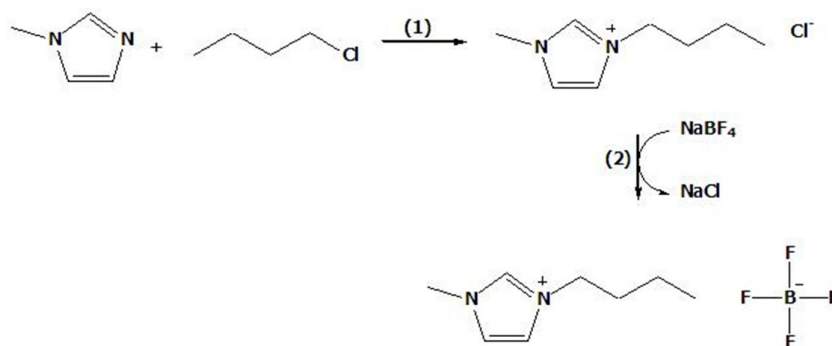


Figure 2.2 General method to synthesis ionic liquids. (1) Quaternization of the cation by alkylation using alkyl halide (2) anion metathesis to form desired anion.

The following section focuses on the preparation of the protic ionic liquids, as the hydroxyl ammonium ionic liquids falls into this category. Protic ionic liquids stand out from other ionic liquids and many other solvents, because of its water like properties in that it can form a three-dimensional hydrogen bonded network and has an equal number of hydrogen donor and acceptor sites [27].

#### 2.1.1.1 Synthesis of Protic Ionic Liquids

Protic ionic liquids are formed through the transfer of a proton from a Brønsted acid to Brønsted base. This leads to its distinguish features from the other ionic liquids, *i.e.*, it has a proton available for hydrogen bonding. The protonation process to form desired protic ionic liquids possesses the advantages which among others are: (i) a wide range of cheap cation sources such as ammonium, and (ii) the protonation reactions generally spontaneous at room temperature. The most common method for the formation of such ionic liquids is simple mixing of the Brønsted acid to Brønsted

base. The reaction is generally quite exothermic, which means that care should be taken when adding the reagents together. Although the products are relatively thermally stable, the build-up of excess local heat can result in decomposition and discoloration of the ionic liquid. This may be prevented either by cooling the mixing vessel or by adding one component to the other in small portions to allow the heat to dissipate naturally [96].

Figure 2.3 presents the schematic formation of protic ionic liquids through proton transfer. The protonation reaction such as used in the formation of ionic liquids ethylammonium nitrate, involves the addition of 3 M nitric acid to a cooled aqueous solution of ethylamine [91]. A slight excess of amine should be left, which is removed along with the water by heating to 60 °C *in vacuo*. The same general process are employed for the preparation of other protic ionic liquids of this type [29, 96-98].

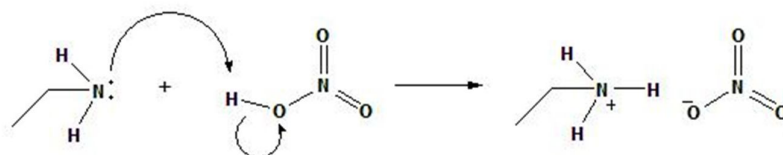


Figure 2.3 Schematic formation of the protic ionic liquids ethylammonium nitrate through proton transfer [91].

The most common cations used in protic ionic liquids are represented in Figure 2.4, including primary, secondary, or tertiary ammonium ions, mono- or di-imidazolium ions, caprolactam, and guanidinium. A large variety of anions have been coupled with these cations, with commonly used ones shown in Figure 2.5. Most of the anion used in protic ionic liquids are alkanoate such as formate, acetate, and lactate; inorganic such as nitrate or hydrogen sulfate; and fluorinated such as bis(trifluoromethanesulfonyl)imide (TFSI), trifluoroacetic acid (TFA), and bis(perfluoroethylsulfonyl)imide (BETI), tetrafluoroborate, or hexafluorophosphate ions [27].

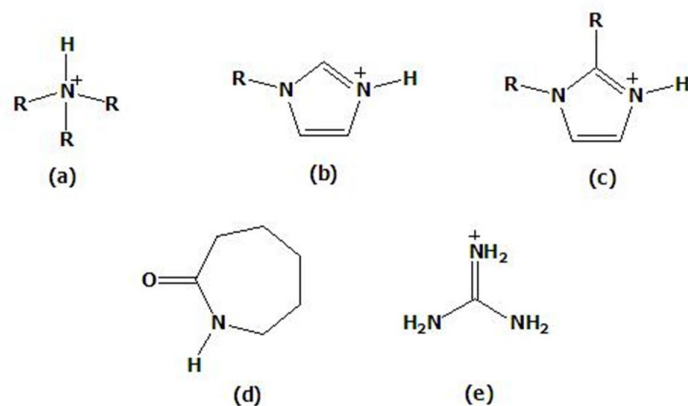


Figure 2.4 Structure of common cations used in protic ionic liquids. (a) primary, secondary, or tertiary ammonium cations, (b) 1-alkylimidazolium cations, (c) 1-alkyl-2-alkylimidazolium cations, (d) caprolactam, and (e) 1,1,3,3-tetramethylguanidine.

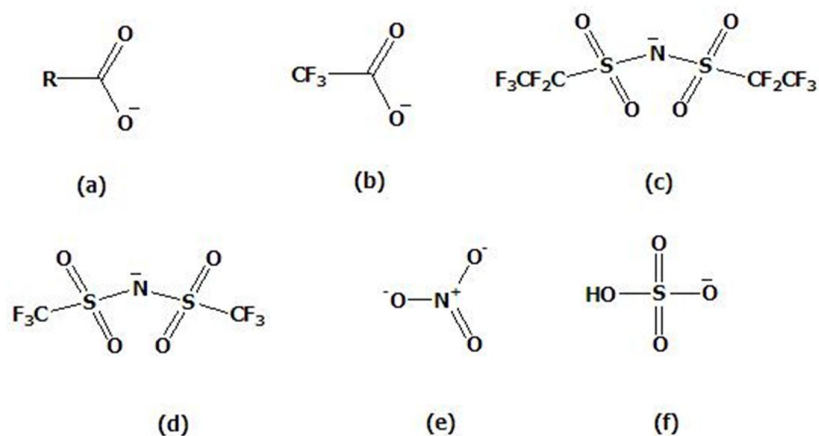


Figure 2.5 Structure of common anions used in protic ionic liquids. (a) carboxylates, (b) trifluoroacetate, (c) bis(perfluoroethylsulfonyl)imide, (d) bis(trifluoromethane sulfonyl)imide, (e) nitrate, and (f) hydrogen sulfate.

### 2.1.2 Purification of Ionic Liquids

The extremely low vapor pressure of the ionic liquids prevents its purification by distillation. The counterpoint to this is that any volatile impurity can, in principle, be separated from an ionic liquid by distillation. In general, it is better to remove as many impurities as possible from the starting materials and, where possible, to use synthetic methods that either generate as few side products as possible, or allow their easy separation from the final ionic liquid product [13].

The presence of impurities in an ionic liquid may have different origins. It may result from solvents used during formation of desired cation on their synthesis, from unreacted starting materials of the protonation reaction or from any volatile organic compound previously dissolved in the ionic liquid. In theory, volatile impurities can be easily removed from the non-volatile ionic liquid by simple evaporation. However, sometimes this process can take a considerable time. Factors that influence the time required for the removal of all volatiles from an ionic liquid (under a given temperature and pressure) are the following: (i) the amount of volatiles; (ii) their boiling points; (iii) the viscosity of the ionic liquid, (iv) the surface of the ionic liquid and – probably most important – (v) their interactions with the ionic liquid [13].

The removal of starting materials is generally achieved easily by heating the ionic liquid under vacuum. Water is generally one of the most problematic to component to be removed, and it is generally recommended that ionic liquids are heated to at least 70 °C for several hours with stirring to achieve an acceptably low degree of water contamination. Thus it is advised that all liquids are dried directly before use. If the amount of water present is of importance, this may be determined using Karl–Fischer titration. The presence of water in an ionic liquid may be a problem for some applications. In all cases one should know the approximate amount of water in the ionic liquid used. Depending on the application, one should be aware of the fact that water in the ionic liquid may not be inert. Moreover, the presence of water can have significant influence on the physicochemical properties of the ionic liquids. Therefore, it is very important to measure the water content of ionic liquids.

## 2.2 Physical Properties of Ionic Liquids

Inhibitor selection begins with the choice of physical properties [1] such as melting and freezing point, degradation, and compatibility with the co-solvent. This list can be extensive, but is important because it defines the domain of possible inhibitors. It must be the first step of the inhibitor evaluation for any new system. These physical measurements are those routinely done as part of minimal quality acceptance testing. Therefore, it is important to measure the physical properties of hydroxyl ammonium ionic liquids as new corrosion inhibitor.

In addition to measurement of physical properties of new corrosion inhibitor, it is also expected to check the compatibility with co-solvent and their physical properties [1, 25]. In practical condition, corrosion inhibitors are mixture of active components, solvents, and surfactant [1]. The corrosion inhibitor is used as its mixture with co-solvent and surfactant. Therefore, the corrosion inhibitor shall compatible with the co-solvent and surfactant used. Among some co-solvent used in the inhibitor solution, alcohol is widely used due to its stability and non-reactive against most of corrosion inhibitor [1]. Thus, the physical properties of inhibitor solution, as well as its pure active components, shall be measured for the new corrosion inhibitor.

Measurement of physical properties such as density, viscosity, and refractive index of ionic liquids and its binary mixture with solvent has a large range of uses in the study of the thermodynamic properties of ionic liquids. The change in density, viscosity, and refractive index upon mixing two miscible liquids tells much about the solvent-solute interactions that have occurred. Relative changes in density, viscosity, and refractive index as a function of temperature and concentration related to the free energy of solute-solvent system and are thus important in the study of thermodynamic. Physical properties of various liquids with different ionic liquids are becoming more widely available in the literature. Binary mixture containing ionic liquids with alcohol [106, 107], alkenes [108], aromatic [109], water [100], and other organic solvent [110, 111] have been reported.

### 2.2.1 Density

Solvent density,  $\rho$ , is an important physical property. This is a particularly used in preparation of specific concentration of ionic liquids in the inhibitor solution. The most direct way of determining density is by combining measurements of the mass of a substance with measurement of its volume. Apparatus based on this method are weighed syringes, pycnometers, and vibrating-tube densimeter [112].

Initial research on the properties of pure ionic liquids concentrated on developing and understanding the relationship between the nature and structure of the cation and anion and the changes in the physical properties [99]. The purity of an ionic liquid is a very important issue when measuring physical properties. Physical properties of pure ionic liquids such as density, viscosity, and refractive index are increasingly published in the literature [21]. Considerable amounts of data on the density of ionic liquids are available in the literature. Ionic liquids are generally denser than either organic solvents or water, with typical density values ranging from 1 to 1.6 g·cm<sup>-3</sup> [100-102].

Given that many of the ionic liquids have a heavy anion it would be expected that their density would be relatively high when compared to organic solvents. Table 2.1 presents density data for ionic liquids and organic solvents at room temperature. As can be seen from Table 2.1, the densities of ionic liquids are higher compared to organic solvent. It also can be seen from Table 2.1, as the alkyl chain length on the imidazolium cation increases from C<sub>4</sub> to C<sub>8</sub>, the density of the corresponding ionic liquids decreases. It has been speculated that the addition of alkyl group to the imidazolium ring results in a reduction of the density for the imidazolium ionic liquids [113]. One possible explanation for this discrepancy is that the densities of ionic liquids are governed by van der Waals forces as well as electrostatic interactions. [113]. The addition of two CH<sub>2</sub> groups to the cation increases the size of the ion, thereby decreasing the electrostatic attraction between the cation and anion. The additional CH<sub>2</sub> groups will also increase the dielectric shielding of the charges. These combined effects will cause density to decrease more rapidly [113].



A literature survey reveals that considerable amounts of data on the density of ionic liquids are available in the literature. The most commonly studied ionic liquids contain an imidazolium cation with varying heteroatom functionality [100-102, 110, 113-121]. However, these data are not available for various types of protic ionic liquids.

Table 2.1 Density for some alcohols and ionic liquids at  $T = 298.15$  K.

Chemicals	$\rho/\text{g}\cdot\text{cm}^{-3}$
Methanol	0.78664 [122], 0.78664 [123]
Ethanol	0.78517 [122], 0.78522 [123], 0.7855 [124], 0.7890 [125]
1-Propanol	0.79952 [122], 0.79940 [123], 0.7996 [124], 0.8036 [125]
[BMIM]BF <sub>4</sub>	1.213 [126], 1.12 [127], 1.208 [128], 1.20 [129]
[BMIM]PF <sub>6</sub>	1.35 [127], 1.373 [128], 1.37 [130], 1.3603 [131], 1.369 [132], 1.32 [133]
[BMIM]Tf <sub>2</sub> N	1.4054 [15], 1.429 [128], 1.51 [129]
[HMIM]Tf <sub>2</sub> N	1.37101 [113], 1.37213 [134], 1.37081 [135]
[OMIM]Tf <sub>2</sub> N	1.31891 [113], 1.317 [132], 1.32076 [136, 137]

### 2.2.1.1 Effect of Temperature on Density of Ionic Liquids

The change of density with temperature can be correlated by the method of least square using the following equation,

$$\rho = a_0T^0 + a_1T + a_2T^2 + \dots + a_nT^n \quad (2.1)$$

where  $a$  is fitting parameter,  $n$  is the number of polynomial degree, and  $T$  is absolute temperature.

Figure 2.6 shows the effect of temperature on density of two ionic liquids 1-Butyl-3-methylimidazolium thiocyanate, [BMIM]SCN [122]; and 1-methyl-1-methylimidazolium methylsulfate, [MMIM]MeSO<sub>4</sub> [138]. The density of these two ionic liquids was found to decrease with increasing temperature.

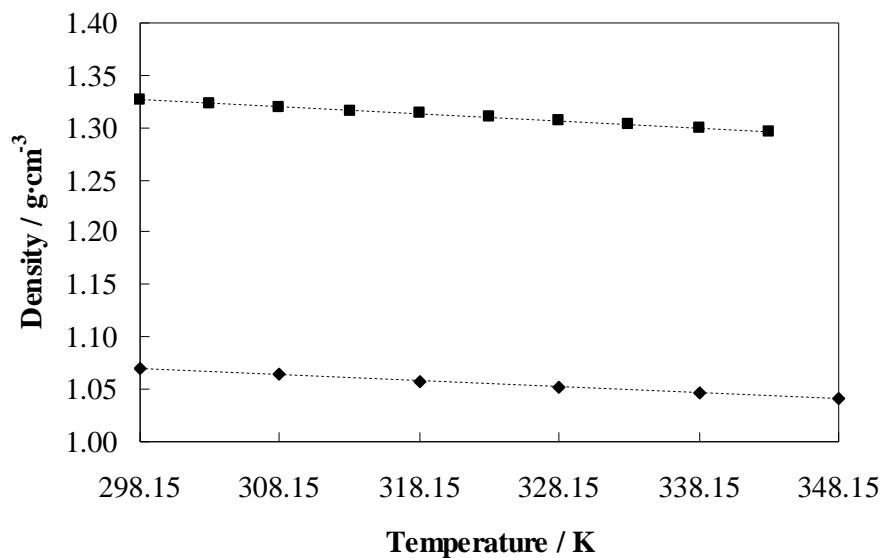


Figure 2.6 Effect of temperature on density of the ionic liquids. Symbols;  $\blacklozenge$ , [BMIM]SCN [122];  $\blacksquare$ , [MMIM]MeSO<sub>4</sub> [138], and (-) Calculated using equation (2.1).

For these ionic liquids, temperature dependence of density can be expressed as,

$$\rho/\text{g}\cdot\text{cm}^{-3} [\text{MMIM}]\text{MeSO}_4 = 1.53839 - (7.08 \times 10^{-4}) T \quad (2.1a)$$

$$\rho/\text{g}\cdot\text{cm}^{-3} [\text{BMIM}]\text{SCN} = 1.26184 - (7.08 \times 10^{-4}) T + (.175 \times 10^{-7}) T^2 \quad (2.1b)$$

### 2.2.1.2 Coefficient of Thermal Expansion

The density-temperature dependence leads to another thermodynamic property, a coefficient of thermal expansion [112]. Coefficient of thermal expansion is the tendency of matter to change in volume in response to a change in temperature. When a substance is heated, its particles begin moving and become active thus maintaining a greater average separation. Coefficient of thermal expansion  $\alpha$  can be defined as,

$$\alpha = \frac{1}{V} \left( \frac{\delta V}{\delta T} \right)_p = -\frac{1}{\rho} \left( \frac{\delta \rho}{\delta T} \right)_p \quad (2.2)$$

under condition of constant pressure. Thus  $\alpha$  can be used to estimate the relative change in volume of liquid for a 1 K increase in temperature. For the ionic liquids [BMIM]SCN and [MMIM]MeSO<sub>4</sub>,  $\alpha = 4 \times 10^{-4}$  and  $5 \times 10^{-4} \text{ K}^{-1}$  at 298.15 K, respectively [122, 138].

### 2.2.2 Viscosity

Viscosity is an important transport property of matter, expressing its resistance to irreversible deformation. More specifically, this property reflects the extent to which relative motion of adjacent liquid layers is retarded and it can be generally regarded as a measure of internal friction of the liquid [112]. From the engineering aspect, the viscosity of ionic liquids can affect transport properties such as diffusion and may be an issue in practical industrial applications [103-105]. It plays a major role in stirring, mixing and pumping operations. The viscosity of many ionic liquids is relatively high compared to conventional solvents, one to three orders of magnitude higher.

Experimentally determined viscosities are generally reported as either absolute viscosity  $\eta$  or kinematics viscosity  $\nu$ . The relationship between absolute viscosity  $\eta$ , density  $\rho$ , and kinematics viscosity  $\nu$  is given by,

$$\eta / \rho = \nu \quad (2.3)$$

The unit of absolute viscosity is the Poise ( $\text{P/g}\cdot\text{cm}^{-1}\text{s}^{-1}$ ) while the unit for kinematics viscosity is the Stoke ( $\text{St/cm}^2\text{s}^{-1}$ ). Several techniques to determine viscosity of liquid based on this method are (1) poiseuille-type viscometers, (2) coutte-type rotational viscometers, (3) Stokesian and falling body viscometers, and (4) dynamic viscometers.

Ionic liquids are more viscous than most common molecular solvent. Table 2.2 presents viscosities of some selected ionic liquids. As can be seen in Table 2.2, within a series of imidazolium ionic liquids containing the same cation, changing the anion clearly impact the viscosity. This trend does not exactly correlate with anion size. This may be due to importance of the effect of other anion properties on the viscosity, such as their ability to form hydrogen bonding with the cation. The viscosity of ionic liquids is also affected by identity of the cation. For ionic liquids with the same anion the trend is larger alkyl substituent on cation lead to more viscous ionic liquids.

Table 2.2 Viscosity of some organic solvents and ionic liquids at  $T = 298.15 \text{ K}$

Chemicals	$\eta/\text{mPa}\cdot\text{s}$
Methanol	0.543 [123], 0.577 [122],
Ethanol	1.085 [123], 1.09 [122], 1.082 [124], 1.0569 [125]
1-Propanol	1.951 [123], 1.94 [122], 2.017 [124], 2.1178 [125]
[BMIM]BF <sub>4</sub>	75 [130], 219 [42, 84, 84], 180 [29, 15], 119.78 [19], 233 [12]
[BMIM]PF <sub>6</sub>	182 [130], 397 [83, 84], 450 [83], 312 [42]
[BMIM]Tf <sub>2</sub> N	87 [130]
[HMIM]Tf <sub>2</sub> N	68 [134]
[OMIM]Tf <sub>2</sub> N	96 [139]

### 2.2.2.1 Effect of Temperature on Viscosity

The viscosity of the ionic liquids is also affected by temperature. Figure 2.7 shows the viscosity changes of the ionic liquids [BMIM]SCN and 1-butyl-1-methylpyrrolidinium bis(trifluorosulfonyl)imide, [BMPyr]NTf<sub>2</sub>, against temperature. It was found that viscosity decreases with increasing temperature, in an exponential rather than linear fashion [122, 140].

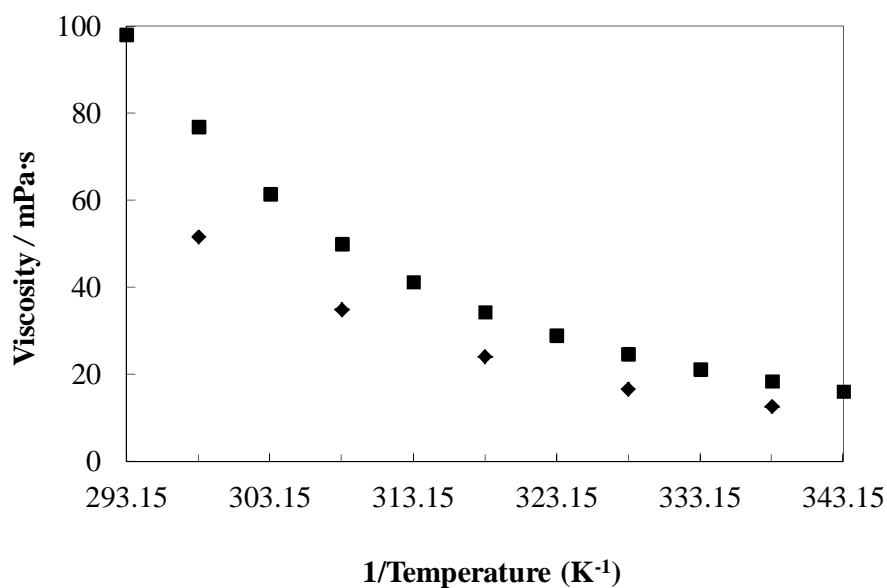


Figure 2.7 Effect of temperature on viscosity of the ionic liquids. Symbols; ♦, [BMIM]SCN [122]; ■, [BMPyr]NTf<sub>2</sub> [140].

The change of viscosity with temperature can be correlated using the method of least square using the following equation,

$$\log \eta = \frac{b_0}{T^0} + \frac{b_1}{T^1} + \dots + \frac{b_n}{T^n} \quad (2.4)$$

where  $b$  is fitting parameter,  $n$  is the number of polynomial degree, and  $T$  is absolute temperature. For ionic liquids [BMIM]SCN and [BMPyr]NTf<sub>2</sub>, the temperature dependence of viscosity can be expressed as,

$$\log \eta/\text{mPa}\cdot\text{s} [\text{BMIM}]\text{SCN} = -3.6364 + \frac{1595.69}{T} \quad (2.4a)$$

$$\log \eta/\text{mPa}\cdot\text{s}[\text{BMPyr}]\text{NTf}_2 = -3.983 - \frac{1837.1}{T} + \frac{539167}{T^2} \quad (2.4b)$$

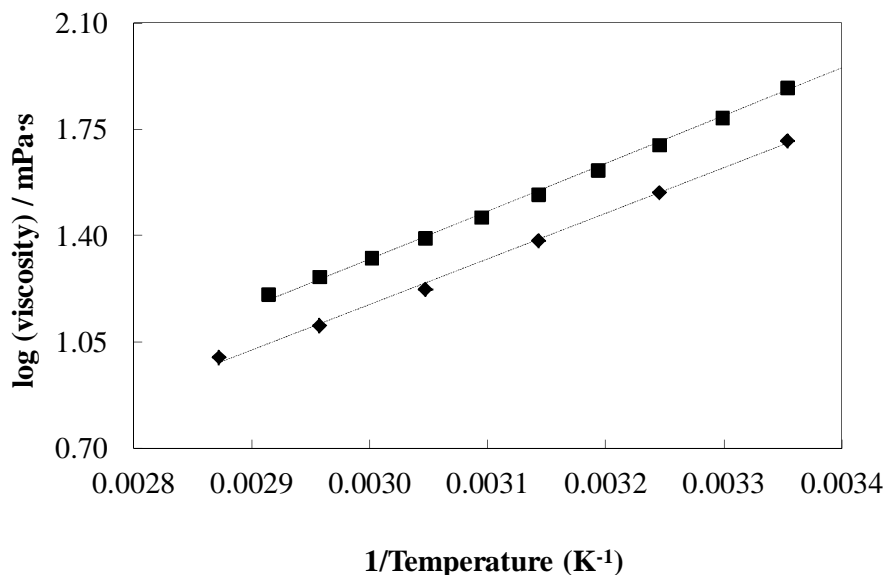


Figure 2.8 Experimental and predicted viscosity for ionic liquids. Symbols; [BMIM]SCN [122]; ■, [BMPyr]NTf<sub>2</sub> [140], (--) Calculated using equation (2.4).

### 2.2.3 Refractive Index

Refractive index,  $n_D$ , is a fundamental physical property of a substance. It is often used to identify a particular substance, confirm its purity, or measure its concentration in mixture [129]. Table 2.3 presents the refractive index of some organic solvent and ionic liquids. As can be seen from Table 2.3, refractive indexes of ionic liquids are higher than common organic solvents. It can be used to identify the presence of ionic liquids in its binary mixture with organic solvents.

Table 2.3 Refractive index of some organic solvents and ionic liquids at temperature 298.15 K

Chemicals	$n_D$
Methanol	1.3269 [104], 1.32687 [123], 1.32687 [141], 1.3272 [142]
Ethanol	1.3593 [143], 1.35960 [123]
1-Propanol	1.38302 [123]
[BMIM]BF <sub>4</sub>	1.42 [129], 1.4626 [144], 1.4219 [145], 1.4197 [146]
[BMIM]PF <sub>6</sub>	1.411 [12], 1.409 [83]
[BMIM]Tf <sub>2</sub> N	1.4271 [128]
[HMIM]Tf <sub>2</sub> N	1.42958 [134]
[OMIM]Tf <sub>2</sub> N	1.43329 [136], 1.43331 [137]

### 2.2.3.1 Effect of Temperature on Refractive Index

The refractive index of the ionic liquids is also affected by temperature. Figure 2.9 shows the refractive index values of the ionic liquids 1-ethyl-3-methylpyridinium ethylsulfate, [empy][EtSO<sub>4</sub>] at several temperatures [147]. As can be seen in Figure 2.8, the refractive index of [empy][EtSO<sub>4</sub>] decreases with increased in the temperature, in a linear fashion.

The change of refractive index with temperature can be correlated using the method of least square using the following equation,

$$n_D = c_0T^0 + c_1T^1 + c_2T^2 + \dots + c_nT^n \quad (2.5)$$

where  $c$  is the fitting parameter and  $T$  is the absolute temperature.

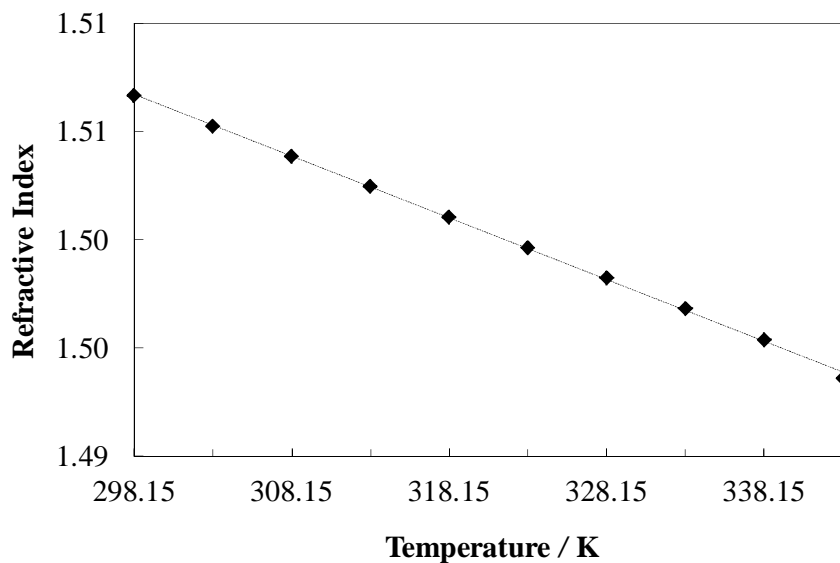


Figure 2.9 Effect of temperature on refractive index of ionic liquids [empy][EtSO<sub>4</sub>] [147]. Symbols;  $\diamond$ , density; (-) correlation using equation (2.5).

For the ionic liquids [empy][EtSO<sub>4</sub>], the temperature dependence of refractive index can be expressed as,

$$n_D = 1.5915 - 0.0003T \quad (2.5a)$$

#### 2.2.4 Effect of Co-solvent on Physical Properties of Ionic Liquids

In practical condition, corrosion inhibitors are mixture of active components, solvents, and surfactant [1]. The corrosion inhibitor should be compatible with co-solvent and surfactant used. Alcohol is widely used as co-solvent for inhibitor solution because it does not react or interfere with the active component. In this work, alcohol such as methanol, ethanol, and 1-propanol are chosen as co-solvent. The following section discusses the literature review on physical properties of binary mixture of ionic liquids with alcohol.



### 2.2.4.1 Density of Binary Mixture and Volumetric Properties

The volume of mixture of two liquids will not equal the sum of the volumes of its pure constituents for a combination of up to reasons: (1) size differences between solvent and solute molecules, (2) shape differences between solvent and solute molecules, (3) structural changes in the molecular ordering of the liquid, (4) interaction differences between like and unlike molecules, and (5) chemical reactions [112].

If a component (1) and component (2) are brought together but not allowed to mix, the total volume  $V$  of (1) and (2) is,

$$V^0 = n_1V_1^0 + n_2V_2^0 \text{ (no mixing)} \quad (2.6)$$

where  $n_1$  and  $n_2$  are the number of moles of component (1) and (2), respectively. If mixing takes place, the volume changes from  $V^0$  to  $V$ . This change can be defined as the excess volume,

$$V^E = V - V^0 \text{ (mixing)} \quad (2.7)$$

It is more convenient to write equation (2.4) in terms of excess molar volumes,

$$V_m^E = \frac{V^E}{n_1 + n_2} \quad (2.8)$$

Combining equation (2.3) and (2.5) gives,

$$V_m^E = V_m - (x_1V_1^0 + x_2V_2^0) \quad (2.9)$$

or

$$V_m^E = \left( \frac{x_1M_1 + x_2M_2}{\rho_{mix}} \right) - \left( \left( \frac{x_1M_1}{\rho_1} \right) + \left( \frac{x_2M_2}{\rho_2} \right) \right) \quad (2.10)$$

where  $\rho_{mix}$  is density of mixture,  $M_i$  is the molar mass of the pure component, and  $x_i$  is the mole fraction of component. The values of  $V_m^E$  depend on temperature and

pressure. Experimental determination of  $V_m^E$  can be accomplished in two ways. One can measure the actual volume change upon mixing, using special mixing or batch-type dilatometers. Alternatively, one can measure changes in density using any of several appropriate techniques. Of these, the vibrating-tube densimeter has become the most popular technique.

Excess molar volumes are useful as a way of describing the mixture of miscible liquids throughout the entire range of mixing ratios ( $0 \leq x \leq 1$ ). Several studies have been conducted to describe the solvent-solute interaction on mixing ionic liquids with solvent. The binary mixture of ionic liquids with alcohol [106, 122, 148-151], water [150, 152, 153], aromatic compound [115] and other organic solvent have been studied extensively [143].

The excess molar volume can be correlated well with composition using Redlich-Kister polynomial equation [154], which for binary mixture is,

$$\Delta Q_{ij} = x_i x_j \sum_{k=0} A_k (x_i - x_j)^k \quad (2.11)$$

where  $x_i$  is the mole fraction of component  $i$ ,  $A_k$  is the polynomial coefficient, and  $k$  is the order of polynomial, which are estimated using the method of least squares. Redlich-Kister polynomial equation, together with excess molar volume, is useful quantity for the description of two completely miscible liquids. To provide a quantitative description for mixing in such cases, one can amend equation (2.6) to account for mixing by defining volume molar partial of component 1 and 2,  $V_{m,1}$  and  $V_{m,2}$ , respectively, in binary mixtures using the following equation,

$$V_{m,1} = V_m^E + V_1^0 + x_2 \left( \frac{\delta V_m^E}{\delta x} \right)_{T,P} \quad (2.12)$$

$$V_{m,2} = V_m^E + V_2^0 + x_1 \left( \frac{\delta V_m^E}{\delta x} \right)_{T,P} \quad (2.13)$$

The derivatives in equation (2.12) and (2.13) are obtained by differentiation of equation (2.6). It leads to the following equation,

$$V_{m,1} = V_{m,1} + x_2^2 \sum_{k=0} A_k (x_1 - x_2)^k - 2x_1 x_2^2 \sum_{k=0} A_k k (x_1 - x_2)^{i-1} \quad (2.14)$$

$$V_{m,2} = V_{m,2} + x_1^2 \sum_{k=0} A_k (x_1 - x_2)^k + 2x_1^2 x_2 \sum_{k=0} A_k k (x_1 - x_2)^{i-1} \quad (2.15)$$

Much of the present interest is focused on the partial molar volume at infinite dilution. The partial properties at infinite dilution are of interest since, at the limit of infinite dilution, the solute–solute interactions disappear. The values of the partial molar volume at infinite dilution provide information about solute–solvent interaction, independent of the composition effect. Therefore, from equation (2.14), by setting  $x_2 = 1$  and  $x_1 = 0$ ,

$$V_{m,1}^{\infty} = V_1^0 + \sum_{k=0} A_k \quad (2.16)$$

Similarly, setting  $x_2 = 0$  in equation (2.15), it gives

$$V_{m,2}^{\infty} = V_2^* + \sum_{k=0} A_k (-1)^k \quad (2.17)$$

Equations (2.16) and (2.17) represent the partial molar volumes of component 1,  $V_{m,1}^{\infty}$ , and component 2,  $V_{m,2}^{\infty}$ , at infinite dilution, respectively. The partial molar volumes are calculated using the Redlich-Kister equation (2.11).

The Redlich–Kister coefficients can be excluded from the determination of the partial molar volumes at infinite dilution by using “the apparent molar volume” approach. The apparent molar volumes of component 1 in component 2,  $V_{\phi,1}$ , and the apparent molar volumes of component 2 in component 1,  $V_{\phi,2}$ , can be expressed as,

$$V_{\phi,1} = \frac{(V_m - x_2 V_{m,2}^{\infty})}{x_1} \quad (2.18)$$

$$V_{\phi,2} = \frac{(V_m - x_1 V_{m,1}^\infty)}{x_2} \quad (2.19)$$

in which  $V_m$  is molar volume of mixture. Combination of equations (2.6), (2.18), and (2.19) leads to,

$$V_{\phi,1} = \bar{V}_1^\infty + \left( \frac{V_m^E}{x_1} \right) \quad (2.20)$$

$$V_{\phi,2} = \bar{V}_2^\infty + \left( \frac{V_m^E}{x_2} \right) \quad (2.21)$$

Figure 2.10 shows the density and excess molar volume for binary mixture of [BMIM]SCN (1) and 1-propanol(2) at  $T=298.15$  K. The densities are highest for pure ionic liquids and are decreasing with increasing mole fraction of alcohol. Figure 2.9 also indicate that  $V_m^E$  exhibit negative deviation from ideality over the entire composition range.

The negative deviation from ideality observed for this system has to be a result of a strong interaction of ionic liquids with methanol. The strength of the intermolecular hydrogen bonding is not only one factor influencing the  $V_m^E$ . The molecular size and shape of the components and the packing effect are equally important factors.

The values for  $V_m^E$  of a mixture formed from two self-associated (H-bonded) substances are result of a number of effects that may contribute terms differing in sign. Disruption of H-bonds makes positive contribution, but specific interaction makes negative contributions to  $V_m^E$ . The free volume effect, which depends on differences in the characteristic pressures and temperatures of the components, makes negative contribution.

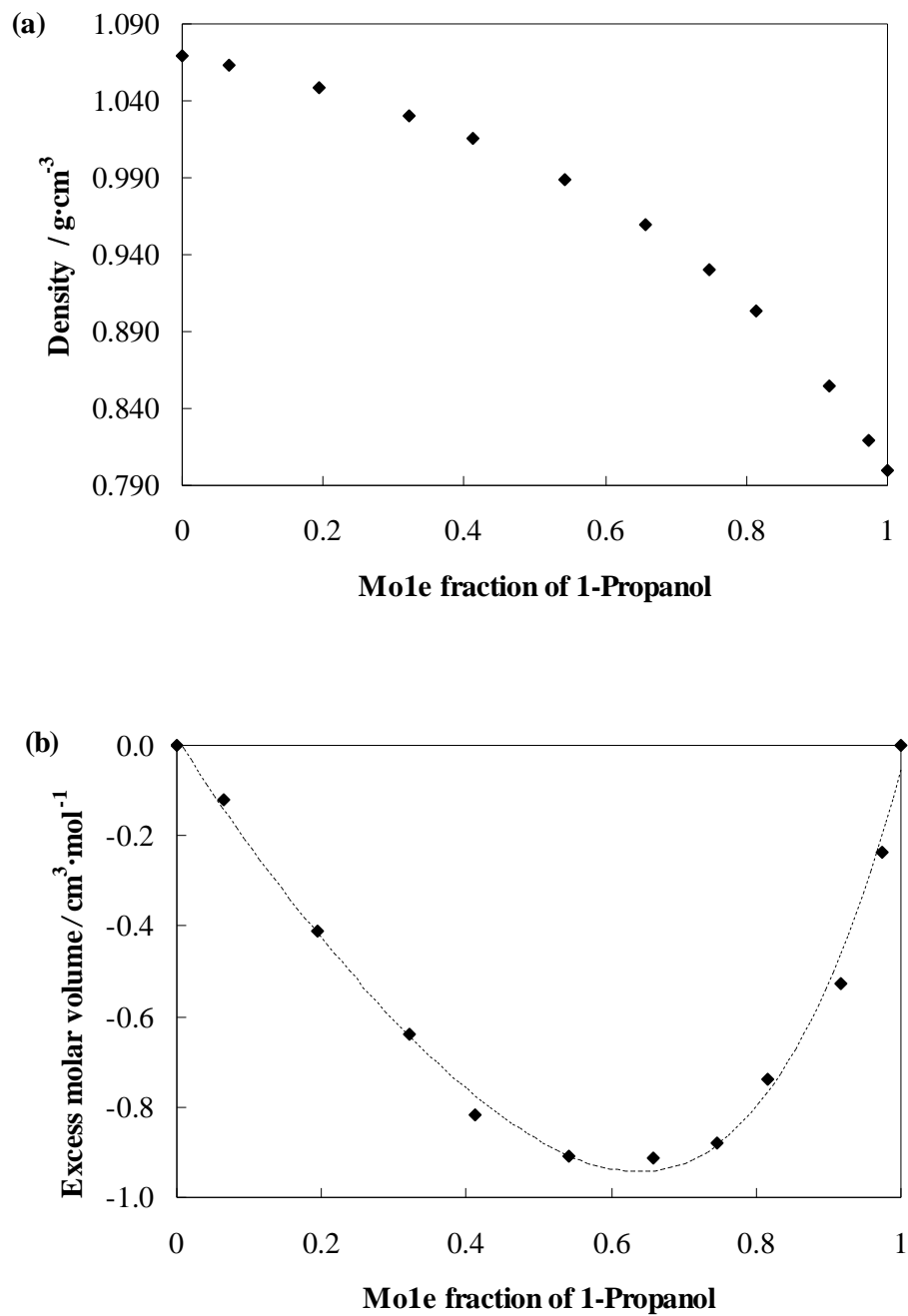


Figure 2.10 Density and excess molar volume ([BMIM]SCN + 1-propanol) binary mixture at  $T = 298.15$  K (a) Effect of composition on density of binary mixture, (b) Excess volume molar of binary mixture, (--) correlated using equation 2.11 [122].

Packing effects or conformational changes of the molecules in the mixtures are more difficult to categorize. However, interstitial accommodation and the effect of the condensation give further negative contributions. In the mixtures, the observed  $V_m^E$  values may be explained by four opposing sets of contributions: (1) expansion of an alcohol due to breaking of some of the hydrogen bonds of an alcohol during addition of the ionic liquids; (2) contraction due to specific interactions of an alcohol molecule with an ionic liquids; (3) size difference; and (4) expansion due to steric repulsion between alkyl chain of an alcohol and that of [BMIM][SCN] van der Waals interactions between the alkane chains [122].

#### 2.2.4.2 Viscosity of Binary Mixture and Viscosity Deviation

The addition of cosolvent to the ionic liquids, to form binary mixture, can result in dramatic reduction in the viscosity. The viscosity of the mixture of two liquids will not be equal to the sum of the viscosity of its pure constituents [112],

$$\Delta\eta = \eta_{mix} - (x_1\eta_1 + x_2\eta_2) \quad (2.22)$$

where  $\eta_{mix}$  is viscosity of mixture and  $x_i$  is the mole fraction of component.

Deviation of viscosity can be also correlated using Redlich Kister. For deviation of viscosity, it can be expressed as,

$$\Delta\eta = x_i x_j \sum_{k=0} A_k (x_i - x_j)^k \quad (2.23)$$

Figure 2.11 shows the viscosity of ([BMIM]SCN + 1-propanol) binary mixture. The observed decrease in viscosity with an increase in methanol content exhibits negative deviation and is particularly strong in dilute solutions of an alcohol in the ionic liquid. Ion-dipole interactions and/or hydrogen bonding between the cation of the ionic liquids and the alcohol will take place when an alcohol is added to the ionic liquids. This weakening of the strong hydrogen bonding interactions between cation and anion of the ionic liquids leads to a higher mobility of the ions and a lower viscosity of the mixture [122].

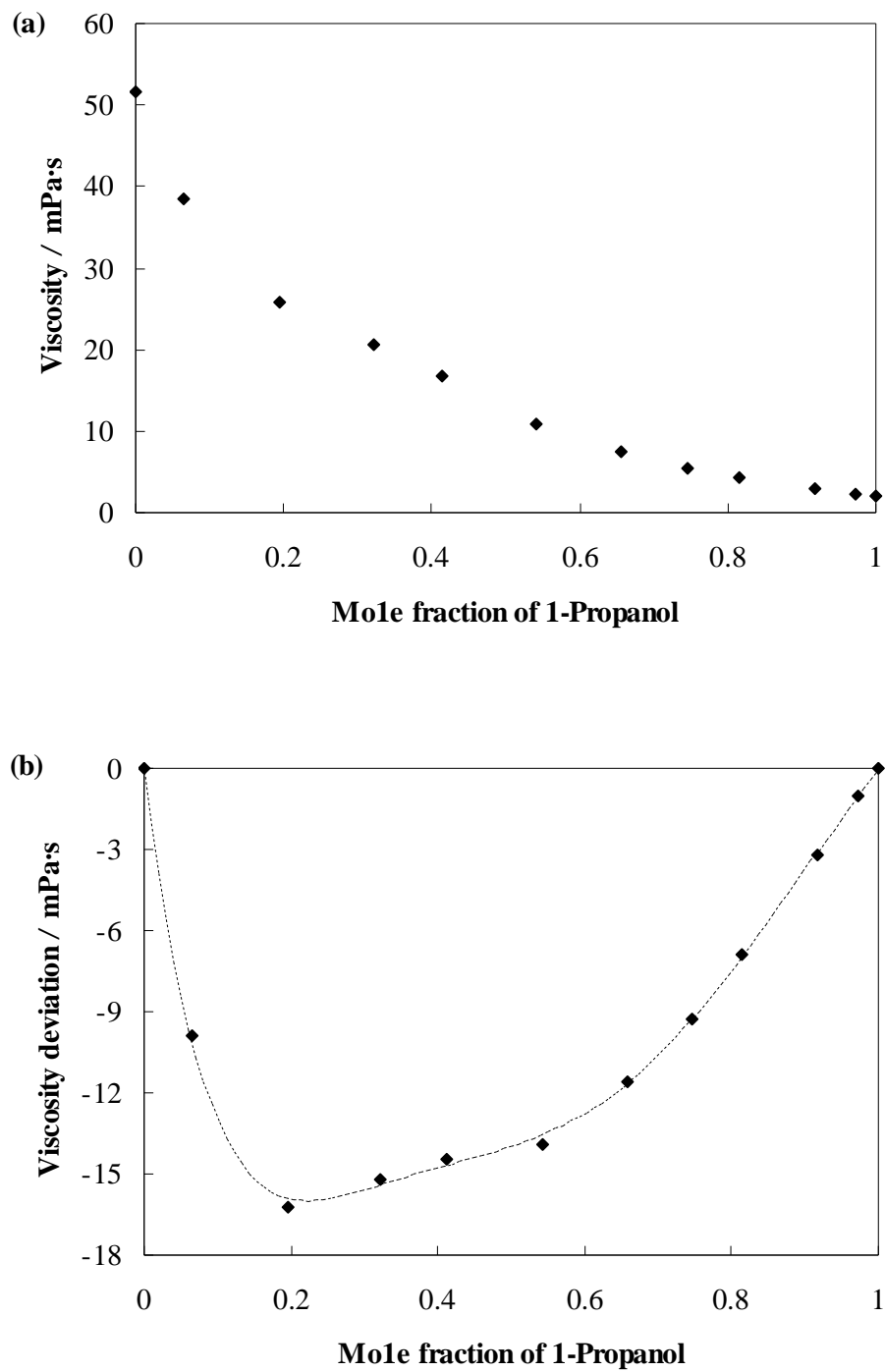


Figure 2.11 Viscosity of ([BMIM]SCN + 1-propanol) binary mixture at  $T = 298.15$  K  
 (a) Effect of composition on viscosity of binary mixture, (b) Deviation of viscosity of binary mixture, (-) correlated using equation 2.11 [122].

Viscosity of binary mixture containing imidazolium ionic liquids have also been studied with a range of cosolvent including water [155, 156], methanol, ethanol [155, 157], 1-propanol [125, 158], ethyl acetate, acetonitrile, and other organic solvent [104]. However, for protic hydroxyl ammonium ionic liquids these data are very scarce or hardly available.

#### 2.2.4.3 *Refractive Index of Binary Mixture and Refractive Index Deviation*

The addition of cosolvent to ionic liquids, to form binary mixture, can result in reduction in the refractive index. Figure 2.11 shows the refractive index of ([empty][EtSO<sub>4</sub>] + ethanol) binary mixture and its deviation of refractive index. As can be seen from Figure 2.11a, the refractive index of the binary mixture decreases with increasing composition of ethanol in the mixture. The refractive index is at maximum at pure ionic liquids and minimum at pure ethanol.

The deviation of refractive index can be expressed as,

$$\Delta n_D = n_{D_{mix}} - (x_1 n_{D,1} + x_2 n_{D,2}) \quad (2.24)$$

Deviation of refractive index can be also correlated using Redlich Kister. For deviation of refractive index, it can be expressed as,

$$\Delta n_D = x_i x_j \sum_{k=0} A_k (x_i - x_j)^k \quad (2.25)$$

Refractive index of binary mixture containing imidazolium ionic liquids have also been studied with a range of cosolvent including water [159, 160], methanol, ethanol [159, 160], 1-propanol [124], ethyl acetate [161], acetonitrile, and other organic solvent [143]. However, for protic hydroxyl ammonium ionic liquids these data are again hardly available



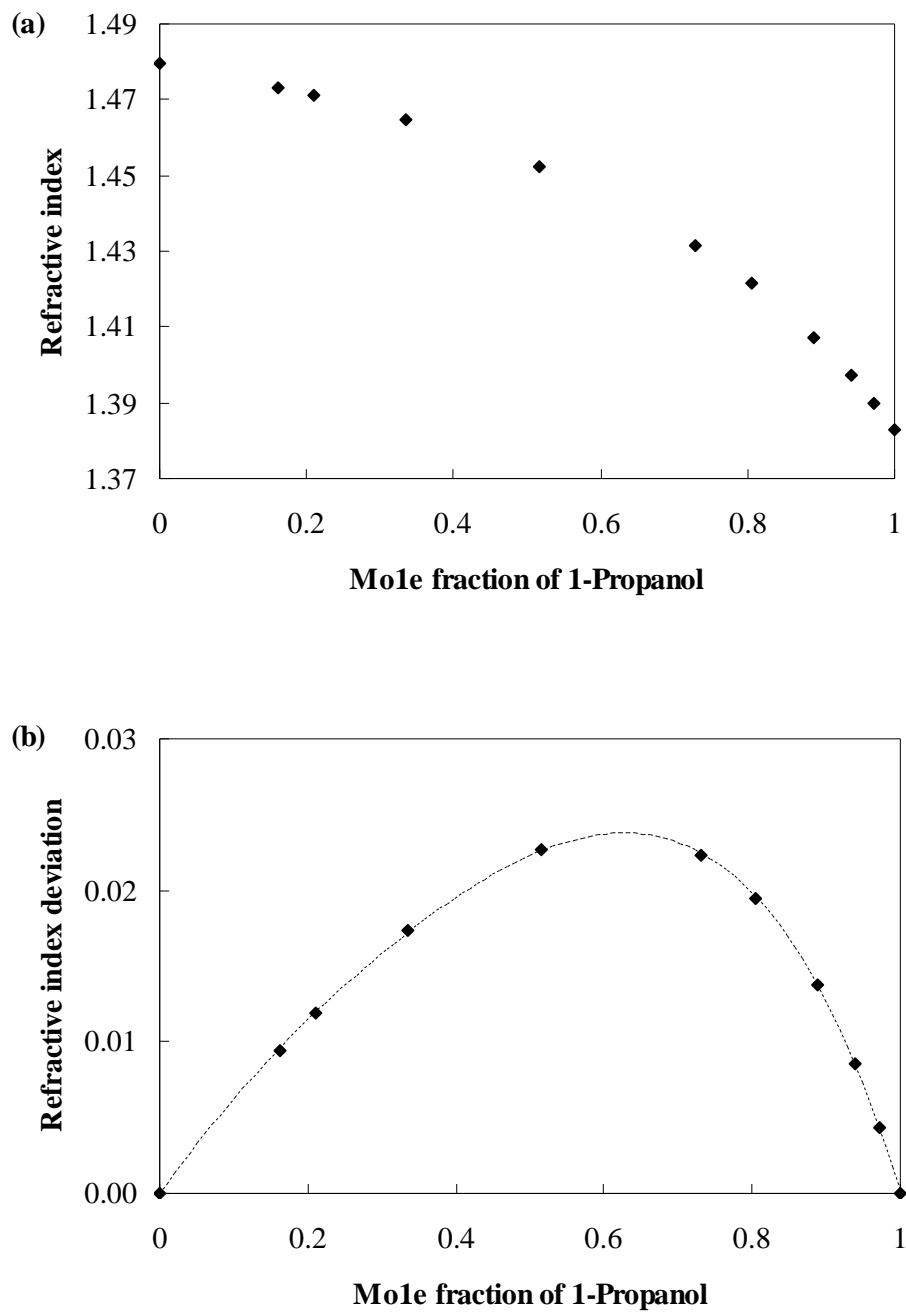


Figure 2.12 Refractive index of ([empy][EtSO<sub>4</sub>] + 1-Propanol) binary mixture at  $T = 298.15$  K (a) Effect of composition on refractive index of binary mixture, (b) Deviation of refractive index of binary mixture, (-) correlated using equation 2.11

### 2.3 Carbon Steel Corrosion in Acidic Media

Carbon steel is used in a wide range of industrial applications such as erecting boilers, drums, heat exchangers, tanks, and many others. On the other hand, acid solutions are widely used in different industries. The most important fields of application are acid pickling, industrial acid cleaning, acid descaling, and oil well acidising. The use of acid solution for those processes has led to the corrosive attack on carbon steel [4-9, 11, 12].

In the case of steel in which iron presents as the major components, the iron is corroded by acidic medium such as hydrochloric acid, HCl, as illustrated by the following chemical reactions [1],



In ionic form the above reaction can be written as follows,



Eliminating Cl<sup>-</sup> from both of sides of the reaction gives,



Therefore, the above reaction can be separated into half reactions consisting of oxidation-reduction as follows;



Commercial HCl usually contains ferric ion, present as iron chloride which makes metals corrode much more rapidly due to availability of two cathodic reactions namely, hydrogen evolution (Equation 2.30) and ferric ion reaction,



The stability of a metal and their alloy when exposed to a given environment depends on a multitude of factors that may vary greatly with the pH and oxidizing or reducing power of that environment. One useful concept to represent the effects of aqueous environments on metals became known as potential-pH (*E*-pH) diagrams, also called predominance or Pourbaix diagrams. The *E*-pH diagrams are typically plotted for various equilibria on normal Cartesian coordinates with potential, *E*, as the ordinate and pH as the abscissa [1]. Some interesting uses of such diagrams, which have been constructed for most metals and a few alloys, are to (1) predict whether or not corrosion can occur; (2) estimate the composition of the corrosion products formed; and (3), predict environmental changes which will prevent or reduce corrosion attack [1].

Figure 2.13 illustrates the *E*-pH diagram for iron at 25°C in the presence of water or corrosive environments. At potentials more positive than -0.6 and at pH values below 9, ferrous ion, Fe<sup>2+</sup>, is the stable substance. This indicates that iron corrodes under these conditions according to the following reaction,



In the other regions of the iron *E*-pH diagram, it can be seen that the corrosion of iron produces ferric ions, Fe<sup>3+</sup>; ferric hydroxide, [Fe(OH)<sub>3</sub>]; ferrous hydroxide, [Fe(OH)<sub>2</sub>]; and at very alkaline conditions, complex HFeO<sub>2</sub><sup>-</sup> ions. In the acidic media, which pH is equal to 1, reaction 2.26 is take place. It means that the carbon steel, which mainly composed by iron, corrodes in acidic media to form Fe<sup>2+</sup>. These diagrams also indicate that if the potential of iron is made sufficiently negative or shifted cathodically below approximately -0.5 V vs. Standard Hydrogen Electrode (SHE) in neutral or acidic environments, iron will less corrode. The addition of corrosion inhibitor into the system shifts the potential of iron into more negative value. It leads to cathodic protection criterion, in which iron will less corrode.

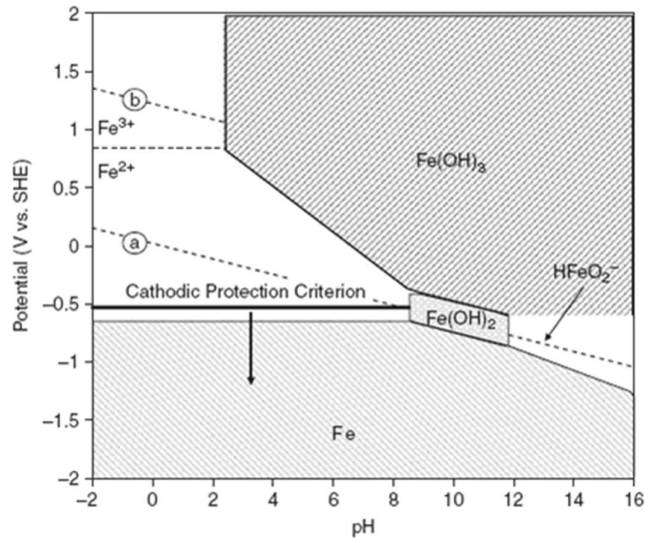


Figure 2.13 The E-pH diagram of iron with the cathodic criterion at 25 °C [1].

The difference between this cathodic potential and line (a) is indicative that such potential will also tend to electrolyze water into hydrogen as indicated in the following equations,



In the acidic media, in which concentration of  $\text{H}^+$  is high, reaction 2.34 takes place.

### 2.3.1 Recent Development on Corrosion Inhibitor in Acidic Media

Among the several methods of corrosion control and prevention, the use of corrosion inhibitors is very popular [4-9, 11, 12, 162-175]. Corrosion inhibitors are substances which when added in small concentrations to corrosive media decrease or prevent the reaction of the metal with the media. Inhibitors are added to many systems viz., cooling systems, refinery units, chemicals, and oil and gas production units.

The acidization of oil and gas wells is probably the most widely used work over and stimulation practice in oil industry. Acidization is oil reservoir stimulation technique for increasing well productivity by removing near-well bore formation damage or by creating alternate flow paths by dissolving small portions of the formation. Generally speaking, acids, or acid-based fluids, are useful in this regard due to their ability to dissolve both formation minerals and contaminants *e.g.*, drilling fluid coating the wellbore or that has penetrated the formation which were introduced into the wellbore/formation during drilling or remedial operations [1].

Different acids are used in conventional acidization treatment. The most common are hydrochloric acid, HCl; hydrofluoric acid, HF; acetic acid, CH<sub>3</sub>COOH; formic acid, HCOOH; sulfamic acid, H<sub>2</sub>NSO<sub>3</sub>H, and chloroacetic acid, ClCH<sub>2</sub>COOH. Among various acids, HCl is widely used for stimulating carbonate-based reservoirs like lime stone and dolomite [1]. Since HCl is strong aggressive medium for oil and gas well equipment. Thus, the effective way to protect these oil well tubular materials is to inject a suitable corrosion inhibitor. Accordingly, corrosion inhibitors must be injected with the HCl solution to avoid the destructive effect of acid on the surface of the pipe lines. Hence it is very important to measure the physical properties, in this case is viscosity, of the new corrosion inhibitor [1].

A number of organic compounds have been reported as corrosion inhibitors [4-9, 11, 12] and the screening of synthetic heterocyclic compounds is still being continued. Most of them are toxic in nature. This has led to the development of non toxic corrosion inhibitors such as amino acid [162-167] and natural product [168-172] such as Khillah [168], pennyroyal oil [169], lawsonia [170], and opuntia [171]. The inhibitive effect of four antibacterial drugs, namely ampicillin, cloxacillin, flucloxacillin and amoxicillin towards the corrosion of aluminium was investigated. The inhibition efficiency follow the order amoxicillin > ampicillin > cloxacillin > flucloxacillin. The inhibition action of these drugs was attributed to blocking the surface via formation of insoluble complexes on the metal surface [173]. Various rhodanine azosulpha drugs were used as a potential class of corrosion inhibitor on 304 stainless steel [174]. El-Naggar have studied the corrosion inhibition activity of sulpha drugs namely sulphaguanidine, sulphamethazine, sulphamethaxazole and

sulphadiazine as corrosion inhibitor for mild steel in hydrochloric acid and sulphuric acid solutions and reported them as potential inhibitors [175]. Even though those compounds show high inhibition performance on carbon steel corrosion in acidic medium, the author did not report its physical properties that needed on practical condition such as density and viscosity [162-175].

The literature data show that organic compounds act as an inhibitor by adsorption on the metal surface [4-9, 11, 12, 162-175]. Inhibitor molecules may adsorb on the carbon steel surface in the form of: (i) neutral molecule via chemisorption mechanism involving the sharing of electrons between the nitrogen atom and iron, (ii) adsorption of inhibitor can occur through electron interactions between the aromatic ring of the molecule and the metal surface, (iii) cationic form with positively charged part of the molecule is oriented toward negatively charged surface [26]. Adsorption can also occur via electrostatic interaction between a negatively charged surface, which is provided with a specifically adsorbed anion on iron and the positive charge of the inhibitor. The inhibiting mechanism is generally explained by the formation of a physically and/or chemically adsorbed film on the carbon steel surface [4-9, 11, 12, 162-175]. The type of adsorbed film on the carbon steel surface is determined by their thermodynamic of adsorption. The thermodynamic of adsorption is reviewed further in section 2.3.5.

Figure 2.14 presents the mechanism of carbon steel corrosion in the absence and presence of inhibitor [176, 177]. In the absence of inhibitors the reaction follows the pathway from (a)  $\rightarrow$  (b)  $\rightarrow$  (c)  $\rightarrow$  (d). When carbon steel immersed in the HCl solution, in the presence of inhibitor (inh), chloride ions are firstly adsorbed to the metal surface, because of smaller degree of hydration. Adsorbed chloride ions create an excess negative charge towards the solution (step a), and favor more adsorption of the cations. The protonated inhibitor molecules are adsorbed on metal surface via  $\text{Cl}^-$  ions which forms interconnecting bridges between the metal atoms and the organic cations (step e). So it can be proposed that, reaction pathway of carbon steel corrosion in the presence of inhibitor is seems to be through (a  $\rightarrow$  e). The equilibrium constant  $k_2$  must be much more bigger than  $k_4$  and reaction (a  $\rightarrow$  e) should be more favored

than (a) → (b) → (c) → (d). Thus, the inhibitor molecules may act as a barrier against corrosion of the iron [176, 177].

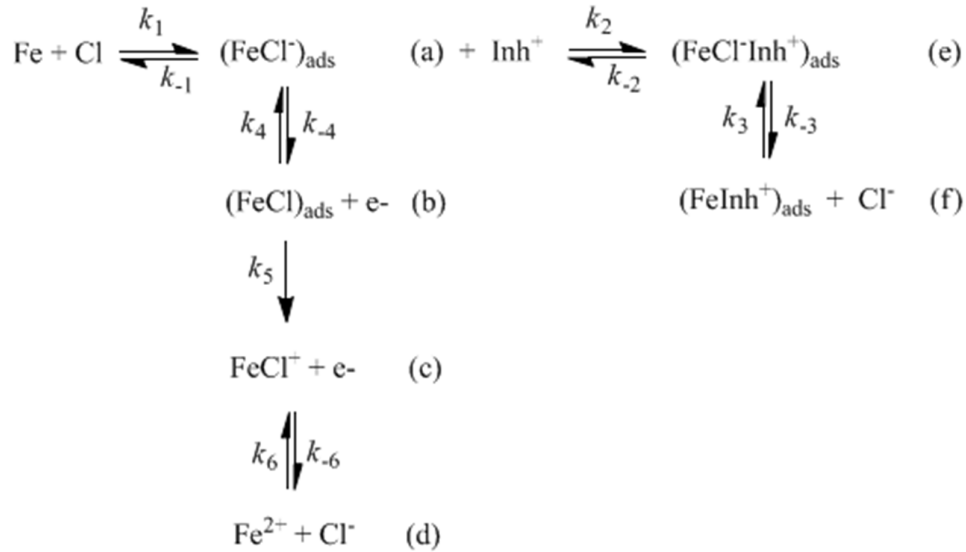


Figure 2.14 Mechanism of carbon steel corrosion in HCl solution in the absence and presence of inhibitor [176, 177].

In the case chemisorption, the same adsorption pathway is observed. In the first step, negative charged metal surface was formed, by chloride ions as explained above, following this step the reaction proceeded through forming  $(\text{FeCl}^- \text{Inh}^+)_{\text{ads}}$  as a new reaction pathway having equilibrium constant, of  $k_3$ ,  $\text{e}^- \rightarrow \text{f}$ . The positively charged inhibitor molecule will replace with  $\text{Cl}^-$  due to more interaction ability of inhibitor, and  $\text{Cl}^-$  is displaced from the metal surface towards solution. Consequently, a new double layer is formed and metal surface is loaded negative charge, against positive charged inhibitor molecule  $(\text{FeInh}^+)_{\text{ads}}$ . The equilibrium constant related with forming of  $(\text{FeInh}^+)_{\text{ads}}$ ,  $k_3$ , is must be bigger than  $k_2$  and  $k_4$ , so the reaction do not stop at step e and proceeds further with replacement of  $\text{Cl}^-$  ions.

Though many synthetic compounds showed good anticorrosive activity, there are some disadvantages with the reported inhibitor such as difficulty in the preparation method and the high material cost. Also it has been reported that the lack of their physical properties data, has limited the design and application of these corrosion inhibitors [4-9, 11, 12, 162-175].

### 2.3.1.1 *Ionic Liquids as Corrosion Inhibitor*

The potential application of imidazolium and pyridinium based ionic liquids as inhibitor on steel corrosion in acidic medium has been reported in open literature [22-24]. Inhibition of corrosion of mild steel in 1M HCl by imidazolium based ionic liquids, namely 1-butyl-3-methylimidazolium chlorides, [BMIM]Cl, and 1-butyl-3-methylimidazolium hydrogen sulfate, [BMIM]HSO<sub>4</sub>, has been investigated using electrochemical impedance, potentiodynamic polarization and weight loss measurements. These two ionic liquids showed good inhibition property for the corrosion of mild steel in 1M HCl solution and the inhibition efficiency was improved significantly with ionic liquids concentration [22]. The adsorption of the inhibitors molecules on the metal surface from 1M HCl solution obeys Langmuir adsorption isotherm. The high value of adsorption equilibrium constant suggested that, the inhibitors are strongly adsorbed on the mild steel surface. In addition, the increase in activation energy after the addition of inhibitors to the 1M HCl solution and the value of standard free energy of the adsorption indicated that the adsorption is more physical than the chemical adsorption. The negative sign of the  $\Delta G_{ads}$  and  $\Delta H$  indicate that the adsorption process is spontaneous and exothermic [22].

The inhibiting property of ionic liquids 1-butyl-3-methylimidazolium bromide, [BMIM]Br, on corrosion of mild steel in 1 M HCl was also evaluated by various corrosion monitoring techniques [23]. Potentiodynamic polarization data indicated that the [BMIM]Br acts essentially as a mixed-type inhibitor. The adsorption of inhibitor on the mild steel is found to follow the Langmuir adsorption isotherm.



More recently, the inhibition performance of imidazolium and pyridinium bromides on mild steel corrosion in aqueous 1 M H<sub>2</sub>SO<sub>4</sub> solution by was evaluated by polarization curves and surface analysis techniques such as SEM, EDX, XRD, and Mössbauer [24]. The results showed that these ionic liquids show a fair corrosion inhibition with average corrosion efficiency within 82-88 % to protect the mild steel corrosion in the aqueous solution of sulfuric acid; their efficiencies are increased with the inhibitor concentration. These compounds affected both anodic and cathodic reactions so they are classified as mixed type inhibitor. The ionic liquids adsorbed on the mild steel surface due to chemisorption and obeyed the Langmuir's isotherm.

### 2.3.2 Method to Measure Corrosion Inhibition

There are many methods to measure corrosion rate and monitor corrosion process. The most common methods are Weight Loss (WL), Tafel Plot, Linear Polarization Resistance (LPR), and Electrochemical Impedance Spectroscopy (EIS) [4-9, 11, 12, 162-175].

#### 2.3.2.1 Weight Loss Method

The weight loss method measurement is based on geometric weight loss measurement. This measurement requires long exposure time to reach measurable corrosion rate. The weight loss method can be used for both corrosion rate measurements and inhibition efficiency of inhibitor on corrosive system. The inhibition efficiency for all inhibitors were calculated using the following equation,

$$\%IE = \frac{CR_{corr} - CR_{corr}^{inh}}{CR_{corr}} \times 100 \quad (2.35)$$

where  $CR_{corr}$  and  $CR_{corr}^{inh}$  are the corrosion rate of carbon steel in the absence and presence of the inhibitor, respectively. Figure 2.15 shows the corrosion rate and inhibition performance of [BMIM]Cl on the mild steel corrosion in 1 M HCl at 303 K using weight loss method and [22]. As can be seen from Figure 2.15 The corrosion

rate of mild steel decreased in the presence of the ionic liquids. It appeared the ionic liquids reduce the corrosion rate of carbon steel in 1 M HCl. The effect is more pronounced with increasing concentration of the ionic liquids. Consequently, the inhibition efficiency increases with increasing concentration of the ionic liquids [22].

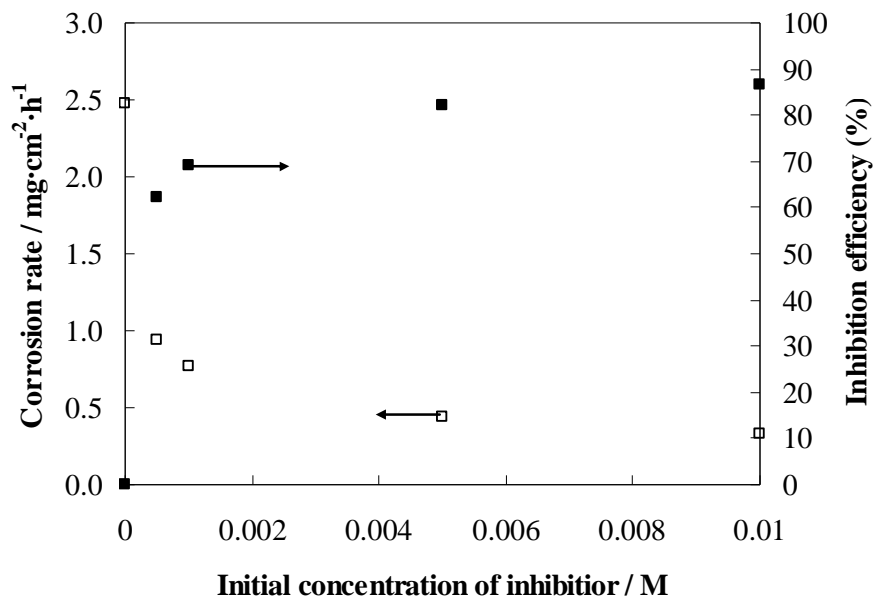


Figure 2.15 Corrosion rate and inhibition efficiency in the absence and presence of [BMIM]Cl for mild steel in 1 M HCl. Symbol: ■, inhibition efficiency; □, corrosion rate [22].

### 2.3.2.2 Tafel Plot

For Tafel Plots measurements, an external potential is imposed on a metal specimen in which the specimen is polarized to about 300 mV anodically and cathodically, from the corrosion potential,  $E_{corr}$ , as shown in Figure 2.15. The corrosion current,  $i_{corr}$ , is then obtained from a Tafel plot by extrapolating the linear portion of the curve to  $E_{corr}$  as shown in Figure 2.16.

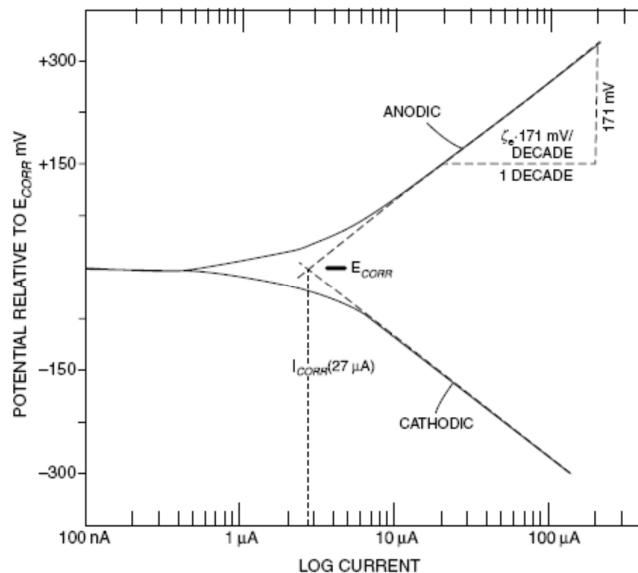


Figure 2.16 Experimentally measured Tafel plot [1].

Figure 2.17 shows the Tafel Plot for mild steel in the presence and absence of [BMIM]Cl at 303 K. The graph indicates that addition of the inhibitors causes more negative shift in corrosion potential,  $E_{corr}$ , especially at high concentrations. The anodic Tafel slopes increase in the presence of the inhibitors and lines, which indicate that the hydrogen evolution reaction is activation controlled and the addition of the studied alkyimidazolium bases does not modify the mechanism of this process. Addition of the alkyimidazolium bases affects both anodic and cathodic reaction. Therefore, those compounds could be classified as mixed type inhibitors [22]. The same behavior was also observed for other imidazolium based ionic liquids [23]. The inhibition efficiency for all inhibitors are calculated using the following equation [22, 23],

$$\%IE = \frac{i_{corr} - i_{corr}^{inh}}{i_{corr}} \times 100 \quad (2.36)$$

where  $i_{corr}$  and  $i_{corr}^{inh}$  are the corrosion current in the absence and presence of inhibitor.

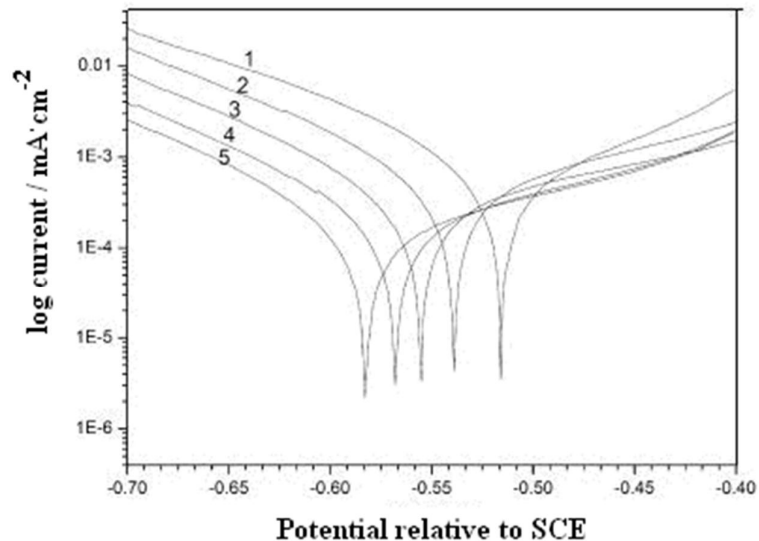


Figure 2.17 Effect of inhibitor concentration on the potentiodynamic polarization response for mild steel in 1M HCl solution at 303 K in various concentration of [BMIM]Cl. Symbols: 1, blank; 2, 0.0005 M; 3, 0.001 M; 4, 0.005 M; 5, 0.01 M [22].

### 2.3.2.3 Linear Polarization Resistance

The linear polarization technique is rapid and gives corrosion rate data, which correlate reasonably well with the weight loss method. The linear polarization resistance (LPR) measurement is performed by scanning through a potential range that is very close to the corrosion potential  $E_{corr}$ . The polarization range is generally  $\pm 20$  mV about  $E_{corr}$ . The resulting current density is plotted versus potential as shown in Figure 2.18.

LPR is widely used for corrosion rate measurement in high conductivity media and also provides a faster corrosion rate measurement. This is not a destructive test so it can be used on the same electrode to monitor long-term corrosion. The inhibition efficiency for inhibitors can be calculated using the following equation [22, 23],

$$\%IE = \frac{R_p^{inh} - R_p}{R_p^{inh}} \times 100 \quad (2.37)$$

where  $R_p$  and  $R_p^{inh}$  are the polarization resistance in the absence and presence of inhibitor.

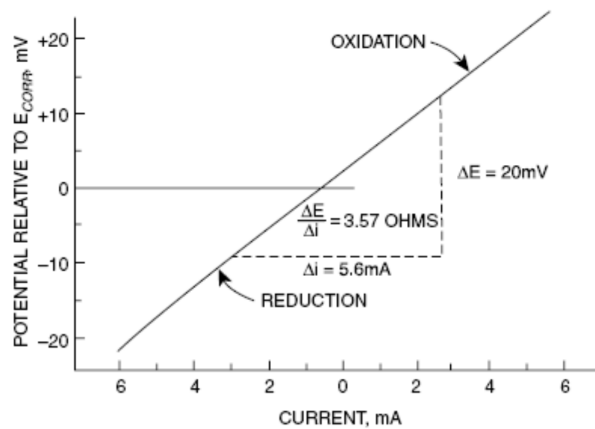


Figure 2.18 Experimentally measured linear polarization resistance [1]

#### 2.3.2.4 Electrochemical Impedance Spectroscopy

Electrochemical Impedance Spectroscopy (EIS) has been successfully applied to the study of the corrosion and its prevention system for over the years because this method yields information on the type of corrosion, the kinetics of the corrosion, and also corrosion rates. An important advantage of EIS over the other conventional laboratory techniques is that it uses very small amplitude signals without disturbing the nature of the metal surface being examined.

The effects of [BMIM]Cl on the impedance behavior of mild steel in 1M HCl solution have been studied by Zhang and Hua [22]. Nyquist plots, Bode diagram, and its electrical circuit analog are given in Figures 2.19, 2.20, and 2.21, respectively. It is clear from Figure 2.19 that the impedance spectra obtained yields a semi circular shape and only one time constant is observed in the Bode format. This indicates the corrosion of the mild steel in 1M HCl solution is mainly controlled by a charge

transfer process. The charge transfer resistance,  $R_t$ , must be corresponding to the resistance between the metal and OHP (Outer Helmholtz plane) and can be calculated from the difference in impedance at lower and higher frequencies. To obtain the double-layer capacitance,  $C_{dl}$ , the frequency at which the imaginary component of the impedance is maximum,  $-Z''_{max}$ , is determined and  $C_{dl}$  values are calculated from the following equation [1],

$$f(-Z''_{max}) = \frac{1}{2\pi C_{dl} R_{ct}} \quad (2.38)$$

From Figure 2.19, it is clear that the corrosion of mild steel is obviously inhibited in the presence of the inhibitors. It is apparent that, the impedance response for mild steel in HCl changes significantly with increasing inhibitor concentration. It is worthy noting that similar profile of the Nyquist plots is observed in the absence and presence of the inhibitors, indicating that addition of inhibitors do not change the mechanism for the dissolution of mild steel in HCl [22].

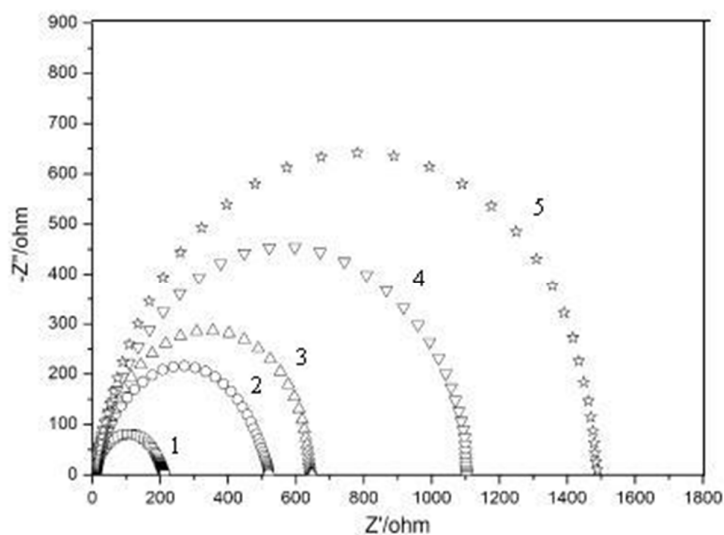


Figure 2.19 Nyquist plot for mild steel in 1M HCl solution at 303.15 K in various concentration of 1-butyl-3-methylimidazolium chloride. Symbols: 1, blank; 2, 0.0005 M; 3, 0.001 M; 4, 0.005 M; 5, 0.01 M [22].

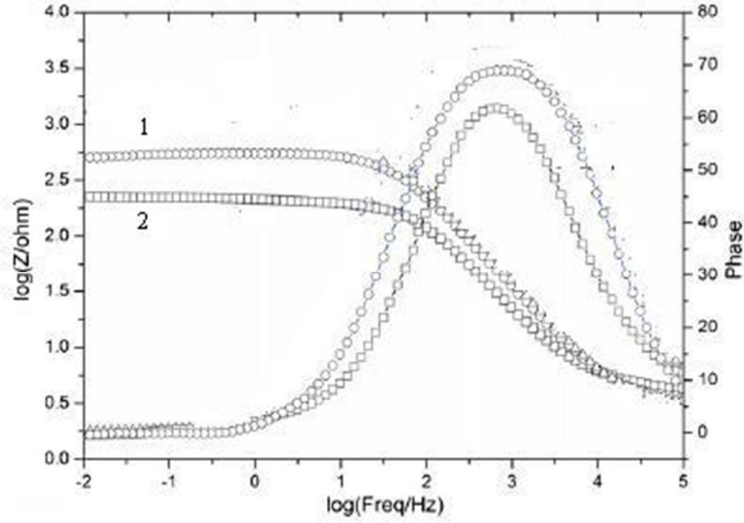


Figure 2.20 Bode plot for mild steel in 1M HCl solution at 303.15 K in various concentration of 1-butyl-3-methylimidazolium chloride. Symbols: 1, blank; 2, 0.005 [22].

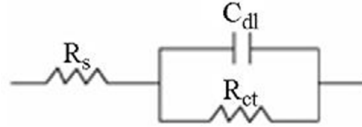


Figure 2.21 Electrical circuit analog corresponded to the Figure 2.19 and 2.20

In the case of the electrochemical impedance spectroscopy, the inhibition efficiency ( $IE$ ) is calculated using charge transfer resistance as follows [22, 23],

$$\%IE = \frac{R_t^{inh} - R_t}{R_t^{inh}} \times 100 \quad (2.39)$$

where  $R_t$  and  $R_t^{inh}$  are the charge transfer resistance values without and with inhibitor for mild steel in 1MHCl, respectively. As the inhibitor concentration increases, the  $R_t$

values increase, while the  $C_{dl}$  values decrease. The decrease in  $C_{dl}$  value is due to the adsorption of inhibitor on the metal surface. The inhibition efficiency increases with increasing inhibitor concentration.

### 2.3.3 Adsorption of Inhibitor on Carbon Steel Surface

A corrosion inhibitor can function in two ways [1]. In some situations the added inhibitors can alter the corrosive environment into a non corrosive or less corrosive environment through its interaction with the corrosive species. In other cases the corrosion inhibitor interacts with the metal surface and as a consequence inhibits the corrosion of the metal. It is well recognized that the first step in inhibition of metallic corrosion is the adsorption of organic inhibitor molecules at the metal/solution interface and that the adsorption depends on the molecules chemical composition, the temperature and the electrochemical potential at the metal/solution interface. In fact, the solvent  $H_2O$  molecules could also adsorb at metal/solution interface. So the adsorption of organic inhibitor molecules from the aqueous solution can be regarded as a quasi-substitution process between the organic compounds in the aqueous phase  $[Org_{(sol)}]$  and water molecules at the electrode surface  $[H_2O_{(ads)}]$  [4-9, 11, 12, 162-175],



where  $n$  is the size ratio, that is, the number of water molecules replaced by one organic inhibitor. For effective adsorption of the inhibitor on a metal surface the forces of interaction of the metal and an inhibitor must be greater than the interaction forces of metal and water molecules.

#### 2.3.3.1 Adsorption Isotherm

Adsorption isotherm is shown to reflect the performance of inhibitors. When the inhibitor is dissolved in a solution, it gets adsorbed on the metal surface and prevents the corrosion. The adsorption changes the nature of electrified interface between



metal and the solution. The adsorption process is influenced by the chemical structures of organic compounds, the distribution of charge in molecule, the nature and surface charge of metal and the type of aggressive media [1].

The adsorption isotherms are given in Table 2.4. Most of the organic corrosion inhibitors obey the Langmuir's isotherm adsorption. The Langmuir's isotherm adsorption model is based on following assumptions: (i) The heat of adsorption is the same for all adsorption sites and is independent of surface coverage, (ii) The total numbers of adsorption sites are constant and each site can hold one adsorbed species, and (iii) The adsorbed species do not interact with each other [1]. Figure 2.22 shows the graph of Langmuir's isotherm adsorption for [BMIM]Cl at temperature 303 K [22]. A straight line was obtained on plotting  $C_{inh}/\theta$  against  $C_{inh}$  as shown in Figure 2.21 which suggested that the adsorption of the inhibitors used from 1M HCl solutions on mild steel follows Langmuir's adsorption isotherm. Ionic liquids 1-butyl-3-methylimidazolium chlorides, 1-butyl-3-methylimidazolium hydrogen sulfate, and 1,3-Dioctadecylimidazolium bromide, and N-Octadecylpyridinium bromide follows Langmuir isotherm adsorption [24].

Table 2.4 Adsorption isotherm [1]

Isotherm	Formula	Equation
Langmuir	$\frac{\theta}{(1-\theta)} = K_{ads} C_{inh}$	(2.41)
Frumkin	$\left[ \frac{\theta}{(1-\theta)} \right] = K_{ads} C_{inh}$	(2.42)
Temkin	$\theta = \left( \frac{1}{f} \right) \ln K_{ads} C_{inh}$	(2.43)
Bockris-Swinkels	$\frac{\theta}{(1-\theta)^n} \left[ \frac{(\theta + n(1-\theta)^{n-1})}{n^n} \right] = \frac{ce^{-K_{ads}}}{55.4}$	(2.44)
Virial Parson	$\theta e^{2f\theta} = K_{ads} C_{inh}$	(2.45)

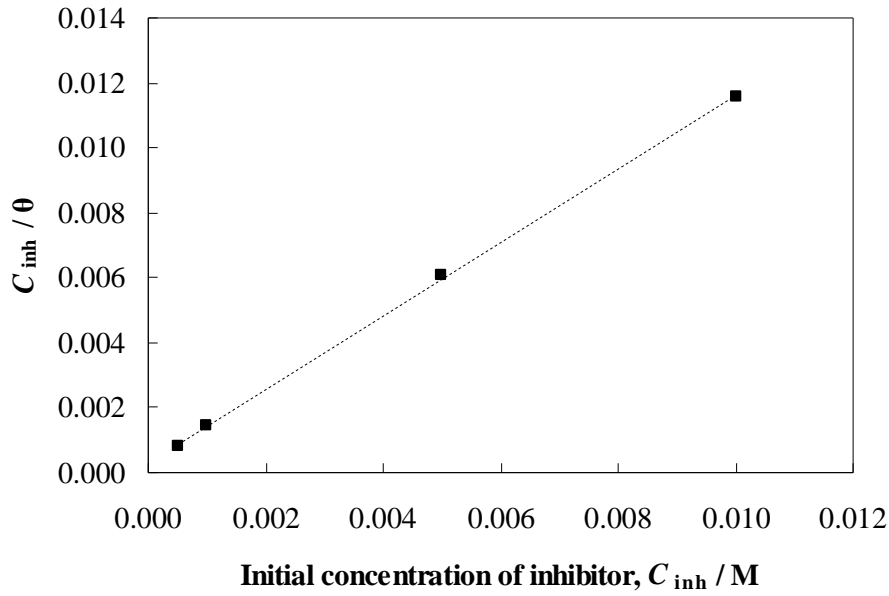


Figure 2.22 Langmuir's isotherm adsorption for ionic liquids 1-Butyl-3-methylimidazolium chloride on the surface of mild steel at temperature 303 K [22].

### 2.3.3.2 Equilibrium Constant of Adsorption

In the case of inhibitors which adsorb on the metal surface and inhibit the corrosion there are two steps, namely: (i) partitioning of inhibitor between electrolyte system and carbon steel surface; and (ii) carbon steel - inhibitor interactions. The equilibrium constant of adsorption,  $K_{ads}$ , reflect the adsorption of corrosion inhibitor from the corrosive environment to the carbon steel surface and is given by [1],

$$K_{ads} = \frac{\theta}{C_{inh}(1-\theta)} \quad (2.46)$$

where  $\theta$  is degree of surface coverage of the metal surface and  $C_{inh}$  is the inhibitor concentration.

Figure 2.23 presents the value of  $K_{ads}$  for adsorption of [BMIM]Cl onto the mild surface in 1 M HCl at several temperatures. The high values for equilibrium constant of adsorption are good indicative for a strong adsorption of the studied inhibitors on mild steel surface. The higher  $K_{ads}$  the stronger and more stable adsorbed layer being forming, this increases the inhibition efficiency. The value of  $K_{ads}$  decreases with increasing temperature. It suggests that the inhibitors are physically adsorbed on the metal surface and desorption process enhances with elevating temperature [1].

### 2.3.4 Thermodynamic of Adsorption

The thermodynamic of adsorption parameters are a useful tool for clarifying the adsorption behavior of an inhibitor. It can be used to understand the effect of concentration and temperature on the adsorption processes of the ionic liquids on the carbon steel surface in 1 M HCl. The thermodynamic parameters include the standard free energy of adsorption, and enthalpy and entropy of activation.

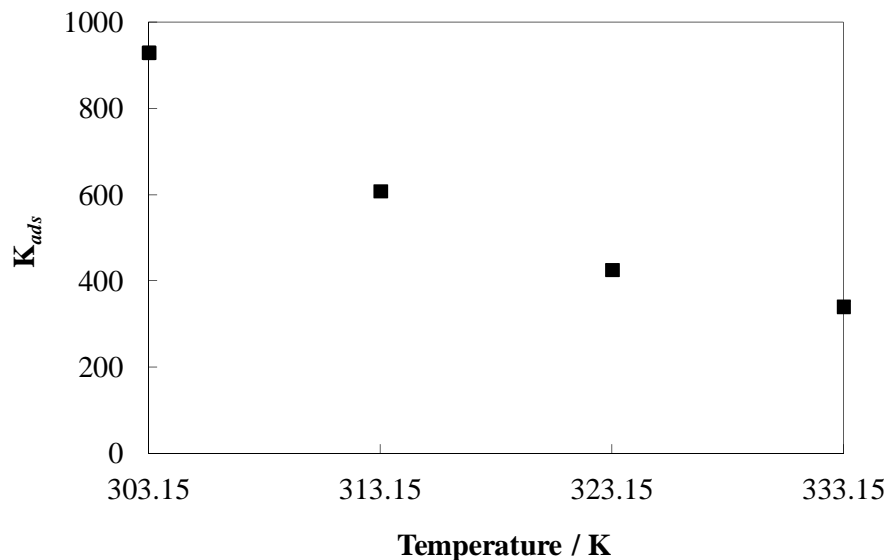


Figure 2.23 Equilibrium constant for mild steel in 1M HCl solution in the presence of 0.005 M [BMIM]Cl at different temperatures [22].

### 2.3.4.1 Standard Free Energy of Adsorption

Adsorption of inhibitors on the carbon steel surface can be due to either physisorption or chemisorption. These types of adsorption are related to their standard free energy of adsorption,  $\Delta G_{ads}$  [1, 22-24],

$$\Delta G_{ads} = -RT \ln(55.5 \times K_{ads}) \quad (2.47)$$

where  $R$  is gas constant,  $T$  is the absolute temperature, and  $K_{ads}$  is the equilibrium constant of adsorption.

Generally, the  $\Delta G_{ads}$  values of  $-20 \text{ kJ}\cdot\text{mol}^{-1}$  or less negative are associated with an electrostatic interaction between charged molecules and charged metal surface, physisorption; those of  $-40 \text{ kJ}\cdot\text{mol}^{-1}$  or more negative involve charge sharing or transfer from the inhibitor molecules to the metal surface to form a coordinate covalent bond, chemisorption [1].

Figure 2.24 shows the standard free energy for adsorption of [BMIM]Cl on the mild surface in 1 M HCl at several temperatures. The values of  $\Delta G_{ads}$  are negative, indicating spontaneous interaction of inhibitor molecule with the corroding mild steel surface. The graph also shows that the values of  $\Delta G_{ads}$  around to be less than  $40 \text{ kJ}\cdot\text{mol}^{-1}$  and higher than  $20 \text{ kJ}\cdot\text{mol}^{-1}$ . It is usually accepted as a threshold value between chemisorption and physisorption

Inhibitors involved in physisorption can be desorbed with ease while inhibitors involved in chemisorption are difficult to be desorbed. Physical adsorption forces are relatively weak and they have low activation energy,  $E_a$ . Chemisorption of inhibitor molecules on metals is slow and involves interaction forces stronger than the forces in physisorption. A coordinate type of bond between the metal and the inhibitor is thought to be present with charge transfer from the inhibitor to the metal. An opposing view is that a chemical bond is not necessarily present in chemisorption of an inhibitor on the metal surface. In some cases the temperature dependence shows higher inhibition efficiency and higher activation energy  $E_a$  than physisorption [1].

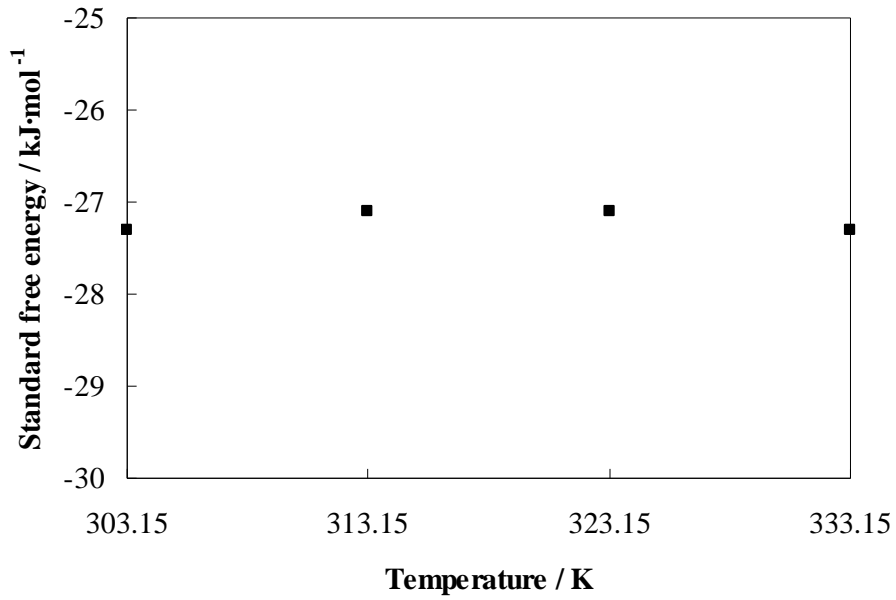


Figure 2.24 Standard free energy for mild steel in 1M HCl solution in the presence of 0.005 M [BMIM]Cl at different temperatures [22].

#### 2.3.4.2 Enthalpy and Entropy of Activation

The enthalpy of activation,  $\Delta H_{act}$ , gives information on the strength of the interaction between metal and dissolved inhibitor whereas the entropy of activation,  $\Delta S_{act}$ , indicates the level of ordering that takes place in the iron/inhibitor mixture. These thermodynamics properties can be determined from the following equation [1],

$$\text{Corrosion rate} = \frac{RT}{Nh} \exp\left(\frac{\Delta S_{act}}{R}\right) \exp\left(-\frac{\Delta H_{act}}{RT}\right) \quad (2.48)$$

Where  $R$  is gas constant,  $T$  is the absolute temperature,  $h$  is the Planck's constant,  $N$  is the Avogadro's number,

Figure 2.25 plots the  $\ln(CR/T)$  against.  $1000/T$  for mild steel in 1 M HCl in the presence of 0.005 M 1-butyl-3-methylimidazolium chloride at several temperatures. A plot of  $\ln(CR/T)$  against.  $1000/T$  give a straight line with a slope of  $(-\Delta H_{act}/R)$  and an intercept of  $[(\ln(R/Nh)) + (\Delta S_{act}/R)]$ , from which the values of  $\Delta H_{act}$  and  $\Delta S_{act}$  are calculated and listed in Table 2.5.

The data show that the  $\Delta H_{act}$  values of the corrosion of mild steel in 1M HCl solution in the presence of the inhibitors are higher than those in the absence of inhibitor. The  $\Delta H_{act}$  value enhance with increasing inhibitor concentration, indicating more energy barrier for the reaction in the presence of the inhibitor. The entropy of activation  $\Delta S_{act}$  in the absence and presence of the inhibitor is large and negative. This indicates the activated complex in the rate determining step represents an association rather than a dissociation step, meaning that, a decrease in disordering takes place on going from reactants to the activated complex [22].

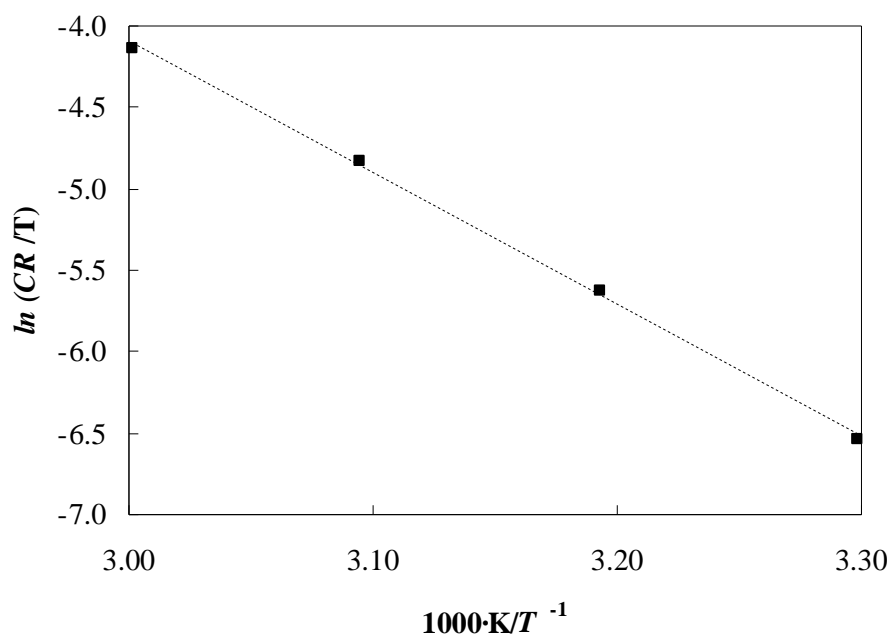


Figure 2.25 Plot the  $\ln(CR/T)$  against.  $1000/T$  for mild steel in 1M HCl solution in the presence of 0.005 M 1-butyl-3-methylimidazolium chloride at different temperatures [22].

Table 2.5 The enthalpy and entropy of activation for mild steel in 1M HCl solution in the absence and presence of [BMIM]Cl

$C_{inh}/M$	$\Delta H_{act}/kJ\cdot mol^{-1}$	$-\Delta S_{act}/(J\cdot K^{-1}\cdot mol^{-1})$
0	46.4	84.3
0.0005	55.2	63.5
0.0010	58.1	55.7
0.0050	67.1	30.1
0.0100	72.6	14.5

### 2.3.5 The Apparent Activation Energy

The apparent activation energy  $E_a$  is calculated using Arrhenius equation [1],

$$\ln(CR) = \frac{-E_a}{RT} + A \quad (2.49)$$

where  $E_a$  is the apparent activation energy for the corrosion of iron in acidic solution,  $R$  is the gas constant,  $A$  is the Arrhenius pre-exponential factor and  $T$  is the absolute temperature.

Figure 2.25 presents the Arrhenius plot for mild steel in 1M HCl solution in the presence of 0.005 M [BMIM]Cl at different temperatures. A plot of the natural logarithm of the corrosion rate of mild steel against  $1000\cdot 1/T$  gives straight lines as shown in Figure 2.15. The apparent activation energy for mild steel in 1M HCl solution in the absence or presence of various concentration of [BMIM]Cl is calculated using equation (2.43), and the values are listed in Table 2.6.

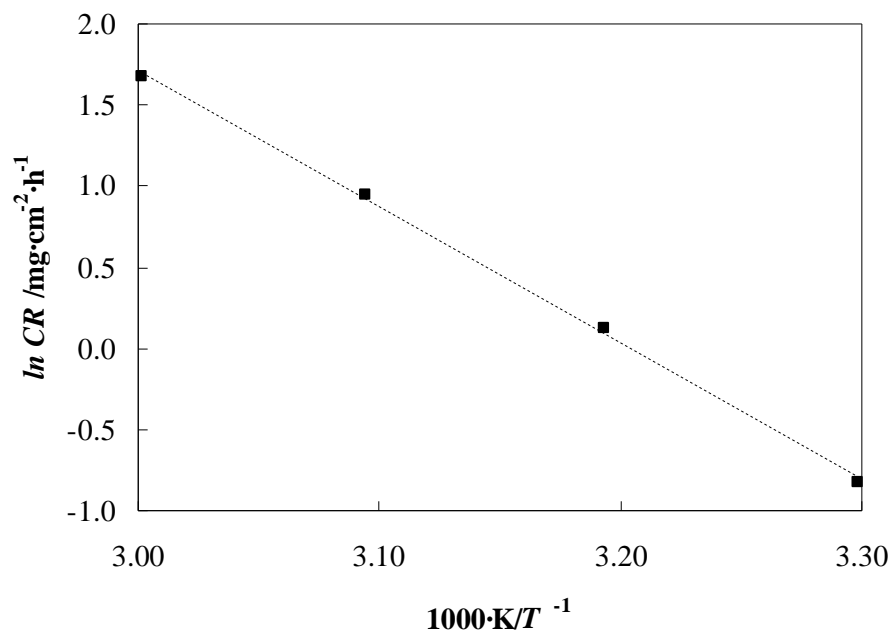


Figure 2.26 Arrhenius plot for mild steel in 1M HCl solution in the presence of 0.005 M 1-butyl-3-methylimidazolium chloride at different temperatures [22].

Table 2.6 The apparent activation energy for mild steel in 1M HCl solution in the absence and presence of [BMIM]Cl [22].

$C_{inh}/M$	$E_a/kJ\cdot mol^{-1}$
0	49.1
0.0005	57.9
0.0010	60.7
0.0050	69.8
0.0100	75.2



The data show that the apparent activation energy of the corrosion of mild steel in 1M HCl solution in the presence of the inhibitors is higher than those in the free acid solution. The value of  $E_a$  enhances with increasing inhibitor concentration, indicating more energy barrier for the reaction in the presence of the inhibitor is attained [22].



## CHAPTER 3

### RESEARCH METHODOLOGY

This chapter covers the experimental part of the present work. Chapter 3.1 presents the preparation of ionic liquids. The preparation includes synthesis and characterization of ionic liquids used for the study of thermodynamic and application of ionic liquids in this work. The structure of ionic liquids is determined using spectroscopy  $^1\text{H}$  and  $^{13}\text{C}$  NMR and Infra-red. The purity of ionic liquids is determined using elemental analysis and water content. Chapter 3.2 presents the measurement of physical properties of ionic liquids and binary mixture of ionic liquids with organic solvents. It includes density, viscosity, and refractive index. Finally, chapter 3.3 presents the experimental setup to measure the inhibition efficiency of ionic liquids on corrosion of carbon steel in acidic medium. Figure 3.1 shows the flow diagram of experimental work in the present work.

#### **3.1 Preparation of Ionic Liquids**

In the present work, ionic liquids were synthesized by protonation of alkanolamines with different organic acids. Ease of manufacturing and commercially available as well as low cost materials are some of the reasons for choosing alkanolamines as the cation source.

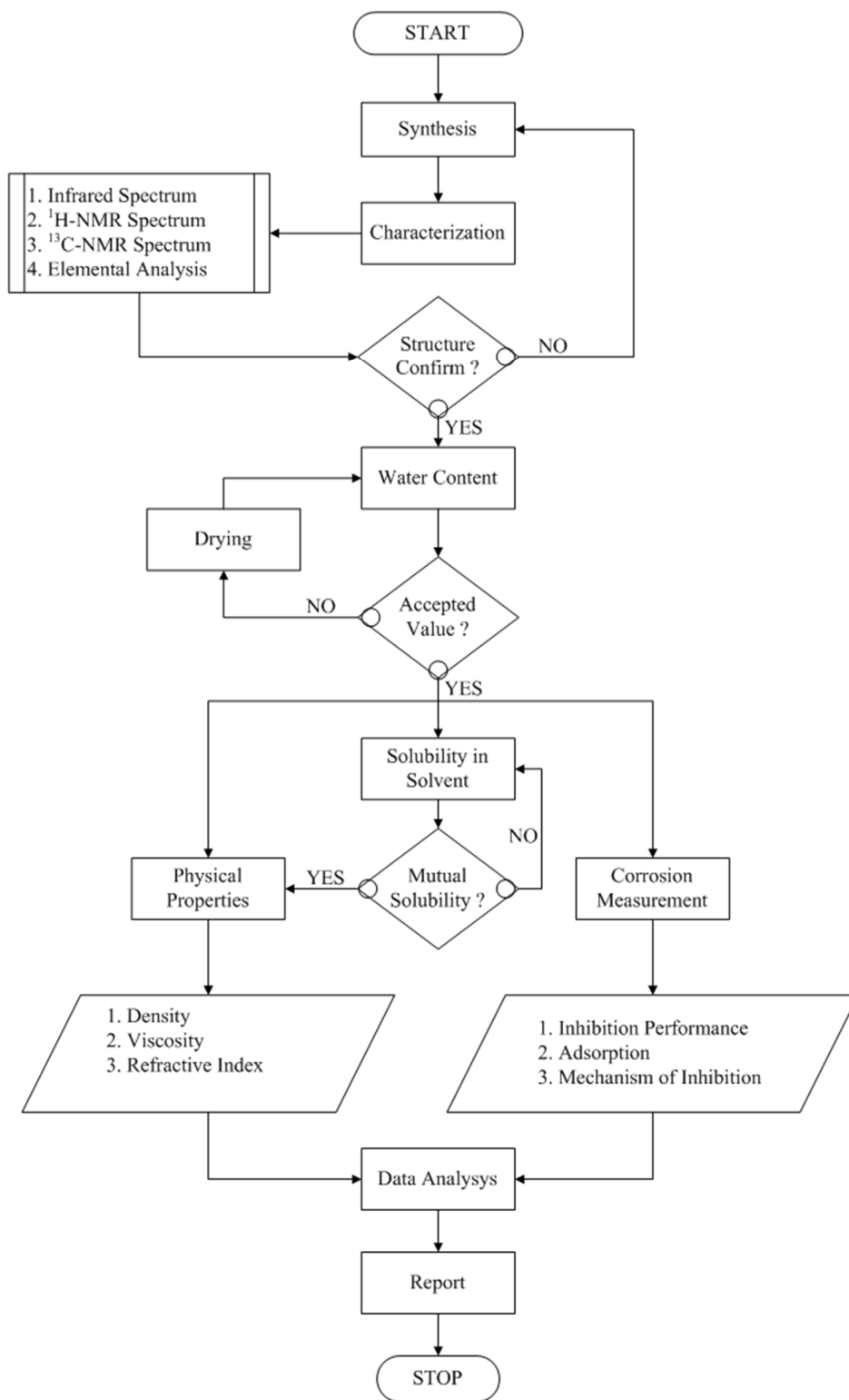


Figure 3.1 Flow diagram of experimental in the present work.

### 3.1.1 Chemicals

Synthetic grade of alkanolamines, such as monoethanolamine (MEA), diethanolamine (DEA), methyldiethanolamine (MDEA), and triethanolamine (TEA) were supplied from Merck® (Merck, Malaysia Sdn. Bhd.). High purity organic acids; such as formic acid, acetic acid, propionic acid, and lactic acid were also supplied from Merck® (Merck, Malaysia Sdn. Bhd.). Alcohol with reagents for pharmacopoeia analysis grade (ACS, ISO, Reag. Ph Eur) were also supplied from Merck® (Merck, Malaysia Sdn. Bhd.). The structure, formula, molar mass, and CAS number of the chemical used in this work are given in Table A.1 of Appendix A.

### 3.1.2 Synthesis of Ionic Liquids

In this work, ionic liquids were synthesized by protonation of alkanolamines using organic acids. Otherwise stated, all chemicals listed in table 3.1 were used as received from the supplier. Figure 3.2 gives the schematic preparation of ionic liquids synthesized in this work. These ionic liquids can be classified as protic ionic liquids as these ionic liquids were synthesized through direct protonation of alkanolamines using organic acids [178].

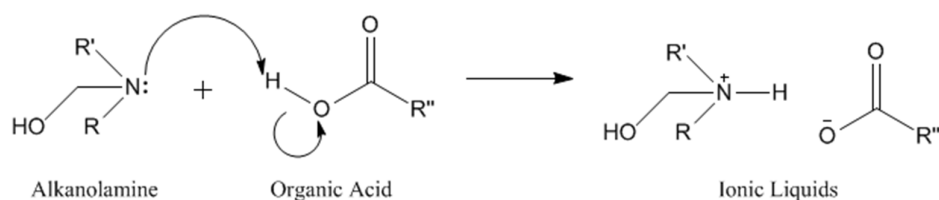


Figure 3.2 Schematic preparation of ionic liquids through protonation of alkanolamine using organic acid

### 3.1.2.1 *Synthesis of 2-hydroxyethanaminium formate*

A solution of 0.5 moles (18.9 mL) of formic acid were added slowly to a solution of 0.5 moles (29.9) mL of MEA in round bottom flask equipped with reflux condenser, a magnetic stirrer, and thermometer. The mixing temperature,  $T_m$ , was kept at 25 °C using ice bath. After all acid was added to the alkanolamine, the reaction mixture was stirred with continues stirring at heating temperature,  $T_h$ , 40 °C. The reaction was monitored by a thin layer chromatography using aluminum sheets silica gel and methanol as eluent. After reaching the reaction time,  $t_r$ , for 24 hours the resulting viscous liquid is washed with methanol and transferred into a rotary evaporator to remove unreacted materials and methanol. To ensure removal of the starting materials and methanol, the resulting viscous liquids is kept under vacuum oven for 24 hours. The ionic liquids are then kept in vial with PTFE septum. For any characterization purpose, ionic liquids are taken out using syringe equipped with needle to avoid atmosphere contamination particularly from the moisture.

### 3.1.2.2 *Synthesis of 2-hydroxyethanaminium Acetate*

The procedure describe above is also used to synthesise 2-hydroxyethanaminium Acetate [HEA]. For synthesis of [HEA], 28.6 ml of acetic acid and 29.9 ml of MEA were used.

### 3.1.2.3 *Synthesis of 2-hydroxyethanaminium Propionate*

The procedure describe above is also used to synthesis 2-hydroxyethanaminium propionate [HEP]. For synthesis of [HEP], 37.1 ml of propionic acid and 29.9 ml of MEA were used.

#### 3.1.2.4 *Synthesis of 2-hydroxyethanaminium Lactate*

The procedure describe above is also used to synthesize 2-hydroxyethanaminium Lactate [HEL]. For synthesis of [HEL], 37.2 ml of acetic acid and 29.9 ml of MEA were used.

#### 3.1.2.5 *Synthesis of Bis(2-hydroxyethyl)ammonium Formate*

The procedure describe above is also used to synthesize bis(2hydroxyethyl)ammonium Formate [BHEAF]. For synthesis of [BHEAF], 18.9 ml of formic acid and 48.2 ml of DEA were used with  $T_m$ ,  $T_h$ , and  $t_r$  set at 40 °C, 50°C, and 48 hours, respectively.

#### 3.1.2.6 *Synthesis of Bis(2-hydroxyethyl)ammonium Acetate*

The procedure describe above is also used to synthesize bis(2hydroxyethyl)ammonium Acetate [BHEAA]. For synthesis of [BHEAA], 28.6 ml of acetic acid and 48.2 ml of DEA were used with  $T_m$ ,  $T_h$ , and  $t_r$  set at 50 °C, 75°C, and 72 hours, respectively.

#### 3.1.2.7 *Synthesis of Bis(2-hydroxyethyl)ammonium Propionate*

The procedure describe above is also used to synthesize bis(2hydroxyethyl)ammonium Propionate [BHEAP]. For synthesis of [BHEAP], 37.1 mL of propionic acid and 48.2 ml of DEA were used with  $T_m$ ,  $T_h$ , and  $t_r$  set at 50 °C, 75°C, and 48 hours, respectively.

#### 3.1.2.8 *Synthesis of Bis(2-hydroxyethyl)ammonium Lactate*

The procedure describe above is also used to synthesize bis(2hydroxyethyl)ammonium Lactate [BHEAL]. For synthesis of [BHEAL], 37.2

mL of lactic acid and 48.2 ml of DEA were used with  $T_m$ ,  $T_h$ , and  $t_r$  set at 50 °C, 75°C, and 48 hours, respectively.

#### 3.1.2.9 *Synthesis of Bis(2-hydroxyethyl)methylammonium Formate*

The procedure describe above is also used to synthesize bis(2hydroxyethyl)methylammonium Formate [BHEMF]. For synthesis of [BHEMF], 18.9 mL of formic acid and 57.3 mL of MDEA were used with  $T_m$ ,  $T_h$ , and  $t_r$  set at 40 °C, 55°C, and 36 hours, respectively.

#### 3.1.2.10 *Synthesis of Bis(2-hydroxyethyl)methylammonium Acetate*

The procedure describe above is also used to synthesize bis(2hydroxyethyl)methylammonium Acetate [BHEMA]. For synthesis of [BHEMA], 28.6 mL of acetic acid and 57.3 mL of MDEA were used with  $T_m$ ,  $T_h$ , and  $t_r$  set at 40 °C, 55°C, and 36 hours, respectively.

#### 3.1.2.11 *Synthesis of Bis(2-hydroxyethyl)methylammonium Propionate*

The procedure describe above is also used to synthesize bis(2hydroxyethyl)methylammonium Propionate [BHEMP]. For synthesis of [BHEMP], 37.1 mL of propionic acid and 57.3 mL of MDEA were used with  $T_m$ ,  $T_h$ , and  $t_r$  set at 40 °C, 55°C, and 36 hours, respectively.

#### 3.1.2.12 *Synthesis of Bis(2-hydroxyethyl)methylammonium Lactate*

The procedure describe above is also used to synthesize bis(2hydroxyethyl)methylammonium Lactate [BHEML]. For synthesis of [BHEML], 37.2 mL of lactic acid and 57.3 mL of MDEA were used with  $T_m$ ,  $T_h$ , and  $t_r$  set at 40 °C, 55°C, and 36 hours, respectively.



### 3.1.2.13 *Synthesis of Tris(2-hydroxyethyl)ammonium Formate*

The procedure describe above is also used to synthesize tris(2hydroxyethyl)ammonium Formate [THEAF]. For synthesis of [THEAF], 18.9 mL of formic acid and 66.6 mL of TEA were used with  $T_m$ ,  $T_h$ , and  $t_r$  set at 50 °C, 75°C, and 72 hours, respectively. After 72 hours, the mixture was brought to room temperature. The resulting white solid obtained is washed with methanol and transferred into a rotary evaporator to remove any unreacted materials and methanol. To ensure complete removal of starting materials and methanol, the resulting white solid is kept under vacuum oven for 24 hours. The ionic liquids were kept in vial with PTFE septum. [THEAF] is solid at room temperature.

### 3.1.2.14 *Synthesis of Tris(2-hydroxyethyl)ammonium Acetate*

The procedure describe above is also used to synthesize tris(2hydroxyethyl)ammonium Acetate [THEAA]. For synthesis of [THEAA], 28.6 mL of acetic acid and 66.6 mL of TEA were used with  $T_m$ ,  $T_h$ , and  $t_r$  set at 50 °C, 60°C, and 72 hours, respectively.

### 3.1.2.15 *Synthesis of Tris(2-hydroxyethyl)ammonium Propionate*

The procedure describe above is also used to synthesize tris(2hydroxyethyl)ammonium Propionate [THEAP]. For synthesis of [THEAP], 37.1 mL of propionic acid and 66.6 mL of TEA were used with  $T_m$ ,  $T_h$ , and  $t_r$  set at 50 °C, 50°C, and 72 hours, respectively.

### 3.1.2.16 *Synthesis of Tris(2-hydroxyethyl)ammonium Lactate*

The procedure describe above is also used to synthesize tris(2hydroxyethyl)ammonium Lactate [THEAL]. For synthesis of [THEAL], 37.2

mL of lactic acid and 66.6 mL of TEA were used with  $T_m$ ,  $T_h$ , and  $t_r$  at 50 °C, 50°C, and 72 hours, respectively.

### 3.1.3 Characterization of Ionic Liquids

The synthesized ionic liquids are characterized using Spectroscopy Infrared (IR) and Nuclear Magnetic Resonance (NMR);  $^1\text{H}$ -NMR, and  $^{13}\text{C}$ -NMR. The composition of synthesized ionic liquids is determined using elemental analysis. The purity of synthesized ionic liquids is determined using water content analysis.

#### 3.1.3.1 *Infrared Spectroscopy*

The infrared (IR) spectra of synthesized ionic liquids are obtained on a Perkin Elmer Spectrum One Fourier Transform Infrared spectrometer. The ionic liquid samples were sandwiched between two plates of a salt. The plates are transparent to the infrared light and do not introduce any lines onto the spectra. The IR spectra produced had wave number range of 600 – 4000  $\text{cm}^{-1}$ .

#### 3.1.3.2 *Spectrum NMR*

In NMR, 5 to 10 mg of sample was dissolved in  $\pm 0.7 \text{ cm}^3$  of Dimethylsulfoxide (DMSO). The  $^1\text{H}$  and  $^{13}\text{C}$  NMR spectra were recorded at room temperature on JEOL JNM-ECA400 or Bruker Avance 300 spectrometer. The  $^1\text{H}$  and  $^{13}\text{C}$  chemical shifts ( $\delta$ ) are reported in parts per million (ppm) references with Tetra methyl silane (TMS) as an internal standard. Multiplicities are abbreviated as s, singlet; d, doublet; t, triplet; and m, multiplet.

### 3.1.3.3 *Elemental Analysis*

The composition of synthesized ionic liquids is determined using Elemental analyses are measured using CHNS-932 (LECO Instruments) elemental analyzer. The instrument was calibrated using standard calibration sample with known chemical composition provided by supplier before each measurement. A sample size of  $\pm 2$ mg was used for each measurement and the analysis for each sample was done at least 3 times and the average values were reported.

### 3.1.3.4 *Water Content*

Apart from routine structure analysis and determination, it is essential that ionic liquids are analyzed for its water content. Measurement of water content is an important aspect in the synthesis and characterization of ionic liquids. Ideally the ionic liquids should be dried until it contains negligible water content. In most cases, the water contents of ionic liquids are reported in the range between 100 to 10000 ppm. In this work, the water content of ionic liquids is determined using a coulometer Karl Fischer titrator, DL 39 (Mettler Toledo) with the Hydranal coulomat AG reagent (Riedel-de Haen).

## 3.2 **Measurement of Physical Properties**

Once the ionic liquids are dried until it contained less than 500 ppm of water, it is then measured for its physical properties. The ionic liquids are kept in vial with PTFE septum under electronic desiccators. For physical properties measurements, the samples are taken using syringe equipped with needle. This is done to avoid absorption of water and moisturizer into the ionic liquids, as the synthesized ionic liquids are highly hygroscopic and the presence of water can affect its physical properties. The physical properties of interest in this work include density, viscosity, and refractive index.

### 3.2.1 Density

The density of pure ionic liquids is measured using a densimeter, Anton Paar DMA 5000 (Anton Paar, Austria). The apparatus is calibrated regularly by measuring the density of Millipore quality water (SH Calibration Service GmbH, Graz) and dried air according to the prescribed manual. The calibrated apparatus is also verified using organic solvents and commercial ionic liquids, and found to be within the adjusted uncertainty of the apparatus. The procedure for the density measurements of all the samples is conducted according to the following steps;

#### 1. Cleaning and drying of measuring cell

Suitable solvents are used to clean and dry the measuring cell. Two solvents are used, the first solvent is used to clean up the measuring cell while the second solvent is used to remove the residue of the first solvent and also to dry the measuring cell. In the present work, methanol and acetone are used as the first and second solvent, respectively. As the synthesized ionic liquids have high solubility in methanol, it will be easy to remove the remaining sample in the measuring cell. The residue of methanol in the measuring cell is removed by adding the second solvent. These solvents are injected several times into the measuring cell using syringe. Later, dry air is blown through the measuring cell using a built in air pump for 5-10 minutes.

#### 2. Measurement settings

The settings for density measurement of all samples are adjusted to work at 'medium equilibrium mode'. For pure ionic liquids, densities are measured at temperature from (273.15 to 353.15) K while for binary mixture, their densities are measured at temperature from (273.15 to 323.15) K. The measurement temperature is adjusted from a low temperature to a high temperature with 5 K step increment from the initial to the final temperature range.

#### 3. Density measurement

The sample is taken from the vial with PTFE septum using syringe and slowly injected into a U-tube measuring sample ensuring that there is no bubble present in

the cell by viewing through the optical window. The preset method is activated to start the density measurement which is then recorded in the data memory.

#### *3.2.1.1 Measurement of Density of 1 M HCl Solution*

In addition to measurement of density of pure ionic liquids and binary mixture of ionic liquids [BHEAF] with alcohol, the density of 1 M HCl solution in the presence of various concentration of ionic liquids [BHEAF] are also measured using pycnometer. Pycnometer is used instead of Anton Paar Densimeter DMA-5000 because its vibrating tube is not compatible with acid solution. For this purpose, an empty 25 ml calibrated-pycnometer is weight using analytical balance (Mettler Toledo, model AS120S) with a precision of  $\pm 0.0001$  g. The pycnometer is then filled with desired solution and weight the mass of pycnometer with the solution. The density is then calculated on the basis of mass change of the volume.

### **3.2.2 Viscosity**

The viscosities are measured using a SVM 3000 Stabinger Viscometer, (Anton Paar, Austria). The apparatus is calibrated using few standard calibration fluids according to instruction given by the supplier. The calibrated apparatus is also verified using organic solvents and commercial ionic liquids, and found to be with in the adjusted uncertainty of the apparatus.

The procedure for the viscosity measurements of all the samples is outlined below;

#### 1. Cleaning and drying of measuring cell

Toluene is used as the solvent to clean and dry the measuring cell. This solvent is injected several times into the measuring cell using syringe. Later, dry air is blown through the measuring cell using a built in air pump for 5-10 minutes.

## 2. Measurement settings

The settings for viscosity measurement of all samples are adjusted to work at 'medium equilibrium method'. For pure ionic liquids, viscosities are measured at temperature from (273.15 to 353.15) K while for binary mixture, their viscosities are measured at temperature from (273.15 to 323.15) K. The measurement temperature is adjusted from a low temperature to a high temperature with 5 K step increment from the initial to the final temperature range.

## 3. Viscosity measurement

The sample is taken from vial with PTFE septum using syringe and slowly injected into U-tube measuring sample ensuring that there is no bubble in the cell and followed by pressing the START button to execute the viscosity measurement.

### 3.2.3 Refractive Index

The refractive indexes of pure ionic liquids and its binary mixtures with organic solvents are determined using ATAGO programmable digital refractometer model RX-5000 alpha, with measuring accuracy of  $\pm 4 \times 10^{-5}$ . The apparatus is calibrated frequently and before each series of sample measurements through determining the refractive index of Millipore quality water. The calibrated apparatus is also verified by measuring the refractive index of organic solvents and commercial ionic liquids. The measuring procedure for refractive index consists of the following steps

#### 1. Cleaning and drying of measuring cell

Water and acetone are used to clean and dry the prism measuring cell. Water is used as synthesized ionic liquids have high solubility in water. Hence the ionic liquids sample can be easily removed. Meanwhile, the water residue is dried using acetone. A few drops of solvents are placed in the prism measuring cell and wiped using tissue.

## 2. Measurement setting

The refractive indexes of ionic liquids and its binary mixture with organic solvents are measured at temperature from (273.15 to 323.15) K. The temperatures are maintained using Julabo F26 water circulation. The measurement temperature is adjusted from a low temperature to a high temperature with 5 K step increment from the initial to the final temperature range.

## 3. Refractive index measurement

A sample is placed on cleaned prism which is covered with a lid followed by pressing the START button to execute the refractive index measurement. The results are displayed on LCD in few seconds.

### 3.2.4 Preparation of Binary Mixture

The binary mixtures of ionic liquids [BHEAF] with methanol, ethanol, and 1-propanol are prepared in glass vials with PTFE septum. Samples are taken from the vial with a syringe through a PTFE septum. The samples are prepared in an inert atmosphere glove box, using an analytical balance (Mettler Toledo, model AS120S) with a precision of  $\pm 0.0001$  g. A glove box is used because the ionic liquids are highly hygroscopic, and small quantities of water can cause considerable change in the physical properties. The possible error in the mole fraction calculations is estimated to be around  $\pm 0.0001$ .

Methanol, Ethanol, and 1-propanol used in the present study are supplied by Merck (Merck, Malaysia) and is degassed ultrasonically and dried over molecular sieves type 4Á, (supplied by Aldrich) and kept in bottles with PTFE septum under electronic desiccators with water contents of less than  $4 \times 10^{-5}$  mass fraction.

The physical properties of interest for the binary mixture of ionic liquids with alcohol include density, viscosity, and refractive index, The measurement method used are the same as before for the pure ionic liquids.

### **3.3 Corrosion Study**

This section provides details of the corrosion experiments conducted, including specimen and solution preparations, experimental setup, experimental procedure, and data analysis. Two methods of corrosion tests were employed; weight loss and electrochemical methods. The weight loss method is the simplest form of corrosion monitoring and predominantly designed to investigate general corrosion. It is used for determining corrosion rates and behavior under long term exposure of carbon steel on the acidic medium. Weighed test specimens are exposed to the acidic medium for a specific period of time and subsequently removed for determining the weight loss of the specimen and ultimately the corrosion rate. The electrochemical method is used for determining the corrosion rate of carbon steel under a shorter term exposure and revealing the corrosion behavior at the mechanistic level. These methods involve Tafel Plot, Linear Polarization Resistance (LPR), and Electrochemical Impedance Spectroscopy (EIS).

#### **3.3.1 Preparation of Solution**

An aqueous solution of 1 M HCl is prepared from a 38% HCl reagent (Merck, Merck Sdn. Bhd.) and deionized water. The solution is loaded with a desired concentration of ionic liquids by mixing the ionic liquids into the solution. The amount of ionic liquids needed is weighed using an analytical balance (Mettler Toledo, model AS120S) with a precision of  $\pm 0.0001$  g.

#### **3.3.2 Preparation of Specimen**

Two types of specimens are used in this work, stainless steel 430 (SS430) and carbon steel BS970. The stainless steel SS 430 is regularly used for standardizing the experimental procedures and instrumentation for electrochemical tests, whereas carbon steel BS970 is used for all actual weight loss and electrochemical test. Composition of carbon steel BS970 is given in Table 3.2.



Table 3.1 The amount of ionic liquids needed to make 0.02, 0.04, 0.06, and 0.08 M of solution

	Concentration of inhibitor / M			
	0.02	0.04	0.06	0.08
HEF	2.14	4.28	6.43	8.57
HEA	2.42	4.85	7.27	9.69
HEP	2.70	5.41	8.11	10.81
HEL	3.02	6.05	9.07	12.09
BHEAF	3.02	6.05	9.07	12.09
BHEAA	3.30	6.61	9.91	13.22
BHEAP	3.58	7.17	10.75	14.34
BHEAL	3.90	7.81	11.71	15.62
BHEMF	3.30	6.61	9.91	13.22
BHEMA	3.58	7.16	10.75	14.33
BHEMP	3.86	7.73	11.59	15.46
BHEML	4.18	8.37	12.55	16.74
THEAF	3.90	7.81	11.71	15.62
THEAA	4.18	8.37	12.55	16.74
THEMP	4.47	8.93	13.40	17.86
THEAL	4.79	9.57	14.36	19.14

Table 3.2 Chemical composition of carbon steel BS 970.

Element	Composition (%)	Element	Composition (%)
C	0.148	Cr	0.069
Si	0.175	Mo	0.014
Mn	0.799	Ni	0.065
P	0.01	Fe	Balance
S	0.032		

Figure 3.3 shows the sketches of specimens used for weight loss and electrochemical experiments. Carbon steel BS970 with outer diameter of 12 mm is cut into 10 mm long cylinder specimens, giving a specimen area of 113 mm<sup>2</sup>. Prior to the tests, the specimens are prepared by wet grinding with 1200 grit silicon carbide paper using isopropanol, cleaned with acetone in an ultrasonic bath and flushed with ethanol. Then the specimens are blow-dried and mounted on the specimen holder. All specimens are kept in a desiccator until it is used.

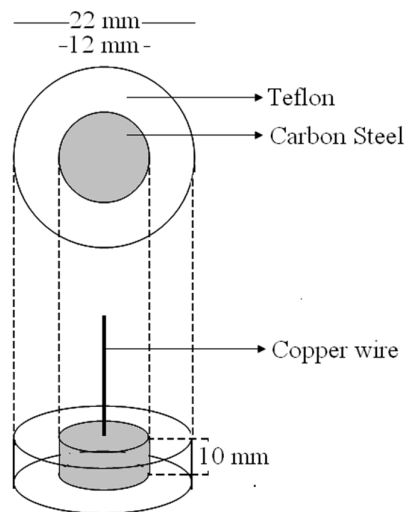


Figure 3.3 Illustration of the working electrode used for measurement of corrosion experiment.

### 3.3.3 Weight Loss Method

This is the oldest, versatile and simplest technique, used both in laboratory and field, to measure the average rate of uniform corrosion. The specimen used for these test is called corrosion coupons. They can be rectangular or round and are usually stamped for identification purposes. Surface finish of these coupons is important because corrosion rate is very sensitive to the presence of surface defects and cold work. Diamond or carbide abrasive papers are used in industries for cleaning the specimens.

The weight loss measurement method is based on the geometric weight loss. This measurement requires long exposure time to reach measurable corrosion rate [1].

### 3.3.3.1 *Experimental Procedures*

The setup consists of 1 L beaker covered with Teflon lids, a heater equipped with thermometer, and a pH meter. The test environment is maintained at the desired temperature by means of the heater. The temperature is checked using thermometers placed directly inside the cell. The weight loss of carbon steel coupon exposed to 1 L of 1 M HCl solution at temperatures of 25, 40, 55, and 70 °C were determined after 24 h for acid solutions in the presence of various concentrations of ionic liquids used [22-24].

### 3.3.3.2 *Method of Cleaning Specimens after Test*

Cleaning the specimens after the experiment is a vital step in the corrosion test procedure. In this work, it is done by washing the specimen under running-tap water, scrubbing and brushing lightly using a non metallic bristle brush to remove loose, bulky corrosion products. Care should be taken to avoid the removal of sound metal. The specimen is then dried with air and weighed [22-24].

### 3.3.3.3 *Calculation of Corrosion Rate*

The corrosion rate of carbon steel in the presence of various concentrations of ionic liquids is calculated according to ASTM G1 - 03, Practice for Preparing, Cleaning, and Evaluating using the following equation,

$$CR = \frac{K \times W}{A \times T \times D} \quad (3.1)$$

where  $CR$  is Corrosion rate in  $\text{g}\cdot\text{m}^{-2}\cdot\text{h}^{-1}$ ,  $K$  is a constant ( $1.00 \times 10^4 \times D$ ),  $T$  is time of exposure in hours to the nearest 0.01 h,  $A$  is area in  $\text{cm}^2$  to the nearest 0.01  $\text{cm}^2$ ,  $W$  is

mass loss in g, to nearest 1 mg (corrected for any loss during cleaning, and  $\rho$  is density of steel in  $\text{g}\cdot\text{cm}^{-3}$ ).

#### 3.3.3.4 Inhibition Calculation

The inhibition efficiency for all inhibitors is calculated using the equation 2.35,

$$\%IE = \frac{CR_{corr} - CR_{corr}^{inh}}{CR_{corr}} \times 100 \quad (2.35)$$

### 3.3.4 Electrochemical Method

The setup consists of a corrosion cell, a potentiostat, a heater equipped with thermometer, a gas supply set, and a data acquisition system. The corrosion cell is a standard three electrode cell [25]. It is a fully equipped glass vessel used for stimulating a corrosive environment. A schematic diagram of the corrosion cell is shown in Figure 3.10. The potentiostat is an electronic device capable of supplying and controlling the potentials of specimen (working electrode) and also measuring the currents produced from the corrosion cell. An ACM potentiostat/galvanostat providing an accuracy of  $\pm 0.2\%$  of the potential and current readings is used. To ensure its performance, the potentiostat is calibrated regularly using a built in calibration function mode.

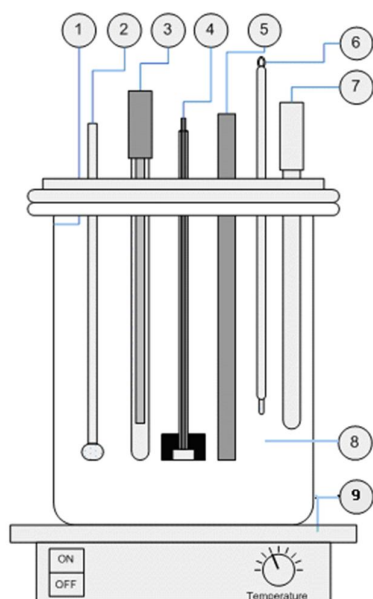


Figure 3.4 General setup for the measurement of corrosion rate using three electrodes configurations. (1) Glass cell, (2) N<sub>2</sub> bubbler, (3) Reference electrode, (4) Working electrode, (5) Counter electrode, (6) Thermometer, (7) pH meter, (8) Electrolyte solution, and (9) Heater.

#### 3.3.4.1 Tafel Plots

Tafel Plots is an electrochemical technique used to obtain some information on the reaction mechanism of the inhibitor and also to evaluate its inhibition efficiency. Unlike weight loss methods, which may take days or weeks, electrochemical experiments is a rapid techniques which could be done in few hours. This is especially useful for corrosion measurement of highly corrosion resistant metal or alloy. A Tafel Plots is performed on a specimen by polarizing the specimen about  $\pm 350$  mV both anodically and cathodically [22-24].

The corrosion cell, as shown in Figure 3.10, is filled with 1 L of 1 M HCl with different concentration of ionic liquids. The top of the corrosion cell is covered with a lid and fixed on the corrosion cell using two screws. A pre-polished coupon, reference electrode, and counter electrode are installed and put the connection through the lid

cover. The three electrodes are connected to the ACM potentiostat/galvanostat and kept for 90 minutes. Then, the potentiostat and the software were started and kept for another 30 minutes to get stable open circuit potential (OCP). When stable OCP is reached, the program is initiated to polarize the test electrode with  $\pm 350$  mV with scan rate of 10 mV/minute. After completion, the data is imported to Excel file for  $R_p$  values calculations. The Tafel Plot data measured by the software is plotted in Excel file as potential vs. current densities for each run [22-24].

The inhibition efficiency for all inhibitors are calculated using the equation (2.36),

$$\%IE = \frac{i_{corr} - i_{corr}^{inh}}{i_{corr}} \times 100 \quad (2.36)$$

#### 3.3.4.2 Linear Polarization Resistance

Linear Polarization Resistance (LPR) techniques is one of the most widely used methods for measuring corrosion rate or inhibition efficiency of new inhibitor. LPR is simple and rapid and when applied to aqueous electrolyte solutions, provides an instantaneous measurement of corrosion rate. In fundamental terms, a small voltage of polarization potential is applied to an electrode in solution. The current needed to maintain a specific voltage shift, typically 10 mV, is directly related to the corrosion on the surface of the electrode in the solution. By measuring the current, a corrosion rate can be calculated. In this work, LPR is done using the same procedure for Tafel plot, but the coupon is given a potential of 10 mV cathodically and anodically, instead of 350 mV [22-24].

The inhibition efficiency for all inhibitors were calculated using equation (2.37),

$$\%IE = \frac{R_p^{inh} - R_p}{R_p^{inh}} \times 100 \quad (2.37)$$

### 3.3.4.3 Electrochemical Impedance Spectroscopy

The Electrochemical Impedance Spectroscopy (EIS) measurements are recorded immediately after the LPR on the same electrode without any further surface treatment. The response of the electrochemical system to alternating current (AC) excitation with a frequency ranging mainly from 95 kHz to 0.1 Hz (in some cases down to 0.03 Hz) and peak to peak amplitude of 10 mV was measured. The lock-in amplifier technique is used in the frequency range of 5 Hz to 100 kHz with 5 points per decade. Measurements below 10 Hz were performed using fast Fourier transformation (FFT) technique with eight data cycles. All EIS are recorded at the open circuit potential, *i.e.*, at the corrosion potential  $E_{corr}$ . Various equivalent circuit models are fitted to the impedance data using a non-linear least squares fit procedure. The inhibition efficiency is calculated using equation (2.33) [22-24],

$$\%IE = \frac{R_t^{inh} - R_t}{R_t^{inh}} \times 100 \quad (2.38)$$





## CHAPTER 4

### SYNTHESIS AND PHYSICAL PROPERTIES OF IONIC LIQUIDS

This chapter presents the experimental result on synthesis and physical properties of the ionic liquids studied. Section 4.1 presents the result on synthesis and characterization of the ionic liquids. The synthesized ionic liquids are characterized using Spectroscopies infrared and  $^1\text{H}$  and  $^{13}\text{C}$ -NMR, CHN analysis, and its water content. The result on measured physical properties of ionic liquids, namely density, viscosity, and refractive index, are reported in section 4.2. The discussion is focused on the effect of temperature on physical properties of the ionic liquids. A correlation is developed to represent the temperature dependence of the physical properties of ionic liquids. Moreover, from the temperature dependence of density, the coefficient of thermal expansion is calculated. Finally, the effect of alcohol on the physical properties of the ionic liquids is presented in section 4.3.

#### **4.1 Hydroxyl Ammonium Ionic Liquids**

In this work, 16 ionic liquids were synthesized. The chemical structure and abbreviation is given in Table A.2 of Appendix A. The synthesized ionic liquids in this work were liquids at room temperature, except for [THEAF]. [THEAF] is a white solid. The same observation is reported in the literature [95]. This phenomenon can be explained by looking through the structure of [THEAF]. [THEAF] has high symmetry of cation with small size of anion thus enabling more efficient ion-ion packing in the crystal cell of [THEAF]. Consequently, [THEAF] is solid at room temperature.

Further investigation using Differential Scanning Calorimetry (DSC) revealed that the melting point of [THEAF] is 59°C. Hence, it still falls under ionic liquids category.

#### 4.1.1 Infrared Spectrum

Figure 4.1 – 4.4 present the infrared (IR) spectra of synthesized ionic liquids in this work. The two important areas for a preliminary examination of an IR spectrum are the regions 4000 – 1300 and 900 – 650  $\text{cm}^{-1}$ . The high-frequency side of the IR spectrum is attributed to the hydroxyl functional group within the ionic liquids. The characteristic stretching frequencies for important functional group of synthesized ionic liquids in this work such as hydroxyl ( $-\text{OH}$ ), ammonium ( $-\text{NH}$ ), and carboxylate ( $-\text{O}-\text{C}=\text{O}$ ) occur in this parts of the spectrum. The conversion of carboxylic acid to a salt, in the case of ionic liquids, shows two characteristic carbonyl absorption bands in addition to an ammonium band in the 2700 – 2200  $\text{cm}^{-1}$  region [179].

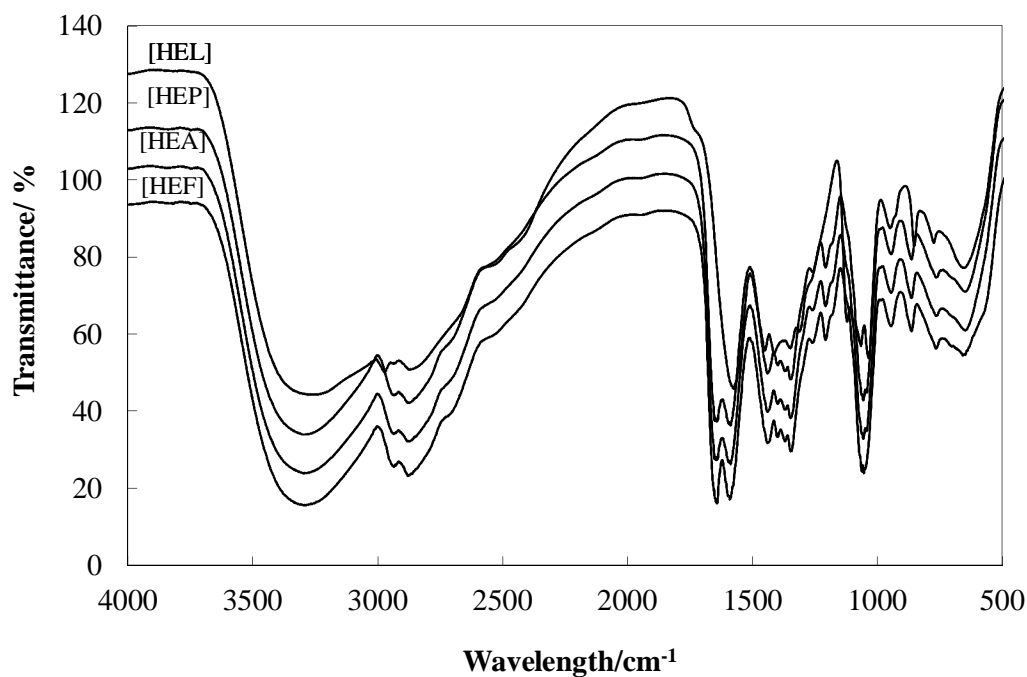


Figure 4.1 Infrared spectra of ionic liquids [HEF], [HEA], [HEP], and [HEL]

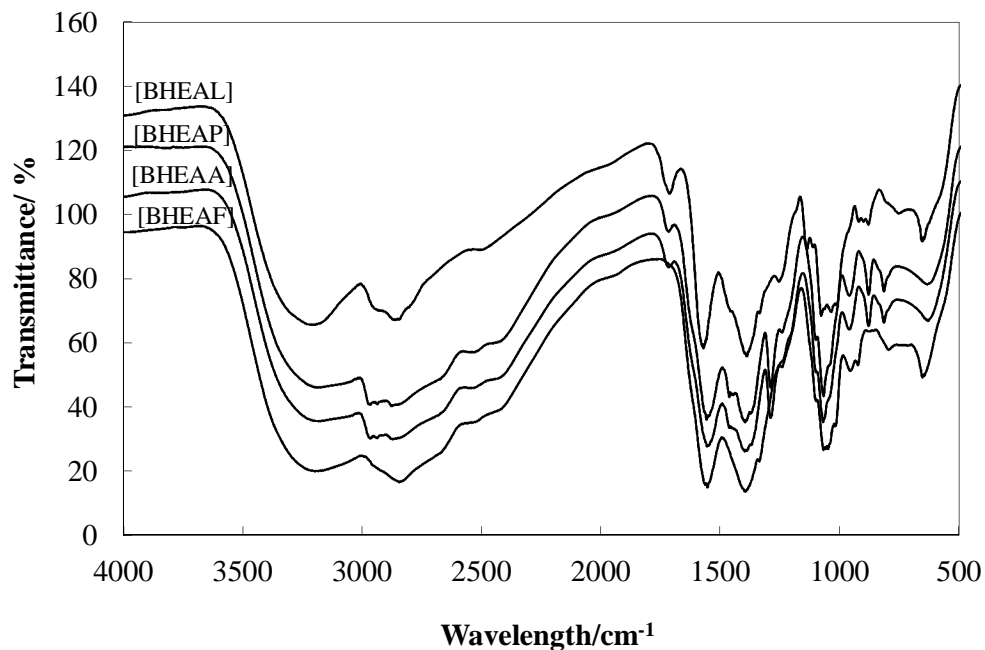


Figure 4.2 Infrared spectra of [BHEAF], [BHEAA], [BHEAP], and [BHEAL]

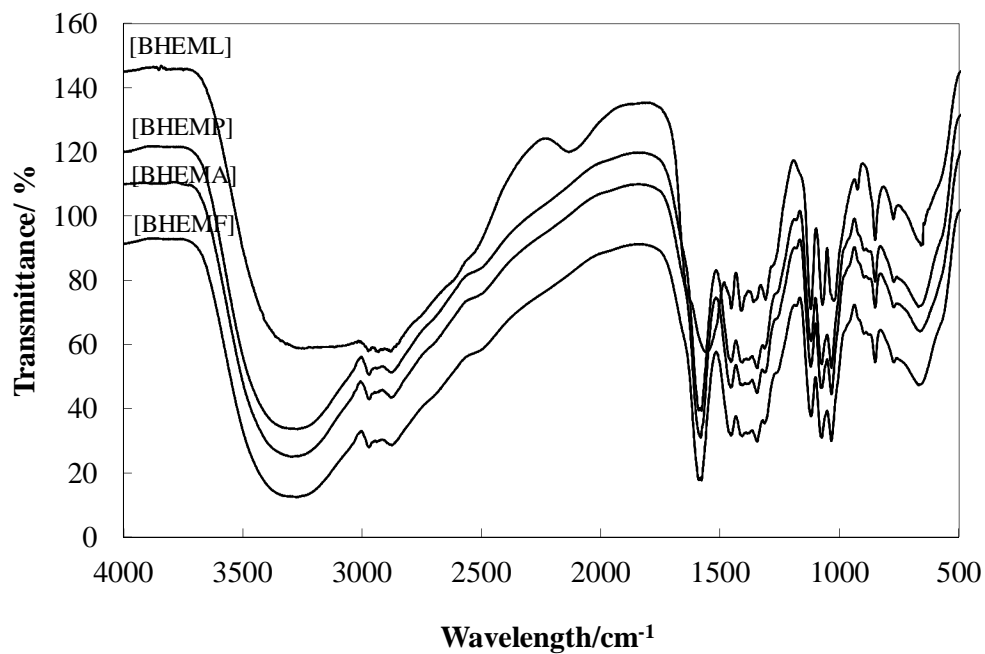


Figure 4.3 Infrared spectra of [BHEMF], [BHEMA], [BHEMP], and [BHEML]

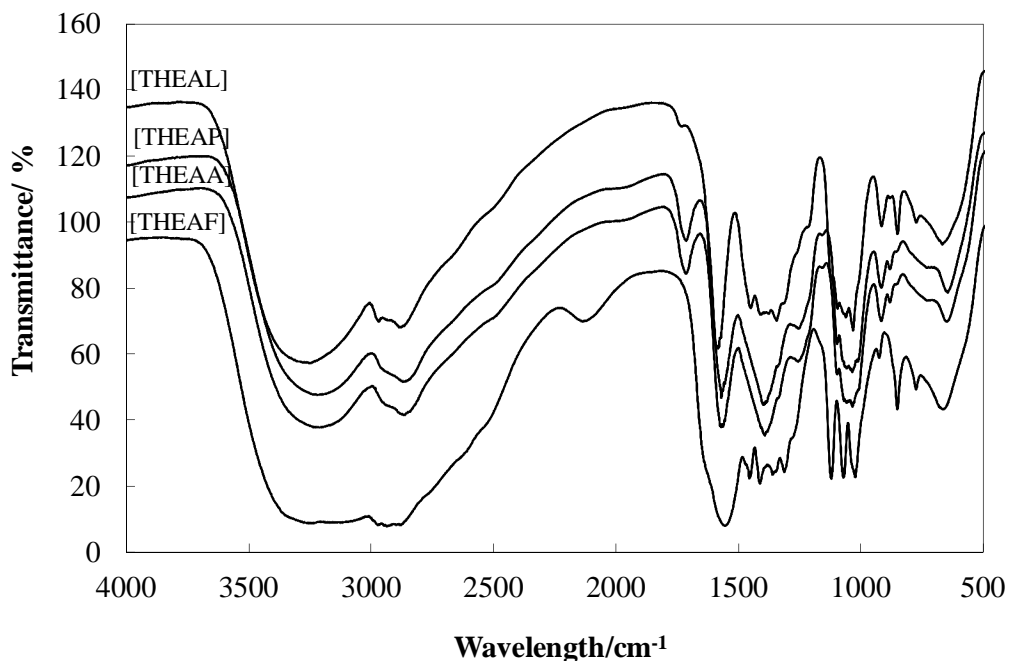


Figure 4.4 Infrared spectra of [THEAF], [THEAA], [THEAP], and [THEAL]

One of the characteristic bands observed in the IR spectra of the ionic liquids resulted from the O–H stretching and C–O stretching. These vibrations are sensitive to hydrogen bonding. Ionic liquids show intermolecular hydrogen bonding as a broad band at  $3172\text{ cm}^{-1}$ . The C–O stretching vibrations produce a peak at  $1066\text{ cm}^{-1}$ . The O–H in-plane bending vibration occurs in the general region of  $1420 - 1330\text{ cm}^{-1}$ . In primary alcohol, as present in ionic liquids, the O–H in-plane bending couples with the C–H wagging vibrations to produce two bands; the first near  $1440\text{ cm}^{-1}$  and the second near  $1330\text{ cm}^{-1}$  [179]. Table 4.1 lists the regular peaks appear in the IR spectrum of the synthesized ionic liquids.

The spectrum infrareds of the synthesized ionic liquids show similar feature, vibration of hydroxyl functional group, amine salts, and carboxylic acid as expected from hydroxyl ammonium ionic liquids. Therefore it can be concluded that the synthesis method used in this work was successful.

Table 4.1 List of peak appear in the infrared spectrum of the synthesized ionic liquids in this work

Peak Number (cm <sup>-1</sup> )	Chemical group assignment [179].
3300 – 3030	N–H stretching vibration
3000 – 2800	asymmetrical and symmetrical stretching in the HN <sup>+</sup> group
3000 – 2700	Salts of secondary amines
2700 – 2200	The conversion of carboxylic acid to a salt, in the case of ionic liquids
1650 – 1550	The carboxylate anion

#### 4.1.2 NMR Spectrum

Figure 4.5 and 4.6 present the <sup>1</sup>H-NMR and <sup>13</sup>C-NMR spectrum of [BHEAF], respectively. The other NMR spectrums of the synthesized ionic liquids are given in Appendix B. Figure 4.5 shows the <sup>1</sup>H-NMR spectra for [BHEAF] which are in good agreement with that reported in literature [95]. The proton at C-1 and C-2 showed triplet peak and being deshielded effect of N<sup>+</sup> ion at 2.81 and 3.48 ppm, respectively. A broad peak is observed and centered at 4.53 ppm due to presence of hydrogen attach to nitrogen and oxygen. Hydrogen attached in carboxylate anion, C-3, showed single peak at 8.40 ppm. No extra peak is observed in the spectra indicating no impurities on the ionic liquids [BHEAF].

Figure 4.3 shows the <sup>13</sup>C-NMR spectra for [BHEAF]. <sup>13</sup>C-NMR (400 MHz, DMSO) δ 163.21 ppm (C carboxylate), 58.89 ppm (C-N), 39.40 (C-O) ppm. There are no data reported in the literature for <sup>13</sup>C-NMR spectrum of the other ionic liquids as comparison. As can be seen from Figure 4.2 and 4.3, the spectrum of <sup>1</sup>H and <sup>13</sup>C-NMR for [BHEAF] indicate that the synthesis of ionic liquids has been successful.

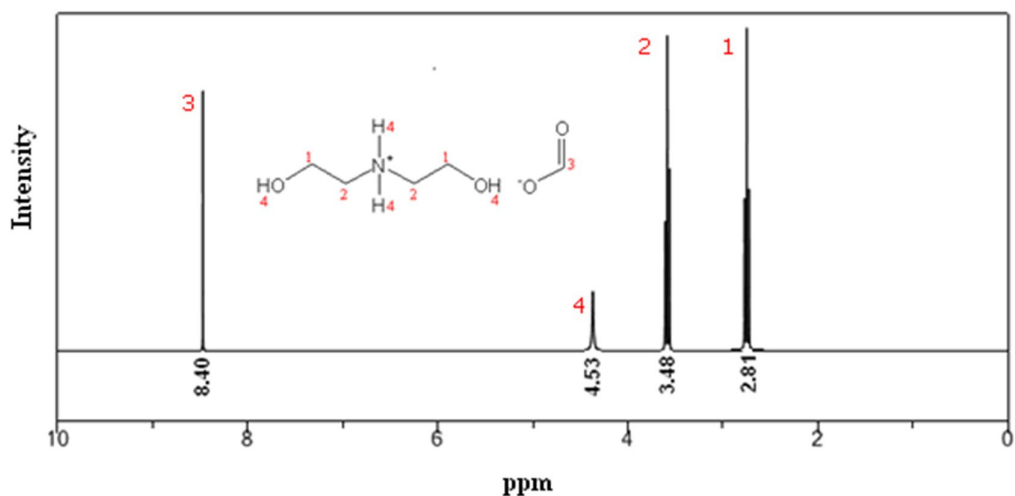


Figure 4.5 <sup>1</sup>H-NMR spectrum of [BHEAF].

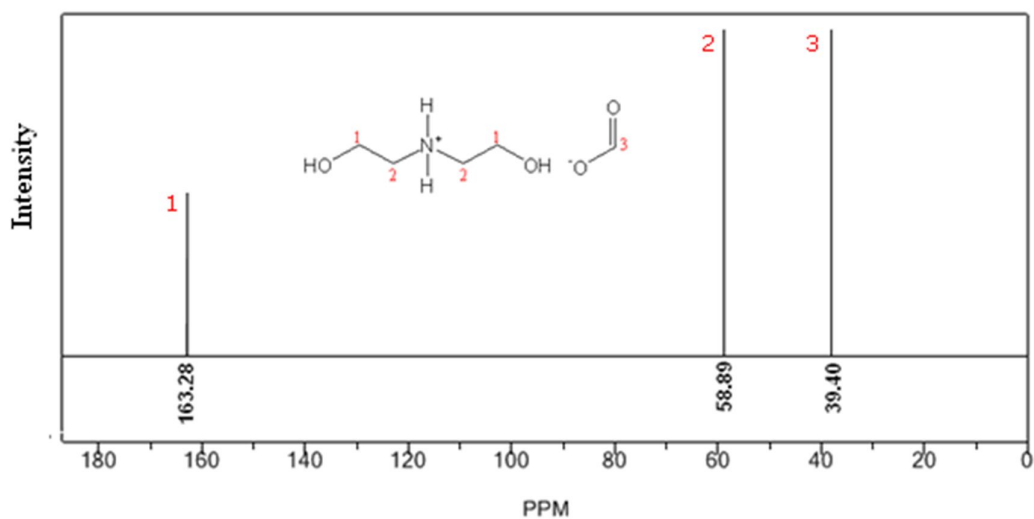


Figure 4.6 <sup>13</sup>C-NMR Spectrum of [BHEAF].

The NMR results of the other ionic liquids show a similar general feature. The number of hydrogen and carbon on the structure of the synthesized ionic liquids were confirmed. Therefore it can be concluded that the synthesis method used in this work was successful.

**[HEF]:**  $^1\text{H-NMR}$  (400 MHz, DMSO)  $\delta$  8.43 ppm (s, 1H, H-COO $^-$ ), 6.12 ppm (broad, 4H, -NH and -OH), 3.60 ppm (t, 2H, -CH $_2$ -N), 2.87 ppm (t, 2H, -O-CH $_2$ ).  $^{13}\text{C-NMR}$  (400 MHz, DMSO)  $\delta$  167.41 ppm (C carboxylate), 58.25 ppm (C-N), 39.80 (C-O) ppm.

**[HEA]:**  $^1\text{H NMR}$  (400 MHz, DMSO)  $\delta$  6.62 ppm (broad, 4H, -NH and -OH), 3.54 ppm (t, 2H, -CH $_2$ -N), 2.77 (t, 2H, -O-CH $_2$ ), 1.72 ppm (s, 3H, H $_3$ C- COO $^-$ ).  $^{13}\text{C-NMR}$  (400 MHz, DMSO)  $\delta$  176.15 ppm (C carboxylate), 59.26 ppm (C-N), 39.68 (C-O), 24.38 ppm (C-COO $^-$ ).

**[HEP]:**  $^1\text{H NMR}$  (400 MHz, DMSO)  $\delta$  5.88 ppm (broad, 4H, -NH $_3$  and -OH), 3.53 (t, 2H, -CH $_2$ -N), 2.77 (t, 2H, -CH $_2$ -N), 1.99 (m, 2H, -CH $_2$ - COO $^-$ ), 0.92 (t, 3H, H $_3$ C-C).  $^{13}\text{C-NMR}$  (400 MHz, DMSO)  $\delta$  178.70 ppm (C carboxylate), 59.77 ppm (C-N), 42.52 (C-O), 30.33 ppm (C-COO $^-$ ), 10.83 ppm (C, terminal carboxylate).

**[HEL]:**  $^1\text{H-NMR}$  (400 MHz, DMSO)  $\delta$  5.88 ppm (broad, 5H, -NH, -OH, and HO-C Lactate), 3.53 ppm (t, 2H, -CH $_2$ -N), 2.80 ppm (t, 2H, -O-CH $_2$ ), 2.52 ppm (m, 1H, -CH- COO $^-$ ), 1.13 ppm (d, 3H, H $_3$ C-C).  $^{13}\text{C-NMR}$  (400 MHz, DMSO)  $\delta$  175.25 ppm (C carboxylate), 67.68 ppm (C-C carboxylate), 60.14 ppm (C-N), 40.06 (C-O), 21.88 (C, terminal carboxylate).

**[BHEAF]:**  $^1\text{H-NMR}$  (400 MHz, DMSO)  $\delta$  8.40 ppm (s, 1H, H-COO $^-$ ), 4.53 ppm (broad, 4H, -NH and -OH), 3.48 ppm (t, 4H, -CH $_2$ -N), 2.81 ppm (t, 2H, -O-CH $_2$ ).  $^{13}\text{C-NMR}$  (400 MHz, DMSO)  $\delta$  163.28 ppm (C carboxylate), 58.89 ppm (C-N), 39.44 (C-O) ppm.

**[BHEAA]:**  $^1\text{H NMR}$  (400 MHz, DMSO)  $\delta$  5.52 ppm (broad, 4H, -NH $_3$  and -OH), 3.55 ppm (t, 4H, -CH $_2$ -N), 2.76 (t, 4H, -O-CH $_2$ ), 1.77 ppm (s, 3H, H $_3$ C- COO $^-$ ).  $^{13}\text{C-NMR}$  (400 MHz, DMSO)  $\delta$  175.25 ppm (C carboxylate), 58.86 ppm (C-N), 40.04 ppm (C-O), 23.41 ppm (C-COO $^-$ ).

**[BHEAP]:**  $^1\text{H NMR}$  (400 MHz, DMSO)  $\delta$  5.86 ppm (broad, 4H, -NH and -OH), 3.55 (t, 4H, -CH $_2$ -N), 2.78 (t, 4H, -CH $_2$ -N), 2.04 (m, 2H, -CH $_2$ - COO $^-$ ), 0.98 (t, 3H, H $_3$ C-C).  $^{13}\text{C-NMR}$  (400 MHz, DMSO)  $\delta$  177.73 ppm (C carboxylate), 58.82 ppm (C-N), 39.74 (C-O), 29.05 ppm (C-COO $^-$ ), 10.53 ppm (C, terminal carboxylate).

**[BHEAL]:**  $^1\text{H-NMR}$  (400 MHz, DMSO)  $\delta$  5.47 ppm (broad, 5H,  $-\text{NH}_2$ ,  $-\text{OH}$ , and  $\text{HO-C Lactate}$ ), 3.65 ppm (t, 4H,  $-\text{CH}_2-\text{N}$ ), 2.97 ppm (t, 4H,  $-\text{O}-\text{CH}_2$ ), 2.52 ppm (m, 1H,  $-\text{CH}-\text{COO}^-$ ), 1.17 ppm (d, 3H,  $\text{H}_3\text{C}-\text{C}$ ).  $^{13}\text{C-NMR}$  (400 MHz, DMSO)  $\delta$  179.31 ppm (C carboxylate), 67.67 ppm (C-C carboxylate), 49.81 ppm (C-N), 40.28 (C-O), 21.52 (C, terminal carboxylate).

**[BHEMF]:**  $^1\text{H-NMR}$  (400 MHz, DMSO)  $\delta$  8.35 ppm (s, 1H,  $\text{HC}-\text{COO}^-$ ), 6.63 ppm (broad, 4H,  $-\text{NH}$  and  $-\text{OH}$ ), 3.64 ppm (t, 6H,  $-\text{CH}_2-\text{N}$ ), 2.91 ppm (t, 6H,  $-\text{O}-\text{CH}_2$ ), 2.56 ppm (m, 3H,  $\text{H}_3\text{C}-\text{N}$ ).  $^{13}\text{C-NMR}$  (400 MHz, DMSO)  $\delta$  166.38 ppm (C carboxylate), 58.57 ppm (C-N), 41.63 (C-O) ppm, 39.48 (C, N-methyl).

**[BHEMA]:**  $^1\text{H NMR}$  (400 MHz, DMSO)  $\delta$  6.48 ppm (broad, 4H,  $-\text{NH}$  and  $-\text{OH}$ ), 3.53 ppm (t, 6H,  $-\text{CH}_2-\text{N}$ ), 2.64 (t, 6H,  $-\text{O}-\text{CH}_2$ ), 2.37 ppm (m, 3H,  $\text{H}_3\text{C}-\text{N}$ ), 1.84 ppm (s, 3H,  $\text{H}_3\text{C}-\text{COO}^-$ ).  $^{13}\text{C-NMR}$  (400 MHz, DMSO)  $\delta$  174.26 ppm (C carboxylate), 58.21 ppm (C-N), 42.22 ppm (C-O), 40.04 ppm (C, N-methyl), 22.50 ppm (C-COO $^-$ ).

**[BHEMP]:**  $^1\text{H NMR}$  (400 MHz, DMSO)  $\delta$  5.61 ppm (broad, 3H,  $-\text{NH}$  and  $-\text{OH}$ ), 3.53 (t, 6H,  $-\text{CH}_2-\text{N}$ ), 2.56 (t, 6H,  $-\text{CH}_2-\text{N}$ ), 2.12 (m, 2H,  $-\text{CH}_2-\text{COO}^-$ ), 0.96 (t, 3H,  $\text{H}_3\text{C}-\text{C}$ ).  $^{13}\text{C-NMR}$  (400 MHz, DMSO)  $\delta$  176.45 ppm (C carboxylate), 59.47 ppm (C-N), 42.83 (C-O), 39.67 ppm (C, N-methyl), 28.15 ppm (C-COO $^-$ ), 10.83 ppm (C, terminal carboxylate).

**[BHEML]:**  $^1\text{H-NMR}$  (400 MHz, DMSO)  $\delta$  5.17 ppm (broad, 4H,  $-\text{NH}$ ,  $-\text{OH}$ , and  $\text{HO-C Lactate}$ ), 3.53 ppm (t, 2H,  $-\text{CH}_2-\text{N}$ ), 2.77 ppm (t, 2H,  $-\text{O}-\text{CH}_2$ ), 2.47 ppm (m, 1H,  $-\text{CH}-\text{COO}^-$ ), 1.19 ppm (d, 3H,  $\text{H}_3\text{C}-\text{C}$ ).  $^{13}\text{C-NMR}$  (400 MHz, DMSO)  $\delta$  178.71 ppm (C carboxylate), 67.00 ppm (C-C carboxylate), 59.21 ppm (C-N), 57.58 (C-O), 39.74 ppm (C, N-methyl), 21.52 (C, terminal carboxylate).

**[THEAF]:**  $^1\text{H-NMR}$  (400 MHz, DMSO)  $\delta$  8.26 ppm (s, 1H,  $\text{H}-\text{COO}^-$ ), 5.07 ppm (broad, 4H,  $-\text{NH}$  and  $-\text{OH}$ ), 3.50 ppm (t, 6H,  $-\text{CH}_2-\text{N}$ ), 2.77 ppm (t, 6H,  $-\text{O}-\text{CH}_2$ ).  $^{13}\text{C-NMR}$  (400 MHz, DMSO)  $\delta$  164.55 ppm (C carboxylate), 58.56 ppm (C-N), 40.40 ppm (C-O).



**[THEAA]:**  $^1\text{H}$  NMR (400 MHz, DMSO)  $\delta$  5.53 ppm (broad, 4H,  $-\text{NH}$  and  $-\text{OH}$ ), 3.65 ppm (t, 6H,  $-\text{CH}_2-\text{N}$ ), 2.79 (t, 6H,  $-\text{O}-\text{CH}_2$ ), 1.67 ppm (s, 3H,  $\text{H}_3\text{C}-\text{COO}^-$ ).  $^{13}\text{C}$ -NMR (400 MHz, DMSO)  $\delta$  175.35 ppm (C carboxylate), 58.96 ppm (C-N), 40.14 ppm (C-O), 23.51 ppm (C- $\text{COO}^-$ ).

**[THEAP]:**  $^1\text{H}$  NMR (400 MHz, DMSO)  $\delta$  5.78 ppm (broad, 4H,  $-\text{NH}$  and  $-\text{OH}$ ), 3.43 (t, 6H,  $-\text{CH}_2-\text{N}$ ), 2.87 (t, 6H,  $-\text{CH}_2-\text{N}$ ), 1.98 (m, 2H,  $-\text{CH}_2-\text{COO}^-$ ), 0.91 (t, 3H,  $\text{H}_3\text{C}-\text{C}$ ).  $^{13}\text{C}$ -NMR (400 MHz, DMSO)  $\delta$  178.72 ppm (C carboxylate), 59.67 ppm (C-N), 42.42 (C-O), 30.43 ppm (C- $\text{COO}^-$ ), 10.82 ppm (C, terminal carboxylate).

**[THEAL]:**  $^1\text{H}$ -NMR (400 MHz, DMSO)  $\delta$  5.29 ppm (broad, 5H,  $-\text{NH}$ ,  $-\text{OH}$ , and  $\text{HO}-\text{C}$  Lactate), 3.58 ppm (t, 6H,  $-\text{CH}_2-\text{N}$ ), 2.90 ppm (t, 2H,  $-\text{O}-\text{CH}_2$ ), 2.57 ppm (m, 1H,  $-\text{CH}-\text{COO}^-$ ), 1.20 ppm (d, 3H,  $\text{H}_3\text{C}-\text{C}$ ).  $^{13}\text{C}$ -NMR (400 MHz, DMSO)  $\delta$  178.32 ppm (C carboxylate), 66.69 ppm (C-C carboxylate), 56.98 ppm (C-N), 39.42 (C-O), 21.23 (C, terminal carboxylate).

#### 4.1.3 Elemental Analysis

The chemical composition is an important aspect in the synthesis and characterization of ionic liquids. It determines the purity of the synthesized ionic liquids. In this work, the chemical composition of the ionic liquids is measured using CHNS-932 (LECO Instruments) elemental analyzer. The instrument was calibrated using standard calibration sample with known chemical composition provided by supplier prior to each measurement. Table 4.2 presents the result for elemental analysis of synthesized ionic liquids. The experimental values are found to be in good agreement with the calculated value. The standard deviation is found to be  $\pm 0.02$  (wt%)

Table 4.2 Elemental analysis of synthesized ionic liquids

Ionic liquids	Experimental (wt %)			Calculated (wt %)		
	C	H	N	C	H	N
[HEF]	33.71	8.41	13.10	33.64	8.47	13.08
[HEA]	39.69	9.11	11.53	39.66	9.15	11.56
[HEP]	44.49	9.60	10.29	44.43	9.69	10.36
[HEL]	39.71	8.60	9.21	39.73	8.67	9.27
[BHEAF]	39.79	8.61	9.21	39.73	8.67	9.27
[BHEAA]	43.62	9.11	8.47	43.63	9.15	8.48
[BHEAP]	46.94	9.52	7.79	46.91	9.56	7.82
[BHEAL]	43.11	8.72	7.15	43.07	8.78	7.18
[BHEMF]	43.70	9.12	8.45	43.63	9.15	8.48
[BHEMA]	46.89	9.52	7.76	46.91	9.56	7.82
[BHEMP]	49.67	9.89	7.29	49.72	9.91	7.25
[BHEML]	46.98	9.10	6.64	45.92	9.15	6.69
[THEAF]	43.11	8.69	7.20	43.07	8.78	7.18
[THEAA]	45.95	9.11	6.65	45.92	9.15	6.69
[THEAP]	48.48	9.42	6.21	48.42	9.48	6.27
[THEAL]	45.21	8.85	5.82	45.18	8.85	5.85

#### 4.1.4 Water Content

Table 4.4 presents the values of the water content of the synthesized ionic liquids in this work. As can be seen from Table 4.3, water content of these ionic liquids is found to be less than 200 ppm. The standard deviation is found to be  $\pm 5$  ppm.

Table 4.3 Water content of synthesized ionic liquids

Ionic liquids	Water content (ppm)	Ionic liquids	Water content (ppm)
[HEF]	108	[BHEMF]	132
[HEA]	117	[BHEMA]	142
[HEP]	105	[BHEMP]	141
[HEL]	174	[BHEML]	139
[BHEAF]	128	[THEAF]	128
[BHEAA]	127	[THEAA]	169
[BHEAP]	115	[THEAP]	121
[BHEAL]	170	[THEAL]	172

#### 4.2 Physical Properties of Ionic Liquids

The physical properties of new corrosion inhibitor must be determined before it applies into the corrosive environment [1, 25]. However, most of the new corrosion inhibitor in the literature is reported without their physical properties [4-9, 11, 12, 162-175]. In this work, the physical properties namely density, viscosity, and refractive index of hydroxyl ammonium ionic liquids as new corrosion inhibitor were measured and reported. In the following section, the results for density, viscosity, and refractive index are discussed. First, the obtained data will be reported and compared with literature where available. Thereafter, the effect of temperature on the respective physical properties is reported and discussed. In general, for the ionic liquids investigated in this study, there were lacks of literature found from previous study.

### 4.2.1 Density

The experimental density for all pure ionic liquids are presented in Table C.1 of Appendix C. Prior to the measurement, the densimeter was calibrated regularly using Millipore water and dried air according to the manual. The calibrated densimeter was verified by measuring density of alcohol and 1-hexyl-3-methylimidazolium ionic liquids. The densities of methanol, ethanol, and 1-propanol from this work are in good agreement with the literature [122, 123, 125].

The density data for some of the studied ionic liquids are already available in the open literature Table 4.4 lists the experimental densities of the ionic liquids measured and compared with literature data. The experimental density values for [HEF] are found to be slightly lower than those reported by Biçak (2005) and Yuan *et al.* (2007) and notably higher than those given by Greave *et al.* (2006) and Igleasias *et al.* (2008). This minor discrepancy could be due to the presence of impurities and the variation of water content in the sample. Unfortunately, the authors have not mentioned the water content in their sample.

Table 4.4 Comparison of density,  $\rho$ , values for pure ionic liquids and alcohol at  $T = 298.15$  K.

Ionic Liquids	$\rho/\text{g}\cdot\text{cm}^{-3}$	
	This work	Literature
[HEF]	1.20025	1.184 [26]
		1.204 [95]
		1.17709 [97]
		1.204 [180]
[HEA]	1.14622	1.176 [26]
		1.120 [95]
[HEP]	1.10963	NA

Table 4.4 Comparison of density,  $\rho$ , values for pure ionic liquids and alcohol at  $T = 298.15$  K (cont).

Ionic Liquids	$\rho/\text{g}\cdot\text{cm}^{-3}$	
	This work	Literature
[HEL]	1.21020	1.228 [26] 1.202 [95]
[BHEAF]	1.18385	1.194041 [96]
[BHEAA]	1.17020	NA
[BHEAP]	1.13940	NA
[BHEAL]	1.22055	NA
[BHEMF]	1.17990	NA
[BHEMA]	1.12490	NA
[BHEMP]	1.09505	NA
[BHEML]	1.18010	NA
[THEAF]	solid	NA
[THEAA]	1.19420	NA
[THEAP]	1.18188	NA
[THEAL]	1.22890	NA

The structure of an ionic liquid directly impacts its density. It is well known that the densities of ionic liquids vary with the choice of anion and cation [13]. In this work, the effects of cation and anion on density of hydroxyl ammonium ionic liquids were also predicted using COSMO-RS method. The predicted density as well as molecular volume and energy produced from COSMO-RS method is given in Table 4.5

Table 4.5 The predicted density for hydroxyl ammonium ionic liquids using COSMO-RS method.

Ionic liquids	$\rho/\text{g}\cdot\text{cm}^{-3}$	$V/\text{nm}^3$	Energy/ $\text{kJ}\cdot\text{mol}^{-1}$			
			H_int	H_MF	H_HB	H_vdW
[HEF]	1.0637	167.22	-48.42	2.63	-43.11	-7.94
[HEA]	1.0029	200.57	-53.48	3.20	-47.66	-9.01
[HEP]	0.9916	226.35	-54.27	3.39	-47.64	-10.02
[HEL]	1.0724	234.06	-45.27	3.13	-38.33	-10.07
[BHEAF]	1.1094	226.27	-41.87	6.13	-38.87	-9.67
[BHEAA]	1.0619	258.31	-46.86	6.66	-43.33	-10.75
[BHEAP]	1.0489	283.72	-48.05	6.45	-43.29	-11.76
[BHEAL]	1.1146	290.83	-40.70	5.00	-34.38	-11.80
[BHEMF]	1.0826	253.38	-30.13	9.59	-29.32	-10.40
[BHEMA]	1.0463	284.42	-34.48	10.09	-33.09	-11.47
[BHEMP]	1.0357	309.83	-36.10	9.55	-33.17	-12.48
[BHEML]	1.0979	316.47	-31.62	7.27	-26.39	-12.51
[THEAF]	Solid					
[THEAA]	1.0060	345.39	-57.48	7.01	-52.01	-12.49
[THEAP]	1.0001	370.70	-58.58	6.88	-51.96	-13.50
[THEAL]	1.0546	376.75	-49.96	5.38	-41.82	-13.52

Figure 4.7 presents the density of ionic liquids with 2-hydroxyethylammonium cation and different anions. The experimental and predicted density using COSMO-RS was found to be in qualitative agreement. It was observed that as the alkyl chain length in the carboxylate anion increases, the density of the corresponding ionic liquids decreases. According to COSMO-RS method, the density of ionic liquids are

influenced by size and interaction energy such as misfit (H\_MF), hydrogen bond (H\_HB), and van der Waals (H\_vdW). As the molecular volume increase from [HEF] to [HEP], the density of the ionic liquids decreases, reflecting higher misfit interaction in the crystal lattice. Hence it was observed that the order of decreasing density for ionic liquids composed of single anion is formate > acetate > propionate. The same trend is also observed for the other three cations when they coupled with this anion.

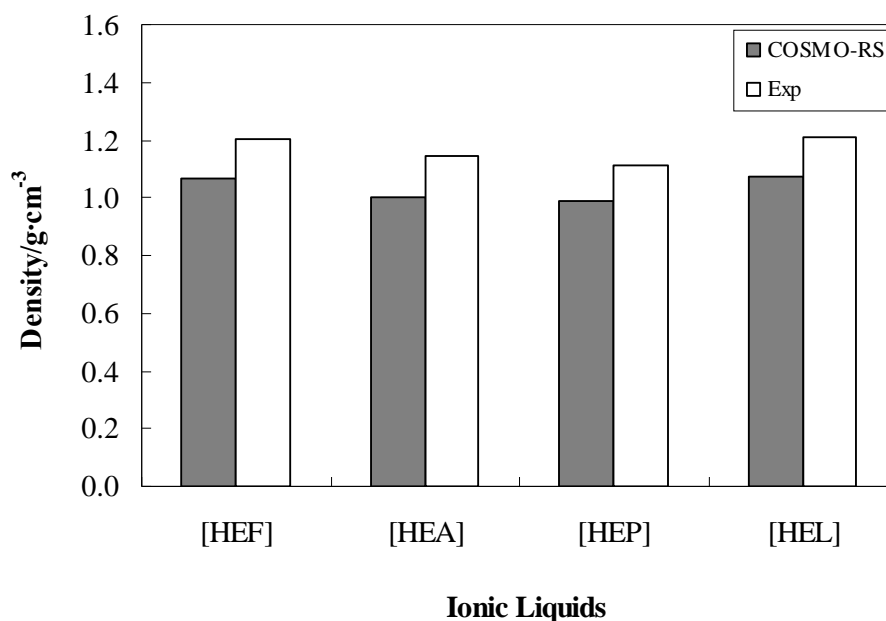


Figure 4.7 Density of ionic liquids Bis(2-hydroxyethyl)ammonium with different anion at temperature 298.15 K.

The misfit energy arises from the unbalance atom to form hydrogen bonding between cation and anion *e.g.* the 2-hydroxyethylammonium contain 3 hydrogen becoming donor, however the anion could only accommodate 1 hydrogen on their oxygen-carboxylate of the anion. The introduction of the (HO<sup>-</sup>) group into propionate anion, as in lactate anion, would increase the density due to the extra hydrogen bonding accommodated. Thus, it reduces the misfit interaction. From Figure 4.7, [HEL] shows the highest value of density. The same trend is also observed with lactate anion coupled with three other cations studied in this work.

The effect of cation size and structure is also studied. Figure 4.8 presents the ionic liquids with different cation coupled with acetate. The presence of (HO-) group would increase the density due to the hydrogen bonding. The experimental and predicted density was found in the same trend, except for the tris(2-hydroxyethyl)ammonium cation. The graph indicates that the order of increasing density for ionic liquids with single cation is [HEA] < [BHEAA] < [THEAA]. However, the predicted density showed that density of [BHEAA] is higher than [THEAA]. The difference maybe caused by the uncompleted conformer used for tris(2-hydroxyethyl)ammonium cation in COSMO-RS.

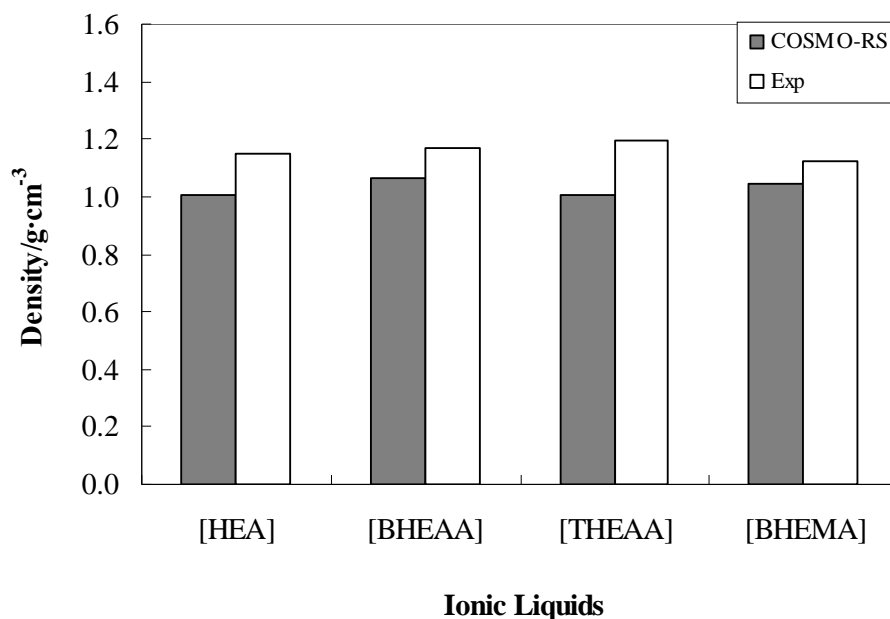


Figure 4.8 Density of ionic liquids with acetate and different cation at temperature 298.15 K.



On the other hand, addition of methyl chain into Bis(2-hydroxyethyl)ammonium cation, as in the case of Bis(2-hydroxyethyl)methylammonium cation, would decrease the density due to bigger size of the latter cation. The same trend was also observed for predicted density data. According to COSMO-RS, addition of methyl chain increase the misfit interaction in the ionic liquids, thus it was observed that, for the same anion, the densities of ionic liquids with Bis(2-hydroxyethyl)methylammonium cation is lower than Bis(2-hydroxyethyl) ammonium cation.

#### 4.2.1.1 Effect of Temperature on Density of Ionic Liquids

The experimental data for the densities of the ionic liquids from temperature (293.15 to 353.15) K were fitted to equation (2.1a) using the method of least squares,

$$\rho = a_0 + a_1T \quad (2.1a)$$

with  $\rho$  is the density of the ionic liquids,  $T$  is absolute temperature;  $a_0$  and  $a_1$  are the fit parameters determined by applying the Newton-Rhapson numerical method with confidence level of 95%. Fit parameters are listed in Table 4.6 along with their standard deviation,  $\sigma$ , calculated using equation (4.1),

$$\sigma = \sqrt{\frac{\sum_i^{n_{DAT}} (Z_{\text{exp}} - Z_{\text{cal}})^2}{n_{DAT}}} \quad (4.1)$$

The standard deviation between experimental density and prediction using equation (2.1a) was found to be less than 0.0015. It indicates that the correlation presented in Table 4.8 can be used to predict the density of the synthesized ionic liquids within the temperature range studied in this work.

Table 4.6 Fit parameter for temperature dependence of density calculated using equation (2.1) and its standard deviation calculated using equation (4.1)

	$a_0$	$10^4 \cdot a_1$	$\sigma$		$a_0$	$10^4 \cdot a_1$	$\sigma$
[HEF]	1.3390	-4.6821	0.0005	[BHEMF]	1.3996	-7.3650	0.0004
[HEA]	1.3048	-5.3114	0.0007	[BHEMA]	1.3598	-7.8792	0.0001
[HEP]	1.2903	-6.0607	0.0002	[BHEMP]	1.4006	-10.2358	0.0011
[HEL]	1.3852	-5.8571	0.0004	[BHEML]	1.3658	-6.2342	0.0004
[BHEAF]	1.3936	-7.0275	0.0005	[THEAF]	1.4276	-6.3500	0.0001
[BHEAA]	1.3441	-5.8375	0.0002	[THEAA]	1.3688	-5.8493	0.0003
[BHEAP]	1.3113	-5.7725	0.0005	[THEAP]	1.3556	-5.8233	0.0004
[BHEAL]	1.4165	-6.5692	0.0008	[THEAL]	1.4015	-5.7942	0.0004

The plot of experimental density as function of temperature for the synthesized ionic liquids is given in Figures 4.9 to 4.12. A decrease in the densities of the studied ionic liquids was observed with an increase in temperature. The experimental data for density of [HEF], [BHEAF], and [THEAF] within the temperature range of 293.15 to 353.15 K and its polynomial correlations using equation (2.1) are plotted with solid lines shown in Figure 4.9. The densities of [THEAF] were found to be in good agreement with literature [96]. On the other hand, the densities of [HEF] in the temperature range studied were slightly higher compared to literature. Meanwhile, the densities of [BHEAF] were slightly lower compared to the literature. The differences may be attributed to the purity and water content of the sample. However, the previous author did not mention on the water content in their ionic liquids [96].

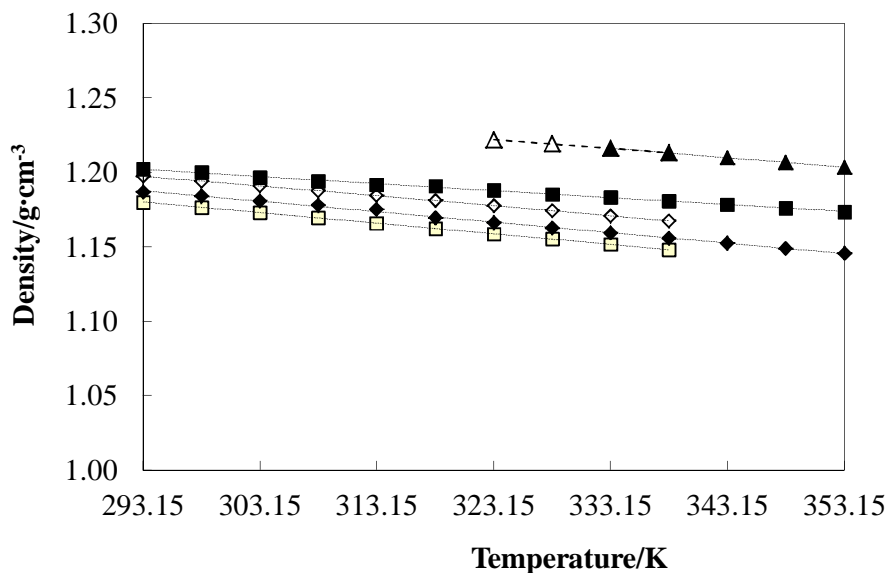


Figure 4.9 Density of ionic liquids with formate anion and different cation as function of temperature. Symbols: ■, [HEF] this work; □, [HEF] [96]; ♦, [BHEAF] this work; ◇, [BHEAF] [96]; ▲, [THEAF] this work; △, [THEAF] [96]; and (---) Correlation using equation (2.1).

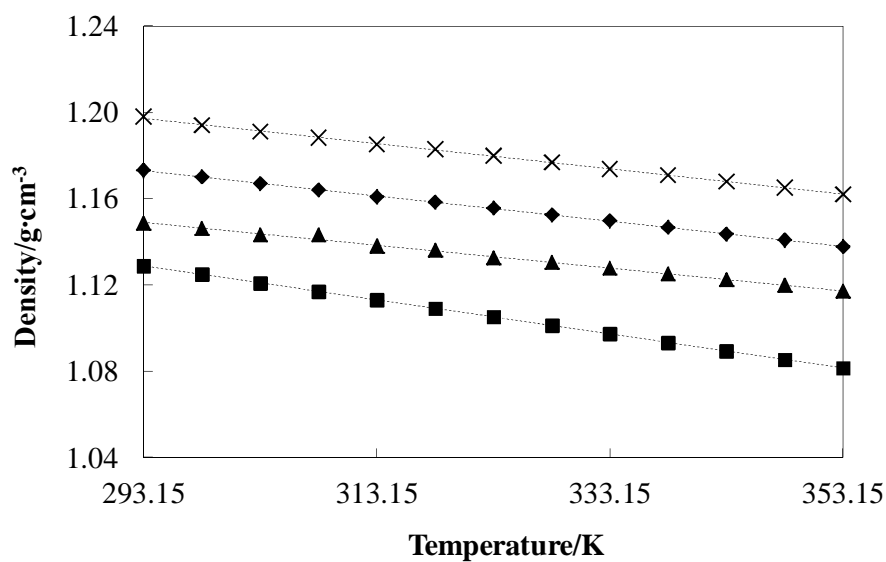


Figure 4.10 Density of ionic liquids with acetate anion and different cation as function of temperature. Symbols: ▲, [HEA]; ♦, [BHEAA]; ■, [BHEMA]; ×, [THEAA]; and (---) Correlation using equation (2.1).

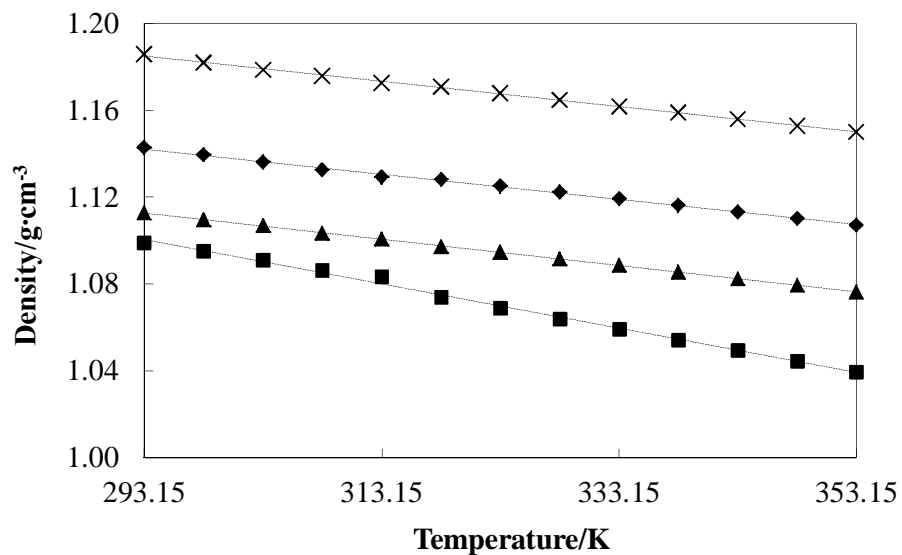


Figure 4.11 Density of ionic liquids with propionate anion and different cation as function of temperature. Symbols: ▲, [HEP]; ◆, [BHEAP]; ■, [BHEMP]; ×, [THEAP]; and (---) Correlation using equation (2.1).

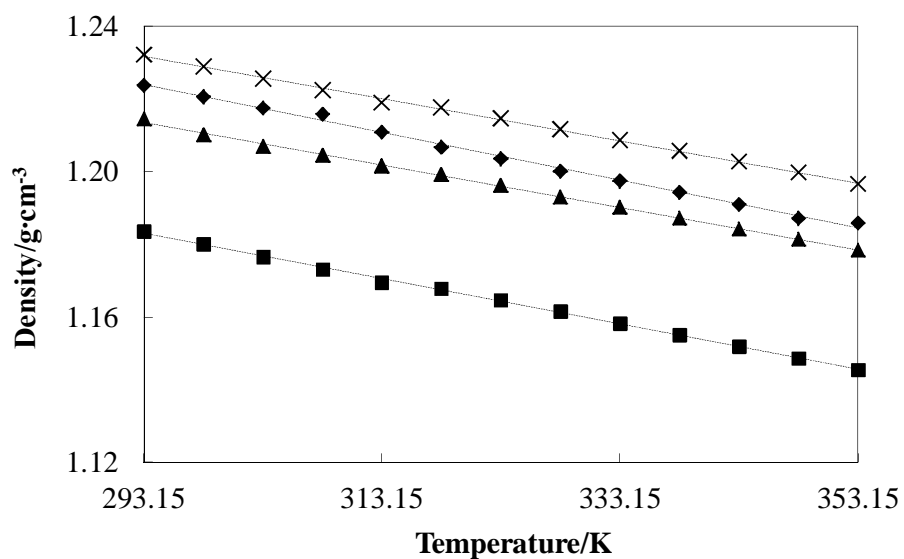


Figure 4.12 Density of ionic liquids with lactate anion and different cation as function of temperature. Symbols: ▲, [HEP]; ◆, [BHEAP]; ■, [BHEMP]; ×, [THEAP]; and (---) Correlation using equation (2.1).

#### 4.2.2 Coefficient of Thermal Expansion

From density-temperature dependence, one can calculate the volume of expansivity or also known as the coefficient of thermal expansion using equation (2.2),

$$\alpha = \frac{1}{V} \left( \frac{\delta V}{\delta T} \right)_P = -\frac{1}{\rho} \left( \frac{\delta \rho}{\delta T} \right)_P \quad (2.2)$$

The results of the analysis for the pure synthesized ionic liquids are listed in Table B.2 of Appendix B. The values are comparable to the coefficient of thermal expansion of the imidazolium and amino acid based ionic liquids [181-192]. Figure 4.13 presents the plots of the coefficient of thermal expansion,  $\alpha$ , for the ionic liquids [HEF], [BHEAF], [THEAF], and methanol as function of temperatures. The coefficient of thermal expansion for [HEF] in this work was found to be slightly lower than literature. This is due to the difference on experimental density, which is slightly higher than literature [96].

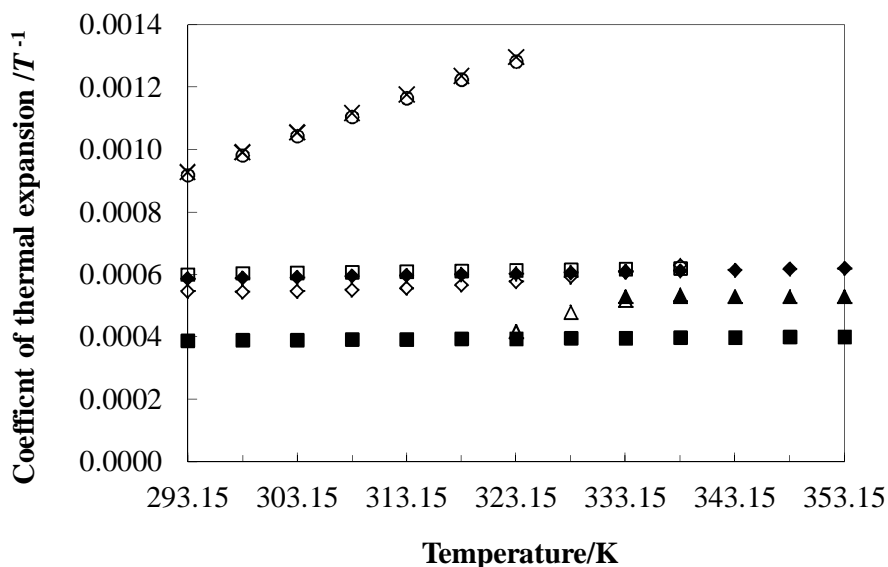


Figure 4.13 Coefficient of thermal expansion of ionic liquids and methanol at several temperatures. Symbols: ■, [HEF] this work; □, [HEF] [96]; ◆, [BHEAF] this work; ◇, [BHEAF] [96]; ▲, [THEAF] this work; △, [THEAF] [96]; ×, methanol, this work; ○, methanol [122].

The coefficients of thermal expansion for both ionic liquids and methanol increased with increasing temperature. This is a typical behavior for fluids in general [112, 122]. The coefficients of thermal expansion of pure ionic liquids are considerably less dependent on temperature when compared to methanol and were found to be at lower values which show the impact of the difference in molecule packing between ionic liquids and alcohol. Ionic liquids composed solely of ions whereas alcohols are molecular solvent. One possible explanation for this phenomena is that the coefficient of thermal expansions for ionic liquids are governed by the van der Waals forces as well as strong electrostatic interactions between cation and anion of the ionic liquids, thus causing it to be less influenced by temperature [101, 113].

### 4.2.3 Viscosity

Table 4.7 presents the experimental viscosity of pure ionic liquids and is compared to the literature data. For the viscosity of [HEF], three data points are available in the literature. Greaves *et al.* determined a viscosity of 220 mPa·s [26]. The authors give no information on their measurements method. They also did not specify the purity of the sample, its water content, and the uncertainty of their measurements. Yuan *et al.* determined a viscosity of 118 mPa·s using NDJ-1 rotary type viscometer [95]. Bicak determined a viscosity of 105 mPa·s at 298.15 K [180]. Viscosity was determined by capillary viscometer method using a Canon-Fenske viscometer in a thermostated bath. The viscosities were given in terms of centi Poise (cp), using distilled water as reference. The author also did not specify the purity of the sample, its water content, and the uncertainty of their measurements. These deviations may be attributed to the difference in the water content and method to measure its viscosity.

Table 4.7 Comparison of viscosity values for pure ionic liquids at  $T = 298.15$  K

Ionic Liquids	$\eta/\text{mPa}\cdot\text{s}$	
	This work	Literature
[HEF]	130.67	118 [95] 220 [26] 105 [180]
[HEA]	409.72	640 [95] 701 [26]
[HEP]	284.14	NA
[HEL]	624.44	1200 [95] 1324 [26]
[BHEAF]	234.93	NA
[BHEAA]	761.43	NA
[BHEAP]	480.18	NA
[BHEAL]	963.05	NA
[BHEMF]	491.4	NA
[BHEMA]	625.31	NA
[BHEMP]	324.81	NA
[BHEML]	679.03	NA
[THEAF]	Solid	NA
[THEAA]	1920.7	NA
[THEAP]	1922.0	NA
[THEAL]	2785.6	NA

In general, the viscosity of ionic liquids is also governed by Coulomb forces like van der Waals interactions and hydrogen bonding besides the entanglement between the molecules. Hasse and co-worker stated in their work that charge delocalization within the anion weakens the intermolecular hydrogen bonding with the cation, leading to lower viscosities if not overcompensated by van der Waals interactions [105]. For the ionic liquids containing the 2-hydroxyethanaminium cation, the highest viscosity found for [HEA] can be explained with the long side chain of the anion, which increases the contributions to viscosity by entanglement and van der Waals interactions. It is worth mentioning that more basic anions lead to tighter ion pairing between the cation and the anion, which also increases the intermolecular bonds such as hydrogen bonding [105]. The formate anion exhibits the lowest viscosity, followed by propionate anion, which is in agreement with the order of the viscosity of the three ionic liquids. Also for the comparison of different ionic liquids containing the same anion, 2-hydroxyethanaminium exhibits the lowest viscosity, followed by bis(2-hydroxyethyl)methylammonium and bis(2-hydroxyethyl)ammonium. It is evident that a higher viscosity is caused by an increasing alkyl chain length of the cation [13, 112].

#### 4.2.3.1 *Effect of Temperature on Viscosity of Ionic Liquids*

Figure 4.14 shows the effect of temperature on viscosities of some ionic liquids. A decrease in the viscosity of the studied ionic liquids was observed with increasing temperature. The same trend was observed for the other synthesized ionic liquids in this work. No previous data as a function of temperature has been reported in literature for these systems for comparison.

The experimental data obtained for viscosities of the ionic liquids within the temperature range of 293.15 to 353.15 K were fitted using the method of least squares to the equation (2.4b) [140],

$$\log \eta = b_0 + \frac{b_1}{T} + \frac{b_2}{T^2} \quad (2.4b)$$



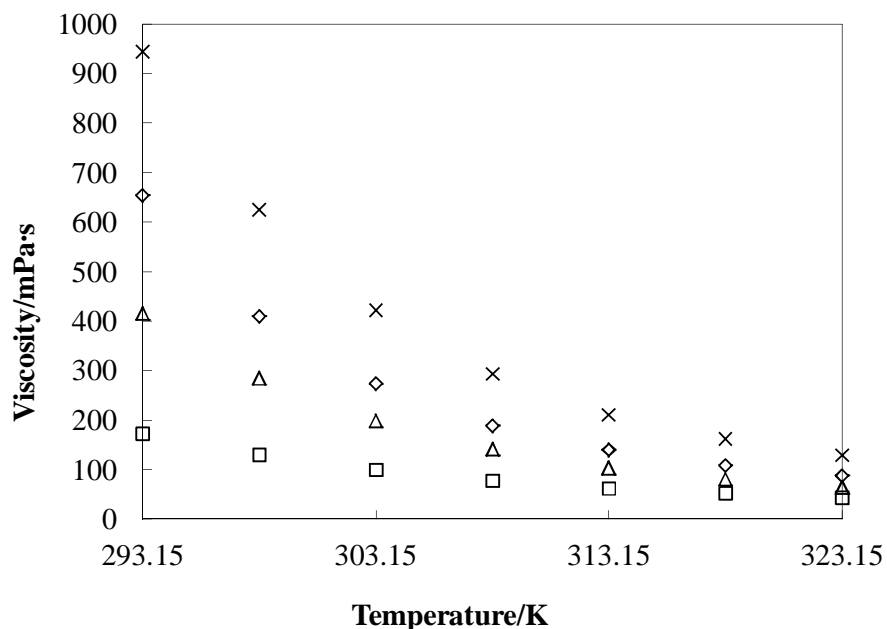


Figure 4.14 Viscosity of ionic liquids as function of temperature. Symbols:  $\square$ , [HEF];  $\diamond$ , [HEA];  $\Delta$ , [HEP]; and  $\times$ , [HEL].

The fitted parameters are listed in Table 4.8, along with their standard deviation calculated using equation (4.1). The experimental data for viscosity of [HEF], [HEA], [HEP], and [HEL] within the temperature range of 293.15 to 353.15 K and its polynomial correlations using equation (4.2) are plotted with solid lines shown in Figure 4.15. The standard deviation between experimental viscosity and prediction using equation (2.4b) was found to be less than 0.005. It indicates that the correlation presented in Table 4.8 can be used to predict the viscosity of the synthesized ionic liquids within the temperature range studied in this work.

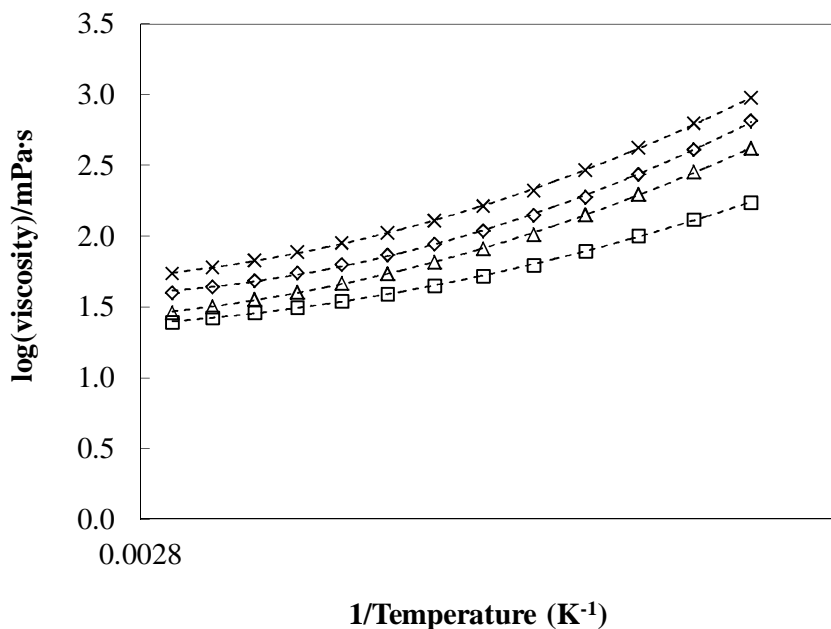


Figure 4.15 Viscosities of ionic liquids from temperature (293.15 to 353.15) K and its polynomial correlation using equation (4.2) (---). Symbols:  $\square$ , [HEF];  $\diamond$ , [HEA];  $\Delta$ , [HEP]; and  $\times$ , [HEL].

Table 4.8 Fit parameter for temperature dependence of viscosity calculated using equation (2.4) and its standard deviation calculated using equation (4.1).

Ionic liquids	$b_0$	$b_1$	$b_2$	$\sigma$
[HEF]	0.8642	47.184	-394.51	0.002
[HEA]	0.9101	60.800	-454.05	0.002
[HEP]	0.7324	65.133	-548.72	0.003
[HEL]	0.9613	68.943	-573.99	0.002
[BHEAF]	0.8219	58.151	-482.28	0.002
[BHEAA]	0.7352	81.203	-687.58	0.002
[BHEAP]	0.8237	69.501	-572.44	0.003
[BHEAL]	0.9180	76.507	-616.41	0.004

Table 4.8 Fit parameter for temperature dependence of viscosity calculated using equation (2.4) and its standard deviation calculated using equation (4.1) (cont)

Ionic liquids	b0	b1	b2	$\sigma$
[BHEMF]	1.0958	59.923	-497.27	0.003
[BHEMA]	0.9578	69.042	-572.98	0.003
[BHEMP]	0.8648	62.050	-518.33	0.003
[BHEML]	1.1997	59.262	-460.97	0.002
[THEAF]	1.5144	119.157	-2088.59	0.001
[THEAA]	1.4257	69.501	-572.44	0.003
[THEAP]	1.1567	78.946	-639.21	0.004
[THEAL]	1.3178	78.946	-639.21	0.004

#### 4.2.4 Refractive Index

The refractive index of the synthesized ionic liquids is measured using ATAGO RX-5000 at a temperature of 293.15 to 353.15 K with intervals of 5 K. The experimental results are given in Table B.4 of Appendix A. Prior to the measurement of the refractive index calibration of the refractometer is done by measuring the refractive index of selected organic solvent and imidazolium ionic liquids with known refractive index within the temperature range of 293.15 to 323.15 K. Apparently there were no previous data reported in literature on refractive index for the ionic liquids studied in this work.

##### 4.2.4.1 *Effect of Temperature on Refractive Index of Ionic Liquids*

The experimental data for the refractive index of the ionic liquids from temperature 293.15 to 353.15 K were fitted using the method of least squares to equation (2.5) in order to determine its coefficient,

$$n_D = c_0 + c_1 T \quad (2.5)$$

where  $n_D$  is density of ionic liquids,  $T$  is absolute temperature, and  $c_0$  and  $c_1$  are the fitted parameters determined by applying the Newton-Rhapson numerical method with confidence level of 95%. Fit parameters are listed in Table 4.9, along with their standard deviation,  $\sigma$ , and calculated using equation (4.1). Figure 4.16 shows the effect of temperature on the refractive index of the ionic liquids. The refractive index of the ionic liquids decreased with increasing temperature. The same trend was observed for the other synthesized ionic liquids in this work. No previous data as a function of temperature has been reported in literature for these systems for comparison.

Table 4.9 Fit parameter for temperature dependence of refractive index calculated using equation (2.5) and its standard deviation calculated using equation (4.1).

ILs	$a_0$	$10^4 \cdot a_1$	$\sigma$	ILs	$a_0$	$10^4 \cdot a_1$	$\sigma$
[HEF]	1.5194	-1.5672	0.0001	[BHEMF]	1.5352	-2.1588	0.0001
[HEA]	1.5135	-1.5611	0.0001	[BHEMA]	1.5322	-2.1546	0.0001
[HEP]	1.5272	-2.0486	0.0005	[BHEMP]	1.5282	-2.1561	0.0001
[HEL]	1.5373	-2.0463	0.0001	[BHEML]	1.5495	-2.6083	0.0001
[BHEAF]	1.5398	-2.2704	0.0002	[THEAF]	Solid		
[BHEAA]	1.5353	-2.2637	0.0001	[THEAA]	1.5479	-2.5100	0.0001
[BHEAP]	1.5307	-2.2457	0.0002	[THEAP]	1.5338	-2.1567	0.0001
[BHEAL]	1.5286	-1.7080	0.0006	[THEAL]	1.5322	-2.2474	0.0002

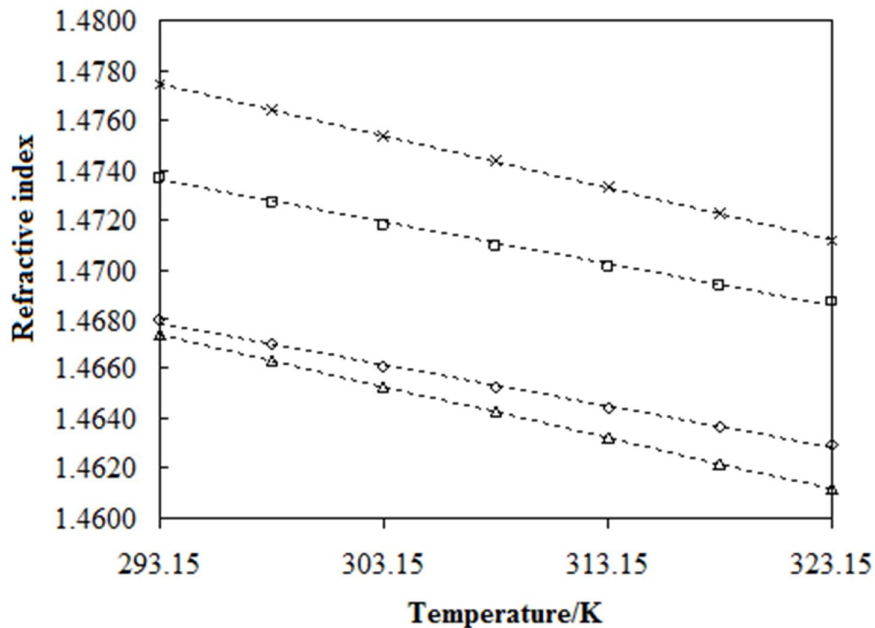


Figure 4.16 Refractive index of ionic liquids as function of temperature and its polynomial correlation using equation (2.1) (····). Symbols: □, [HEF]; ◇, [HEA]; △, [HEP]; and ×, [HEL].

### 4.3 Effect of Alcohol on Physical Properties of Ionic Liquids

In practical condition, corrosion inhibitor is mixture between active components, co-solvent, and surfactant. Thus, it is important to understand the behavior of ionic liquids, as the active component, and co-solvent [1, 25]. The co-solvent used shall not react with the active component. For this purpose, alcohol is widely used as co-solvent [1, 25]. In this work, co-solvents used were methanol, ethanol, and 1-propanol. Ionic liquids [BHEAF] was chosen as the model for ionic liquids, since it has the highest inhibition efficiency.

### 4.3.1 Density of Binary Mixture and Volumetric Properties

Prior to measuring the density of {[BHEAF](1) + alcohol(2)} binary mixture, the densimeter was used to measure the density of a mixture containing [HEF] and methanol for testing. The data are plotted in Figure 4.17 and compared with literature [97]. As can be seen from Figure 4.17, the densities of {[HEF](1) + methanol(2)} binary mixture increases with increasing mole fraction of ionic liquids and are in good agreement with data from literature [97].

To study the effect of alcohol composition and temperature on the density of {[BHEAF](1) + alcohol(2)} binary mixture, 13 different composition of {[BHEAF](1) + alcohol(2)} binary mixtures were prepared and their density measured at several temperature from 293.15 to 323.15 K. The results are given in Table C.1 of Appendix C.

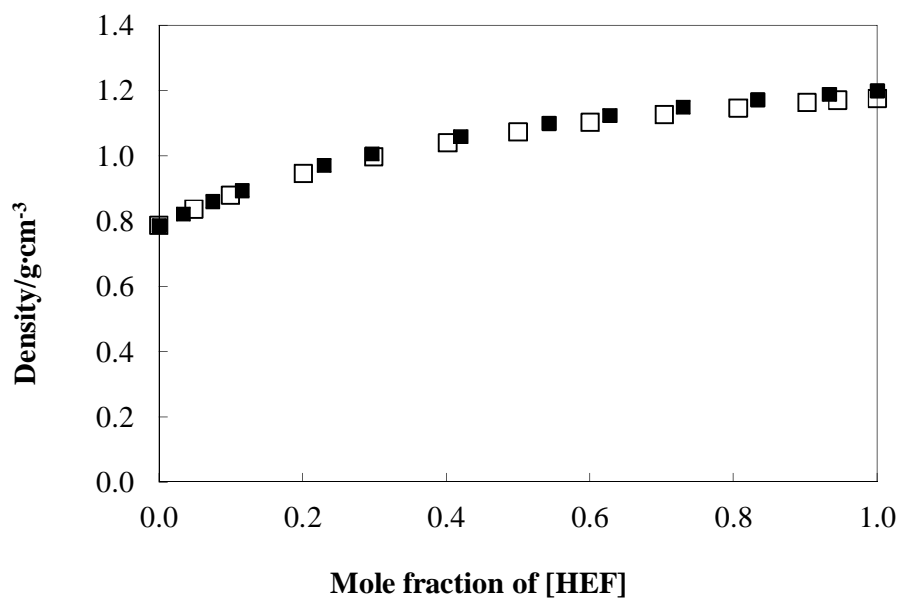


Figure 4.17 Densities of {[HEF](1) + methanol(2)} binary mixture at temperature 298.15 K Symbols: ■, this work; □, Iglesias *et al.* [97]

Figure 4.18 presents the experimental result for densities of {[BHEAF](1) + alcohol(2)} at temperature 298.15 K. As can be seen from Figure 4.18, the densities of the binary mixture of ionic liquids with alcohol were affected by the composition of alcohol in the system. The densities of {[BHEAF](1) + alcohol(2)} binary mixture were lowest at pure alcohol and its value increases with increasing mole fraction of ionic liquids in the system reaching the highest value at pure ionic liquids. The same trend was also observed for other binary system containing ionic liquids [HEF] and alcohol [97].

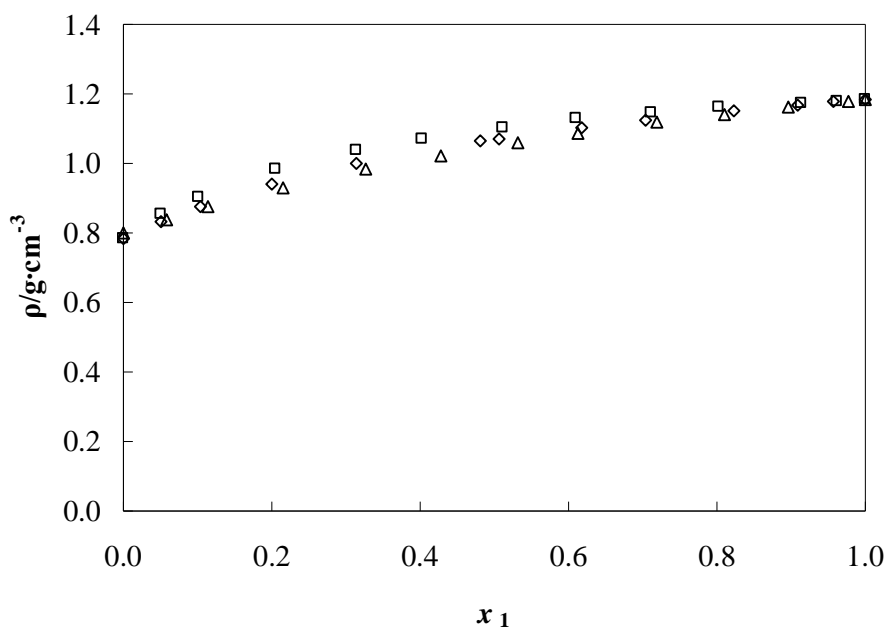


Figure 4.18 Densities of binary mixture of ionic liquids with alcohol at temperature 298.15 K. Symbols: □, {[BHEAF](1) + methanol(2)}; ◇, {[BHEAF](1) + ethanol(2)}; Δ, {[BHEAF](1) + 1-propanol(2)}

Like the density of pure ionic liquids, the density values for binary mixture of ionic liquids with alcohol were also affected by temperature. The density-temperature dependence were correlated using the method of least square based on the equation (2.1a) below,

$$\rho = a_0 + a_1T \quad (2.1)$$

Fitted parameters are listed in Table C.2 of Appendix C, along with their standard deviation calculated using equation (4.1). Equation (2.1a) suitably correlates, as a function of the temperature, not only the densities of the pure ionic liquids but also the densities of the mixtures for the binary systems through the composition range.

The experimental data for densities of {[BHEAF](1) + methanol(2)} binary mixture at several mole fraction of [BHEAF] and temperature from (293.15 to 353.15) K and its polynomial correlations are plotted with solid lines in Figure 4.19.

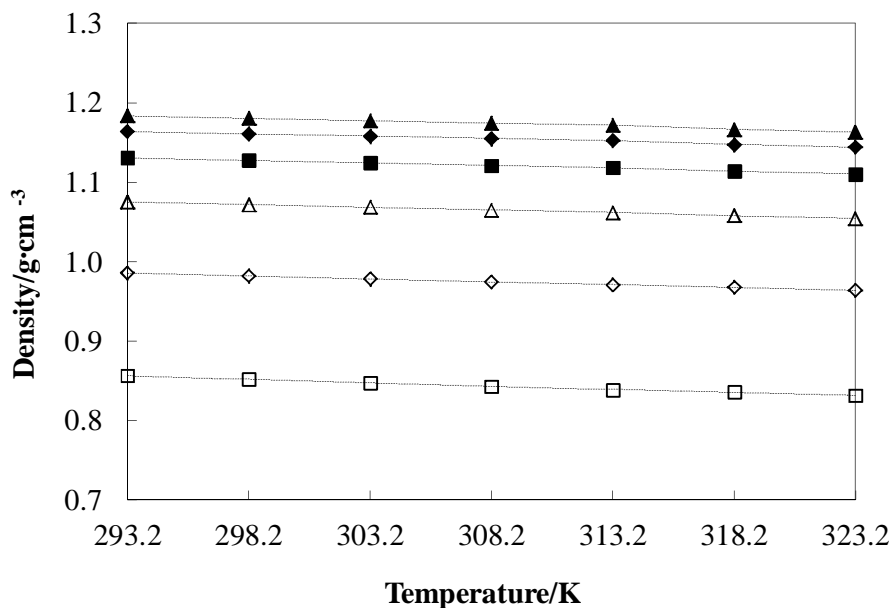


Figure 4.19 Density-temperature dependence of {[BHEAF](1) + methanol(2)} binary mixtures with different moles fraction of [BHEAF]. Symbols: □, 0.0508; ◇, 0.2050; △, 0.4016; ■, 0.6114; ◆, 0.8019, and ▲, 0.9618



#### 4.3.1.1 Excess Molar Volume

The excess molar volumes for the binary mixture of ionic liquids with alcohol are calculated using equation (2.10),

$$V_m^E = \left( \frac{x_1 M_1 + x_2 M_2}{\rho_{mix}} \right) - \left( \left( \frac{x_1 M_1}{\rho_1} \right) + \left( \frac{x_2 M_2}{\rho_2} \right) \right) \quad (2.10)$$

The values of  $V_m^E$  for binary mixture of ionic liquids with alcohol are listed in Table C.3 of Appendix C.

The excess molar volume are fitted with the Redlich-Kister polynomial equation,

$$\Delta Q_{ij} = x_i x_j \sum_{k=0} A_k (x_i - x_j)^k \quad (2.11)$$

The fitted parameters of the Redlich-Kister polynomial equation for excess molar volume of binary mixture of ionic liquids with alcohol are listed in Table C.4 of Appendix C.

The values of excess molar volume for {[BHEAF](1) + methanol(2), or ethanol(2), or 1-propanol(2)} binary mixture at temperature 298.15 K, as well as its Redlich-Kister fits are plotted in Figure 4.20. The graphs of  $V_m^E$  indicate that all mixture of {[BHEAP](1) + alcohol(2)} exhibit negative deviations from ideality over the entire composition range. The negative excess molar volumes indicate that a tighter packing and/or attractive interaction occurred when the ionic liquids and alcohol were mixed. The same behavior was also observed for binary mixture of imidazolium ionic liquids and alcohol [122-124]. Graphs depict also the unsymmetrical behavior of the changes in the excess molar volumes with composition for these systems. The values of  $V_m^E$  become more negative from 1-propanol to methanol. The excess molar volume in these mixtures decreases as the chain length of the alcohol decreases [122-124].

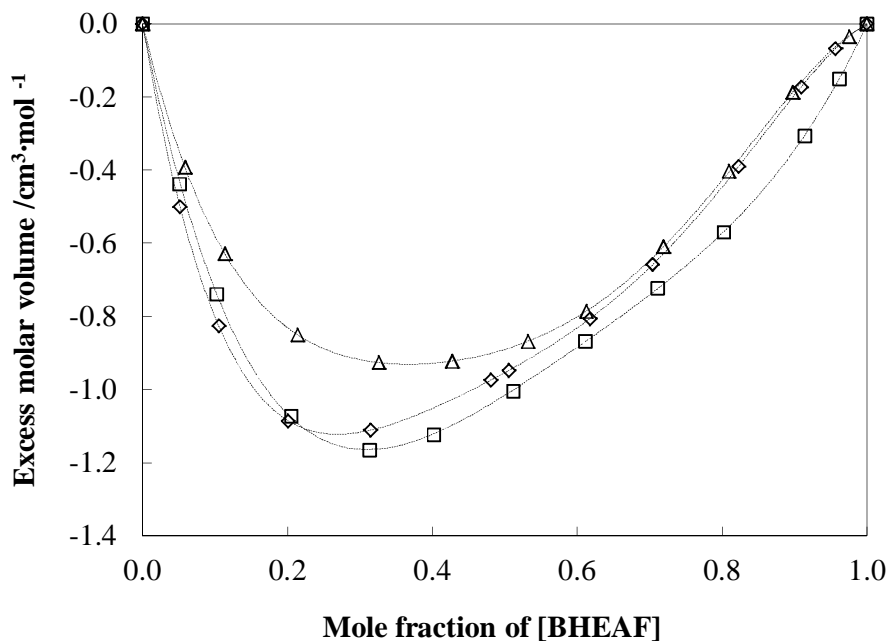


Figure 4.20 Excess molar volume,  $V_m^E$ , for {[BHEAF](1) + Alcohol(2)} binary mixture at temperature 298.15 K. Symbols:  $\square$ , {[BHEAF](1) + methanol(2)};  $\diamond$ , {[BHEAF](1) + ethanol(2)};  $\Delta$ , {[BHEAF](1) + 1-propanol(2)}.

Figure 4.21 present the graph of excess molar volume for {[BHEAF](1) + methanol(2)} binary mixture as a function of temperature. The graph indicates that with increasing temperature, the value for the minimum  $V_m^E$  shifts to a lower one. The same trends were also observed for the other two alcohol system. The excess molar volume data become less negative in the following order: methanol < ethanol < 1-propanol. It is known that in the series of alcohols, the dielectric constants increase with decreasing carbon-chain length. Therefore, the strength of ion-dipole interactions between the [BHEAF] and the alcohols is in agreement with the increasing order observed. At higher temperatures, the minimum  $V_m^E$  shifts to the lower values.

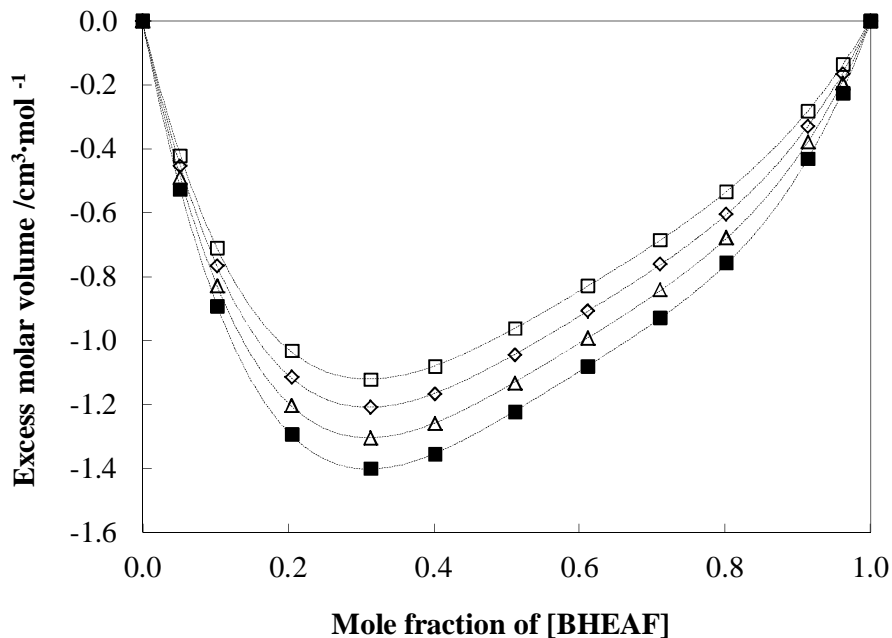


Figure 4.21 Excess molar volume,  $V_m^E$ , for {[BHEAF](1) + methanol(2)} binary mixture at several temperature. Symbols: □, 293.15 K; ◇, 303.15 K; △, 313.15 K; ■, 323.15 K

The high negative deviation from ideality, observed for these systems was a result of strong intermolecular interactions between the ionic liquids and the alcohols. In this binary mixtures, the observed  $V_m^E$  values may be explained by four opposing sets of contributions: (1) weakening of interaction between the cation and the anion of ionic liquids during addition of alcohol; (2) contraction of ionic liquids due to specific interactions with the alcohol; (3) size difference; and (4) expansion due to steric repulsion between alkyl chain of an alcohol *i.e.*, 1-propanol, and that of [BHEAF], van der Waals interactions between the alkane chains. The same behaviors of excess molar volume were also reported for imidazolium based ionic liquids with methanol, ethanol, and 1-propanol [122-124].

#### 4.3.1.2 Partial Molar Volume

The partial molar volume at infinite dilution is a fundamental property of the mixture that helps to explain the solute-solvent interactions, where solvent-solvent interactions are vanishing [112]. The thermodynamic behavior of the dilute mixtures is important for understanding the solute and solvent molecular interactions and the microscopic structure of the solutions. The partial molar volume for {[BHEAF](1) + alcohol(2)} binary mixture are given in Table C.5 of Appendix C. Figure 4.22 shows the apparent molar volume,  $V_\phi$ , for {[BHEAF](1) + methanol(2)} binary mixture at temperature 298.15 K.

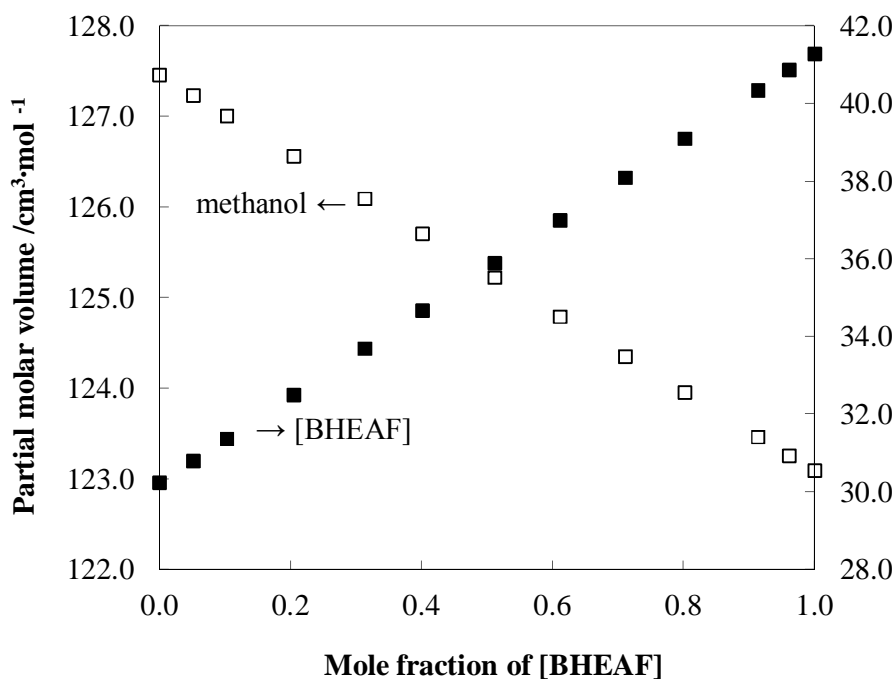


Figure 4.22 Partial molar volume,  $V_\phi$ , for {[BHEAF](1) + methanol(2)} binary mixture at temperature 298.15 K.

The graph indicates that the partial molar volume of species at infinite dilution is smaller than corresponding molar volume of pure species. The partial molar volume for the other two systems also shows the same pattern. The same trend was also observed for the partial molar volume of imidazolium based ionic liquids with alcohol [122-124]. This can be explained by the fact that alcohol molecule partially fit into the open or empty spaces in ionic liquids. At infinite dilution, each ion is surrounded only by the solvent molecules and being infinitely distant from the other ions. It follows that the apparent molar volume at infinite dilution is unaffected by interaction among ions and it is a pure measurement of the (ion + solvent) interaction [122-124].

#### 4.3.2 Coefficient of Thermal Expansion for Binary Mixture

A frequently applied derived value for industrial mixtures is the temperature dependence of volume, which is expressed as coefficient of thermal expansion. As in the case of pure chemicals it can be calculated using equation (2.2),

$$\alpha = \frac{1}{V} \left( \frac{\delta V}{\delta T} \right)_P = -\frac{1}{\rho} \left( \frac{\delta \rho}{\delta T} \right)_P \quad (2.2)$$

Coefficient of thermal expansion for {[BHEAF](1) + alcohol(2)} binary mixture is given in Appendix C.6 of Appendix C. Figure 4.23 presents the plot of coefficient of thermal expansion for {[BHEAF](1) + alcohol(2)} binary mixture at temperature 298.15 K.

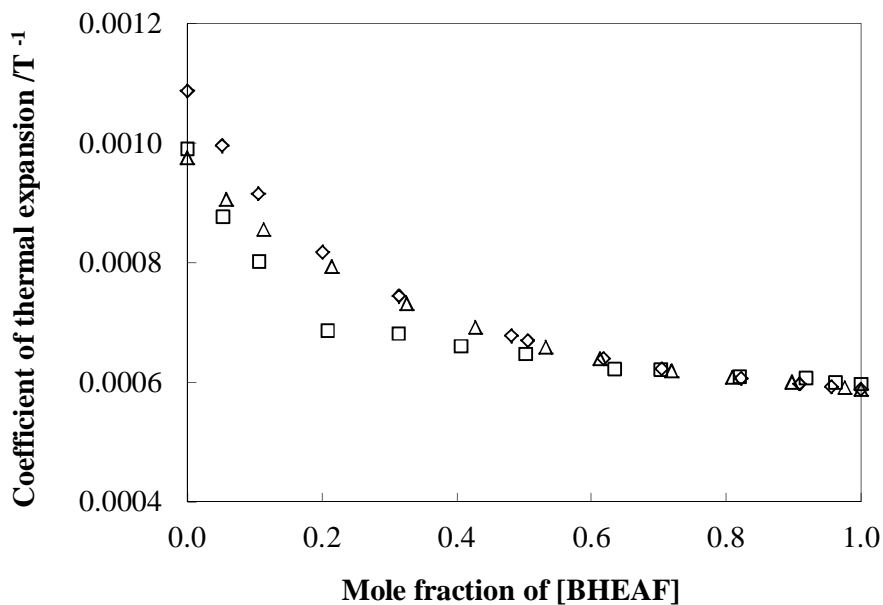


Figure 4.23 Coefficient of thermal expansion for binary mixture of ionic liquids with alcohol at temperature 298.15 K. Symbols: □, {[BHEAF](1) + methanol(2)}; ◇, {[BHEAF](1) + ethanol(2)}; △, {[BHEAF](1) + 1-propanol(2)}

The graph indicates that the coefficient of thermal expansion for {[BHEAF](1) + alcohol(2)} binary mixture decreases with increasing concentration of ionic liquids. The coefficient of thermal expansion is highest at pure alcohol and the value decreases with increasing mole fraction of ionic liquids, and it reaches the lowest value at pure ionic liquids. At mole fraction of ionic liquids above 0.2, the coefficients of thermal expansion are less dependants on temperature compared to those observed for mole fraction of ionic liquids below 0.2. The same trend was also observed at higher temperature, as can be seen in Figure 4.24.

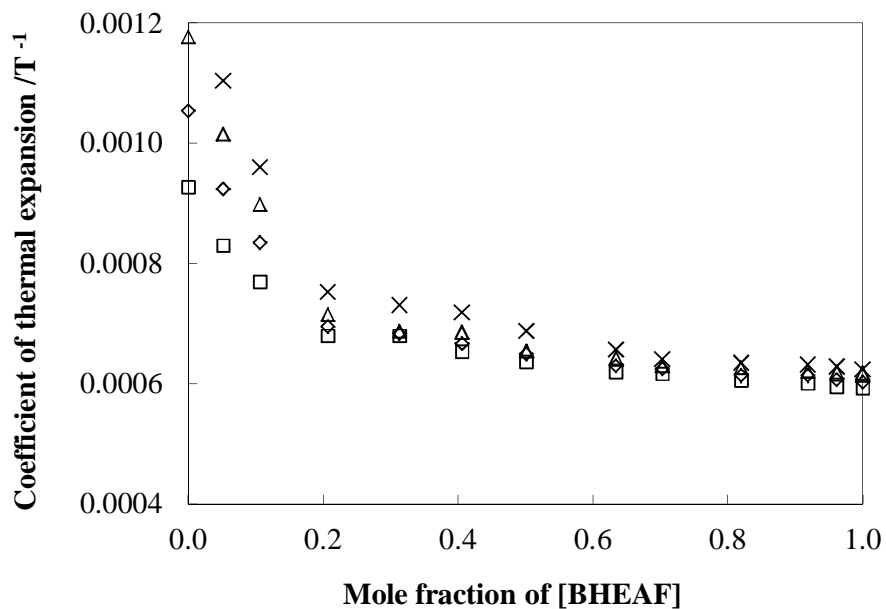


Figure 4.24 Coefficient of thermal expansion for {[BHEAF](1) + methanol(2)} binary mixture at several temperatures. Symbols: □, 293.15 K; ◇, 303.15 K; △, 313.15 K; ×, 323.15 K.

### 4.3.3 Viscosity of Binary Mixture

The viscosities of {[BHEAF](1) + alcohol(2)} binary mixture were measured using vibrating-tube viscometer, SVM 3000 (Anton Paar, Austria) at temperature range from 293.15 to 353.15 K with interval 5 K. The experimental results are given in Table C.7 of Appendix C. Prior to the measurement of the viscosities of ionic liquids; calibrations on the viscometer were done by measuring the viscosity of selected organic solvent and some imidazolium ionic liquids which the viscosity are known.

The changes of dynamic viscosities with composition is presented in Figure 4.25 for {[BHEAF](1) + alcohol(2)} binary mixture. The viscosities of binary mixture of ionic liquids with alcohol were affected by the composition of alcohol in the system. The viscosities of {[BHEAF](1) + alcohol(2)} binary mixture were lowest at pure alcohol and its value increases with increasing mole fraction of ionic liquids in the system, and reaches the highest value at pure ionic liquids. The observed decrease in viscosity with an increase in the alcohol content is particularly more significant in dilute solutions of an alcohol in the ionic liquid. As discussed above, ion-dipole interactions and/or hydrogen bonding between the cation of the ionic liquids and an alcohol will take place when an alcohol is added to the ionic liquid. This weakening of the strong hydrogen bonding interactions between cation and anion of the ionic liquid leads to a higher mobility of the ions and a lower viscosity of the mixture.

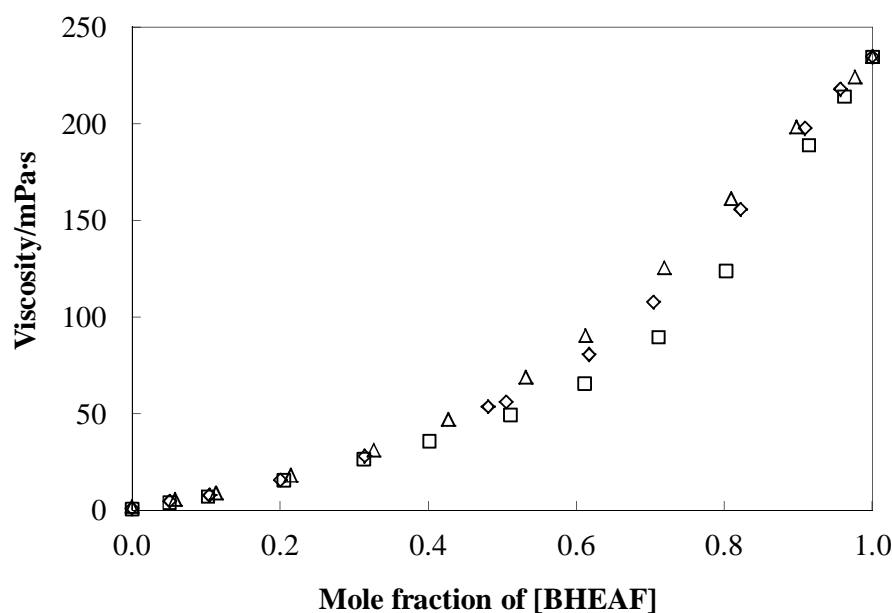


Figure 4.25 Viscosity of binary mixture of ionic liquids with alcohol at temperature 298.15 K. Symbols: □, {[BHEAF](1) + methanol(2)}; ◇, {[BHEAF](1) + ethanol(2)}; △, {[BHEAF](1) + 1-propanol(2)}



Figure 4.26 presents the viscosity of {[BHEAF](1) + methanol(2)} binary mixture at several temperature. The observed decrease in viscosity {[BHEAF](1) + methanol(2)} of the binary mixture with increasing temperature is due to higher mobility of the ions at higher temperature. The effect becomes more obvious at higher temperature. The same effect was also observed for binary mixture of ionic liquids and alcohol [122-124].

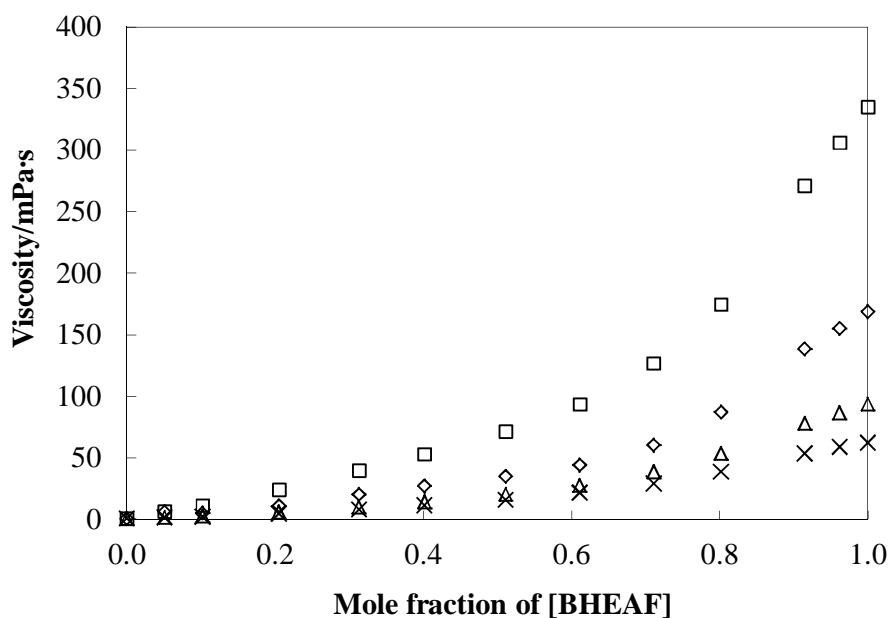


Figure 4.26 Viscosity of {[BHEAF](1) + methanol(2)} binary mixture at several temperatures. Symbols: □, 293.15 K; ◇, 303.15 K; △, 313.15 K; ×, 323.15 K

#### 4.3.3.1 Viscosity Deviation From Ideal Mixtures

The viscosity deviation,  $\Delta\eta$ , for binary mixture of ionic liquids with alcohol were calculated using equation (2.23),

$$\Delta\eta = \eta_{mix} - (x_1\eta_1 + x_2\eta_2) \quad (2.23)$$

The values of  $\Delta\eta$  for binary mixture of ionic liquids with alcohol are listed in Table C.8 of Appendix C.

Deviation of viscosity can be also correlated using the Redlich Kister equation. For deviation of viscosity, it can be calculated using equation (2.23),

$$\Delta\eta = x_i x_j \sum_{k=0} A_k (x_i - x_j)^k$$

The fitted parameters for the Redlich-Kister polynomial equation for viscosity deviation of the binary mixture of ionic liquids with alcohol are listed in Table C.9 of Appendix C. The viscosity deviation for {[BHEAF](1) + alcohol(2)} binary mixture at temperature 298.15 K, as well as their Redlich-Kister correlation are plotted in Figure 4.21. Whereas, the effect of temperature on viscosity deviation of {[BHEAF](1) + methanol(2)} at several temperatures is plotted in Figure 4.22.

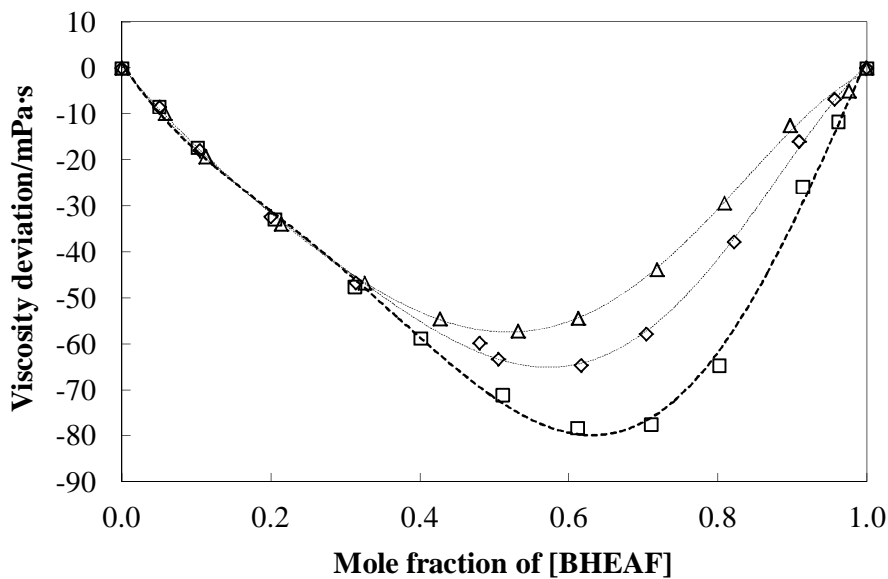


Figure 4.27 Viscosity deviation,  $\Delta\eta$ , for for {[BHEAF](1) + alcohol(2)} binary mixture at temperature 298.15 K. Symbols: □, {[BHEAF](1) + methanol(2)}; ◇, {[BHEAF](1) + ethanol(2)}; △, {[BHEAF](1) + 1-propanol(2)}.

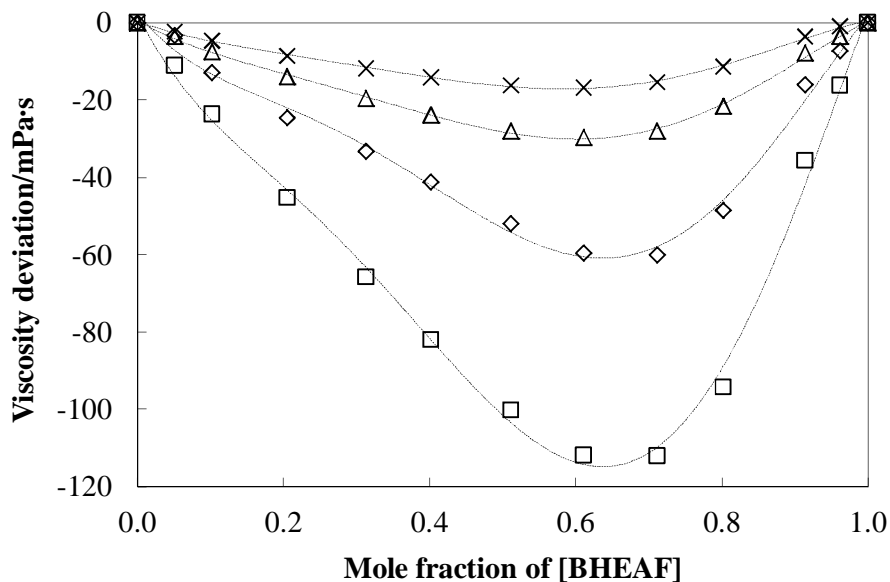


Figure 4.28 Viscosity deviation,  $\Delta\eta$ , for {[BHEAF](1) + methanol(2)} binary mixture at several temperature. Symbols: □, 293.15 K; ◇, 303.15 K; △, 313.15 K; ×, 323.15 K.

These graphs indicate that the viscosity deviations are negative over the whole composition range. The extent of the deviation reduces as temperature increases and this behavior is similar for all systems. The viscosity deviation is particularly significant in solutions with dilute alcohol content due to the high differences in the viscosity of the two pure compounds. The viscosity deviation at 293.15 K is greater than at 303.15 K or 318.15 K or 323.15 K due to the larger reduction in the viscosity of the pure ionic liquid at higher temperature. This agrees well with the result reported for the mixture of the other ionic liquids with alcohol in general [122-124].

#### 4.3.4 Refractive Index of Binary Mixture and Refractive Index Deviation

The refractive index of {[BHEAF](1) + alcohol(2)} binary mixture were measured using ATAGO programmable digital refractometer model RX-5000 alpha at temperature range from 293.15 to 353.15 K with intervals of 10 K. The experimental results are given in Table C.10 of Appendix C. Prior to the measurement of the viscosities of the ionic liquids; calibrations of the viscometer were done by measuring the refractive index of selected organic solvent and some imidazolium ionic liquids which their refractive index values were predetermined. The trend for the changes in the refractive index for {[BHEAF](1) + alcohol(2)} binary mixture with composition is presented in Figure 4.23.

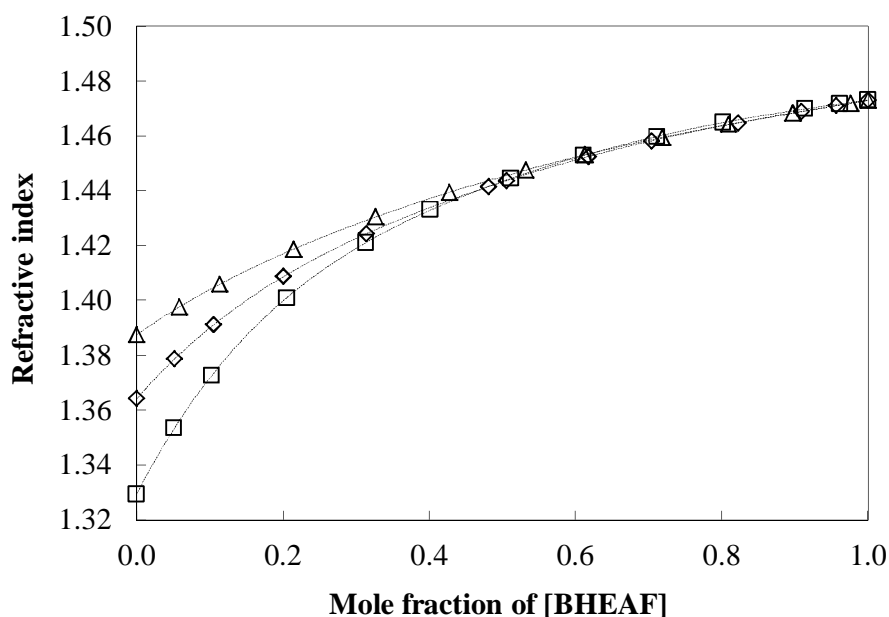


Figure 4.29 Refractive index of binary mixture of ionic liquids with alcohol at temperature 298.15 K. Symbols:  $\square$ , {[BHEAF](1) + methanol(2)};  $\diamond$ , {[BHEAF](1) + ethanol(2)};  $\Delta$ , {[BHEAF](1) + 1-propanol(2)}

As can be seen from Figure 4.23, the refractive index of the binary mixture of ionic liquids with alcohol was also affected by the composition of alcohol in the system. The viscosities of {[BHEAF](1) + alcohol(2)} binary mixture were lowest at pure alcohol and its value increases with the mole fraction of ionic liquids in the system, and reaches the highest value at pure ionic liquids, for the same reason as discussed above for excess molar volume and viscosity deviation.

Figure 4.24 presents the refractive index of {[BHEAF](1) + methanol(2)} binary mixture at several temperature. The graph indicates that the refractive index of the binary mixture decreases with increasing temperature. The same trend was also observed for the other two ionic liquids.

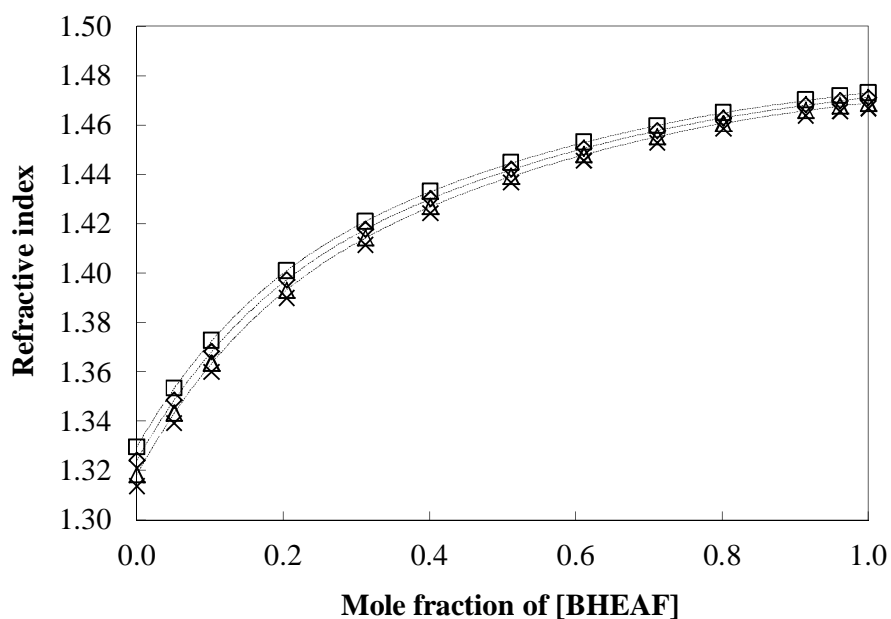


Figure 4.30 Refractive index of {[BHEAF](1) + methanol(2)} binary mixture at several temperatures. Symbols: □, 293.15 K; ◇, 303.15 K; △, 313.15 K; ×, 323.15 K

#### 4.3.4.1 Refractive Index Deviation from Ideal Mixtures

The viscosity deviation,  $\Delta n_D$ , for binary mixture of ionic liquids with alcohol were calculated using equation (2.24),

$$\Delta n_D = n_{D_{mix}} - (x_1 n_{D,1} + x_2 n_{D,2}) \quad (2.24)$$

The values of  $\Delta n_D$  for binary mixture of ionic liquids with alcohol are listed in Table C.11 of Appendix C.

Refractive index deviation can also be correlated using Redlich Kister equation. For refractive index deviation, it can be calculated using equation (2.25),

$$\Delta n_D = x_i x_j \sum_{k=0} A_k (x_i - x_j)^k \quad (2.25)$$

The fitted parameters for the Redlich-Kister polynomial equation for refractive index deviation of the binary mixture of ionic liquids with alcohol are listed in Table C.12 of Appendix C.

The refractive index deviation for {[BHEAF](1) + alcohol(2)} binary mixture at temperature 298.15 K, as well as their Redlich-Kister correlation are plotted in Figure 4.31. The effect of temperature on refractive index deviation of {[BHEAF(1) + methanol(2)} at several temperatures is plotted in Figure 4.32. The two graphs indicate that the refractive index deviations are positive over the whole composition range. The extent of the deviations become less positive as the temperature increases, and this behavior was observed for all system.

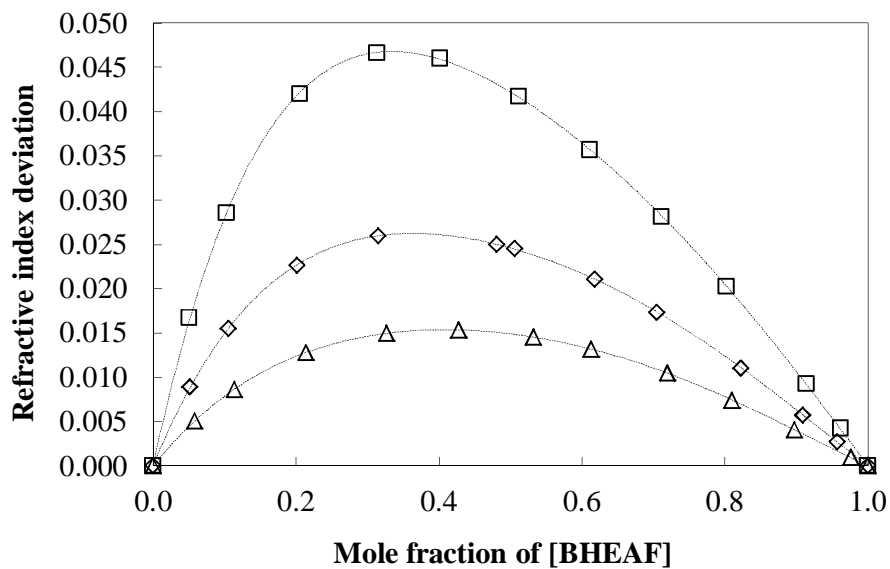


Figure 4.31 Refractive index deviation,  $\Delta n_D$ , for for {[BHEAF](1) + alcohol(2)} binary mixture at temperature 298.15 K. Symbols:  $\square$ , {[BHEAF](1) + methanol(2)};  $\diamond$ , {[BHEAF](1) + ethanol(2)};  $\Delta$ , {[BHEAF](1) + 1-propanol(2)}.

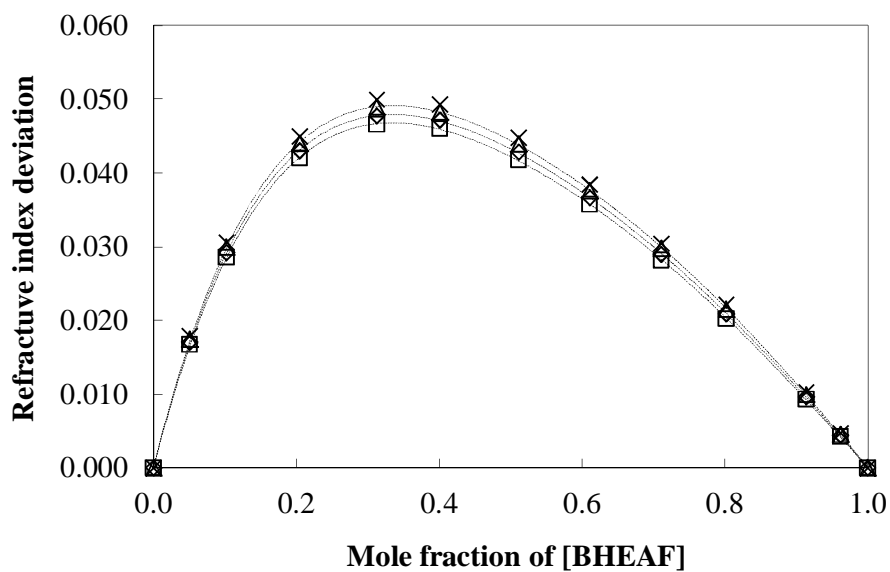


Figure 4.32 Refractive index deviation,  $\Delta n_D$ , for {[BHEAF](1) + methanol(2)} binary mixture at several temperature. Symbols:  $\square$ , 293.15 K;  $\diamond$ , 303.15 K;  $\Delta$ , 313.15 K;  $\blacksquare$ , 323.15 K

#### 4.4 Density of 1 M HCl

The density of corrosive solution, 1 M HCl in the various concentrations of ionic liquids [BHEAF] was measured at temperatures 303.15, 313.15, 323.15, and 333.15 K. The results are presented in Figure 4.33. The density of 1 M HCl slightly increases with increasing concentration of ionic liquids and decreases with increasing temperature. It is also noticed that the density of 1 M HCl in the presence of 0.08 M of [BHEAF] has least effected by change of temperature. This is due to presence of ionic liquids, which is known to be considerably less dependent on temperature [101, 113]. The temperature dependence of density is correlated using equation (2.1). Table 4.10 presents the fit parameter meanwhile Figure 4.34 presents the density of 1 M HCl in the presence of various concentrations of ionic liquids [BHEAF] and their correlation equation.

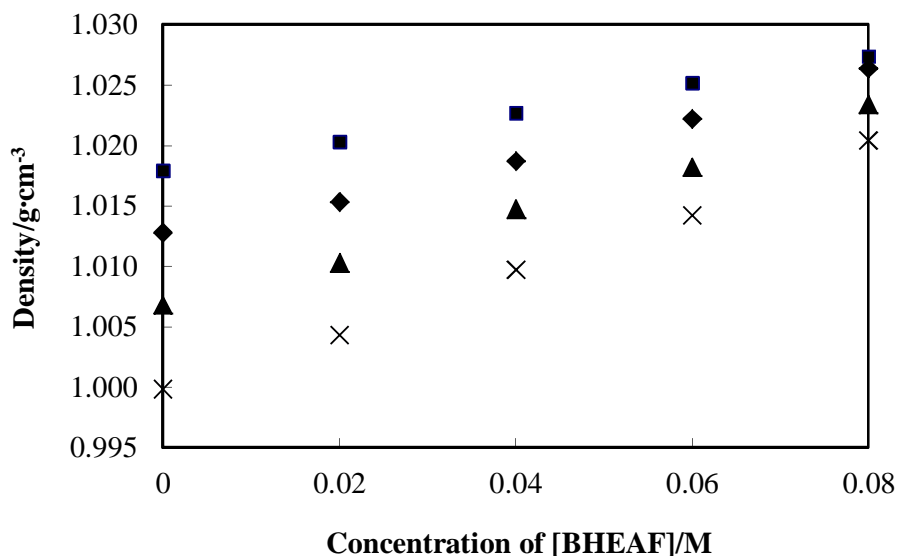


Figure 4.33 Density of 1 M HCl solution in the presence of various concentration of ionic liquids [BHEAF] at several temperatures. Symbols: ■,  $T = 303.15$  K; ♦,  $T = 313.15$  K; ▲,  $T = 323.15$  K; and ×,  $T = 333.15$  K



As can be seen from Table 4.10 and 4.34, the temperature dependence of 1 M HCl in the presence of various concentration of ionic liquids [BHEAF] is well correlated using equation (2.1). The fit parameter given in Table 4.10 may helpful to predict the density of 1 M HCl in the presence of 0 – 0.08 M ionic liquids [BHEAF]

Table 4.10 Fit parameter for temperature dependence of density of 1 M HCl with the various concentrations of [BHEAF] calculated using equation (2.1) and its standard deviation calculated using equation (4.1)

[BHEAF]/M	0.00	0.02	0.04	0.06	0.08
$a_0$	1.2012	1.1812	1.1533	1.1377	1.1008
$10^4 \cdot a_1$	-6.03	-5.30	-4.30	-3.70	-2.40

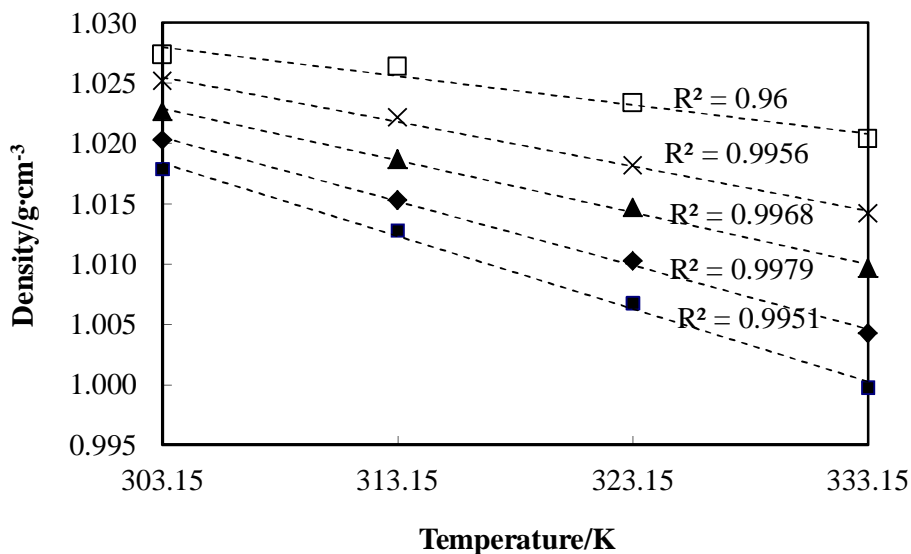


Figure 4.34 Temperature dependence of density of 1 M HCl solution in the presence of various concentration of ionic liquids [BHEAF] at several temperatures. Symbols: ■, 0 M; ◆, 0.02 M; ▲, 0.04 M; ×, 0.06 M; and □, 0.08 M

#### 4.5 Concluding Remarks

There are various commercial ionic liquids available in the market. However, their prices are relatively higher compared to commercial corrosion inhibitor. An alternative way is to find cheaper ionic liquids that can be applied as corrosion inhibitor for carbon steel in acidic medium. Hydroxyl ammonium ionic liquids could potentially be the alternatives. In this research, 16 different hydroxyl ammonium ionic liquids were synthesized and characterized. The synthesis was carried out by direct protonation of alkanolamines with acid. Ease of manufacturing as well as low cost materials are some of the reasons for choosing alkanolamine as the cation source. The structure of the synthesized ionic liquids was confirmed through infrared and NMR spectra. The chemical composition of the synthesized ionic liquids was established from CHN analysis.

Prior to applying ionic liquids for industrial application such as corrosion inhibitor, the physical properties of the ionic liquids have to be determined. The properties such as density and viscosity of the ionic liquids must be examined and reported together with their performance for corrosion inhibition. However, most of the published reports on corrosion inhibitor lack these physical properties data. In this research, physical properties such as density, viscosity, and refractive index of pure synthesized hydroxyl ammonium ionic liquids were measured at several temperatures. The density and viscosity of the synthesized ionic liquids were found to be higher than some organic solvent. The synthesized ionic liquids showed high solubility in polar solvent such as methanol, ethanol, and 1-propanol. Further investigation was conducted to study the solute-solvent behavior of ionic liquids with alcohol by measuring physical properties of {ionic liquids(1) + alcohol(2)} binary mixture. The obtained result indicated that a tighter packing and/or attractive interaction occurred when the ionic liquids and alcohol were mixed. The extent of the packing tightness and/or attractive interaction increases with increased in temperature. The partial molar volumes of the ionic liquids in infinite dilution in alcohol showed that volume of ionic liquids in solution is smaller compared to its pure system.

The high solubility of the synthesized ionic liquids in polar solvent such as alcohol and HCl, may provide some advantages when used as corrosion inhibitor. Firstly, it ensures that the synthesized ionic liquids could be completely mixed with the HCl acid, thus reducing the concentration of the corrosive species down to an acceptable level. Secondly, the physical properties of the ionic liquids such as viscosity could also be reduced leading to a lower shear stress of the production fluid.

From this chapter, the synthesis, characterization, and physical properties of the studied ionic liquids is well presented. In addition, the physical property of the synthesized ionic liquids with alcohol is also reported. This analysis could be a good platform to study the application of ionic liquids as corrosion inhibitor that will be considered in the next chapter.



## CHAPTER 5

### APPLICATION OF IONIC LIQUIDS AS INHIBITOR ON CARBON STEEL CORROSION IN ACIDIC MEDIUM

This chapter presents the test performed to measure the potential of applying the synthesized ionic liquids as corrosion inhibitor on carbon steel under acidic medium. Section 5.1 discusses the effect of concentration and temperature on inhibition efficiency of the ionic liquids on carbon steel corrosion in acidic medium. The inhibition potential is also discussed in terms of Tafel Plots and Electrochemical Impedance Spectroscopy. The adsorption and thermodynamics of adsorption are discussed in section 5.2. Section 5.3 presents the proposed inhibiting mechanism of the carbon steel corrosion in acidic medium in the presence of the ionic liquids corrosion inhibitor.

#### **5.1 Effect of Concentration of Ionic Liquids on Corrosion Rate of Carbon Steel Corrosion**

The effect of ionic liquids concentration on carbon steel corrosion in 1 M HCl was determined from concentration of 0.001 to 1 M. Figure 5.1 shows the effect of ionic liquids concentration on corrosion rate of carbon steel in 1 M HCl at 298.15 K. It was observed that the corrosion rate of carbon steel in 1 M HCl decrease with increasing concentration of ionic liquids. It indicates that the addition of ionic liquids reduce the corrosion rate of carbon steel in 1 M HCl. The same trend was observed for all synthesized ionic liquids in this work.

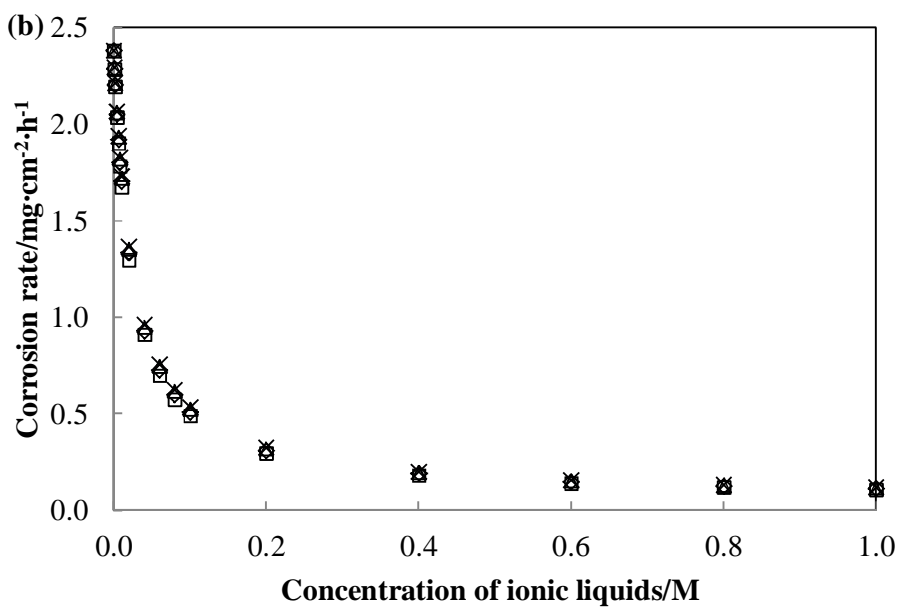
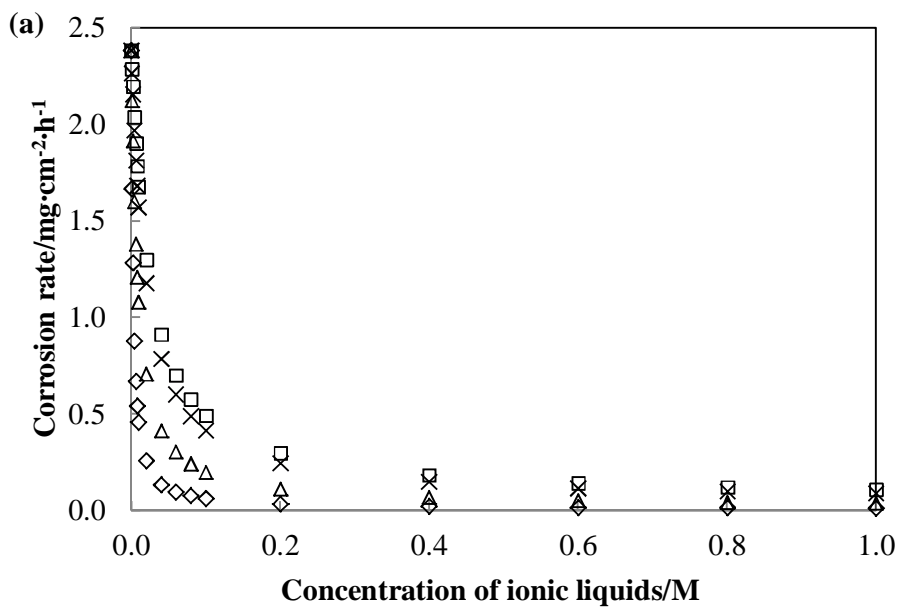


Figure 5.1 Effect of ionic liquids concentration on corrosion rate of carbon steel in 1 M HCl in 1 M HCl at 298.15 K determined using weight loss method. (a) Ionic liquids with formate anion. Symbols: □, [HEF]; ◇, [BHEAF]; △, [BHEMF], and ×, [THEAF]. (b) Ionic liquids with 2-hydroxyethylammonium cation. Symbols: □, [BHEAF]; ◇, [BHEAA]; △, [BHEAP], and ×, [BHEAL].

The corrosion rate of carbon steel in 1 M HCl decreases in the presence of ionic liquids. It is due to ionic liquids adsorbed themselves on the carbon steel surface. Quaternary ammonium salts were reported to inhibit corrosion of carbon steel in acid media [3, 10, 11, 193-197]. As the charged nitrogen in such a molecule has no free orbital for covalent bonding to the surface, it is likely to prevent corrosion by geometrical blocking of the surface [193, 194]. Adsorption of alkyltrimethylammonium bromides with carbon chains (C12–C18) were investigated using quartz crystal microbalance (QCM) on model surfaces of iron and cementite [197]. The adsorption was shown to be reversible and to reach a maximum near the critical micelle concentration. It was concluded that the surfactants adsorbed as discrete aggregates rather than as a film, since the amount adsorbed was less than what was needed to form a monolayer [197]. This conclusion is further supported by comparison to adsorption experiments on other hydrophilic surfaces [195], where adsorption of discrete micelles has been observed by means of atomic force microscopy.

In this work, the inhibition efficiency of the synthesized ionic liquids on carbon steel corrosion in 1 M HCl at temperatures of 298.15, 313.15, 328.15, and 343.15 K is measured using two methods, namely weight loss and electrochemical methods. The effects of various parameters such as concentration of the ionic liquids, temperature, and addition of alcohol on the efficiency of the ionic liquids as inhibitors are studied.

### 5.1.1 Weight Loss Method

The inhibition efficiency for all the synthesized ionic liquids was calculated using the equation (2.29) as shown below,

$$IE(WL) / \% = \frac{CR_{corr} - CR_{corr}^{inh}}{CR_{corr}} \times 100 \quad (2.29)$$

The inhibition efficiency for the carbon steel in 1 M HCl solution at 298.15, 313.15, 328.15, and 343.15 K in the presence of different types of ionic liquids are given in Table D.2 of Appendix D.

Figure 5.2 show the inhibition efficiency of various ionic liquids with different cation and anion on carbon steel corrosion in 1 M HCl at 298.15 K. In general, the inhibition efficiency increases with increasing concentration, reaching a limiting value, which depends on the used inhibitor and practically, is not influenced by further concentration increase. The difference between the inhibitors is best seen in the middle concentration range, reflecting the influence of the molecular structure on their protective properties. Hence, in this study, the inhibition efficiencies are discussed at concentration (0.02, 0.04, 0.06, and 0.08) M of ionic liquids.

#### 5.1.1.1 *Effect of Anion*

The effect of the anion type on the inhibiting performance is investigated by looking at four different anions namely Formate, Acetate, Propionate, and Lactate. Figure 5.3 shows the inhibition efficiency of the respective ionic liquids with different anions coupled with bis(2-hydroxyethyl)ammonium as the cation. The inhibition efficiency increases with increasing concentration of the ionic liquids. The ionic liquids [BHEAF] shows the highest inhibition efficiency. It is followed by [BHEAA], then [BHEAP] and [BHEAL] showing almost the same inhibition efficiency. Hence, for the bis(2-hydroxyethyl)ammonium cation, the type of anion of the ionic liquids can be ranked according to Formate > Acetate > Propionate > Lactate. It appears that the inhibition effect of the anion decreases with increasing molecular size of the anion. Increasing molecular size of the anion leads to decrease on the electrostatic interaction with their cation, hence forming less dense protective layer on the carbon steel surface.



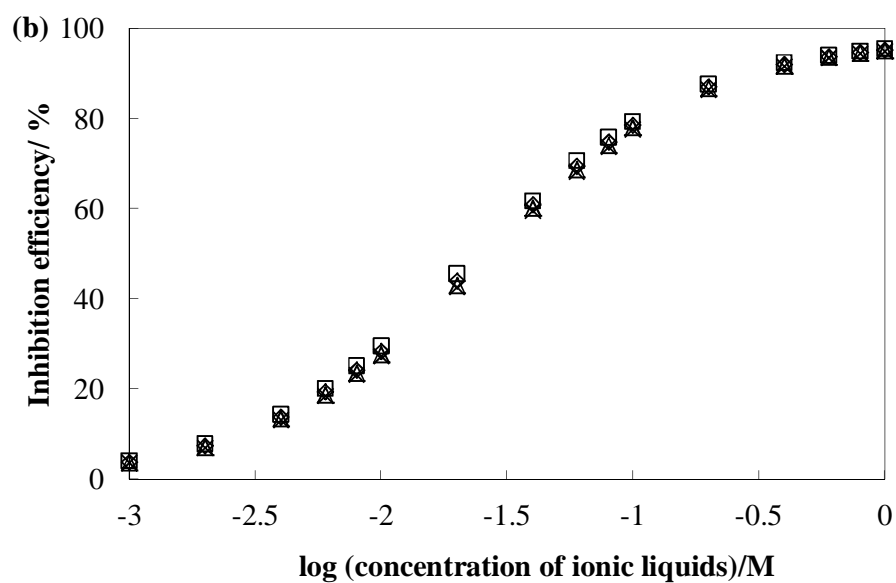
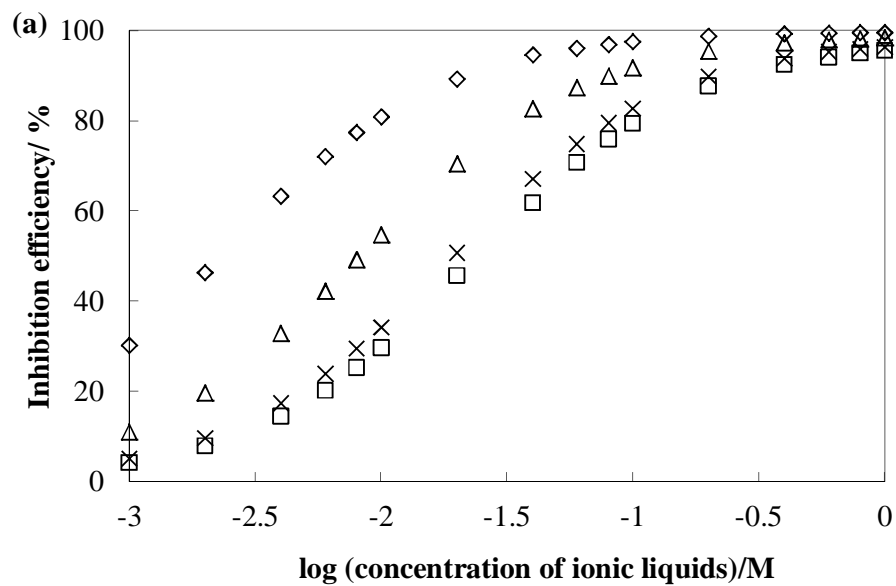


Figure 5.2 Corrosion rate of carbon steel in 1 M HCl in the presence of various concentrations of ionic liquids [BHEAF] at 298.15 K measured using weight loss method. (a) Ionic liquids with formate anion. Symbols:  $\square$ , [HEF];  $\diamond$ , [BHEAF];  $\Delta$ , [BHEMF], and  $\times$ , [THEAF]. (b) Ionic liquids with 2-hydroxyethylammonium cation. Symbols:  $\square$ , [BHEAF];  $\diamond$ , [BHEAA];  $\Delta$ , [BHEAP], and  $\times$ , [BHEAL].

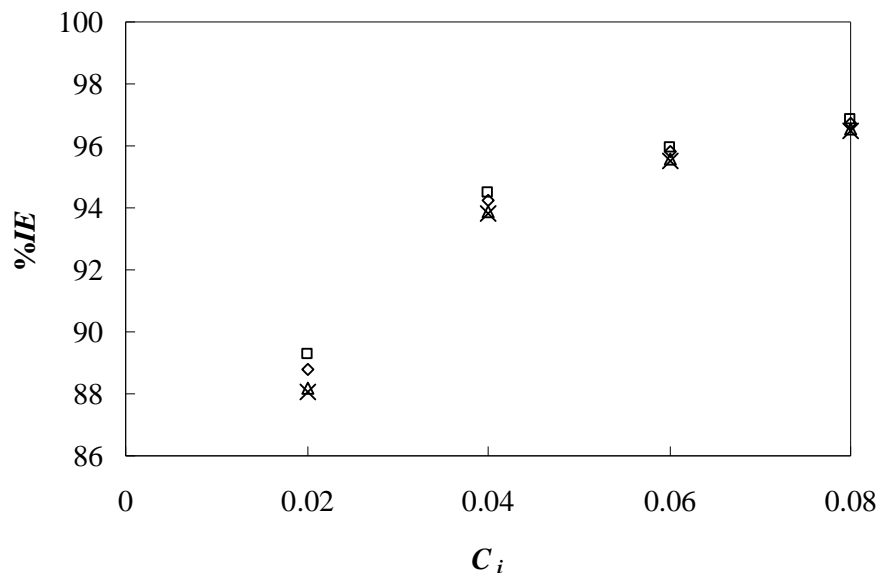


Figure 5.3 Effect of anion on concentration dependence of inhibition efficiency of ionic liquids on corrosion of carbon steel in 1 M HCl at temperature 298.15 K using weight loss method. Symbols:  $\square$ , [BHEAF];  $\diamond$ , [BHEAA];  $\Delta$ , [BHEAP]; and  $\times$ , [BHEAL].

From Figure 5.3, the inhibition efficiency for [BHEAA] and [BHEAF] at 0.02 M which are 88.79 and 89.26 %, respectively. The difference in the inhibition efficiency for the different types of anions is smaller when compared to the cations. One possible explanation for this observation is that the ionic liquids adsorbed on the carbon steel surface are through its cations, instead of its anion. The same observations were also reported for the imidazolium based cation [22-24] and ammonium-salt corrosion inhibitor [3, 10, 11, 193-197].

As can be seen from Table D.1 and D.2 of Appendix D, the same trend of the anion was also observed when it coupled with the three other cations studied in this work. Hence, the effect of anion on the inhibition performance can be ranked in the order of formate > acetate > propionate > lactate.

### 5.1.1.2 Effect of Cation

The effect of the cations on the inhibition performance was investigated by looking at four different type of cations: 2-hydroxyethanaminium, bis(2-hydroxyethyl)ammonium, bis(2-hydroxyethyl)methylammonium and tris(2-hydroxyethyl)ammonium with formate as the anion. Figure 5.4 shows the inhibition efficiency of ionic liquids with different types of cations coupled with formate as the anion.

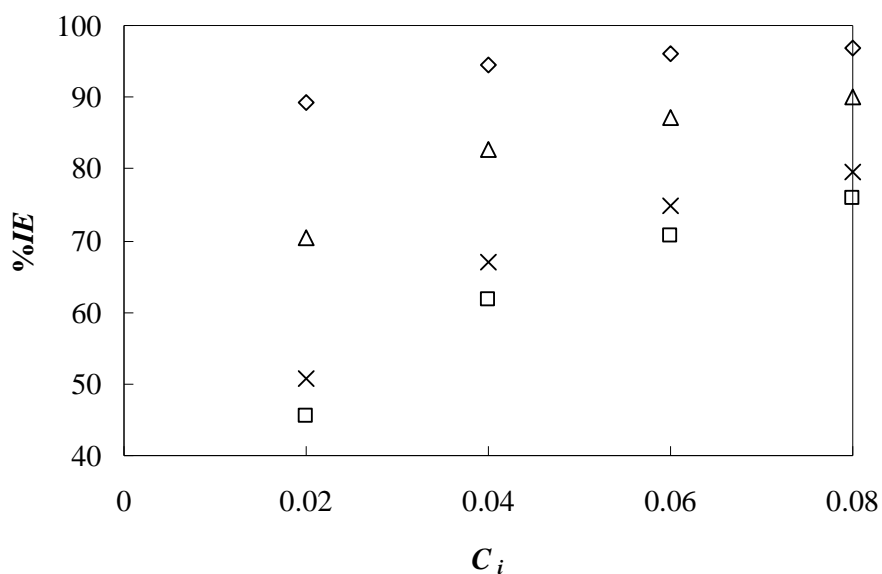


Figure 5.4 Effect of cation on concentration dependence of inhibition efficiency of ionic liquids on corrosion of carbon steel in 1 M HCl at temperature 298.15 K using weight loss method. Symbols:  $\square$ , [HEF];  $\diamond$ , [BHEAF];  $\Delta$ , [BHEMF]; and  $\times$ , [THEAF].

From Figure 5.4, the inhibition efficiency increases with increasing concentration of the ionic liquids. The ionic liquids [BHEAF] shows the highest inhibition efficiency. It is followed by [BHEMF], then [THEAF] and [HEF]. Hence, for the formate anion, the type of cation of the ionic liquids can be ranked according to bis(2-hydroxyethyl)ammonium > bis(2-hydroxyethyl)methylammonium > tris(2-hydroxyethyl)ammonium > 2-hydroxyethylammonium. As also shown in Figure 5.3, the ionic liquids with bis(2-hydroxyethyl)ammonium has a considerably higher inhibition efficiency than the other three cations. A significant increase in inhibition efficiency is observed for [HEF] and [BHEAF]. While [HEF] could not exceed 80 %*IE* at concentration of 0.08 M, [BHEAF] shows more than 95 %*IE*. It appears that the structure of the ionic liquids cation has dominant effect on their inhibition efficiency. The same observations were also reported for the ammonium-salt corrosion inhibitors [3, 10, 11, 193-197].

According to Sastri [1], stereochemical structures of the inhibitor determine their effectiveness of corrosion protection capabilities. This effectiveness depends on the packing of the inhibitor molecule on the carbon steel surface which depends on the configuration of the inhibitor molecule; the denser the layer formed on the carbon steel surface leads to higher inhibition efficiency [1].

The bis(2-hydroxyethyl)ammonium cation has the highest inhibition efficiency compared to the three other cations. It is due to linear structure and two hydroxyl functional groups attached at the end of both alkyl groups that lead to highest dense protective layer on the carbon steel surface. Addition of methyl group and hydroxyl functional group into the bis(2-hydroxyethyl)ammonium cation, such as on the bis(2-hydroxyethyl)methylammonium and tris(2-hydroxyethyl)ammonium cation, respectively, leads to decrease in inhibition efficiency. It is due to the steric effect of which prevents these cations to have denser packing protective layer on the surface of the carbon steel.

On the other hands, 2-hydroxyethylammonium cation has the least inhibition efficiency compared to the three other cations. It is due to smaller molecular volume of this cation compared to the other three studied cations. The smaller volume of the cation leads to lower degree of surface coverage.

From Table D.1 and D.2 of Appendix D, the same trend of the cation was also observed when it coupled with the three other anions studied in this work. Hence, the effect of the cation on the inhibition performance can be ranked as bis(2-hydroxyethyl)ammonium > bis(2-hydroxyethyl)methylammonium > tris(2-hydroxyethyl)ammonium > 2-hydroxyethylammonium.

#### 5.1.1.3 *Effect of Anion and Cation*

Figure 5.5 shows the effect of the anion and cation of the ionic liquids on the inhibition performance. The ionic liquids [BHEAF] has the highest inhibition efficiency, it is then followed by [BHEAA] > [BHEAP] > [BHEAL] > [BHEMF] > [BHEMA] > [BHEMP] > [BHEML] > [THEAF] > [THEAA] > [THEAP] > [THEAL] > [HEF] > [HEA] > [HEP] > [HEL].

From Figure 5.5, it can be seen clearly that differences of *IE*% values between two different cations is much larger compared to different anions. As can be seen from Table D.1 and D.2 of Appendix D, The same trend was also observed at different concentration ionic liquids used and at three other temperatures studied in this work. Thus, it can be concluded that the cation of the ionic liquids is responsible on the adsorption on the carbon steel surface.

The following discussion is focused on the ionic liquids [BHEAF] as this ionic liquids has the highest inhibition efficiency. However, it can also be used to understand the inhibition performance of the other synthesized ionic liquids described in this work.

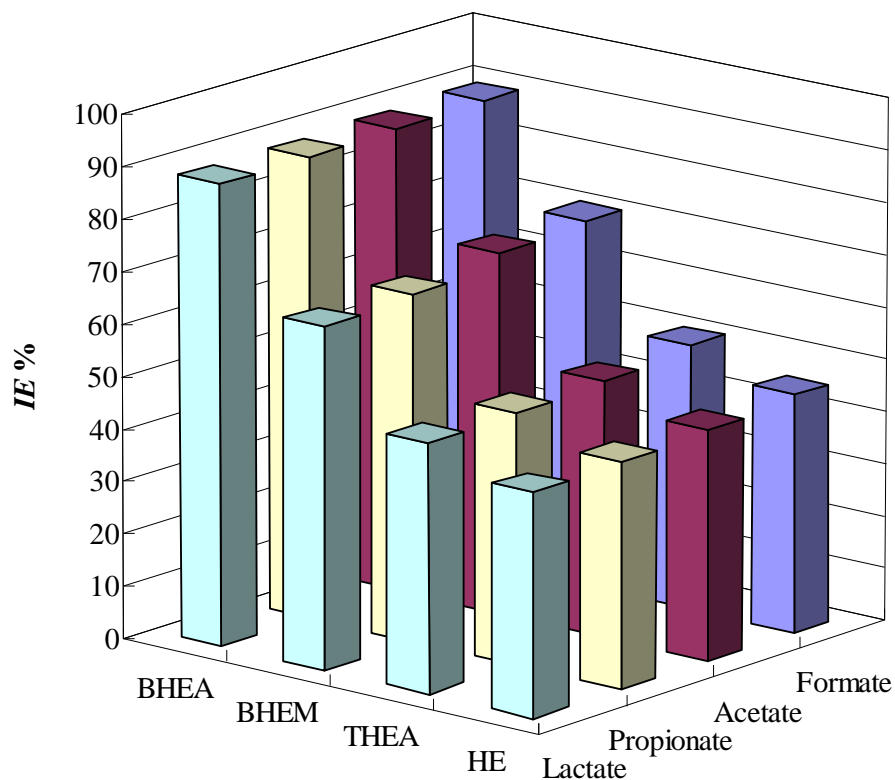


Figure 5.5 Effect of the cation and anion on the inhibition efficiency of 0.02 M ionic liquids on carbon steel corrosion at 298.15 K.

#### 5.1.1.4 SEM Analyses

The surface morphology of the carbon steel specimen before and after immersion in 1 M HCl in the absence and presence of 0.08 M of ionic liquids [BHEAF] is shown in Figure 5.6. It could be observed from Figure 5.6(b) that the carbon steel was strongly damaged in the absence of ionic liquids. SEM images of the carbon steel surface after immersion in 1 M HCl in the presence of 0.08 M of [BHEAF], is shown in Figure 5.6(c). It could be observed that in the presence of ionic liquids, the rate of carbon steel corrosion was suppressed. One possible explanation is that the adsorbed ionic liquids on the carbon steel surface form a protective film which was responsible for the inhibition of carbon steel corrosion in 1 M HCl [3, 10, 11, 193-197].

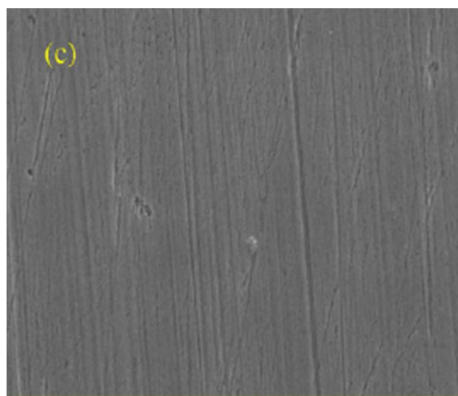
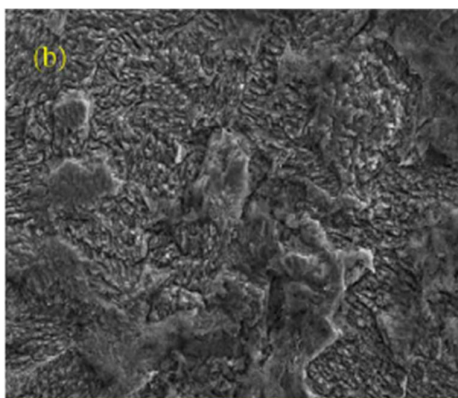


Figure 5.6 SEM micrographs of carbon steel specimens (magnificent scale 3000x). (a) Before immersion, (b) After immersion in 1 M HCl solution without inhibitor, and (c) after immersion in 1 M HCl solution in the presence of 0.08 M of ionic liquids [BHEAF].

### 5.1.2 Tafel Plots

The Tafel Plots for the carbon steel in acidic medium was measured in the various concentrations of the ionic liquids and at temperatures of 298.15, 313.15, 328.15, and 343.15 K. The Tafel Plots of carbon steel specimens in 1 M HCl were obtained at the potential range from -350 to +350 mV at a scan rate of 10 mV/minute. The respective kinetic parameters including corrosion current density,  $i_{\text{corr}}$ , and inhibition efficiency, %IE, are given in Table D.3 and D.4 of Appendix D.

Figure 5.7 shows the Tafel Plots for carbon steel in 1 M HCl in the presence of various concentration of [BHEAF] at 298.15 K. It is observed that the cathodic current potential curves give rise to parallel Tafel lines indicating that the hydrogen evolution reaction is activation controlled. The Tafel Plots also indicate that the ionic liquids manage to suppress both anodic and cathodic reactions on the active site of the carbon steel surface. It means that the ionic liquids reduce the corrosion rate of carbon steel by simple adsorption mode and the mechanism of carbon steel corrosion is the same both with and without the presence of the ionic liquids. Moreover, the value of  $E_{\text{corr}}$  in the presence of the ionic liquids [BHEAF] is nearly constant. This is a typical of mixed type inhibitors with cathodic predominance. The same behavior was also observed for imidazolium and pyridinium based ionic liquids corrosion inhibitor [22-24] and ammonium-salt corrosion inhibitors [3, 10, 11, 193-197].

The addition of the ionic liquids changes the corrosion current density, Figure 5.8 shows the relation between the concentration of ionic liquids with the corrosion current density,  $i_{\text{corr}}$ , and inhibition efficiency. It shows that increasing the concentration of the ionic liquids decreases the  $i_{\text{corr}}$  and increases its inhibition efficiency. The same trend is also observed for other ionic liquids studied. This can be attributed to the adsorption mode of the ionic liquids. The ionic liquids inhibitor molecules were adsorbed on the carbon steel surface thus blocking the surface active sites. When the concentration of the ionic liquids increases, more surface active sites will be protected because more ionic liquids molecules were adsorbed on the carbon steel surface [22-24].



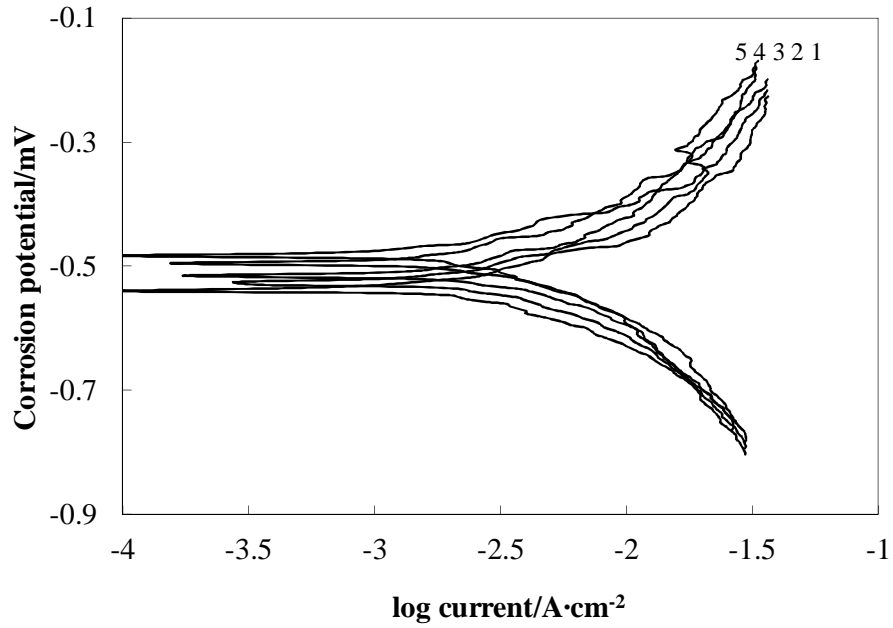


Figure 5.7 Tafel Plots of carbon steel dissolution in 1 M HCl at 298.15 K in the presence of various concentrations of ionic liquids [BHEAF]. Symbols: 1, Blank; 2, 0.02 M; 3, 0.04 M; 4, 0.06 M; and 5, 0.08 M.

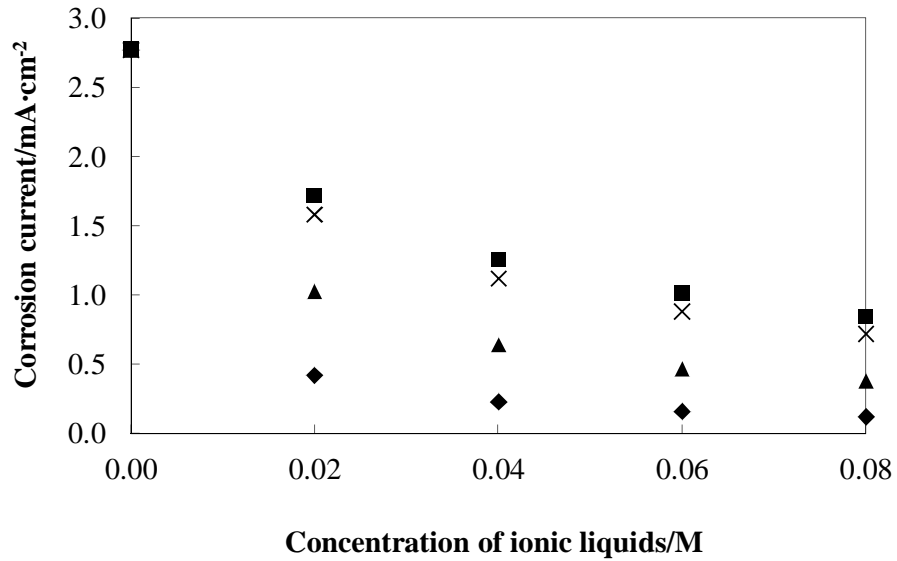


Figure 5.8 The effect of concentration of the ionic liquids on corrosion current density of carbon steel in 1 M HCl at 298.15 K measured using Tafel Plots. Symbols: ■, [HEF]; ♦, [BHEAF]; ▲, [BHEMF]; and ×, [THEAF].

The inhibition efficiency measured using Tafel Plots was calculated using equation (2.30),

$$\%IE = \frac{i_{corr} - i_{corr}^{inh}}{i_{corr}} \times 100 \quad (2.30)$$

with  $i$  and  $i_{inh}$  are corrosion current in the absence and presence of the ionic liquids, respectively. The inhibition efficiency of ionic liquids under study was calculated from Tafel Plots is also given in Table D.2 of Appendix D. Figure 5.9 shows the inhibition efficiency of some selected ionic liquids determined using Tafel Plot at temperature 298.15 K. The inhibition efficiency increases with increases concentration of ionic liquids. The result is found to be in good agreement with the values calculated from the weight loss method.

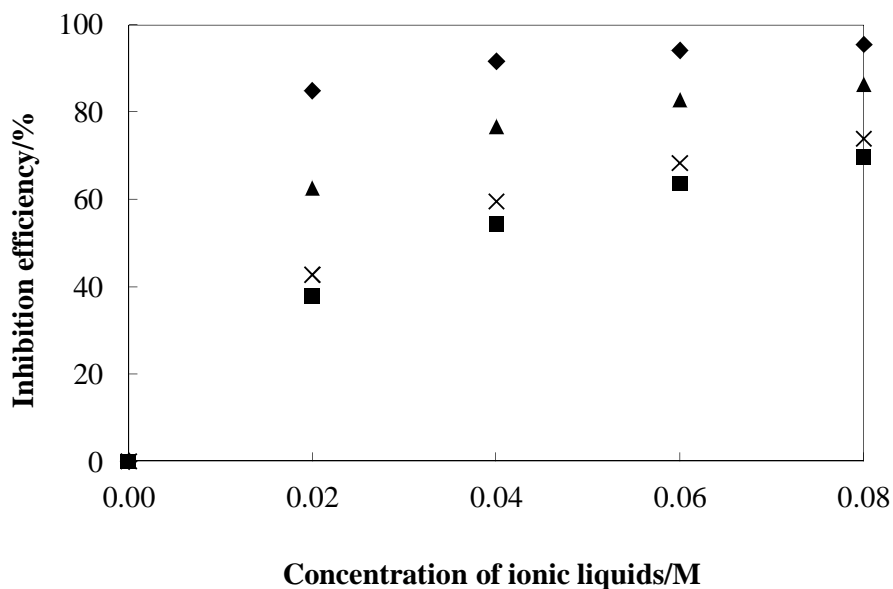


Figure 5.9 The inhibition efficiency of ionic liquids determined using Tafel Plot at 298.15 K. Symbols: ■, [HEF]; ♦, [BHEAF]; ▲, [BHEMF]; and ×, [THEAF].

### 5.1.3 Linear Polarization Resistance

The linear polarization resistance (LPR) for the carbon steel in acidic medium was measured in various concentrations of the ionic liquids and at temperatures of 298.15, 313.15, 328.15, and 343.15 K. The LPR of the carbon steel specimens in 1 M HCl were obtained in the potential range from -10 to +10 mV at a scan rate of 1 mV/minute. The respective kinetic parameter such as polarization resistance,  $R_p$ , is given in Table D.7 and D.8 of Appendix D.

Figure 5.10 shows the effect of concentration of some selected ionic liquids on the  $R_p$  values of carbon steel in 1 M HCl at 298.15. Increasing the concentration of the ionic liquids increases the  $R_p$  value. This may be due to ionic liquids are adsorbed on the carbon steel surface [3, 10, 11, 193-197]. It appears that the adsorbed ionic liquids on the carbon steel increase the polarization resistance of carbon steel in acidic medium. The same observations were also observed for ammonium-salt corrosion inhibitor [3, 10, 11, 193-197].

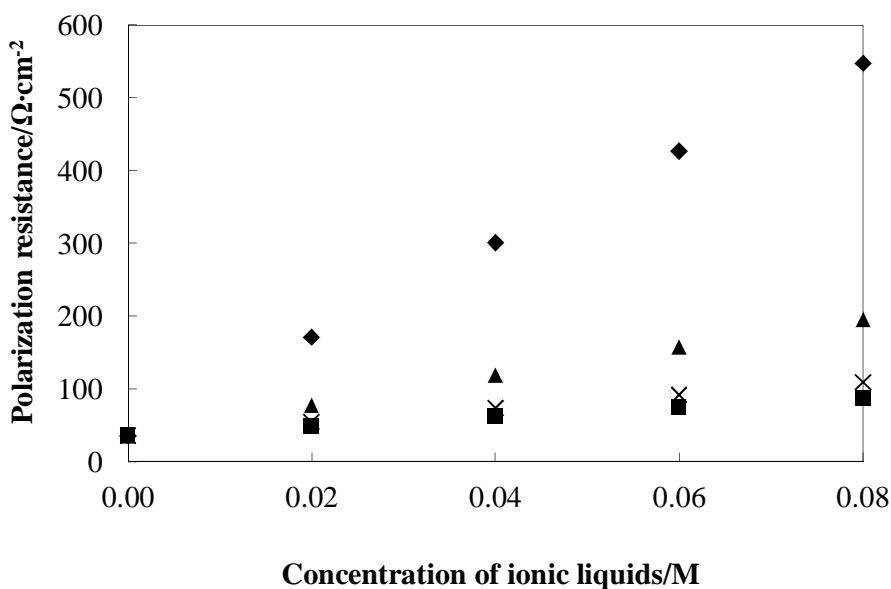


Figure 5.10 The effect of concentration of the ionic liquids on polarization resistance of carbon steel in 1 M HCl at 298.15 K measured using Linear Polarization Resistance. Symbols: ■, [HEF]; ◆, [BHEAF]; ▲, [BHEMF]; and ×, [THEAF].

The inhibition efficiency from LPR measurement was calculated using equation (2.31),

$$\%IE = \frac{R_p^{inh} - R_p}{R_p^{inh}} \times 100 \quad (2.31)$$

with  $R_p$  and  $R_p^{inh}$  are polarization resistance in the absence and presence of the ionic liquids, respectively.

The polarization resistance,  $R_p$ , and inhibition efficiency,  $IE\%$ , for all the studied ionic liquids in this work are given in Table D.7 and D.8 of Appendix D. Figure 5.11 presents the inhibition efficiency determined using LPR method at temperature 298.15 K. The inhibition efficiency increases with increasing concentration of ionic liquids. The result is also in good agreement with the values calculated from weight loss method and Tafel Plots.

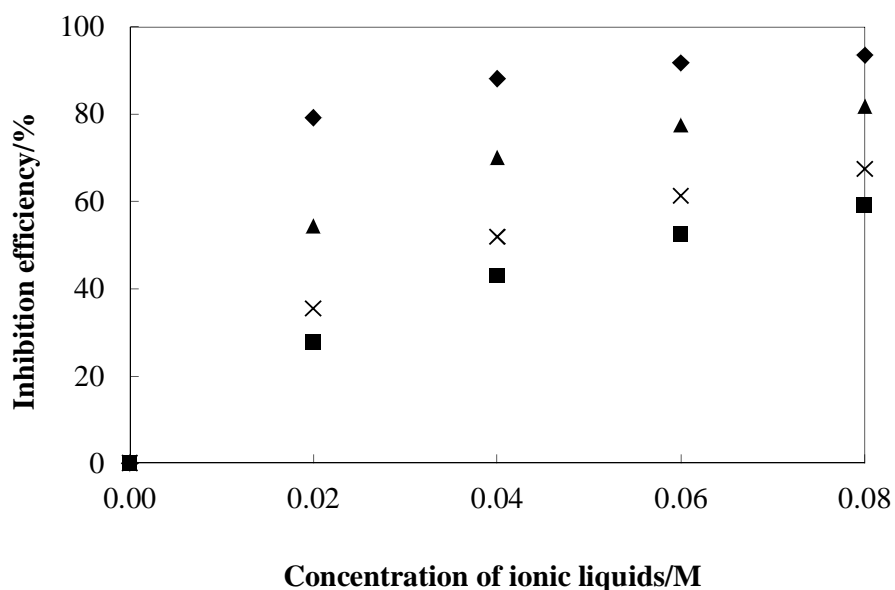


Figure 5.11 The inhibition efficiency of ionic liquids determined using Tafel Plot at 298.15 K. Symbols: ■, [HEF]; ♦, [BHEAF]; ▲, [BHEMF]; and ×, [THEAF].

#### 5.1.4 Electrochemical Impedance Spectroscopy

The electrochemical impedance spectroscopy (EIS) for the carbon steel in acidic medium was measured in the various concentrations of the ionic liquids and at temperatures 298.15, 313.15, 328.15, and 343.15 K. The result is discussed based on the term Nyquist and Bode plot, and its equivalent electrical circuit. The electrochemical impedance parameters were obtained by fitting the EIS experimental data using a circuit model via a non-linear least square program accompanying with ACM potentiostat/galvanostat system. The electrochemical impedance parameters and the corresponding inhibition efficiencies for carbon steel in 1 M HCl in the absence and presence of ionic liquids inhibitor is given in Table D.5 and D.6 of Appendix D.

The typical EIS spectrum of carbon steel in 1 M HCl in the presence of various concentrations of the ionic liquids [BHEAF] at 298.15 K is shown in Figure 5.12 to 5.13. The Nyquist spectra obtained yields a semi circular shape and only one time constant is observed in its Bode plot. This indicates the corrosion of carbon steel in 1 M HCl is mainly controlled by a charge transfer process [3, 10, 11, 193-197]. The Nyquist plots exhibit depressed semicircles centered below  $Z'$  axis. The diameter of semicircle increases with increasing concentration of ionic liquids. It indicates that the charge transfer resistance increase with increasing concentration of ionic liquids. This may be due to ionic liquids were adsorbed on the carbon steel surface. It formed a protective layer on carbon steel surface. The formation of layer can be known by change of the charge transfer resistance [3, 10, 11, 193-197].

According to Sastri [1], this deviations from the semicircle with a center at the  $Z'$  axis is due to the thin films formed on the carbon steel surface, which gives rise to a distribution in relaxation times for interfacial charge transfer reactions. The diameter of these semicircles increases with increase in concentration of the ionic liquids. It indicates that charge transfer resistance increases with increasing concentration of the ionic liquids which lead to improved inhibition efficiency. The charge transfer resistance was also responsible for the inhibition performance of imidazolium and pyridinium based ionic liquids [22-24] and ammonium-salt corrosion inhibitor [3, 10, 11, 193-197].

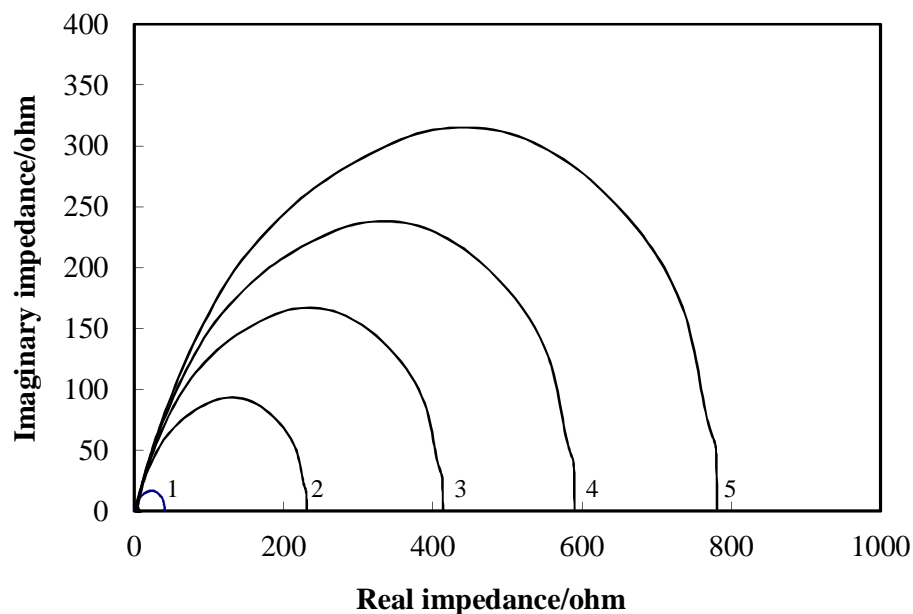


Figure 5.12 Nyquist plot of carbon steel in 1 M HCl with various concentrations of ionic liquids at 298.15 K. Symbols: 1, Blank; 2, 0.02 M; 3, 0.04 M; 4, 0.06 M; and 5, 0.08 M.

Electrical equivalent circuits were used to interpret these electrochemical processes. Several electrical circuit analogs tried to fit to the experimental data. A simple electrochemical circuit, as shown in Figure 5.14, gives the higher  $R^2$  compared to the other electrochemical circuit. In this electrochemical circuit,  $R_s$  is the solution resistance,  $R_t$  is the charge transfer resistance, and  $C_{dl}$  is the double layer capacitance that characterizes the separation of the metal/electrolyte interface. The same electrical equivalent circuit was also used to describe the electrochemical impedance parameters of carbon steel in 1 M HCl in the presence of imidazolium and pyridinium based ionic liquids [22-24].

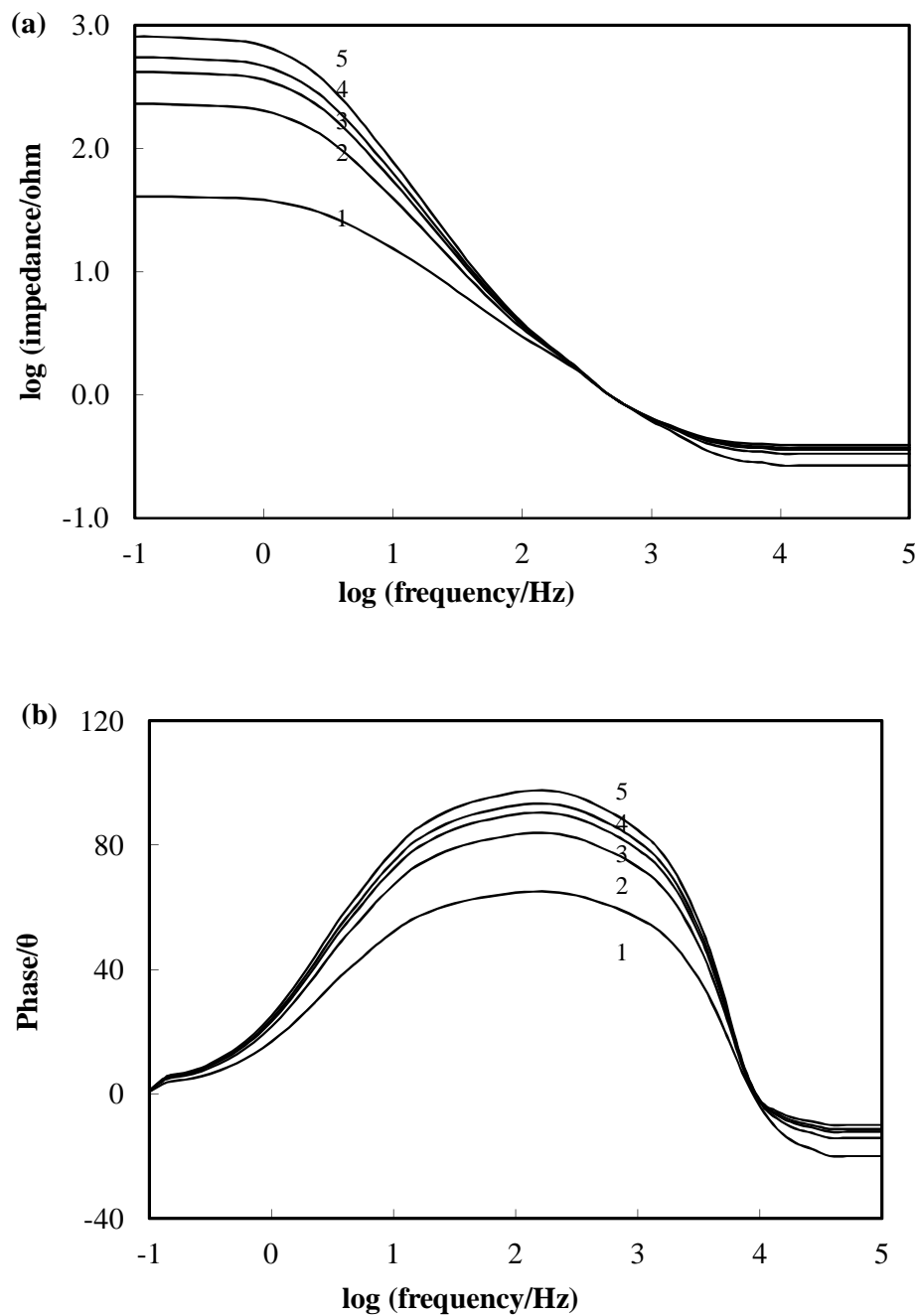


Figure 5.13 Electrochemical impedance spectrum of carbon steel in 1 M HCl with various concentrations of ionic liquids [BHEAF] at 298.15 K. Symbols: 1, Blank; 2, 0.02 M; 3, 0.04 M; 4, 0.06 M; and 5, 0.08 M.

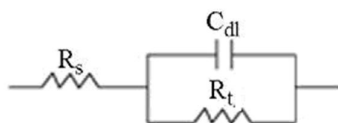


Figure 5.14 Electrical Circuit Analog

Table 5.1 presents the electrochemical impedance parameters;  $R_s$ ,  $R_t$ , and  $C_{dl}$  and the corresponding inhibition efficiencies for carbon steel in 1 M HCl in the presence of various concentrations of ionic liquids [BHEAF] at 298.15 K. From Table 5.1, the solution resistance,  $R_s$ , almost constant for the carbon steel in the absence and presence of different concentration of the ionic liquids [BHEAF]. However, the charge transfer resistance,  $R_t$ , values changes with the addition of the ionic liquids inhibitor. It appears that the presence of the ionic liquids increase the charge transfer resistance that leads to the rise of corrosion efficiency. The effect is more pronounced with increasing concentration of the ionic liquids inhibitor.

Table 5.1 Electrochemical impedance parameters and the corresponding inhibition efficiency for carbon steel in 1 M HCl in the presence of various concentrations of ionic liquids [BHEAF] at 298.15 K.

$C_i/M$	$R_s/\Omega \cdot cm^2$	$R_t/\Omega \cdot cm^2$	$C_{dl}/\mu F \cdot cm^{-2}$	$IE\%$
0.00	2.7	40.8	270	0.00
0.02	2.7	230.6	148	94.30
0.04	2.8	413.0	142	96.06
0.06	2.8	588.5	140	96.96
0.08	2.9	757.5	139	97.51



On the other hand the values of  $C_{dl}$  decrease with increasing the inhibitor concentration. As the inhibitor adsorbed onto the carbon steel surface, the capacitance of the interface starts decreasing [3, 10, 11, 193-197].. The adsorbed ionic liquids on the carbon steel surface forms protective film that reduces the dielectric constant between the metal and electrolyte. Increasing concentration of the ionic liquids, increase the thickness of the film and decrease the dielectric constant [3, 10, 11, 193-197] .

In the case of the electrochemical impedance spectroscopy, the inhibition efficiency was calculated using charge transfer resistance,  $R_t$ , according to equation (2.33),

$$\%IE = \frac{R_t^{inh} - R_t}{R_t^{inh}} \times 100\% \quad (2.33)$$

The inhibition efficiency of the synthesized ionic liquids on carbon steel corrosion in 1 M HCl at 298.15 is given in Table C.4 of Appendix C. As expected, the inhibition efficiency increases with increasing concentration of the ionic liquids. The result is in good agreement with the values calculated from weight loss, Tafel Plots, and Linear Polarization Resistance.

In general, all the synthesized ionic liquids showed high inhibition performance on carbon steel corrosion in 1 M HCl. The inhibition efficiency measured from weight loss, Tafel Plots, LPR, and EIS were in good agreement. However, as can be seen from Table D.5 and D.6 of Appendix D, the  $IE\%$  values calculated from weight loss method were slightly higher than the other three methods used. It is due to time needed to conduct the experiment; 24 hours for weight loss, 2 hours for Tafel Plots and EIS, and 10 minutes for LPR. It assumes that equilibrium between metal and electrolyte was reached during weight loss experiment. Thus, for further discussion, the data is taken from weight loss method.

### 5.1.5 Effect of Temperature

In this work, the inhibition performances of the synthesized ionic liquids were measured at four different temperatures of 298.15, 313.15, 328.15, and 343.15 K using weight loss and electrochemical methods. The results are given in Table D.1 to D.8 of Appendix D. In general, the inhibition efficiency decreases with increasing temperature. A decrease in inhibition efficiency with increasing temperature indicates that the adsorption of the ionic liquids molecules on the carbon steel surface is by physisorption. This observation is supported by their standard free energy of adsorption which was discussed in section 5.2.2.2.

A representation of temperature dependence of corrosion rate of carbon steel in 1 M HCl is given in Figure 5.15. It shows the corrosion rate of carbon steel in 1 M HCl in the presence of various concentrations of ionic liquids [BHEAF] at the temperature of 298.15, 313.15, 328.15, and 343.15 K using weight loss method. The corrosion rate of carbon steel increased with increasing temperature. In the absence of the ionic liquids, the corrosion rate of carbon steel increases significantly with increasing temperature. However, in the presence of ionic liquids, the corrosion rate of carbon steel decreased. It appears that the ionic liquids reduces corrosion rate of the carbon steel in 1 HCl. It also suggests that the synthesized ionic liquids acted as good inhibitor on carbon steel corrosion at the temperature of 298.15 – 343.15 K.

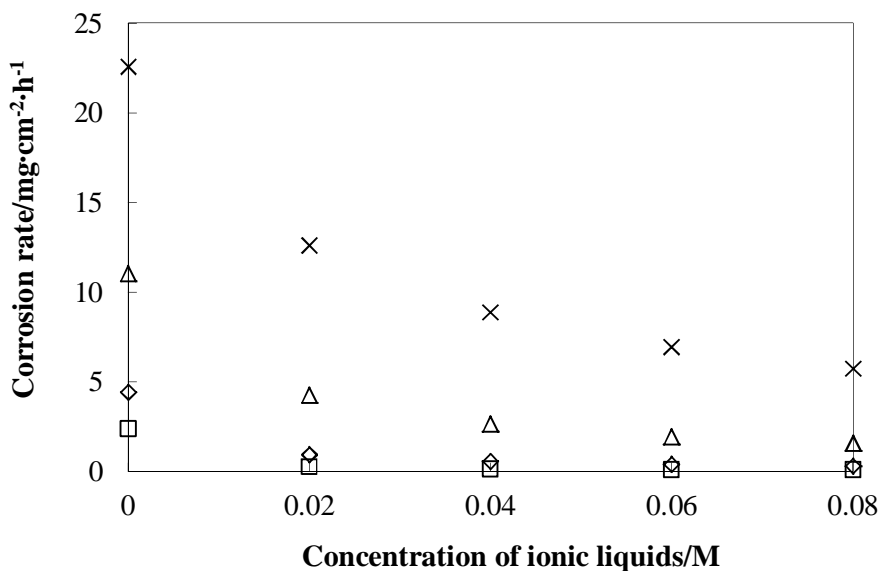


Figure 5.15 Corrosion rate of carbon steel in 1 M HCl with the presence of various concentrations of ionic liquids [BHEAF] at several temperatures using weight loss method. Symbols:  $\square$ ,  $T = 298.15$  K;  $\diamond$ ,  $T = 313.15$ ;  $\Delta$ ,  $T = 328.15$  K; and  $\times$ ,  $T = 343.15$  K.

The inhibition efficiency at the temperatures of 313.15, 328.15, and 343.15 K were calculated using the same equation used at temperature 298.15 K. Figure 5.12 shows the inhibition performance of the ionic liquids [BHEAF] carbon steel in 1 M HCl at temperature (298.15, 313.15, 328.15, and 343.15) K using weight loss method. It can be observed that the inhibition efficiency decreases with increasing temperature. It can be interpreted on the basis that the ionic liquids exert their action by adsorbing themselves on the carbon steel surface and an increase in temperature resulted in desorption of some adsorbed inhibitor molecules leading to a decrease in the inhibition efficiency. The same behavior was also observed for the other studied ionic liquids in this work. Thus, it can be concluded that the synthesized ionic liquids acted as good inhibitor on carbon steel corrosion in 1 M HCl at temperatures (298.15 – 343.15) K.

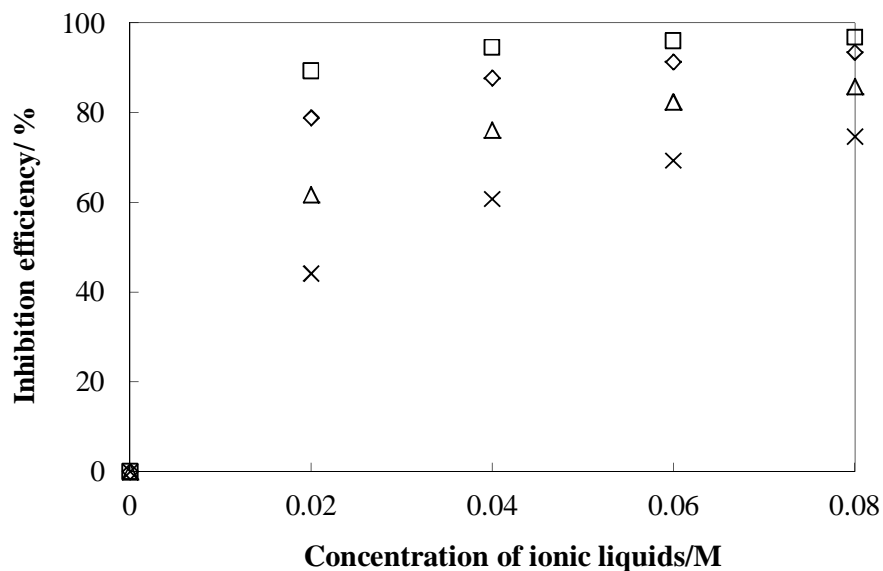


Figure 5.16 Temperature dependence of inhibition efficiency of [BHEAF] on corrosion of carbon steel in 1 M HCl at several temperatures using weight loss method. Symbols: □,  $T = 298.15$  K; ◇,  $T = 313.15$ ; Δ,  $T = 328.15$  K; and ×,  $T = 343.15$  K.

### 5.1.6 Effect of Alcohol

In this section, the effectiveness of the ionic liquids as the active inhibition ingredient alone and in combination with organic solvents is evaluated. Three organic solvents; methanol, ethanol, and 1-propanol, are used in this work. These are typical organic solvent used in many commercial inhibitor packages [25]. The effect of alcohol on inhibition efficiency of ionic liquids [BHEAF] on carbon steel corrosion at the temperatures of 298.15 – 343.15 K was also studied using weight loss and electrochemical methods. The results are given in Table D.9 of Appendix D.

A representative of inhibition performance of the ionic liquids [BHEAF] in the presence of alcohol is given in Figure 5.17. It presents the inhibition efficiency of 0.08 M [BHEAF] in the absence and presence of methanol, ethanol, and 1 propanol on the corrosion of carbon steel in 1 M HCl at temperature 298.15 using weight loss methods. From Figure 5.13, the inhibition efficiency of [BHEAF] in the presence of alcohol is found to be almost equal to the inhibition efficiency of [BHEAF] alone. It is observed that the addition of alcohol did not change the inhibition efficiency, Tafel Plot, or the electrochemical impedance parameters. The same phenomena are also observed at higher temperatures. Thus, it can be concluded that these alcohols can be used as cosolvent with ionic liquids, without reducing the ionic liquids performance. The organic solvent is particularly helpful for reducing the viscosity of ionic liquids which is known to be highly viscous, as discussed in Section 4.3.3.

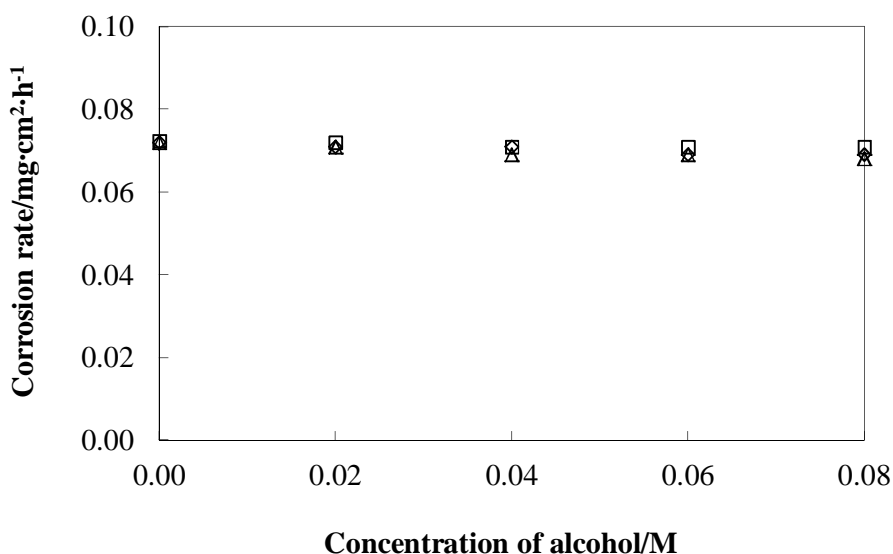


Figure 5.17 Effect of alcohol on inhibition performance of 0.08 M of [BHEAF] on carbon steel corrosion in acidic medium. Symbols; □, methanol; ◇, ethanol; Δ, 1-propanol

## 5.2 Adsorption of Ionic Liquids on the Carbon Steel Surface

The inhibiting effect of ammonium salt is attributed to either geometrical blocking of the surface by the adsorbate or deactivating coverage, *i.e.* blocking of active surface sites [3, 10, 11, 193-197]. In such cases the reduction in corrosion rate may be caused by mass transfer restrictions or geometrical blocking. The adsorbed corrosion inhibitor may be geometrically blocking the surface as a layer, thereby restricting the access of corrosive species to the surface, or the transfer of corrosion products away from it, or it may be blocking reaction sites by adsorption of inhibitor molecules [193, 194]. In this work, an attempt to study the protection-film formed by hydroxyl ammonium ionic liquids was conducted using spectroscopy infrared and Raman. The film formed was very thick that could not be detected by the instruments. Other attempt was made by putting the carbon steel specimen into 100 ml pure ionic liquids. Due to fluorescence effect, the spectroscopy Raman could not be used to detect the interaction between ionic liquids and carbon steel. Future work is recommended to use other method, such as quartz crystal microbalance (QCM) [197] or by means of atomic force microscopy [195].

Taking into account that hydroxyl ammonium ionic liquids are ammonium salt, it is believed that it reduces the corrosion rate of carbon steel by adsorbing themselves on the carbon steel surface [3, 10, 11, 193-197]. The following section discussed the adsorption of the hydroxyl ammonium ionic liquids on the carbon steel surface in 1 M HCl.

### 5.2.1 Adsorption Isotherm

The adsorption isotherm used in this work refers to the relationship between the inhibition efficiency and the concentration of inhibitors at constant temperature and it gives an insight into the adsorption process. The type of the adsorption isotherm can provide information on the properties of the tested compounds. Through adsorption isotherm equations, the degree of surface coverage,  $\theta$ , or its function with concentration of inhibitors,  $C_{inh}$ , can be correlated. The dependence of  $\theta$  on  $C_{inh}$  is

used to obtain the best fitting for adsorption isotherm. It is assumed that %IE is comparable to the degree of coverage of metal surface by an inhibitor,  $\theta$  [22, 23].

In this study, several adsorption isotherm equations; Langmuir, Frumkin, and Temkin, were considered. It found that the Langmuir's isotherm was the best to represent the adsorption behavior of the studied ionic liquids. The Langmuir isotherm was represented by equation (2.35),

$$\frac{C_{inh}}{\theta} = \frac{1}{K_{ads}} + C_{inh} \quad (2.35)$$

A representative of the plot of  $C_{inh}/\theta$  against  $C_{inh}$  is given in Figure 5.18. It is shown that the plot of  $C_{inh}/\theta$  against  $C_{inh}$  for ionic liquids [BHEAF] on carbon steel surface at temperature (298.15 – 343.15) K gives straight lines, with  $R^2$  are almost equal to 1. The same trend was also observed for plot  $C_{inh}/\theta$  against  $C_{inh}$  of the other synthesized ionic liquids. It confirms that the adsorption of the ionic liquids in 1 M HCl acid obeys the Langmuir isotherm adsorption within the temperature range studied. The isotherm parameters for all the synthesized ionic liquids are listed in Table D.9 of Appendix D.

According to Sastri [1], Langmuir adsorption isotherm assumes that the metal surface has a fixed number of adsorption sites which could be occupied by the absorbed species. In other words, the ionic liquids form a layer which covers all the active sites on the surface of carbon steel without distinguishing between anodic and cathodic sites. The same isotherm adsorption is also observed for other ionic liquids based on imidazolium cation [22-24]. Thus, it can be concluded that the ionic liquids suppresses the corrosion rate by adsorbing themselves on the carbon steel surface. The adsorbed ionic liquids on the carbon steel surface form a protective layer. Increasing the concentration of the ionic liquids leads to the increase in the thickness of protective layer, which give higher energy barrier. This result is supported by their apparent activation energy that discussed in Section 5.2.4.

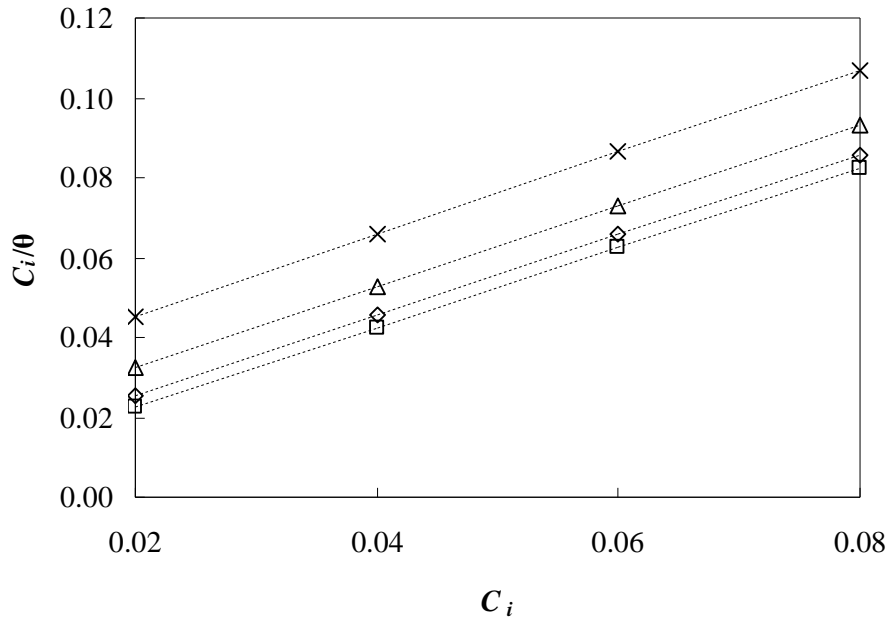


Figure 5.18 Plots of Langmuir's isotherm adsorption of [BHEAF] at several temperatures using weight loss method. Symbols: □,  $T = 298.15$  K; ◇,  $T = 313.15$ ; Δ,  $T = 328.15$  K; ×,  $T = 343.15$  K and (---) Correlation using equation (2.35).

### 5.2.2 Equilibrium Constant of Adsorption Process

The equilibrium constant of the adsorption process,  $K_{ads}$  is calculated using equation (2.40),

$$K_{ads} = \frac{\theta}{C_{inh}(1-\theta)} \quad (2.40)$$

The values of  $K_{ads}$  are listed in Table D.10 of Appendix D. A representative plot of  $K_{ads}$  as function of temperature is given in Figure 5.19.



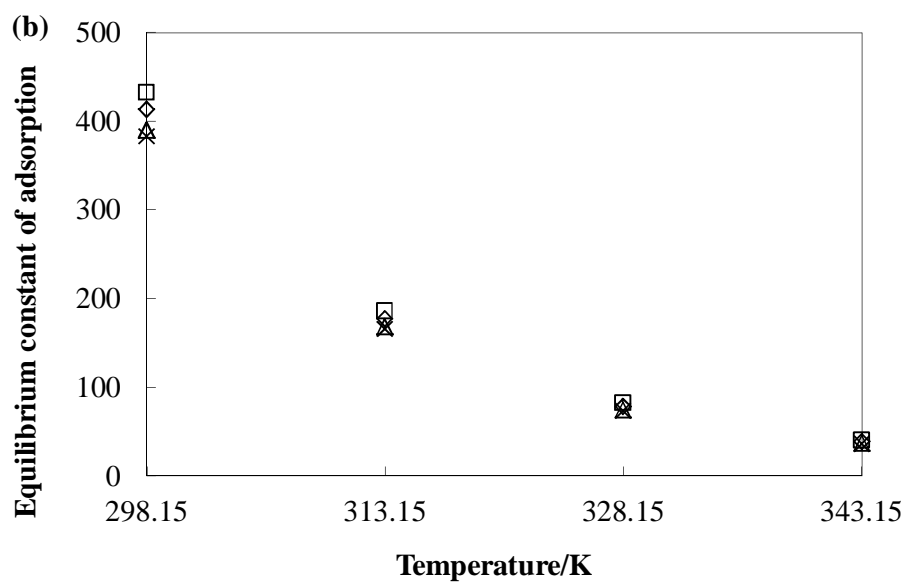
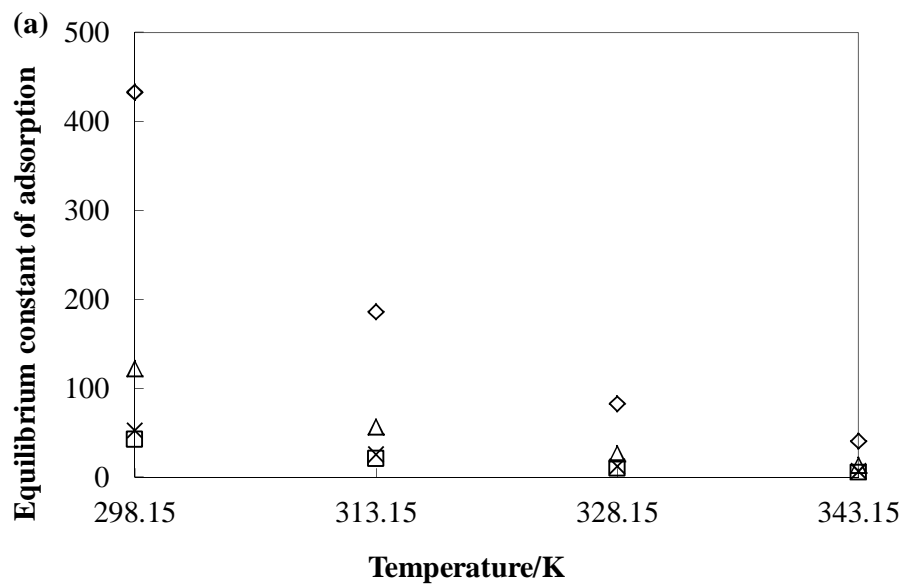


Figure 5.19 Plots of equilibrium constant of adsorption process of ionic liquids on carbon steel surface at several temperatures. (a) Symbols: □, [HEF]; ◇, [BHEAF]; △, [BHEMF]; and ×, [THEAF]. (b) Symbols: □, [BHEAF]; ◇, [BHEAA]; △, [BHEP]; and ×, [BHEAL].

Figure 5.19(a) shows the effect of the cation on the equilibrium constant of adsorption process of the ionic liquids on carbon steel surface at temperature 298.15, 313.15, 328.15, and 343.15 K. The bis(2-hydroxyethyl)ammonium cation has the highest  $K_{ads}$  and it is followed by bis(2-hydroxyethyl)methylammonium, tris(2-hydroxyethyl) ammonium, and 2-hydroxyethanaminium cation, regardless the anion. This result is consistent with their inhibition efficiency behavior. Effect of the cation on the equilibrium constant of adsorption process of the ionic liquids on carbon steel surface is more dominant when it compared to their anion. The values of  $K_{ads}$  at 298.15 K are 42.43 to 432.81 for [HEF] and [BHEAF], respectively. The difference of  $K_{ads}$  between the two cations is much higher when it is compared to the two anions. Hence, it can be concluded that the cation has more effect on the equilibrium constant of adsorption process of the ionic liquids on carbon steel surface. The same observations were also reported for the imidazolium cation of ionic liquids [22-24] and ammonium-salt corrosion inhibitor [3, 10, 11, 193-197].

As can be seen from Figure 5.19(a), the format anion shows the highest equilibrium constant of adsorption, followed by acetate, propionate, and lactate. This result is in good agreement with their inhibition efficiency order as discussed in section 5.1.1.1. The effect of anion on the equilibrium constant of adsorption process of the ionic liquids on carbon steel surface is minor compared to the cation. The values of  $K_{ads}$  at 298.15 K are 413.47 and 432.81 for [BHEAA] and [BHEAF], respectively. The difference of  $K_{ads}$  between the two anions is smaller when it is compared to the two cations. It might be attributed to the adsorption mode of ionic liquids through their cation, rather than their anion, as discussed above.

Increasing temperature leads to decrease in the  $K_{ads}$ . The same observation is observed all the synthesized ionic liquids in this work. Such behavior can be interpreted on the basis that the inhibitors exert their action by adsorbing themselves on the metal surface and an increase in temperature resulted in desorption of some adsorbed inhibitor molecules leading to a decrease in their values of  $K_{ads}$ . According to Sastri [1], if the increases in temperature cause the decreases in  $K_{ads}$ , it means that

the adsorption of the inhibitor on the steel surface is physical adsorption. This physical adsorption of ionic liquids on the carbon steel surface is confirmed by their standard free energy of adsorption, as discussed in section 5.2.3.1.

### 5.2.3 Thermodynamics of Adsorption Process

The thermodynamics adsorption parameter is another useful tool to explain the mechanism of inhibition on carbon steel corrosion. It can be used to understand the effect of concentration and temperature on the adsorption processes of the ionic liquids on the carbon steel surface in 1 M HCl. The thermodynamic parameters include standard free energy of adsorption, enthalpy and entropy of activation [22-24].

#### 5.2.3.1 Standard Free Energy of Adsorption

The standard free energy of adsorption,  $\Delta G_{ads}$  is related to  $K_{ads}$ , by the equation (2.41),

$$\Delta G_{ads} = -RT \ln(55.5 \times K_{ads}) \quad (2.41)$$

The standard free energy values for all studied ionic liquids are presented in Table D.11 in Appendix D. A representative plot of  $\Delta G_{ads}$  at different temperature is given in Figure 5.20. The calculated values of  $\Delta G_{ads}$  are negative which indicate the adsorption of ionic liquids molecules on the surface of carbon steel are a spontaneous reaction.

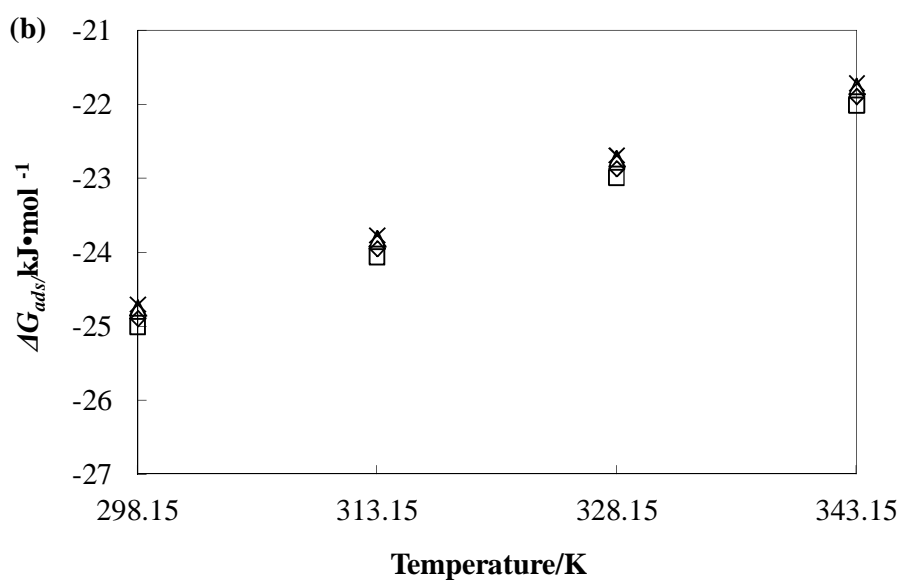
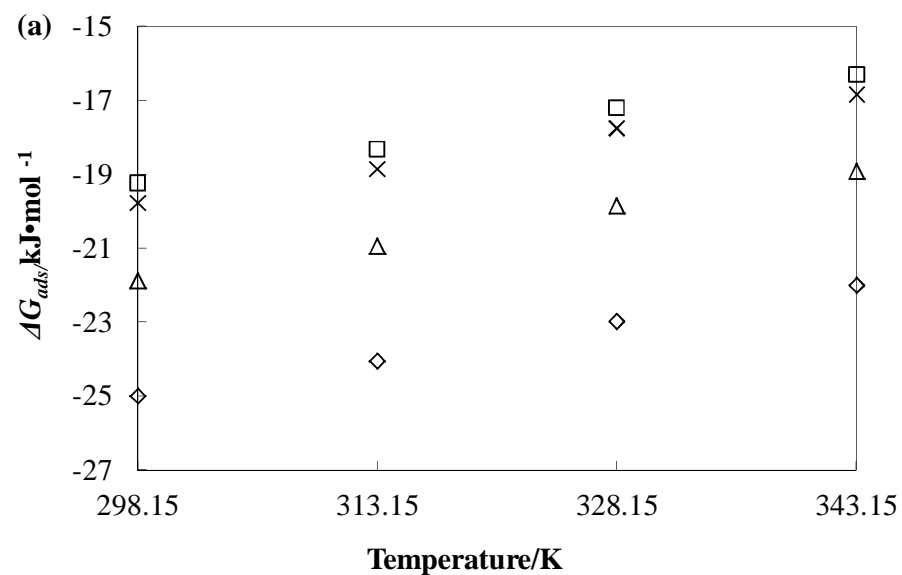


Figure 5.20 Plots of standard free energy of adsorption process of ionic liquids on carbon steel surface at several temperatures. (a) Symbols: □, [HEF]; ◇, [BHEAF]; Δ, [BHEMF]; and ×, [THEAF]. (b) Symbols: □, [BHEAF]; ◇, [BHEAA]; Δ, [BHEP]; and ×, [BHEAL].

According to Sastri [1] the values of  $\Delta G_{ads}$  around  $-20 \text{ kJ}\cdot\text{mol}^{-1}$  or lower consistent with physisorption process which is an electrostatic interaction between charged molecules and the charged metal surface; those around  $-40 \text{ kJ}\cdot\text{mol}^{-1}$  or higher are consistent with chemisorption, it involves charge sharing or transfer from organic molecules to the metal surface to form a coordinate type of metal bond [1]. In this work, the calculated  $\Delta G_{ads}$  values are around  $-20 \text{ kJ}\cdot\text{mol}^{-1}$ , thus indicating that the adsorption of the ionic liquids molecules on the surface of carbon steel is by physisorption.

Figure 5.20(a) shows the effect of the cation on the equilibrium constant of adsorption process of the ionic liquids on carbon steel surface at temperature 298.15, 313.15, 328.15, and 343.15 K. The bis(2-hydroxyethyl)ammonium cation has the highest  $\Delta G_{ads}$  and it is followed by bis(2-hydroxyethyl)methylammonium, tris(2-hydroxyethyl) ammonium, and 2-hydroxyethanaminium cation, regardless the anion. This result is consistent with their inhibition efficiency behavior. Effect of the cation on the standard free energy of adsorption of the ionic liquids on carbon steel surface is more dominant when it compared to their anion. The values of  $\Delta G_{ads}$  at 298.15 K are  $-19.25$  to  $-25.00 \text{ kJ}\cdot\text{mol}^{-1}$  for [HEF] and [BHEAF], respectively, meanwhile the values of  $\Delta G_{ads}$  for [BHEAF] and [BHEAA] are  $-25.00$  and  $-24.89 \text{ kJ}\cdot\text{mol}^{-1}$ , respectively. The difference of  $\Delta G_{ads}$  between the two cations is much higher when it is compared to the two anions. Hence, it can be concluded that the cation has more effect on the equilibrium constant of adsorption process of the ionic liquids on carbon steel surface.

As can be seen from both 5.20(a) and (b) the value of  $\Delta G_{ads}$  decreases with increasing temperature. An increase in temperature resulted in desorption of some adsorbed inhibitor molecules leading to a decrease in their values of  $\Delta G_{ads}$ , which is typical physical adsorption [1]. This result is also consistent with its equilibrium constant of adsorption. The same observation is observed all the synthesized ionic liquids in this work and for ammonium-salt corrosion inhibitor in acidic medium [3, 10, 11, 193-197].

### 5.2.3.2 Enthalpy and Entropy of Activation

The enthalpy and entropy of activation are calculated using equation (2.42),

$$CR = \frac{RT}{Nh} \exp\left(\frac{\Delta S_{act}}{R}\right) \exp\left(-\frac{\Delta H_{act}}{RT}\right) \quad (2.42)$$

The enthalpy and entropy of activation for carbon steel corrosion in the absence and presence of various ionic liquids concentration is calculated by linear regression between  $\ln(CR/T)$  against  $1/T$ . A representative for the plot of  $\ln(CR/T)$  against  $1/T$  is shown in Figure 5.21. The plot of  $\ln(CR/T)$  in the presence of various concentrations of ionic liquids [BHEAF] against  $1/T$  is linear, with slope of  $(-\Delta H_{act}/R)$  and an intercept of  $[\ln(R/Nh) + (\Delta S_{act}/R)]$  from which the values of  $\Delta H_{act}$  and  $\Delta S_{act}$  are calculated. The  $\Delta H_{act}$  and  $\Delta S_{act}$  values for all the synthesized ionic liquids are given in Table D.12 and D.13 of Appendix D. Figure 5.22 and present the effect of ionic liquids on the enthalpy and entropy of activation .

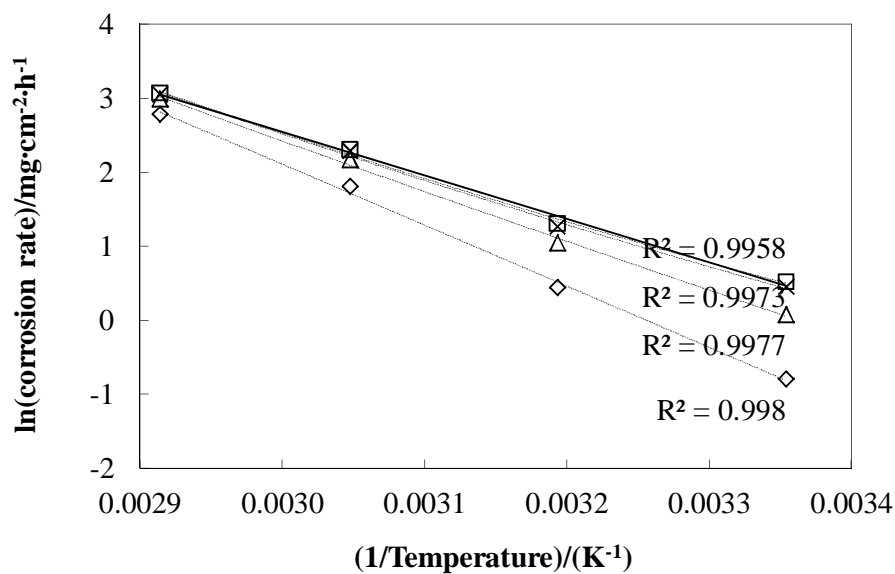


Figure 5.21 Plot of  $\ln(CR/T)$  against  $1/T$  for ionic liquids. Symbols: □, [BHEAF]; ◇, [BHEAA]; △, [BHEP]; and ×, [BHEAL].

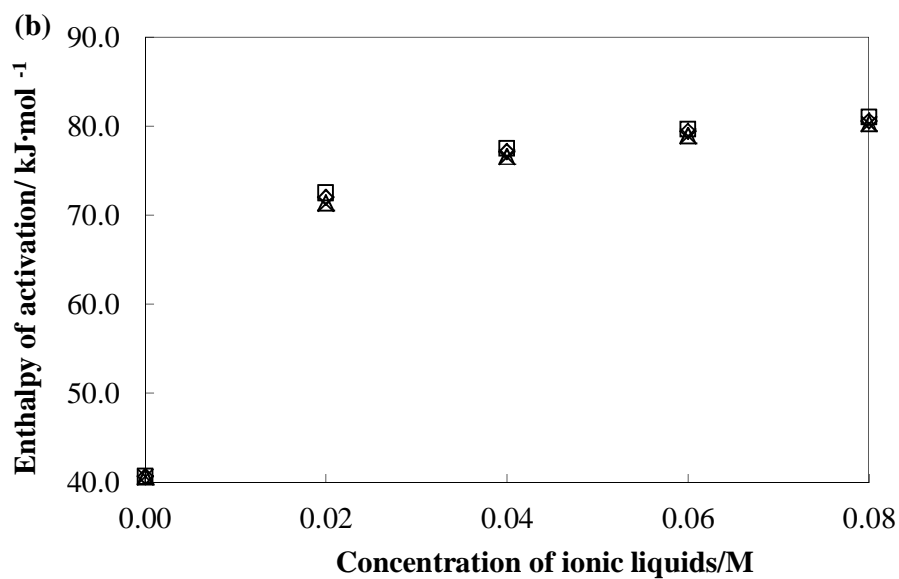
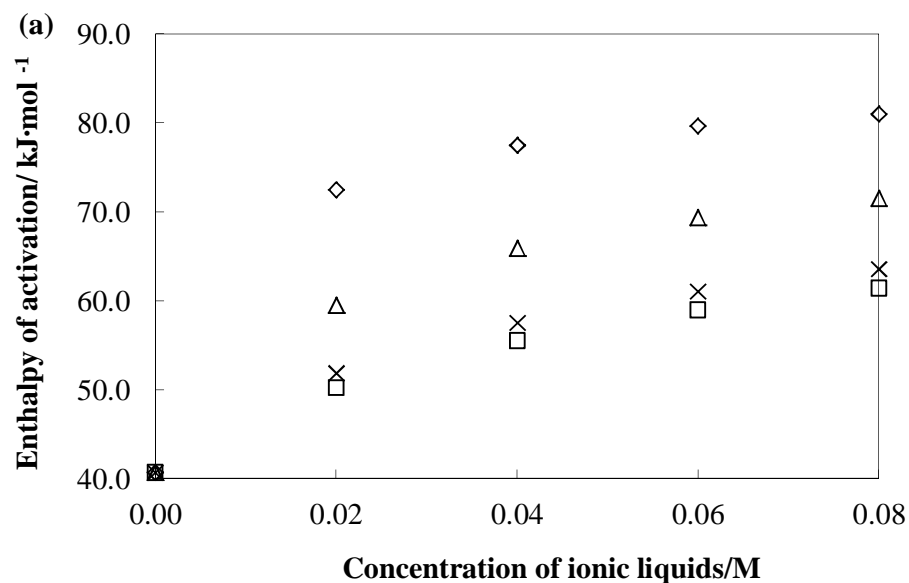


Figure 5.22 Plots of enthalpy of activation for carbon steel corrosion in the presence of various concentrations of ionic liquids. (a) Symbols: □, [HEF]; ◇, [BHEAF]; Δ, [BHEMF]; and ×, [THEAF]. (b) Symbols: □, [BHEAF]; ◇, [BHEAA]; Δ, [BHEP]; and ×, [BHEAL].

The enthalpy of activation in the presence of ionic liquids is higher than without the presence of the ionic liquids. Also, the value of the enthalpy of activation increases with increasing concentration of the ionic liquids. One possible explanation for this phenomenon is the adsorbed ionic liquids on the carbon steel surface form a protective layer thus protecting it from corrosion. For this reason higher energy is required for corrosion to take place in the presence of ionic liquids [1]. Figure 5.22(b) shows the effect of the cation on the enthalpy activation of carbon steel corrosion in 1 M HCl and in the absence and presence of various concentrations of ionic liquids. The bis(2-hydroxyethyl)ammonium cation has the highest enthalpy of activation within the concentration range and followed by bis(2-hydroxyethyl)methylammonium, tris(2-hydroxyethyl)ammonium, and 2-hydroxy ethanaminium cation, regardless the anion. This result is consistent with their inhibition efficiency behavior. The effect of the cation on the enthalpy of activation for the ionic liquids on carbon steel surface is more dominant when it compared to their anion. The values of  $\Delta H_{act}$  in the presence of 0.02 M [HEF] and [BHEAF] are 50.27 and 72.46 kJ·mol<sup>-1</sup>, respectively. Meanwhile, the values of  $\Delta H_{act}$  in the presence of 0.02 M of [BHEAF] and [BHEAA] are 72.46 and 72.00 kJ·mol<sup>-1</sup>, respectively. The difference of apparent activation energy between the two cations is much higher when it is compared to the two anions. Hence, it can be concluded that the cation has more effect on the enthalpy activation of the ionic liquids on carbon steel surface. It might be attributed to the same reason for their inhibition efficiency.

Figure 5.23 shows the effect of ionic liquids on the entropy of activation for carbon steel corrosion in 1 M HCl and in the absence and presence of various concentrations of ionic liquids. The value of  $\Delta S_{act}$  for the carbon steel corrosion in the presence of ionic liquids is higher than in the absence of ionic liquids. The value becomes higher and positive with increasing ionic liquids concentration. This indicates that the activated complex in the rate determining step represents an association rather than a dissociation step, meaning that, a decrease in disordering takes place going from reactants to the activated complex [3, 10, 11, 193-197].



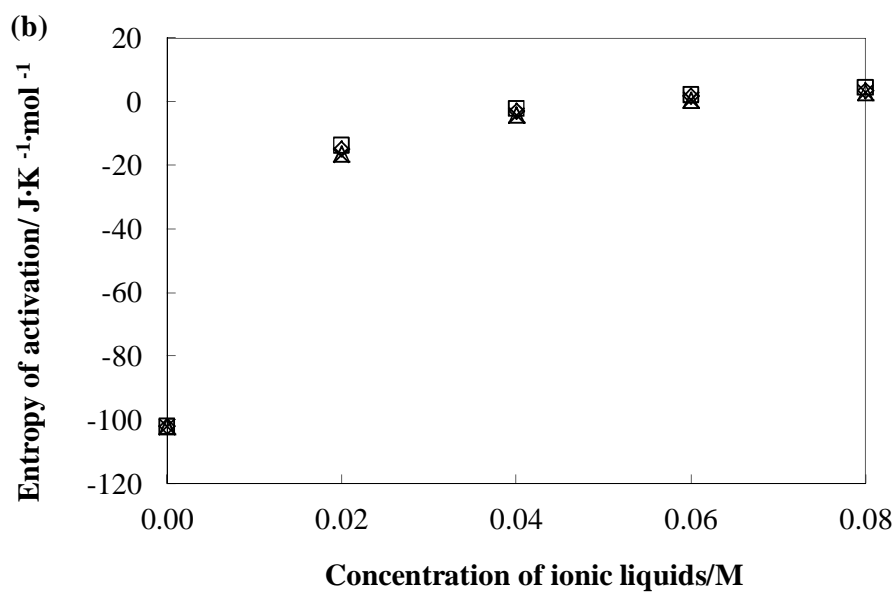
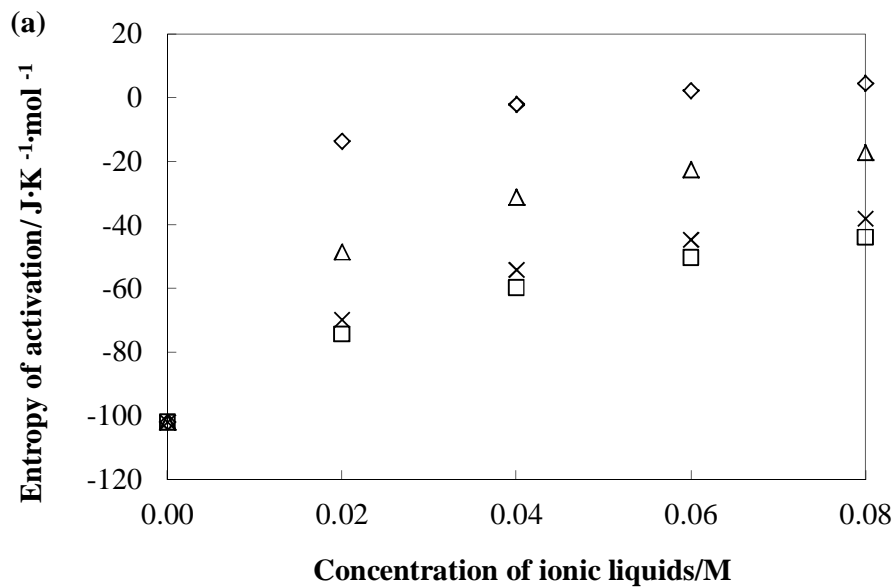


Figure 5.23 Plots of entropy of activation for carbon steel corrosion in the presence of various concentrations of ionic liquids. (a) Symbols: □, [HEF]; ◇, [BHEAF]; Δ, [BHEMF]; and ×, [THEAF]. (b) Symbols: □, [BHEAF]; ◇, [BHEAA]; Δ, [BHEP]; and ×, [BHEAL].

The bis(2-hydroxyethyl)ammonium cation has the highest entropy of activation within the concentration range and followed by bis(2-hydroxyethyl)methyl ammonium, tris(2-hydroxyethyl)ammonium, and 2-hydroxyethanaminium cation, regardless the anion. This result is consistent with their inhibition efficiency behavior. The effect of the cation on the entropy of activation for the ionic liquids on carbon steel surface is more dominant when it compared to their anion. The values of  $\Delta S_{act}$  in the presence of 0.02 M of [HEF] and [BHEAF] are -74.50 and -13.63 J·K<sup>-1</sup>·mol<sup>-1</sup>, respectively. Meanwhile, the values of  $\Delta S_{act}$  in the presence of 0.02 M of [BHEAF] and [BHEAA] are -13.63 and -14.84 J·K<sup>-1</sup>·mol<sup>-1</sup>, respectively. The difference of the entropy of activation between the two cations is much higher when it is compared to the two anions. Hence, it can be concluded that the cation has more effect on the entropy of activation for the ionic liquids on carbon steel surface. It might be attributed to the same reason for their inhibition efficiency.

#### 5.2.4 The Apparent Activation Energy

The apparent activation energies,  $E_a$ , of ionic liquids are calculated using equation (2.43),

$$\ln(CR) = \frac{-E_a}{RT} + A \quad (2.43)$$

where  $E_a$  represents the apparent activation energy,  $R$  the universal gas constant,  $T$  the absolute temperature, and  $A$  is the pre-exponential factor. The apparent activation energies for carbon steel corrosion in the absence and presence of various ionic liquids concentration is calculated by linear regression between  $\ln CR$  and  $1/T$ . A representative for the plot of  $\ln CR$  against  $1/T$  is shown in Figure 5.24. The plot of  $\ln CR$  in the presence of various concentrations of ionic liquids against  $1/T$  shows a linear relation, with  $R^2$  coefficients are close to 1. The slope of the straight line is equal to  $-E_a/R$ . The linear regression coefficient values,  $R^2$ , for all the synthesized ionic liquids are listed in Table D.14 of Appendix D. All the  $R^2$  coefficients are close to 1, indicating that the carbon steel corrosion in hydrochloric acid can be elucidated

using Arrhenius model. The activation energy values for the carbon steel corrosion in 1 M HCl in the presence of the synthesized ionic liquids are also given in Table D.14 of Appendix D.

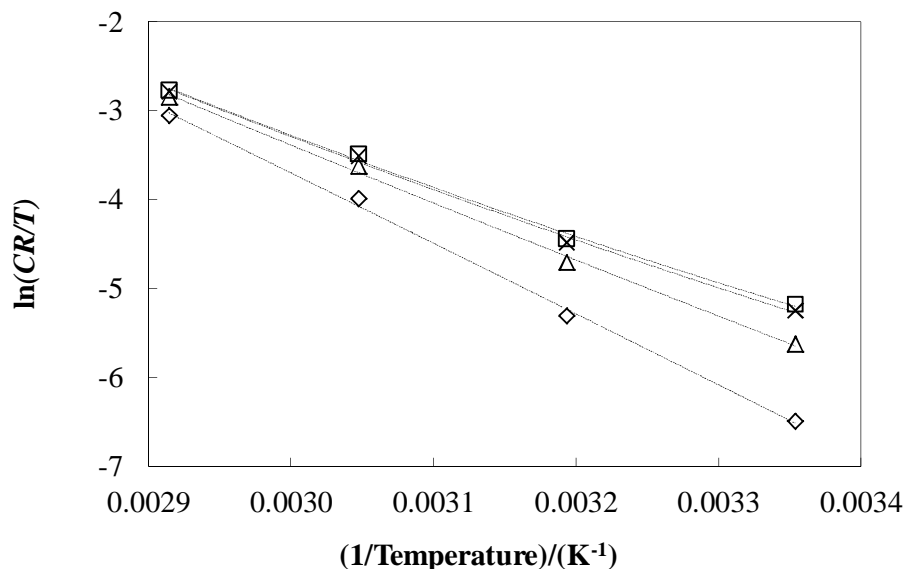


Figure 5.24 Plot of  $\ln(C/R)$  against  $1/T$  for ionic liquids. Symbols:  $\square$ , [BHEAF];  $\diamond$ , [BHEAA];  $\Delta$ , [BHEP]; and  $\times$ , [BHEAL].

Figure 5.25 presents the apparent activation energy in the presence of various concentrations of ionic liquids. The apparent activation energy in the presence of the ionic liquids is higher than in the absence of the ionic liquids. It means higher energy is required for carbon steel corrosion in the presence of the ionic liquids. Furthermore, it is found that the energy barrier for the carbon steel corrosion reaction increases with increasing the ionic liquids concentration, indicating that higher energy barrier is brought by the presence of the ionic liquids. It is often interpreted by physical adsorption lead to the formation of an adsorptive film of electrostatic character [1].

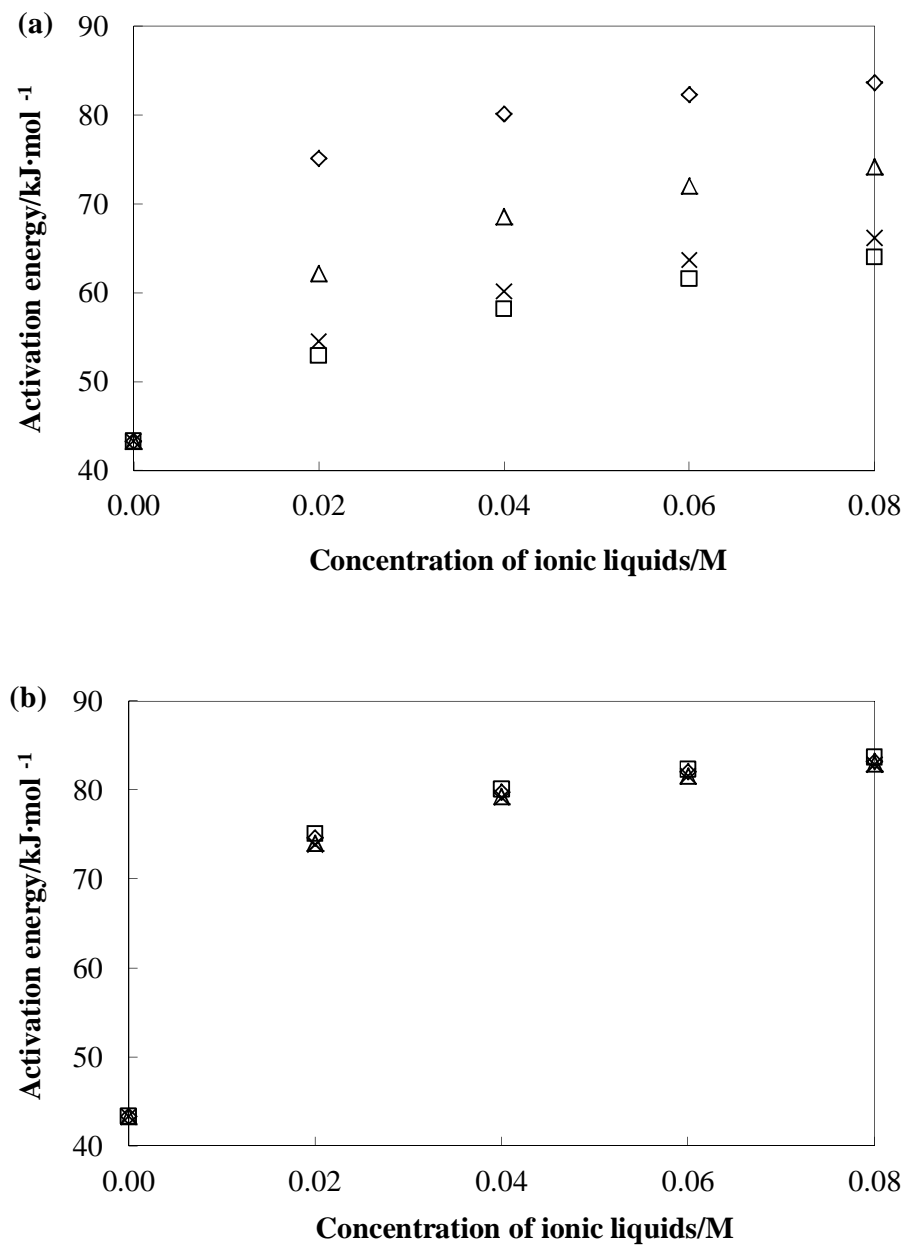


Figure 5.25 Plots of entropy of activation for carbon steel corrosion in the presence of various concentrations of ionic liquids. (a) Symbols: □, [HEF]; ◇, [BHEAF]; Δ, [BHEMF]; and ×, [THEAF]. (b) Symbols: □, [BHEAF]; ◇, [BHEAA]; Δ, [BHEP]; and ×, [BHEAL].

Figure 5.25(a) shows the effect of cation on the apparent activation energy for the carbon steel. The bis(2-hydroxyethyl)ammonium cation has the highest apparent activation energy within the concentration range and followed by bis(2-hydroxyethyl)methylammonium, tris(2-hydroxyethyl)ammonium, and 2-hydroxy ethanaminium cation, regardless the anion. This result is consistent with their inhibition efficiency behavior. Meanwhile, Figure 5.23(b) shows effect of the anion on the apparent activation energy for the carbon steel corrosion in the absence and presence of various concentrations of the ionic liquids. The format anion shows the highest apparent activation energy within the concentration range, followed by acetate, propionate, and lactate, regardless the cation. This result is in good agreement with their inhibition efficiency as discussed in section 5.1.1.1. The effect of anion on the apparent activation energy of the ionic liquids on carbon steel surface is also minor compared to the cation. As can be seen from Figure 5.23(b), the values of  $E_a$  in the presence of 0.02 M of [BHEAF] and [BHEAA] are 75.12 and 74.65 kJ·mol<sup>-1</sup>, respectively. The difference of the apparent activation energy between the anions is smaller when it is compared to the cations. It might be attributed to the same reason for their inhibition efficiency.

### 5.3 Inhibiting Mechanism

The aim of this study is to gain some insight into the effect of adding the synthesized ionic liquids on the carbon steel corrosion in 1 M HCl and to describe the adsorption mechanisms for the synthesized ionic liquids. The ionic liquids [BHEAF] is chosen as model for inhibiting mechanism as it has the highest inhibition efficiency among the studied ionic liquids in this work. The following mechanism is proposed for the carbon steel corrosion in 1 M HCl in the presence of the ionic liquids based on their adsorption and its thermodynamic as discussed earlier.

In the absence of the ionic liquids, the following reaction takes place when the carbon steel immersed in the 1 M HCl [1],

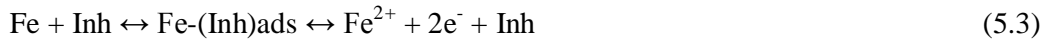




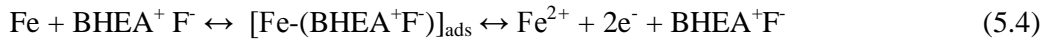
The number of electron,  $n$ , involved in equation (5.1) depends on the corrosion potential,  $E_{\text{corr}}$ , of the carbon steel in acidic medium. From section 5.1.2, the  $E_{\text{corr}}$  value for carbon steel in the absence and presence of ionic liquids was around -0.5 V (vs SHE). Using  $E$ -pH diagram of iron as given in Figure 2.13, the number of electron involved in equation (5.1) is two. Thus, equation (5.1) can be written as,



In acidic media, the ionic liquids exist in the form of cation and anion species. According to Bockris and Drazic (1962), the inhibition mechanism can be explained by the  $\text{Fe}(\text{Inh})_{\text{ads}}$  reaction intermediates,



For [BHEAF] it can be written as follow,



The  $[\text{Fe}(\text{BHEA}^+\text{F}^-)]_{\text{ads}}$  intermediate forms an adsorption layer through cation of the ionic liquids. This fact is supported by their inhibition efficiency, as discussed in sections 5.1.1.1 and 5.1.1.2, in which the cation is responsible for the protective behavior of the ionic liquids. Also, as discussed in section 5.2.3.1, the adsorption of the ionic liquids on the carbon steel surface is thermodynamically favored. Hence the ionic liquids are adsorbed spontaneously on the carbon steel surface in 1 M HCl.

The adsorption layer acts as a hindrance to the hydrochloric acid solution and enhances the protection of the metal surface. Initially when there is insufficient  $[\text{Fe}(\text{BHEA}^+\text{F}^-)]_{\text{ads}}$  to cover the carbon steel surface, because the inhibitor concentration is low or because the adsorption rate is slow, metal dissolution takes place at sites on the carbon steel surface free of  $[\text{Fe}(\text{BHEA}^+\text{F}^-)]_{\text{ads}}$ . With high inhibitor concentration a compact and coherent inhibitor over layer is formed on the carbon steel surface, reducing chemical attack of the metal. This fact is also supported from their apparent

activation energy, as discussed in 5.2.4, in which an increase in the concentration of ionic liquids increases the inhibition efficiency.

Reactions 5.3 and 5.4 take place on the anodic sites of the carbon steel. The ionic liquids molecules also adsorbed at cathodic sites in competition with hydrogen ion. In the presence of the ionic liquids, by the following mechanism:



As can be seen from equation (5.5), addition of the ionic liquids leads to the formation of the adsorption layer  $[\text{Fe}-(\text{BHEA}^+\text{F}^-)]_{\text{ads}}$  to cover the carbon steel surface. Initially when there is insufficient  $[\text{Fe}-(\text{BHEA}^+\text{F}^-)]_{\text{ads}}$  to cover the carbon steel surface, because the inhibitor concentration is low or because the adsorption rate is slow, hydrogen reduction takes place at sites on the carbon steel surface free of  $[\text{Fe}-(\text{BHEA}^+\text{F}^-)]_{\text{ads}}$ . With high inhibitor concentration a compact and coherent inhibitor over layer is formed on the carbon steel surface, reducing the hydrogen reduction.

Therefore, addition of the ionic liquids suppresses both the dissolution of metal in the anodic site and the reduction of hydrogen in the cathode site. This result support the observation resulted from Tafel Plots, as discussed in section 5.1.2.

#### 5.4 Concluding Remarks

Ionic liquids have become important as an environmentally acceptable and readily available for a wide range of needed inhibitors. However, their price is relatively higher compared to the commercially available corrosion inhibitor. An alternative way is to find cheaper ionic liquids that can be applied as corrosion inhibitor on carbon steel corrosion in acidic medium. Hydroxyl ammonium ionic liquids are relatively cheap and easy to produce in purity greater than 99%. In order to develop

low cost corrosion inhibitors, the recent investigations on application of the ionic liquids as inhibitor on corrosion of carbon steel in 1 M HCl, seem really worthwhile.

In this work, the inhibition performance of the synthesized ionic liquids on carbon steel corrosion in 1 M HCl at temperatures (298.15 – 343.15) K was measured using weight loss and electrochemical method. The electrochemical method included Tafel Plot, LPR, and EIS. The result showed that the synthesized ionic liquids managed to reduce the corrosion rate of carbon steel in 1 M HCl at temperature range studied in this work. The inhibition performance could reach up to 96.87% in the presence of 0.08 M [BHEAF]. The ionic liquids inhibited the corrosion rate of carbon steel by absorbing themselves on the surface of carbon steel. The adsorption process of the ionic liquids on the carbon steel surface was spontaneous and it obeyed Langmuir isotherm adsorption.

The ionic liquids adsorbed on the surface of carbon steel surface through its cation. It was absorbed without distinguishing the cathode and anode site. The adsorbed ionic liquids on the carbon steel surface forms a protective film that give energy barrier between metal and electrolyte inter phase. Increasing concentration increased the thickness of the protective film, which leads to higher energy barrier.

The inhibition performance decreased with increasing temperature. This is due to desorption of some adsorbed inhibitor molecules leading to a decrease in the inhibition efficiency. However, within the temperature range studied in this work, the synthesized ionic liquids still showed high inhibition performance. It suggests that all the synthesized ionic liquid in this work has the potential to be used as inhibitor on carbon steel corrosion in 1 M HCl.



## CHAPTER 6

### CONCLUSIONS AND RECOMMENDATIONS

#### 6.1 Conclusions

The following conclusions can be drawn based on the result from this work

1. The synthesis of hydroxyl ammonium ionic liquids was successful. The structure of the synthesized ionic liquids was confirmed through Infrared and NMR spectra. Moreover, chemical composition of the synthesized ionic liquids were verify from the elemental analysis measurement.
2. The physical properties, namely density, viscosity, and refractive index, of the pure ionic liquids and binary mixture of ionic liquids with alcohols were measured from temperature 293.15 to 353.15 K. The physical properties were highest at pure ionic liquids and decreased with increasing concentration of the alcohol, reaching the lowest value at pure alcohols. Furthermore, the physical properties of the pure ionic liquids and its binary mixture with alcohol were found to be decreased with increase in temperature. The temperature dependence of physical properties of these systems can be correlated using empirical method.
3. The synthesized ionic liquids could reduce the corrosion rate of carbon steel in 1 M HCl at temperature from 298.15 K to 343.15 K. The ionic liquids reduced the corrosion rate by adsorbing themselves on the carbon steel surface and obeyed the Langmuir's isotherm adsorption. It formed protective layer on carbon steel surface which give higher energy barrier for corrosion to take place. The inhibition

performance was more pronounced with increasing concentration of the ionic liquids. Moreover, the adsorption of the ionic liquids on the carbon steel surface was spontaneous within the temperature studied in this work. It suggests that all the synthesized ionic liquid in this work has the potential to be used as inhibitor on carbon steel corrosion in 1 M HCl.

4. Addition of alcohol on ionic liquids did not alter the inhibition efficiency. Thus, it can be concluded that these alcohols can be used as cosolvent with ionic liquids, without reducing the ionic liquids performance. The organic solvent is particularly helpful for reducing the viscosity of ionic liquids which is known to be highly viscous.

## **6.2 Recommendations**

This research work has open up for several opportunities for further study. The following issues are recommended for future work in investigating the application of the ionic liquids on carbon steel corrosion in acidic media.

1. The organic corrosion inhibition is the most effective means of protecting the severely internal corrosion of carbon steel pipelines for well acidising. The acid solutions are required to be transported to the respective well. Transporting the acid solution makes the corrosion problems even worse. Therefore it is also worthwhile to consider the effect of the solution flow on the corrosion inhibition of the synthesized ionic liquids.

2. In the industries, the equipments are often submitted to aggressive conditions such as high temperature and pressure, involving the early apparition of corrosion. Thus corrosion and corrosion inhibition studies under these conditions are very important for industrial applications. Therefore to compliment results obtained in this work, additional experiment can be done to study the effect of high temperature and pressure on the inhibition performance of the synthesized ionic liquids.

## PUBLICATION

### A. Journal

1. **Kiki A. Kurnia**, M.I. Abdul Mutallib, B. Ariwahjoedi, “Estimation of Physical Properties of Ionic Liquids [H<sub>2</sub>N-C<sub>2</sub>mim][BF<sub>4</sub>] and [H<sub>2</sub>N-C<sub>3</sub>mim][BF<sub>4</sub>]”, *Journal of Chemical and Engineering Data* 2011, 56 (5), pp. 2557-2562.
2. M.C. Fatah, M.C. Ismail, B. Ari-Wahjoedi, **Kiki A. Kurnia**, “Effects of sulphide ion on the corrosion behaviour of X52 steel in a carbon dioxide environment at temperature 40 °C “, *Materials Chemistry and Physics* 2011, 127(1-2) : 347-352.
3. **Kiki A. Kurnia**, M.I. Abdul Mutalib, T. Murugesan, and B. Ariwahjoedi, “Physicochemical Properties of Binary Mixture of the Protic Ionic Liquid Bis(2-hydroxyethyl)methylammonium Formate with Methanol, Ethanol, and 1-Propanol”, *Journal of Solution Chemistry*, 2011, 40 (5), pp. 818-831.
4. **Kiki Adi Kurnia**, M.I. Abdul Mutalib, T. Murugesan, “Densities, Refractive Indices and Excess Molar Volumes for Binary Mixtures of Protic Ionic Liquids with Methanol at  $T = (293.15 \text{ to } 313.15) \text{ K}$ ”, *Journal of Molecular Liquids*, 2011, 159 (3), pp. 211-219.
5. **Kiki A. Kurnia**, M.I. Abdul Mutalib, T. Murugesan, and B. Ariwahjoedi, “Density and Excess Molar Volume of Protic Ionic Liquids Bis(2-hydroxyethyl)ammonium Acetate with Alcohol”, *Journal of Solution Chemistry*, 2011, 40 (3), pp. 470-480.
6. **Kiki A. Kurnia** and M.I. Abdul Mutalib, “Densities and Viscosities of Binary Mixture of the Ionic Liquid Bis(2-hydroxyethyl)ammonium Propionate with Methanol, Ethanol, and 1-Propanol at  $T = (293.15, 303.15, 313.15, \text{ and } 323.15) \text{ K}$  and at  $P = 0.1 \text{ MPa}$ ”, 2011, *Journal of Chemical and Engineering Data*, 2011, 56 (1), pp. 79-83.
7. Faisal Harris, **Kiki Adi Kurnia**, M. I. Abdul Mutalib and Thanapalan Murugesan, “Heat Capacity of Sodium Aminoacetate Solutions before and after CO<sub>2</sub> Absorption”, *Journal of Chemical and Engineering Data*, 2010, 55 (1), pp. 547-550
8. **Kiki A. Kurnia**, F. Harris, Cecilia D. Wilfred, M. I. Abdul Mutalib, T. Murugesan, “Thermodynamic of Carbon Dioxide Solubility in Hydroxyl Ammonium Ionic Liquids”, *The Journal of Chemical Thermodynamic*, 2009, 41 (10), pp. 1069-1073.
9. F. Harris, **Kiki A. Kurnia**, , M. I. Abdul Mutalib, T. Murugesan, “Density and Solubility of Carbon Dioxide in aqueous solution of Sodium Glycinate for absorption at high pressure”, *Journal of Chemical and Engineering Data*, 2009, 54 (1), pp. 144-147.

10. **Kiki A. Kurnia**, Cecilia D. Wilfred, T. Murugesan, "Thermochemical properties of Hydroxyl Ammonium Ionic Liquids", *The Journal of Chemical Thermodynamic*, 2009, 41 (4), pp. 517-521.

B. Conference

1. **Kiki A. Kurnia**, Hasiah Kamarudin, M.R. Mohamed Ramli, M.I. Abdul Mutalib, Zakaria Man, M. Azmi Bustam, "Separation of aromatic from aliphatic hydrocarbon using ionic liquids. A COSMO-RS screening for potential ionic liquids", Workshop on Graduate Research Trends in France and in Malaysia: Compare and Contrast, SEACARL UTP - IFP, Malaysia, 2011.
2. **Kiki A. Kurnia**, M.I.A. Mutalib, and T. Murugesan, "Protic ionic liquids: A new class of inhibitor on corrosion of carbon steel in acidic medium", Accepted in Asia Pacific Conference on Ionic Liquids and Green Processes, Dalian, China, 2010.
3. **Kiki A. Kurnia**, A.A.A. Khan, M. Fatah, B. Ariwahjoedi, M.I.A. Abdul Mutalib, and T. Murugesan, "Effect of Bis(2-Hydroxyethyl)ammonium Formate on Corrosion of Carbon Steel in Acidic Medium", Accepted in International Conference on Functional Material and Design 2010, University of Malaya, 2010
4. A.A.A. Khan, **Kiki A. Kurnia**, and M.A. Abdullah, "Montmorillonite-Modified Carbon Ionic Liquid Electrode for Cadmium (II) and Lead (II) Detection", Accepted in International Conference on Functional Material and Design 2010, University of Malaya, 2010
5. A.A.A. Khan, **Kiki A. Kurnia**, and M.A. Abdullah, "Cadmium (II) Detection by Montmorillonite-Modified Carbon Ionic Liquids", Accepted in International Conference of Green Technologies for Greener Environment, India, 2009
6. **Kiki A. Kurnia**, Mohamed Ibrahim Abdul Mutalib, and Thanabalan Murugesan, "Inhibition Effect of 2-Hydroxyethanaminium Acetate on Corrosion of Carbon Steel in Acidic Medium", Accepted in Regional Conference on Ionic Liquids, University of Malaya, Malaysia, 2009.
7. **Kiki A. Kurnia**, F. Harris, Cecilia D. Wilfred, M. I. Abdul Mutalib, T. Murugesan, "Solubility of Carbon Dioxide in Hydroxyl Ammonium Ionic Liquids", Accepted in 2<sup>nd</sup> International Conference on Mathematic and Natural Science, 2008.
8. **Kiki A. Kurnia**, Cecilia D. Wilfred, T. Murugesan, "Thermal Properties of Hydroxyl Ammonium Ionic Liquids", Proceeding on Symposium of Malaysian Chemical Engineers, Malaysia, 2006

## REFERENCES

- [1]. V.S. Sastri, E. Ghali, M. Elboudjaini, "Corrosion Prevention and Protection: Practical Solutions", John Wiley & Sons Ltd., The Atrium, Southern Gate, Chichester, West Sussex PO19 8SQ, England, 2007.
- [2]. M. El Azhar, M. Traisnel, B. Mernari, L. Gengembre, F. Bentiss, M. Lagrenée. (2002). Electrochemical and XPS studies of 2,5-bis(n-pyridyl)-1,3,4-thiadiazoles adsorption on mild steel in perchloric acid solution. *Appl. Surf. Sci.* 185 (3-4), pp. 197-205
- [3]. H.A. Nasr-El-Din, A.M. Al-Othman, K.C. Taylor, A.H. Al-Ghamdi. (2004). Surface tension of HCl-based stimulation fluids at high temperatures. *Journal of Petroleum Science and Engineering.* 43 (1-2), pp. 57-73
- [4]. I.B. Obot, N.O. Obi-Egbedi, N.W. Odozi. (2010). Acenaphtho [1,2-b] quinoxaline as a novel corrosion inhibitor for mild steel in 0.5 M H<sub>2</sub>SO<sub>4</sub>. *Corros. Sci.* 52 (3), pp. 923-926
- [5]. S.M.A. Hosseini, A. Azimi. (2009). The inhibition of mild steel corrosion in acidic medium by 1-methyl-3-pyridin-2-yl-thiourea. *Corros. Sci.* 51 (4), pp. 728-732
- [6]. F. Bentiss, C. Jama, B. Mernari, H.E. Attari, L.E. Kadi, M. Lebrini, M. Traisnel, M. Lagrenée. (2009). Corrosion control of mild steel using 3,5-bis(4-methoxyphenyl)-4-amino-1,2,4-triazole in normal hydrochloric acid medium. *Corros. Sci.* 51 (8), pp. 1628-1635
- [7]. A.A. Al-Sarawy, A.S. Fouda, W.A.S. El-Dein. (2008). Some thiazole derivatives as corrosion inhibitors for carbon steel in acidic medium. *Desalin.* 229 (1-3), pp. 279-293
- [8]. G.E. Badr. (2009). The role of some thiosemicarbazide derivatives as corrosion inhibitors for C-steel in acidic media. *Corros. Sci.* 51 (11), pp. 2529-2536
- [9]. A. Popova, M. Christov, A. Vasilev. (2007). Inhibitive properties of quaternary ammonium bromides of N-containing heterocycles on acid mild steel corrosion. Part I: Gravimetric and voltammetric results. *Corros. Sci.* 49 (8), pp. 3276-3289

- [10]. S.A. Ali, M.T. Saeed. (2001). Synthesis and corrosion inhibition study of some 1,6-hexanediamine-based N,N-diallyl quaternary ammonium salts and their polymers. *Polymer*. 42 (7), pp. 2785-2794
- [11]. T.Y. Soror, M.A. El-Ziady. (2003). Effect of cetyl trimethyl ammonium bromide on the corrosion of carbon steel in acids. *Mater. Chem. Phys.* 77 (3), pp. 697-703
- [12]. S. Bilgiç, M. Sahin. (2001). The corrosion inhibition of austenitic chromium-nickel steel in H<sub>2</sub>SO<sub>4</sub> by 2-butyn-1-ol. *Mater. Chem. Phys.* 70 (3), pp. 290-295
- [13]. P. Wasserscheid, T. Welton, "Ionic Liquids in Synthesis", 2<sup>nd</sup> Edition ed., WILEY-VCH Verlag GmbH & Co. KGaA, Darmstadt, Federal Republic of Germany, 2009.
- [14]. F.F.C. Bazito, Y. Kawano, R.M. Torresi. (2007). Synthesis and characterization of two ionic liquids with emphasis on their chemical stability towards metallic lithium. *Electrochim. Acta.* 52 (23), pp. 6427-6437
- [15]. C.P. Fredlake, J.M. Crosthwaite, D.G. Hert, S.N.V.K. Aki, J.F. Brennecke. (2004). Thermophysical Properties of Imidazolium-Based Ionic Liquids. *J. Chem. Eng. Data.* 49 (4), pp. 954-964
- [16]. A. Fernández, J.S. Torrecilla, J. García, F. Rodríguez. (2007). Thermophysical Properties of 1-Ethyl-3-methylimidazolium Ethylsulfate and 1-Butyl-3-methylimidazolium Methylsulfate Ionic Liquids. *J. Chem. Eng. Data.* 52 (5), pp. 1979-1983
- [17]. A.A. Strechan, Y.U. Paulechka, A.G. Kabo, A.V. Blokhin, G.J. Kabo. (2007). 1-Butyl-3-methylimidazolium Tosylate Ionic Liquid: Heat Capacity, Thermal Stability, and Phase Equilibrium of Its Binary Mixtures with Water and Caprolactam. *J. Chem. Eng. Data.* 52 (5), pp. 1791-1799
- [18]. I. Bandrés, D.F. Montañó, I. Gascón, P. Cea, C. Lafuente. (2010). Study of the conductivity behavior of pyridinium-based ionic liquids. *Electrochim. Acta.* 55 (7), pp. 2252-2257
- [19]. S.-H. Yeon, K.-S. Kim, S. Choi, H. Lee, H.S. Kim, H. Kim. (2005). Physical and electrochemical properties of 1-(2-hydroxyethyl)-3-methyl imidazolium and N-(2-hydroxyethyl)-N-methyl morpholinium ionic liquids. *Electrochim. Acta.* 50 (27), pp. 5399-5407
- [20]. J.E. Bara, D.E. Camper, D.L. Gin, R.D. Noble. (2009). Room-Temperature Ionic Liquids and Composite Materials: Platform Technologies for CO<sub>2</sub> Capture. *Acc. Chem. Res.* 43 (1), pp. 152-159

- [21]. S.J. Zhang, X.M. Lu, Q. Zhou, X. Li, X. Zhang, S. Lu, "Ionic Liquids: Physicochemical Properties", 1<sup>st</sup> Edition ed., Elsevier, Oxford - United Kingdom, 2009.
- [22]. Q.B. Zhang, Y.X. Hua. (2009). Corrosion inhibition of mild steel by alkylimidazolium ionic liquids in hydrochloric acid. *Electrochim. Acta.* 54 (6), pp. 1881-1887
- [23]. H. Ashassi-Sorkhabi, M. Es'haghi. (2009). Corrosion inhibition of mild steel in acidic media by [BMIm]Br Ionic liquid. *Mater. Chem. Phys.* 114 (1), pp. 267-271
- [24]. N.V. Likhanova, M.A. Domínguez-Aguilar, O. Olivares-Xometl, N. Nava-Entzana, E. Arce, H. Dorantes. (2010). The Effect of Ionic Liquids with Imidazolium and Pyridinium Cations on the Corrosion Inhibition of Mild Steel in Acidic Environment. *Corros. Sci.* 52 pp. 2088-2097
- [25]. R. Baboian, "NACE Corrosion Engineer's Reference Book", NACE International, 1440 South Creek Drive, Houston, TX 77084, 2002.
- [26]. T.L. Greaves, A. Weerawardena, C. Fong, I. Krodkiewska, C.J. Drummond. (2006). Protic Ionic Liquids: Solvents with Tunable Phase Behavior and Physicochemical Properties. *J. Phys. Chem. B.* 110 (45), pp. 22479-22487
- [27]. T.L. Greaves, C.J. Drummond. (2007). Protic Ionic Liquids: Properties and Applications. *Chem. Rev.* 108 (1), pp. 206-237
- [28]. T.L. Greaves, A. Weerawardena, C. Fong, C.J. Drummond. (2007). Formation of Amphiphile Self-Assembly Phases in Protic Ionic Liquids. *J. Phys. Chem. B.* 111 (16), pp. 4082-4088
- [29]. T.L. Greaves, A. Weerawardena, I. Krodkiewska, C.J. Drummond. (2008). Protic Ionic Liquids: Physicochemical Properties and Behavior as Amphiphile Self-Assembly Solvents. *J. Phys. Chem. B.* 112 (3), pp. 896-905
- [30]. X. Yuan, S. Zhang, J. Liu, X. Lu. (2007). Solubilities of CO<sub>2</sub> in hydroxyl ammonium ionic liquids at elevated pressures. *Fluid Phase Equilib.* 257 (2), pp. 195-200
- [31]. K.A. Kurnia, F. Harris, C.D. Wilfred, M.I. Abdul Mutalib, T. Murugesan. (2009). Thermodynamic properties of CO<sub>2</sub> absorption in hydroxyl ammonium ionic liquids at pressures of (100-1600) kPa. *J. Chem. Thermodyn.* 41 (10), pp. 1069-1073
- [32]. L. Zhai, Q. Zhong, C. He, J. Wang. (2010). Hydroxyl ammonium ionic liquids synthesized by water-bath microwave: Synthesis and desulfurization. *J. Hazard. Mater.* 177 pp. 807-813

- [33]. C. Zhao, G. Burrell, A.A.J. Torriero, F. Separovic, N.F. Dunlop, D.R. MacFarlane, A.M. Bond. (2008). Electrochemistry of Room Temperature Protic Ionic Liquids. *J. Phys. Chem. B.* 112 (23), pp. 6923-6936
- [34]. A.G.e. Böwing, A. Jess. (2007). Kinetics and reactor design aspects of the synthesis of ionic liquids—Experimental and theoretical studies for ethylmethylimidazole ethylsulfate. *Chem. Eng. Sci.* 62 pp. 1760-1769
- [35]. D. Torres-Martínez, R. Melgarejo-Torres, M. Gutiérrez-Rojas, L. Aguilera-Vázquez, M. Micheletti, G.J. Lye, S. Huerta-Ochoa. (2009). Hydrodynamic and oxygen mass transfer studies in a three-phase (air-water-ionic liquid) stirred tank bioreactor. *Biochem. Eng. J.* 45 (3), pp. 209-217
- [36]. H. Xin, Q. Wu, M. Han, D. Wang, Y. Jin. (2005). Alkylation of benzene with 1-dodecene in ionic liquids [Rmim]+Al<sub>2</sub>Cl<sub>6</sub>X<sup>-</sup> (R = butyl, octyl and dodecyl; X = chlorine, bromine and iodine). *Appl. Catal., A.* 292 pp. 354-361
- [37]. Z. Zhao, Z. Li, G. Wang, W. Qiao, L. Cheng. (2004). Friedel-Crafts alkylation of 2-methylnaphthalene in room temperature ionic liquids. *Appl. Catal., A.* 262 (1), pp. 69-73
- [38]. K. Qiao, Y. Deng. (2001). Alkylations of benzene in room temperature ionic liquids modified with HCl. *J. Mol. Catal. A: Chem.* 171 (1-2), pp. 81-84
- [39]. P. Wasserscheid, M. Sessing, W. Korth. (2002). Hydrogensulfate and tetrakis(hydrogensulfato)borate ionic liquids: synthesis and catalytic application in highly Bronsted-acidic systems for Friedel-Crafts alkylation. *Green Chemistry.* 4 (2), pp. 134-138
- [40]. C.G. Blanco, D.C. Banciella, M.D.G. Azpíroz. (2006). Alkylation of naphthalene using three different ionic liquids. *J. Mol. Catal. A: Chem.* 253 (1-2), pp. 203-206
- [41]. A.M. Scurto, W. Leitner. (2006). Expanding the useful range of ionic liquids: melting point depression of organic salts with carbon dioxide for biphasic catalytic reactions. *Chemical Communications.* (35), pp. 3681-3683
- [42]. M.H. Valkenberg, C. deCastro, W.F. Hölderich. (2001). Friedel-Crafts acylation of aromatics catalysed by supported ionic liquids. *Appl. Catal., A.* 215 (1-2), pp. 185-190
- [43]. M.J. Earle, U. Hakala, C. Hardacre, J. Karkkainen, B.J. McAuley, D.W. Rooney, K.R. Seddon, J.M. Thompson, K. Wahala. (2005). Chloroindate(iii) ionic liquids: recyclable media for Friedel-Crafts acylation reactions. *Chemical Communications.* (7), pp. 903-905
- [44]. M.J. Earle, U. Hakala, B.J. McAuley, M. Nieuwenhuyzen, A. Ramani, K.R. Seddon. (2004). Metal bis{(trifluoromethyl)sulfonyl}amide complexes: highly



- efficient Friedel-Crafts acylation catalysts. *Chemical Communications*. (12), pp. 1368-1369
- [45]. B. Murphy, P. Goodrich, C. Hardacre, M. Oelgemoller. (2009). Green photochemistry: photo-Friedel-Crafts acylations of 1,4-naphthoquinone in room temperature ionic liquids. *Green Chemistry*. 11 (11), pp. 1867-1870
- [46]. M. Haumann, A. Riisager. (2008). Hydroformylation in Room Temperature Ionic Liquids (RTILs): Catalyst and Process Developments. *Chem. Rev.* 108 (4), pp. 1474-1497
- [47]. L.c. Leclercq, I. Suisse, F. Agbossou-Niedercorn. (2008). Biphasic hydroformylation in ionic liquids: interaction between phosphane ligands and imidazolium triflate, toward an asymmetric process. *Chemical Communications*. (3), pp. 311-313
- [48]. J. Durand, E. Teuma, M. Gómez. (2007). Ionic liquids as a medium for enantioselective catalysis. *C.R. Chim.* 10 (3), pp. 152-177
- [49]. M. Zou, X. Mu, N. Yan, Y. Kou. (2007). Selective Hydrogenation of Cinnamaldehyde by Ionic Copolymer-Stabilized Pt Nanoparticles in Ionic Liquids. *Chin. J. Catal.* 28 (5), pp. 389-391
- [50]. Y. Deng, F. Shi, J. Beng, K. Qiao. (2001). Ionic liquid as a green catalytic reaction medium for esterifications. *J. Mol. Catal. A: Chem.* 165 (1-2), pp. 33-36
- [51]. J. Gui, X. Cong, D. Liu, X. Zhang, Z. Hu, Z. Sun. (2004). Novel Brønsted acidic ionic liquid as efficient and reusable catalyst system for esterification. *Catal. Commun.* 5 (9), pp. 473-477
- [52]. H. Zhao, C.L. Jones, J.V. Cowins. (2009). Lipase dissolution and stabilization in ether-functionalized ionic liquids. *Green Chemistry*. 11 (8), pp. 1128-1138
- [53]. J. Mutschler, T. Rausis, J.-M. Bourgeois, C. Bastian, D. Zufferey, I.V. Mohrenz, F. Fischer. (2009). Ionic liquid-coated immobilized lipase for the synthesis of methylglucose fatty acid esters. *Green Chemistry*. 11 (11), pp. 1793-1800
- [54]. B. Major, I. Kelemen-Horvath, Z. Csanadi, K. Belafi-Bako, L. Gubicza. (2009). Microwave assisted enzymatic esterification of lactic acid and ethanol in phosphonium type ionic liquids as co-solvents. *Green Chemistry*. 11 (5), pp. 614-616
- [55]. H. Zhang, F. Xu, X. Zhou, G. Zhang, C. Wang. (2007). A Bronsted acidic ionic liquid as an efficient and reusable catalyst system for esterification. *Green Chemistry*. 9 (11), pp. 1208-1211

- [56]. J. Arras, D. Ruppert, P. Claus. (2009). Supported ruthenium catalysed selective hydrogenation of citral in presence of [NTf<sub>2</sub>]- based ionic liquids. *Appl. Catal., A*. 371 (1-2), pp. 73-77
- [57]. A. Chrobok, S. Baj, W. Pudlo, A. Jarzebski. (2009). Supported hydrogensulfate ionic liquid catalysis in Baeyer-Villiger reaction. *Appl. Catal., A*. 366 (1), pp. 22-28
- [58]. S. Gago, S.S. Balula, S. Figueiredo, A.D. Lopes, A.A. Valente, M. Pillinger, I.S. Gonçalves. (2010). Catalytic olefin epoxidation with cationic molybdenum(VI) cis-dioxo complexes and ionic liquids. *Appl. Catal., A*. 372 (1), pp. 67-72
- [59]. C.M. Gordon. (2001). New developments in catalysis using ionic liquids. *Appl. Catal., A*. 222 (1-2), pp. 101-117
- [60]. J. Joni, M. Haumann, P. Wasserscheid. Continuous gas-phase isopropylation of toluene and cumene using highly acidic Supported Ionic Liquid Phase (SILP) catalysts. *Appl. Catal., A*. 372 (1), pp. 8-15
- [61]. J.-P.T. Mikkola, P.P. Virtanen, K. Kordás, H. Karhu, T.O. Salmi. (2007). SILCA--Supported ionic liquid catalysts for fine chemicals. *Appl. Catal., A*. 328 (1), pp. 68-76
- [62]. E. Öchsner, K. Schneiders, K. Junge, M. Beller, P. Wasserscheid. (2009). Highly enantioselective Ru-catalyzed asymmetric hydrogenation of [beta]-keto ester in ionic liquid/methanol mixtures. *Appl. Catal., A*. 364 (1-2), pp. 8-14
- [63]. J. Fraga-Dubreuil, K. Bourahla, M. Rahmouni, J.P. Bazureau, J. Hamelin. (2002). Catalysed esterifications in room temperature ionic liquids with acidic counteranion as recyclable reaction media. *Catal. Commun.* 3 (5), pp. 185-190
- [64]. M. Herbert, A. Galindo, F. Montilla. (2007). Catalytic epoxidation of cyclooctene using molybdenum(VI) compounds and urea-hydrogen peroxide in the ionic liquid [bmim]PF<sub>6</sub>. *Catal. Commun.* 8 (7), pp. 987-990
- [65]. S. Breitenlechner, M. Fleck, T.E. Müller, A. Suppan. (2004). Solid catalysts on the basis of supported ionic liquids and their use in hydroamination reactions. *J. Mol. Catal. A: Chem.* 214 (1), pp. 175-179
- [66]. N.V. Gwala, N. Deenadayalu, K. Tumba, D. Ramjugernath. (2010). Activity coefficients at infinite dilution for solutes in the trioctylmethylammonium bis(trifluoromethylsulfonyl)imide ionic liquid using gas-liquid chromatography. *J. Chem. Thermodyn.* 42 (2), pp. 256-261
- [67]. T.M. Letcher, U. Domanska, M. Marciniak, A. Marciniak. (2005). Activity coefficients at infinite dilution measurements for organic solutes in the ionic liquid 1-butyl-3-methyl-imidazolium 2-(2-methoxyethoxy) ethyl sulfate using

- g.l.c. at T = (298.15, 303.15, and 308.15) K. *J. Chem. Thermodyn.* 37 (6), pp. 587-593
- [68]. M. Sobota, V. Dohnal, P. Vrbka. (2009). Activity Coefficients at Infinite Dilution of Organic Solutes in the Ionic Liquid 1-Ethyl-3-methyl-imidazolium Nitrate. *J. Phys. Chem. B.* 113 (13), pp. 4323-4332
- [69]. G.W. Meindersma, A.B. de Haan. (2008). Conceptual process design for aromatic/aliphatic separation with ionic liquids. *Chem. Eng. Res. Des.* 86 (7), pp. 745-752
- [70]. A.B. Pereiro, F.J. Deive, J.M.S.S. Esperança, A. Rodríguez. (2010). Alkylsulfate-based ionic liquids to separate azeotropic mixtures. *Fluid Phase Equilib.* 291 (1), pp. 13-17
- [71]. A.B. Pereiro, A. Rodríguez. (2008). Separation of Ethanol–Heptane Azeotropic Mixtures by Solvent Extraction with an Ionic Liquid. *Ind. Eng. Chem. Res.* 48 (3), pp. 1579-1585
- [72]. A.B. Pereiro, A. Rodríguez. (2009). Effective extraction in packed column of ethanol from the azeotropic mixture ethanol + hexane with an ionic liquid as solvent. *Chem. Eng. J.* 153 (1-3), pp. 80-85
- [73]. D.R. MacFarlane, M. Forsyth, P.C. Howlett, J.M. Pringle, J. Sun, G. Annat, W. Neil, E.I. Izgorodina. (2007). Ionic Liquids in Electrochemical Devices and Processes: Managing Interfacial Electrochemistry. *Acc. Chem. Res.* 40 (11), pp. 1165-1173
- [74]. Q. Dai, D.B. Menzies, D.R. MacFarlane, S.R. Batten, S. Forsyth, L. Spiccia, Y.-B. Cheng, M. Forsyth. (2010). Dye-sensitized nanocrystalline solar cells incorporating ethylmethylimidazolium-based ionic liquid electrolytes. *C.R. Chim.* 9 (5-6), pp. 617-621
- [75]. K. Suzuki, M. Yamaguchi, M. Kumagai, N. Tanabe, S. Yanagida. (2006). Dye-sensitized solar cells with ionic gel electrolytes prepared from imidazolium salts and agarose. *C.R. Chim.* 9 (5-6), pp. 611-616
- [76]. V. Baranchugov, E. Markevich, E. Pollak, G. Salitra, D. Aurbach. (2007). Amorphous silicon thin films as a high capacity anodes for Li-ion batteries in ionic liquid electrolytes. *Electrochem. Commun.* 9 (4), pp. 796-800
- [77]. J.N. Barisci, G.G. Wallace, D.R. MacFarlane, R.H. Baughman. (2004). Investigation of ionic liquids as electrolytes for carbon nanotube electrodes. *Electrochem. Commun.* 6 (1), pp. 22-27
- [78]. J. Jin, H.H. Li, J.P. Wei, X.K. Bian, Z. Zhou, J. Yan. (2009). Li/LiFePO<sub>4</sub> batteries with room temperature ionic liquid as electrolyte. *Electrochem. Commun.* 11 (7), pp. 1500-1503

- [79]. R.F. de Souza, J.C. Padilha, R.S. Gonçalves, J. Dupont. (2003). Room temperature dialkylimidazolium ionic liquid-based fuel cells. *Electrochem. Commun.* 5 (8), pp. 728-731
- [80]. G. Lakshminarayana, M. Nogami. (2010). Inorganic-organic hybrid membranes with anhydrous proton conduction prepared from tetramethoxysilane/methyl-trimethoxysilane/trimethylphosphate and 1-ethyl-3-methylimidazolium-bis (trifluoromethanesulfonyl) imide for H<sub>2</sub>/O<sub>2</sub> fuel cells. *Electrochim. Acta.* 55 (3), pp. 1160-1168
- [81]. A. Balducci, U. Bardi, S. Caporali, M. Mastragostino, F. Soavi. (2004). Ionic liquids for hybrid supercapacitors. *Electrochem. Commun.* 6 (6), pp. 566-570
- [82]. D. Wei, T.W. Ng. (2009). Application of novel room temperature ionic liquids in flexible supercapacitors. *Electrochem. Commun.* 11 (10), pp. 1996-1999
- [83]. J.L. Anderson, J.K. Dixon, J.F. Brennecke. (2007). Solubility of CO<sub>2</sub>, CH<sub>4</sub>, C<sub>2</sub>H<sub>6</sub>, C<sub>2</sub>H<sub>4</sub>, O<sub>2</sub>, and N<sub>2</sub> in 1-Hexyl-3-methylpyridinium Bis(trifluoromethylsulfonyl)imide: Comparison to Other Ionic Liquids. *Acc. Chem. Res.* 40 (11), pp. 1208-1216
- [84]. J. Kumelan, D. Tuma, G. Maurer. (2009). Partial molar volumes of selected gases in some ionic liquids. *Fluid Phase Equilib.* 275 (2), pp. 132-144
- [85]. A.M. Schilderman, S. Raeissi, C.J. Peters. (2007). Solubility of carbon dioxide in the ionic liquid 1-ethyl-3-methylimidazolium bis(trifluoromethylsulfonyl)imide. *Fluid Phase Equilib.* 260 (1), pp. 19-22
- [86]. T. Wang, C. Peng, H. Liu, Y. Hu. (2006). Description of the pVT behavior of ionic liquids and the solubility of gases in ionic liquids using an equation of state. *Fluid Phase Equilib.* 250 (1-2), pp. 150-157
- [87]. Á.P.-S. Kamps, D. Tuma, J. Xia, G. Maurer. (2003). Solubility of CO<sub>2</sub> in the Ionic Liquid [bmim][PF<sub>6</sub>]. *J. Chem. Eng. Data.* 48 (3), pp. 746-749
- [88]. X. Li, M. Hou, B. Han, X. Wang, L. Zou. (2008). Solubility of CO<sub>2</sub> in a Choline Chloride + Urea Eutectic Mixture. *J. Chem. Eng. Data.* 53 (2), pp. 548-550
- [89]. S. Raeissi, C.J. Peters. (2008). Carbon Dioxide Solubility in the Homologous 1-Alkyl-3-methylimidazolium Bis(trifluoromethylsulfonyl)imide Family. *J. Chem. Eng. Data.* 54 (2), pp. 382-386
- [90]. M.B. Shiflett, A. Yokozeki. (2007). Solubility of CO<sub>2</sub> in Room Temperature Ionic Liquid [hmim][Tf<sub>2</sub>N]. *J. Phys. Chem. B.* 111 (8), pp. 2070-2074
- [91]. P. Walden. (1914). *Bulletin of Academia and Imperial Science (St. Petersburg).* (8), pp. 405-422

- [92]. M. Anouti, M. Caillon-Caravanier, Y. Dridi, J. Jacquemin, C. Hardacre, D. Lemordant. (2009). Liquid densities, heat capacities, refractive index and excess quantities for {protic ionic liquids + water} binary system. *J. Chem. Thermodyn.* 41 (6), pp. 799-808
- [93]. J.-P. Belieres, C.A. Angell. (2007). Protic Ionic Liquids: Preparation, Characterization, and Proton Free Energy Level Representation. *J. Phys. Chem. B.* 111 (18), pp. 4926-4937
- [94]. C.A. Angell, N. Byrne, J.-P. Belieres. (2007). Parallel Developments in Aprotic and Protic Ionic Liquids: Physical Chemistry and Applications. *Acc. Chem. Res.* 40 (11), pp. 1228-1236
- [95]. X.L. Yuan, S.J. Zhang, X.M. Lu. (2007). Hydroxyl Ammonium Ionic Liquids: Synthesis, Properties, and Solubility of SO<sub>2</sub>. *J. Chem. Eng. Data.* 52 (2), pp. 596-599
- [96]. I. Cota, R. Gonzalez-Olmos, M. Iglesias, F. Medina. (2007). New Short Aliphatic Chain Ionic Liquids: Synthesis, Physical Properties, and Catalytic Activity in Aldol Condensations. *J. Phys. Chem. B.* 111 (43), pp. 12468-12477
- [97]. M. Iglesias, A. Torres, R. Gonzalez-Olmos, D. Salvatierra. (2008). Effect of temperature on mixing thermodynamics of a new ionic liquid: {2-Hydroxy ethylammonium formate (2-HEAF) + short hydroxylic solvents}. *J. Chem. Thermodyn.* 40 (1), pp. 119-133
- [98]. M. Anouti, A. Vigeant, J. Jacquemin, C. Brigouleix, D. Lemordant. (2010). Volumetric properties, viscosity and refractive index of the Protic Ionic Liquid, pyrrolidinium octanoate, in molecular solvents. *J. Chem. Thermodyn.* 42 (7), pp. 834-845
- [99]. K.N. Marsh, J.A. Boxall, R. Lichtenthaler. (2004). Room temperature ionic liquids and their mixtures--a review. *Fluid Phase Equilib.* 219 (1), pp. 93-98
- [100]. E. Rilo, J. Pico, S. García-Garabal, L.M. Varela, O. Cabeza. (2009). Density and surface tension in binary mixtures of C<sub>n</sub>MIM-BF<sub>4</sub> ionic liquids with water and ethanol. *Fluid Phase Equilib.* 285 (1-2), pp. 83-89
- [101]. R.L. Gardas, H.F. Costa, M.G. Freire, P.J. Carvalho, I.M. Marrucho, I.M.A. Fonseca, A.G.M. Ferreira, J.A.P. Coutinho. (2008). Densities and Derived Thermodynamic Properties of Imidazolium-, Pyridinium-, Pyrrolidinium-, and Piperidinium-Based Ionic Liquids. *J. Chem. Eng. Data.* 53 (3), pp. 805-811
- [102]. J.M.S.S. Esperança, H.J.R. Guedes, M. Blesic, L.P.N. Rebelo. (2005). Densities and Derived Thermodynamic Properties of Ionic Liquids. 3. Phosphonium-Based Ionic Liquids over an Extended Pressure Range. *J. Chem. Eng. Data.* 51 (1), pp. 237-242

- [103]. O. Borodin, G.D. Smith, H. Kim. (2009). Viscosity of a Room Temperature Ionic Liquid: Predictions from Nonequilibrium and Equilibrium Molecular Dynamics Simulations. *J. Phys. Chem. B.* 113 (14), pp. 4771-4774
- [104]. M.T. Zafarani-Moattar, R. Majdan-Cegincara. (2007). Viscosity, Density, Speed of Sound, and Refractive Index of Binary Mixtures of Organic Solvent + Ionic Liquid, 1-Butyl-3-methylimidazolium Hexafluorophosphate at 298.15 K. *J. Chem. Eng. Data.* 52 (6), pp. 2359-2364
- [105]. B. Hasse, J. Lehmann, D. Assenbaum, P. Wasserscheid, A. Leipertz, A.P. Frba. (2009). Viscosity, Interfacial Tension, Density, and Refractive Index of Ionic Liquids [EMIM][MeSO<sub>3</sub>], [EMIM][MeOHPO<sub>2</sub>], [EMIM][OcSO<sub>4</sub>], and [BBIM][NTf<sub>2</sub>] in Dependence on Temperature at Atmospheric Pressure. *J. Chem. Eng. Data.* 54 (9), pp. 2576-2583
- [106]. U. Domanska, M. Królikowska, M. Królikowski. (2010). Phase behaviour and physico-chemical properties of the binary systems {1-ethyl-3-methylimidazolium thiocyanate, or 1-ethyl-3-methylimidazolium tosylate + water, or + an alcohol}. *Fluid Phase Equilib.* In Press, Accepted Manuscript pp.
- [107]. M.G. Freire, L.M.N.B.F. Santos, I.M. Marrucho, J.A.P. Coutinho. (2007). Evaluation of COSMO-RS for the prediction of LLE and VLE of alcohols + ionic liquids. *Fluid Phase Equilib.* 255 (2), pp. 167-178
- [108]. A. Heintz, D.V. Kulikov, S.P. Verevkin. (2001). Thermodynamic Properties of Mixtures Containing Ionic Liquids. 1. Activity Coefficients at Infinite Dilution of Alkanes, Alkenes, and Alkylbenzenes in 4-Methyl-n-butylpyridinium Tetrafluoroborate Using Gas-Liquid Chromatography. *J. Chem. Eng. Data.* 46 (6), pp. 1526-1529
- [109]. S.P. Verevkin, J. Safarov, E. Bich, E. Hassel, A. Heintz. (2005). Thermodynamic properties of mixtures containing ionic liquids: Vapor pressures and activity coefficients of n-alcohols and benzene in binary mixtures with 1-methyl-3-butyl-imidazolium bis(trifluoromethyl-sulfonyl) imide. *Fluid Phase Equilib.* 236 (1-2), pp. 222-228
- [110]. Y. Geng, T. Wang, D. Yu, C. Peng, H. Liu, Y. Hu. (2008). Densities and Viscosities of the Ionic Liquid [C<sub>4</sub>mim][PF<sub>6</sub>]+ N, N-dimethylformamide Binary Mixtures at 293.15 K to 318.15 K. *Chin. J. Chem. Eng.* 16 (2), pp. 256-262
- [111]. S.P. Verevkin, T.V. Vasiltsova, E. Bich, A. Heintz. (2004). Thermodynamic properties of mixtures containing ionic liquids: Activity coefficients of aldehydes and ketones in 1-methyl-3-ethyl-imidazolium bis(trifluoromethyl-sulfonyl) imide using the transpiration method. *Fluid Phase Equilib.* 218 (2), pp. 165-175

- [112]. B.W. Rossiter, R.C. Baetzold, "Physical Methods of Chemistry", 2<sup>nd</sup> Edition ed., John Wiley & Sons, Inc., United States of America, 1992.
- [113]. M. Tariq, P.A.S. Forte, M.F.C. Gomes, J.N.C. Lopes, L.P.N. Rebelo. (2009). Densities and refractive indices of imidazolium- and phosphonium-based ionic liquids: Effect of temperature, alkyl chain length, and anion. *J. Chem. Thermodyn.* 41 (6), pp. 790-798
- [114]. M.A. Iglesias-Otero, J. Troncoso, E. Carballo, L. Roman. (2008). Densities and Excess Enthalpies for Ionic Liquids + Ethanol or + Nitromethane. *J. Chem. Eng. Data.* 53 (6), pp. 1298-1301
- [115]. Y. Zhong, H. Wang, K. Diao. (2007). Densities and excess volumes of binary mixtures of the ionic liquid 1-butyl-3-methylimidazolium hexafluorophosphate with aromatic compound at T = (298.15 to 313.15) K. *J. Chem. Thermodyn.* 39 (2), pp. 291-296
- [116]. A.B. Pereiro, P. Verdía, E. Tojo, A. Rodríguez. (2007). Physical Properties of 1-Butyl-3-methylimidazolium Methyl Sulfate as a Function of Temperature. *J. Chem. Eng. Data.* 52 (2), pp. 377-380
- [117]. Q. Zhou, L.-S. Wang, H.-P. Chen. (2006). Densities and Viscosities of 1-Butyl-3-methylimidazolium Tetrafluoroborate + H<sub>2</sub>O Binary Mixtures from (303.15 to 353.15) K. *J. Chem. Eng. Data.* 51 (3), pp. 905-908
- [118]. Chan Han, Shuqian Xia, Peisheng Ma, F. Zeng. (2009). Densities of Ionic Liquid [BMIM][BF<sub>4</sub>] + Ethanol, + Benzene, and + Acetonitrile at Different Temperature and Pressure. *J. Chem. Eng. Data.* 54 (10), pp. 2971-2977
- [119]. A.N. Soriano, B.T. Doma Jr, M.-H. Li. (2010). Density and refractive index measurements of 1-ethyl-3-methylimidazolium-based ionic liquids. *J. Taiwan Inst. Chem. Eng.* 41 (1), pp. 115-121
- [120]. P. Kilaru, G.A. Baker, P. Scovazzo. (2007). Density and Surface Tension Measurements of Imidazolium-, Quaternary Phosphonium-, and Ammonium-Based Room-Temperature Ionic Liquids: Data and Correlations. *J. Chem. Eng. Data.* 52 (6), pp. 2306-2314
- [121]. W. Fan, Q. Zhou, J. Sun, S. Zhang. (2009). Density, Excess Molar Volume, and Viscosity for the Methyl Methacrylate + 1-Butyl-3-methylimidazolium Hexafluorophosphate Ionic Liquid Binary System at Atmospheric Pressure. *J. Chem. Eng. Data.* 54 (8), pp. 2307-2311
- [122]. U. Domanska, M. Laskowska. (2009). Temperature and Composition Dependence of the Density and Viscosity of Binary Mixtures of {1-Butyl-3-methylimidazolium Thiocyanate + 1-Alcohols}. *J. Chem. Eng. Data.* 54 (7), pp. 2113-2119

- [123]. E.J. González, L. Alonso, Á. Domínguez. (2006). Physical Properties of Binary Mixtures of the Ionic Liquid 1-Methyl-3-octylimidazolium Chloride with Methanol, Ethanol, and 1-Propanol at T = (298.15, 313.15, and 328.15) K and at P = 0.1 MPa. *J. Chem. Eng. Data.* 51 (4), pp. 1446-1452
- [124]. B. González, N. Calvar, E. Gomez, I. Dominguez, A. Dominguez. (2009). Synthesis and Physical Properties of 1-Ethylpyridinium Ethylsulfate and its Binary Mixtures with Ethanol and 1-Propanol at Several Temperatures. *J. Chem. Eng. Data.* 54 (4), pp. 1353-1358
- [125]. B. Mokhtarani, A. Sharifi, H.R. Mortaheb, M. Mirzaei, M. Mafi, F. Sadeghian. (2009). Density and viscosity of 1-butyl-3-methylimidazolium nitrate with ethanol, 1-propanol, or 1-butanol at several temperatures. *J. Chem. Thermodyn.* 41 (12), pp. 1432-1438
- [126]. C.A. Ohlin, P.J. Dyson, G. Laurency. (2004). Carbon monoxide solubility in ionic liquids: determination, prediction and relevance to hydroformylation. *Chemical Communications.* (9), pp. 1070-1071
- [127]. J.G. Huddleston, A.E. Visser, W.M. Reichert, H.D. Willauer, G.A. Broker, R.D. Rogers. (2001). Characterization and comparison of hydrophilic and hydrophobic room temperature ionic liquids incorporating the imidazolium cation. *Green Chemistry.* 3 (4), pp. 156-164
- [128]. A. Berthod, M. Ruiz-Angel, S. Carda-Broch. (2008). Ionic liquids in separation techniques. *J. Chromatogr. A.* 1184 pp. 6-18
- [129]. K.-S. Kim, B.-K. Shin, H. Lee, F. Ziegler. (2004). Refractive index and heat capacity of 1-butyl-3-methylimidazolium bromide and 1-butyl-3-methylimidazolium tetrafluoroborate, and vapor pressure of binary systems for 1-butyl-3-methylimidazolium bromide + trifluoroethanol and 1-butyl-3-methylimidazolium tetrafluoroborate + trifluoroethanol. *Fluid Phase Equilib.* 218 (2), pp. 215-220
- [130]. H. Tokuda, K. Hayamizu, K. Ishii, M.A.B.H. Susan, M. Watanabe. (2006). How Ionic Are Room-Temperature Ionic Liquids? An Indicator of the Physicochemical Properties. *J. Phys. Chem. B.* 110 (39), pp. 19593-19600
- [131]. Z. Gu, J.F. Brennecke. (2002). Volume Expansivities and Isothermal Compressibilities of Imidazolium and Pyridinium-Based Ionic Liquids. *J. Chem. Eng. Data.* 47 (2), pp. 339-345
- [132]. S.H. Lee, S.B. Lee. (2005). The Hildebrand solubility parameters, cohesive energy densities and internal energies of 1-alkyl-3-methylimidazolium-based room temperature ionic liquids. *Chemical Communications.* (27), pp. 3469-3471



- [133]. R. Fortunato, C.A.M. Afonso, M.A.M. Reis, J.G. Crespo. (2004). Supported liquid membranes using ionic liquids: study of stability and transport mechanisms. *J. Membr. Sci.* 242 (1-2), pp. 197-209
- [134]. A. Muhammad, M.I. Abdul Mutalib, C.D. Wilfred, T. Murugesan, A. Shafeeq. (2008). Thermophysical properties of 1-hexyl-3-methyl imidazolium based ionic liquids with tetrafluoroborate, hexafluorophosphate and bis(trifluoromethylsulfonyl)imide anions. *J. Chem. Thermodyn.* 40 (9), pp. 1433-1438
- [135]. R. Gomes de Azevedo, J.M.S.S. Esperança, J. Szydłowski, Z.P. Visak, P.F. Pires, H.J.R. Guedes, L.P.N. Rebelo. (2005). Thermophysical and thermodynamic properties of ionic liquids over an extended pressure range: [bmim][NTf<sub>2</sub>] and [hmim][NTf<sub>2</sub>]. *J. Chem. Thermodyn.* 37 (9), pp. 888-899
- [136]. L. Alonso, A. Arce, M. Francisco, A. Soto. (2007). Measurement and Correlation of Liquid-Liquid Equilibria of Two Imidazolium Ionic Liquids with Thiophene and Methylcyclohexane. *J. Chem. Eng. Data.* 52 (6), pp. 2409-2412
- [137]. L. Alonso, A. Arce, M. Francisco, A. Soto. (2008). (Liquid + liquid) equilibria of [C8mim][NTf<sub>2</sub>] ionic liquid with a sulfur-component and hydrocarbons. *J. Chem. Thermodyn.* 40 (2), pp. 265-270
- [138]. A.B. Pereiro, A. Rodríguez. (2008). A study on the liquid-liquid equilibria of 1-alkyl-3-methylimidazolium hexafluorophosphate with ethanol and alkanes. *Fluid Phase Equilib.* 270 (1-2), pp. 23-29
- [139]. B.D. Fitchett, T.N. Knepp, J.C. Conboy. (2004). 1-Alkyl-3-methylimidazolium Bis(perfluoroalkylsulfonyl)imide Water-Immiscible Ionic Liquids. *Journal of Electrochemical Society.* 151 (7), pp. E219-E225
- [140]. A.B. Pereiro, H.I.M. Veiga, J.M.S.S. Esperança, A. Rodríguez. (2009). Effect of temperature on the physical properties of two ionic liquids. *J. Chem. Thermodyn.* 41 (12), pp. 1419-1423
- [141]. E.J. González, B. González, N. Calvar, Á. Domínguez. (2007). Physical Properties of Binary Mixtures of the Ionic Liquid 1-Ethyl-3-methylimidazolium Ethyl Sulfate with Several Alcohols at T = (298.15, 313.15, and 328.15) K and Atmospheric Pressure. *J. Chem. Eng. Data.* 52 (5), pp. 1641-1648
- [142]. H. Shekaari, S.S. Mousavi. (2010). Volumetric properties of ionic liquid 1,3-dimethylimidazolium methyl sulfate + molecular solvents at T = (298.15-328.15) K. *Fluid Phase Equilib.* 291 (2), pp. 201-207
- [143]. M.A. Iglesias-Otero, J. Troncoso, E. Carballo, L. Romaní. (2008). Density and refractive index in mixtures of ionic liquids and organic solvents: Correlations and predictions. *J. Chem. Thermodyn.* 40 (6), pp. 949-956

- [144]. W. Liu, T. Zhang, H. Wang, M. Yu. (2006). The Physical Properties of Aqueous Solutions of the Ionic Liquid [BMIM][BF<sub>4</sub>] J. Solution Chem. 35 pp. 1337-1346
- [145]. M.A. Iglesias-Otero, J. Trancoso, E. Carballo. (2007). Density and Refractive Index for Binary Systems of the Ionic Liquid [Bmim][BF<sub>4</sub>] with Methanol, 1,3-Dichloropropane, and Dimethyl Carbonate. J. Solution Chem. 26 pp. 1219-1230
- [146]. A. Kumar. (2008). Estimates of Internal Pressure and Molar Refraction of Imidazolium Based Ionic Liquids as a Function of Temperature. J. Solution Chem. 37 pp. 203-214
- [147]. B. González, N. Calvar, E. Gomez, E.A. Macedo, A. Dominguez. (2008). Synthesis and Physical Properties of 1-Ethyl 3-methylpyridinium Ethylsulfate and Its Binary Mixtures with Ethanol and Water at Several Temperatures. J. Chem. Eng. Data. 53 (8), pp. 1824-1828
- [148]. A. Goldon, K. Dbrowska, T. Hofman. (2007). Densities and Excess Volumes of the 1,3-Dimethylimidazolium Methylsulfate + Methanol System at Temperatures from (313.15 to 333.15) K and Pressures from (0.1 to 25) MPa. J. Chem. Eng. Data. 52 (5), pp. 1830-1837
- [149]. T. Hofman, A. Goldon, A. Nevines, T.M. Letcher. (2008). Densities, excess volumes, isobaric expansivity, and isothermal compressibility of the (1-ethyl-3-methylimidazolium ethylsulfate + methanol) system at temperatures (283.15 to 333.15) K and pressures from (0.1 to 35) MPa. J. Chem. Thermodyn. 40 (4), pp. 580-591
- [150]. J. Ortega, R. Vreekamp, E. Penco, E. Marrero. (2008). Mixing thermodynamic properties of 1-butyl-4-methylpyridinium tetrafluoroborate [b4mpy][BF<sub>4</sub>] with water and with an alkan-1-ol (methanol to pentanol). J. Chem. Thermodyn. 40 (7), pp. 1087-1094
- [151]. M. Abareshi, E.K. Goharshadi, S.M. Zebarjad. (2009). Thermodynamic properties of the mixtures of some ionic liquids with alcohols using a simple equation of state. J. Mol. Liq. 149 (3), pp. 66-73
- [152]. I. Bou Malham, P. Letellier, A. Mayaffre, M. Turmine. (2007). Part I: Thermodynamic analysis of volumetric properties of concentrated aqueous solutions of 1-butyl-3-methylimidazolium tetrafluoroborate, 1-butyl-2,3-dimethylimidazolium tetrafluoroborate, and ethylammonium nitrate based on pseudo-lattice theory. J. Chem. Thermodyn. 39 (8), pp. 1132-1143
- [153]. S. Wang, J. Jacquemin, P. Husson, C. Hardacre, M.F. Costa Gomes. (2009). Liquid-liquid miscibility and volumetric properties of aqueous solutions of ionic liquids as a function of temperature. J. Chem. Thermodyn. 41 (11), pp. 1206-1214

- [154]. O. Redlich, A.T. Kister. (1948). Algebraic Representation of Thermodynamic Properties and the Classification of Solutions. *Ind. Eng. Chem.* 40 (2), pp. 345-348
- [155]. A. Arce, A. Soto, J. Ortega, G. Sabater. (2008). Viscosities and Volumetric Properties of Binary and Ternary Mixtures of Tris(2-hydroxyethyl) Methylammonium Methylsulfate + Water + Ethanol at 298.15 K. *J. Chem. Eng. Data.* 53 (3), pp. 770-775
- [156]. I. Bou Malham, M. Turmine. (2008). Viscosities and refractive indices of binary mixtures of 1-butyl-3-methylimidazolium tetrafluoroborate and 1-butyl-2,3-dimethylimidazolium tetrafluoroborate with water at 298 K. *J. Chem. Thermodyn.* 40 (4), pp. 718-723
- [157]. J. Restolho, A.P. Serro, J.L. Mata, B. Saramago. (2009). Viscosity and Surface Tension of 1-Ethanol-3-methylimidazolium Tetrafluoroborate and 1-Methyl-3-octylimidazolium Tetrafluoroborate over a Wide Temperature Range. *J. Chem. Eng. Data.* 54 (3), pp. 950-955
- [158]. B. González, N. Calvar, E. González, Á. Domínguez. (2008). Density and Viscosity Experimental Data of the Ternary Mixtures 1-Propanol or 2-Propanol + Water + 1-Ethyl-3-methylimidazolium Ethylsulfate. Correlation and Prediction of Physical Properties of the Ternary Systems. *J. Chem. Eng. Data.* 53 (3), pp. 881-887
- [159]. E. Gómez, B. González, N. Calvar, Á. Domínguez. (2008). Excess molar properties of ternary system (ethanol + water + 1,3-dimethylimidazolium methylsulphate) and its binary mixtures at several temperatures. *J. Chem. Thermodyn.* 40 (8), pp. 1208-1216
- [160]. B. González, N. Calvar, E. Gómez, Á. Domínguez. (2008). Physical properties of the ternary system (ethanol + water + 1-butyl-3-methylimidazolium methylsulphate) and its binary mixtures at several temperatures. *J. Chem. Thermodyn.* 40 (8), pp. 1274-1281
- [161]. E. Vercher, F.J. Llopis, M.V. Gonzalez-Alfaro, A. Martinez-Andreu. (2009). Density, Speed of Sound, and Refractive Index of 1-Ethyl-3-methylimidazolium Trifluoromethanesulfonate with Acetone, Methyl Acetate, and Ethyl Acetate at Temperatures from (278.15 to 328.15) K. *J. Chem. Eng. Data.* 55 (3), pp. 1377-1388
- [162]. M.A. Kiani, M.F. Mousavi, S. Ghasemi, M. Shamsipur, S.H. Kazemi. (2008). Inhibitory effect of some amino acids on corrosion of Pb-Ca-Sn alloy in sulfuric acid solution. *Corros. Sci.* 50 (4), pp. 1035-1045
- [163]. N.H. Helal, M.M. El-Rabiee, G.M.A. El-Hafez, W.A. Badawy. (2008). Environmentally safe corrosion inhibition of Pb in aqueous solutions. *Journal of Alloys and Compounds.* 456 (1-2), pp. 372-378

- [164]. K. Barouni, L. Bazzi, R. Salghi, M. Mihit, B. Hammouti, A. Albourine, S. El Issami. (2008). Some amino acids as corrosion inhibitors for copper in nitric acid solution. *Mater. Lett.* 62 (19), pp. 3325-3327
- [165]. M. Spah, D.C. Spah, B. Deshwal, S. Lee, Y.-K. Chae, J.W. Park. (2009). Thermodynamic studies on corrosion inhibition of aqueous solutions of amino/carboxylic acids toward copper by EMF measurement. *Corros. Sci.* 51 (6), pp. 1293-1298
- [166]. D.-Q. Zhang, Q.-R. Cai, X.-M. He, L.-X. Gao, G.-D. Zhou. (2008). Inhibition effect of some amino acids on copper corrosion in HCl solution. *Mater. Chem. Phys.* 112 (2), pp. 353-358
- [167]. D.-Q. Zhang, Q.-R. Cai, L.-X. Gao, K.Y. Lee. (2008). Effect of serine, threonine and glutamic acid on the corrosion of copper in aerated hydrochloric acid solution. *Corros. Sci.* 50 (12), pp. 3615-3621
- [168]. P.B. Raja, M.G. Sethuraman. (2008). Natural products as corrosion inhibitor for metals in corrosive media -- A review. *Mater. Lett.* 62 (1), pp. 113-116
- [169]. A.Y. El-Etre. (2006). Khillah extract as inhibitor for acid corrosion of SX 316 steel. *Appl. Surf. Sci.* 252 (24), pp. 8521-8525
- [170]. A. Bouyanzer, B. Hammouti, L. Majidi. (2006). Pennyroyal oil from *Mentha pulegium* as corrosion inhibitor for steel in 1 M HCl. *Mater. Lett.* 60 (23), pp. 2840-2843
- [171]. A.Y. El-Etre, M. Abdallah, Z.E. El-Tantawy. (2005). Corrosion inhibition of some metals using lawsonia extract. *Corros. Sci.* 47 (2), pp. 385-395
- [172]. A.Y. El-Etre. (2003). Inhibition of aluminum corrosion using *Opuntia* extract. *Corros. Sci.* 45 (11), pp. 2485-2495
- [173]. M. Abdallah. (2004). Antibacterial drugs as corrosion inhibitors for corrosion of aluminium in hydrochloric solution. *Corros. Sci.* 46 (8), pp. 1981-1996
- [174]. M. Abdallah. (2002). Rhodanine azosulpha drugs as corrosion inhibitors for corrosion of 304 stainless steel in hydrochloric acid solution. *Corros. Sci.* 44 (4), pp. 717-728
- [175]. M.M. El-Naggar. (2007). Corrosion inhibition of mild steel in acidic medium by some sulfa drugs compounds. *Corros. Sci.* 49 (5), pp. 2226-2236
- [176]. H. Keles, M. Keles, I. Dehri, O. Serindag. (2008). Adsorption and inhibitive properties of aminobiphenyl and its Schiff base on mild steel corrosion in 0.5 M HCl medium. *Colloids and Surfaces A: Physicochemical and Engineering Aspects.* 320 (1-3), pp. 138-145

- [177]. H. Keles, M. Keles, I. Dehri, O. Serindag. (2008). The inhibitive effect of 6-amino-m-cresol and its Schiff base on the corrosion of mild steel in 0.5 M HCl medium. *Mater. Chem. Phys.* 112 (1), pp. 173-179
- [178]. K.A. Kurnia, "Development of Ionic Liquids for CO<sub>2</sub> Absorption", M.Sc. Thesis, Department of Chemical Engineering, Universiti Teknologi PETRONAS, Tronoh, Malaysia, 2008
- [179]. R.M. Silverstein, F.X. Webster, D.J. Kiemle, "Spectrometric Identification of Organic Compounds", 7<sup>th</sup> Edition ed., John Wiley & Sons, Inc., New York, United States of America, 2005.
- [180]. N. Bicak. (2005). A new ionic liquid: 2-hydroxy ethylammonium formate. *J. Mol. Liq.* 116 (1), pp. 15-18
- [181]. S.-l. Zang, D.-W. Fang, J.-x. LI, Y.-Y. Zhang, S. Yue. (2009). Estimation of Physicochemical Properties of Ionic Liquid HPrEO4 Using Surface Tension and Density. *J. Chem. Eng. Data.* 54 (9), pp. 2498-2500
- [182]. J. Tong, M. Hong, W. Guan, J.-B. Li, J.-Z. Yang. (2006). Studies on the thermodynamic properties of new ionic liquids: 1-Methyl-3-pentylimidazolium salts containing metal of group III. *J. Chem. Thermodyn.* 38 (11), pp. 1416-1421
- [183]. J.-Z. Yang, Q.-G. Zhang, F. Xue. (2006). Studies on the properties of EMIGaCl<sub>4</sub>. *J. Mol. Liq.* 128 (1-3), pp. 81-84
- [184]. J. Tong, Q.-S. Liu, W. Guan, J.-Z. Yang. (2007). Estimation of Physicochemical Properties of Ionic Liquid C<sub>6</sub>MIGaCl<sub>4</sub> Using Surface Tension and Density. *J. Phys. Chem. B.* 111 (12), pp. 3197-3200
- [185]. J. Tong, Q.-S. Liu, W.-G. Xu, D.-W. Fang, J.-Z. Yang. (2008). Estimation of Physicochemical Properties of Ionic Liquids 1-Alkyl-3-methylimidazolium Chloroaluminate. *J. Phys. Chem. B.* 112 (14), pp. 4381-4386
- [186]. S.-G. Sun, Y. Wei, D.-W. Fang, Q.-G. Zhang. (2008). Estimation of properties of the ionic liquid BMIZn<sub>3</sub>Cl<sub>7</sub>. *Fluid Phase Equilib.* 273 (1-2), pp. 27-30
- [187]. S.-l. Zang, D.-W. Fang, J.-x. Li, Y.-Y. Zhang, S. Yue. (2009). The estimation of physico-chemical properties of ionic liquid N-propylpyridine rheniumate. *Fluid Phase Equilib.* 283 (1-2), pp. 93-96
- [188]. S.-L. Zang, Q.-G. Zhang, M. Huang, B. Wang, J.-Z. Yang. (2005). Studies on the properties of ionic liquid EMInCl<sub>4</sub>. *Fluid Phase Equilib.* 230 (1-2), pp. 192-196
- [189]. Q.-G. Zhang, J.-Z. Yang, X.-M. Lu, J.-S. Gui, M. Huang. (2004). Studies on an ionic liquid based on FeCl<sub>3</sub> and its properties. *Fluid Phase Equilib.* 226 pp. 207-211

- [190]. Q.-S. Liu, J. Tong, Z.-C. Tan, U. Welz-Biermann, J.-Z. Yang. (2010). Density and Surface Tension of Ionic Liquid [C2mim][PF3(CF2CF3)3] and Prediction of Properties [Cnmim][PF3(CF2CF3)3] (n = 1, 3, 4, 5, 6). *J. Chem. Eng. Data.* 55 pp. 2586-2589
- [191]. J.-y. Wang, F.-Y. Zhao, R.-j. Liu, Y.-q. Hu. (2010). Thermophysical properties of 1-methyl-3-methylimidazolium dimethylphosphate and 1-ethyl-3-methylimidazolium diethylphosphate. *J. Chem. Thermodyn.* 43 (1), pp. 47-50
- [192]. J.-Z. Yang, Q.-G. Zhang, B. Wang, J. Tong. (2006). Study on the Properties of Amino Acid Ionic Liquid EMIGly. *J. Phys. Chem. B.* 110 (45), pp. 22521-22524
- [193]. R.J. Meakins. (1963). Alkyl quaternary ammonium compounds as inhibitors of the acid corrosion of steel. *Journal of Applied Chemistry.* 13 pp. 339-345
- [194]. V. Branzoi, F. Branzoi, M. Baibarac. (2000). The inhibition of the corrosion of ARMCO iron in HCl solutions in the presence of surfactants of the type of N-alkyl quaternary ammonium salts *Mater. Chem. Phys.* 65 pp. 288-297
- [195]. S.B. Velegol, B.D. Fleming, S. Biggs, E.J. Wanless, R.D. Tilton. (2000). Counterion effects on hexadecyltrimethylammonium surfactant adsorption and self-assembly on silica. *Langmuir.* 16 pp. 2548-2556
- [196]. G. Bereket, A. Yurt. (2002). Inhibition of the corrosion of low carbon steel in acidic solution by selected quaternary ammonium compounds. *Anti-Corrosion Methods and Materials.* 49 pp. 210-220
- [197]. M. Knag, J. Sjoblom, G. Oye, E. Gulbrandsen. (2005). A quartz crystal microbalance study of the adsorption of quaternary ammonium derivatives on iron and cementite. *Colloids and Surfaces A—Physicochemical and Engineering Aspects.* 250 (269-278),